

Carbon Budget and Cycling in Perennially Ice-Covered Lake Untersee, East Antarctica

NICOLE MARSH

Thesis submitted to the University of Ottawa
in partial fulfillment of the requirements for the
Master of Science

Department of Earth and Environmental Science
Faculty of Science
University of Ottawa

Under the supervision of:
Dr. Ian Clark (Department of Earth and Environmental Science)
Dr. Denis Lacelle (Department of Geography)

© Nicole Marsh, Ottawa, Canada, 2019

Acknowledgements

First, I want to thank my supervisors Dr. Ian Clark and Dr. Denis Lacelle. I'm very fortunate to have supervisors that are as knowledgeable on polar environments and as invested in this work as the both of you. It's been an absolute pleasure working with and learning from you.

Many thanks are owed to Dr. Dale Andersen (Carl Sagan Center, SETI Institute), who led the expedition to the Undersee Oasis and brought a team of scientists together for a grand adventure to one of the most extraordinary locations on Earth. Thank-you for your guidance in the field and with the science, and constant entertainment with your stories. I'd also like to thank the other expedition members for their help in the field and memories in South Africa; Benoit Faucher and Dr. Denis Lacelle (University of Ottawa), George Shamilshvily (St. Petersburg University, Russia), and Elliott Steele (University of Queensland, Australia).

The expedition was possible due to funding from the TAWANI Foundation and the Trottier Family Foundation, logistical support by the Antarctic Logistics Centre International (ALCI), and collaboration with the Arctic/Antarctic Research Institute and Russian Antarctic Expedition (RAE). Funding for analytical work was generously provided by NSERC.

I am grateful for the training, technical guidance and countless hours of analytical work performed by the lab technicians and collaborators at the University of Ottawa. Thank-you to Carley Crann, Sarah Murseli, Christabel Jean, Monika Wilk, and Dr. Xiaolei Zhao at the A.E. Lalonde AMS Laboratory, Paul Middlestead, Wendy Abdi, Patricia Wickham and Kerry Klassen at the Ján Veizer Stable Isotope Laboratory, and Smitarani Mohanty and Nimal De Silva at the Geochemistry Laboratory. Thanks to Sarina Cotroneo for her Sr-isotope work and Husnain Anwar for assisting with the lake cores. A special thanks to Benoit Faucher from whom I've received constant support in the field, laboratory and in scientific discussion.

I feel very fortunate to have been apart of this project, and for the friends and family that supported me every step of the way. You have my love and gratitude.

Abstract

Perennially ice-covered lake Untersee is one of the largest (8.7 km²) and deepest (~160 m) freshwater lakes in East Antarctica. Water mass balance of Lake Untersee shows it receives ~45% of its annual input from melting of the glacial-wall beneath the ice-cover and ~55% from subglacial meltwater; with loss by sublimation of the ice-cover. The lake floor hosts active photosynthetic microbial mats despite weak irradiance through the ice-cover (<5% PAR). This study aims to characterize the carbon content and its isotopic composition ($\delta^{13}\text{C}$ and ^{14}C) in the lake-waters and microbial mats to develop a carbon budget in order to define carbon sources and its cycling in the lake ecosystem. The DIC in the oxic and alkaline water column (pH 10.4) is very low and of atmospheric origin (0.3–0.4 ppm, $\delta^{13}\text{C}_{\text{DIC}} = -7$ to -10‰ , $F^{14}\text{C}_{\text{DIC}}$ of 0.41 to 0.60). The organic-C content of microbial mats is 0.857 kg C m⁻² and the surface layer has very similar $\delta^{13}\text{C}$ (-9 to -12‰) to the DIC in the water column. The ^{14}C ages of the top and bottom mat layers range from 9,524 to 10,052 years BP, with the age of the bottom mat layers (12,031–13,049 years BP) corresponding to the inferred timing of formation of the lake. Mass balance shows that the rate of the incoming carbon from both subglacial meltwater and englacial melting (8×10^4 g C y⁻¹) is insufficient to account for the carbon sequestered by the microbial mats ($4\text{--}8 \times 10^9$ gC). This suggests that Lake Untersee developed a summer moat when it initially developed (~12 to 13 kya), which allowed for open-exchange with atmospheric CO₂ and replenishment of DIC in the water column. This is supported by a higher growth rate observed in the deepest microbial mats. Since the permanent ice-cover developed, growth rate has decreased, and given the $F^{14}\text{C}_{\text{DIC}}$ and $F^{14}\text{C}_{\text{DOC}}$ in oxic waters ($^{14}\text{C} = 4,119$ to $7,079$ years BP), Lake Untersee has been well-sealed from atmosphere and the water-column subsequently became starved in carbon. These results demonstrate the capacity of microbial communities to adapt to harsh and shifting conditions in Earth's most extreme environments.

Contents

Acknowledgements.....	ii
Abstract.....	iii
Contents	iv
List of Tables	vii
List of Figures.....	viii
1 Introduction	1
1.1 Research Objectives.....	2
2 Study Area.....	4
2.1 Site Location and Climate.....	4
2.2 Glacial History	5
2.3 Geology and Surface Deposits.....	5
2.4 Lake Untersee.....	7
2.5 Lake Water Chemistry	7
2.6 Lake Ecosystem.....	8
2.7 Lacustrine Sediments	10
Chapter 2 Figures	11
3 Methodology.....	16
3.1 Field Logistics	16
3.2 Field Measurements and Sampling	17
3.3 Laboratory Analyses	19
3.3.1 Major Ions, Rare Earth Elements and Trace Metals in Waters.....	19
3.3.2 Carbon Content and $\delta^{13}\text{C}$ in Waters.....	20

3.3.3	Radiocarbon Analysis of TIC and TOC in Waters	20
3.3.4	Strontium (⁸⁷ Sr/ ⁸⁶ Sr) Isotopes in Waters.....	22
3.3.5	Sulfur Isotopes of Sulfate and Sulfide in Waters.....	23
3.3.6	Nitrogen and Oxygen Isotopes of Nitrate in Waters.....	24
3.3.7	Tritium (³ H) in Waters	25
3.3.8	Radioiodine (¹²⁹ I) in Waters.....	25
3.3.9	Microbial Mats Sample Preparation	26
3.3.10	Organic–Carbon Content and δ ¹³ C of Microbial Mats	27
3.3.11	Radiocarbon Measurements of Microbial Mats.....	28
3.4	Carbon Budget.....	29
	Chapter 3 Tables	31
	Chapter 3 Figures.....	32
4	Results	36
4.1	North Basin Water Column.....	36
4.2	South Basin Water Column.....	38
4.3	Moraine Ponds.....	40
4.4	Microbial Mats	41
	Chapter 4 Tables	43
	Chapter 4 Figures.....	51
5	Discussion.....	62
5.1	Lake and Pond Chemistry	62
5.2	Lake Carbon Model and Budget	69
5.2.1	Carbon Reservoirs.....	70
5.2.2	Glacial CO ₂ Input.....	72

5.2.3	Carbon Output.....	75
5.2.4	Carbon Mass Balance and Implications.....	76
5.2.5	Carbon Cycling in the Sediment Microbiome	80
Chapter 5 Tables		83
Chapter 5 Figures.....		87
6	Conclusions	90
6.1	Future Work	91
References.....		93
Appendix A: External Laboratory (IT2) Methodology for Analysis of Nitrogen and Oxygen of Nitrate ($\delta^{15}\text{N}$ and $\delta^{18}\text{O}$).....		102
Appendix B: Lake and Pond Water Data.....		105
Appendix C: Microbial Mat Data		180
Appendix D: Geochemical Modelling (PHREEQC) Output		192

List of Tables

Table 3–1 Field sampling locations	31
Table 3–2 Water sample summary.....	31
Table 4–1 Major ion summary.....	43
Table 4–2 Radiocarbon results of lake and pond waters.....	44
Table 4–3 Strontium isotopes in lake and pond waters.....	45
Table 4–4 Nitrogen and oxygen isotopes of nitrate in pond and lake waters	46
Table 4–5 Sulfur isotopes of sulfate and sulphide in pond and lake waters	47
Table 4–6 Tritium (³ H) results for lake and pond water samples	48
Table 4–7 Radioiodine results for lake and pond water samples.....	48
Table 4–8 Lake core organic carbon abundance and stable isotope summary	49
Table 4–9 Core microbial mat organic carbon mass and content	49
Table 4–10 Radiocarbon results of the organic carbon component from Core 1 and Core 3.....	50
Table 5–1 Geochemical modelling (PHREEQC) summary.....	83
Table 5–2 Radiogenic strontium isotope summary.....	84
Table 5–3 Data from literature used in the carbon mass–balance calculations	85
Table 5–4 Measured data from this study used in the carbon mass–balance calculations.....	85
Table 5–5 Carbon budget and mass balance	86

List of Figures

Figure 2–1 Satellite imagery of Dronning Maud Land, East Antarctica (left) and Untersee Oasis (right). The image was captured by the Landsat 8 satellite (download via LIMA database from United States Geographical Survey).....	11
Figure 2–2 Schematic of the glacial history of the Untersee Oasis. Modified from Schwab et al. (1998). Stage 1: valley is filled by advancing glacier. Stage 2 and Stage 3: glacier retreat to indicated positions. Stage 4: present position of the glacier.	12
Figure 2–3 Pressure ridge at the intersect of the Anuchin Glacier (left) and Lake Untersee (right). Photograph by Benoit Faucher.....	13
Figure 2–4 Schematic cross–section of Lake Untersee, showing hydrological inputs (subaqueous melt and potential subglacial melt and/or groundwater) and loss by sublimation of the ice cover. Figure modified from Faucher <i>et al.</i> (2019).	14
Figure 2–5 Underwater photograph of microbial mats on the lake bottom, including prostrate mats and conical structures (Andersen <i>et al.</i> , 2011).....	15
Figure 3–1 Lake Untersee field camp (top). Red WeatherHaven and orange Stronghold tents on the lake ice (bottom).	32
Figure 3–2 Lake water and sediment core sampling sites at Lake Untersee. The image was captured by the Landsat 8 satellite (download via LIMA database from United States Geographical Survey).....	33
Figure 3–3 Niskin water sampling bottle.	34
Figure 3–4 Split Core 3 prior to sampling (left), and sampling of the microbial mat laminae (right) at the Department of Geography laboratory facilities at the University of Ottawa.	35
Figure 4–1 Temperature, pH, specific conductivity (Sp. Cond.), dissolved oxygen (DO) and chlorophyll profiles of the northern basin at location NB. Data from previous expeditions (2015, 2016) were collected by Benoit Faucher.	51
Figure 4–2 Piper plot of lake and moraine pond major ion data.....	52

Figure 4–3 North Basin (NB) profiles of total inorganic carbon (TIC) concentrations (left) and $\delta^{13}\text{C}_{\text{TIC}}$ VPBD (right). Stable carbon values for modern atmospheric CO_2 from (Clark, 2015a), and East Antarctica ice core CO_2 compilation data from Eggleston et al. (2016). 53

Figure 4–4 North basin (NB) and south basin (SB) profiles of sulfur isotope ratios of sulfate (solid lines) and sulfide (dashed line) with lateral moraine pond $\delta^{34}\text{S}_{\text{SO}_4}$ results (cyan asterisk). Grey shaded area is the range of $\delta^{34}\text{S}_{\text{SO}_4}$ (total) and $\delta^{34}\text{S}_{\text{SO}_4}$ (no sea salt) values published for Dome C and Vostok ice cores spanning ages from 2.5–130 kya (Alexander *et al.*, 2003)..... 54

Figure 4–5 Chondrite normalized (C1, after McDonough and Sun, 1995) REE pattern for lake waters (NB, SB) and lateral moraine pond waters (Moraine Ponds). Gruber Anorthosite whole rock sample REE data from Ravikant et al. (2011). Note y-axis change for water results versus whole rock anorthosite data. 55

Figure 4–6 Temperature, pH, specific conductivity (Sp. Cond.), dissolved oxygen (DO) and chlorophyll profiles of the southern basin (SB). Data from previous expeditions (2015, 2016) were collected by Benoit Faucher..... 56

Figure 4–7 South Basin (SB) total inorganic carbon (TIC) concentrations (left), total organic carbon (TOC) concentrations and $\delta^{13}\text{C}_{\text{TIC}}$ and $\delta^{13}\text{C}_{\text{TOC}}$ (right). Stable carbon values for modern atmospheric CO_2 from Clark, (2015a), East Antarctica ice core $\delta^{13}\text{C}\text{--CO}_{2(\text{g})}$ compilation data from Eggleston et al. (2016). 57

Figure 4–8 Temperature, pH, specific conductivity (Sp. Cond.), dissolved oxygen (DO) and chlorophyll profiles of the lateral moraine ponds. 58

Figure 4–9 Core 3 microbial mat nitrogen abundance and isotope ratios. The $^{15}\text{N}/^{14}\text{N}$ ratios are normalized to air and reported as $\delta^{15}\text{N}$ 59

Figure 4–10 Core microbial mat organic carbon abundance, stable isotopes ($\delta^{13}\text{C}$) and radiocarbon results reported as fraction modern carbon ($F^{14}\text{C}$). 60

Figure 4–11 Bathymetry map (modified from Kaup, 1988) showing core sampling locations and radiocarbon ages of top laminae reported for each core (years before 1950). Cores from this study

(Core 2 and Core 3) were collected within a 30 m radius of the diving hole. Radiocarbon dates in pink from Andersen *et al.*, (2011) and radiocarbon dates in black from Schwab (1998)..... 61

Figure 5–1 Ranges in $\delta^{34}\text{S}$ contents of sulphur and sulphur compounds in different materials and environments. Figure modified from (Krouse, 1980)..... 87

Figure 5–2 Accrued carbon input to the lake by glacial input of CO_2 by combined glacial input of subaqueous melting of the glacial wall and subglacial melt (using $[\text{C}]_{\text{melt}} = 0.0165 \text{ gC L}^{-1}$). Mass of estimated total carbon reservoirs for 50%, 75% and 100% matt coverage scenarios denoted by black dashed lines. 88

Figure 5–3 Carbon cycling in the sediment microbiome. Image of photosynthetic bacteria (Cyanobacteria) from Andersen *et al.*, (2011) and stock heterotrophic bacteria image by Denis Kunkel (<http://www.denniskunkel.com/>)..... 89

1 Introduction

Perennially ice-covered lakes in polar regions provide a unique opportunity to examine limnological processes under a rather unique set of environmental conditions. Limnological processes in ice-covered lakes are largely influenced by: 1) the source of water feeding the lakes; and 2) the ice-cover which precludes atmospheric gas exchange and reduces light penetration, both key factors to lake biogeochemistry (Hawes *et al.*, 2016). Hundreds of ice-covered lakes have been inventoried in Antarctica, largely in cold and dry ice-free regions such as the McMurdo Dry Valley (MDV), Vestfold Hills, Schirmacher Oasis, and Syowa Coast (Matsumoto *et al.*, 1992; Bormann and Fritzsche, 1995; Perriss and Laybourn-Parry, 1997). The lakes can be classified based on their ice-cover regime; coastal lakes typically develop a seasonal ice-cover and are typically recharged by a combination of local precipitation, runoff and glacial meltwater (e.g., Gibson *et al.*, 2002; Lyons *et al.*, 2013). Further inland where the climate is colder and drier, lakes are perennially ice-covered yet develop a zone of open water along the margin in the summer (moat) and are largely fed by glacial melt-streams. These ice-covered surface lakes differ, of course, from the many subglacial lakes, such as Lake Vostok, which have been discovered beneath the Antarctic ice sheet (Wright and Siegert, 2012).

Lake Untersee is a large perennially ice-covered lake in Dronning Maud Land that is unlike most of the lakes in Antarctica. Lake Untersee developed at about 12,000–10,000 years before present (yr BP) following the retreat of the Anuchin Glacier (Bormann and Fritzsche, 1995; Schwab, 1998). Unlike most ice-covered lakes, Lake Untersee does not develop a summer moat, thus sealing the lake to atmospheric exchange, and is recharged solely by subaqueous glacial melt and subglacial meltwater (Hermichen, Kowski and Wand, 1985; Kaup *et al.*, 1988; Andersen, McKay and Lagun, 2015). The 2–4 m thick ice cover and absence of summer moating at Lake Untersee ensures that irradiance received in the water-column is only across the photosynthetic active radiation (PAR) spectrum (450–800 nm) and decreases from 5% just beneath the ice-cover to <1%

at the lake bottom (Andersen *et al.*, 2011; Faucher *et al.*, 2019). Despite the low–light conditions and nutrient–starved lake waters (*e.g.*, C, P and Fe), the lake–bed is colonized by a microbial ecosystem that develop mats, pinnacles and cone structures, with some cones rising ~0.5 m above the lake bottom (Andersen *et al.*, 2011). Metagenomic sequencing of the 16S rRNA gene showed that the top layer of the mats are composed of phototrophic microbial community (*Cyanobacteria: Phormidium sp., Leptolyngbya sp., and Pseudanabaena sp*) that shift to a heterotrophic microbial community in the underlying layers (*Actinobacteria, Verrucomicrobia, Proteobacteria, and Bacteroidetes*) (Koo *et al.*, 2017). The benthic photosynthetic psychrophiles in Lake Untersee appear to be well adapted to their environment; however, it is unclear if their metabolic functioning is light–, nutrient– or carbon–limited, and whether the rate of biomass accumulation has changed during the Holocene. It is also unknown how their activity might affect the lake water chemistry and carbon cycling.

1.1 Research Objectives

The aim of the thesis is to characterize the carbon content and isotopic composition of the lake–waters and sediments to better understand source and cycling in Lake Untersee and the role of the microbial mats in sequestering carbon in the lake. These objectives were accomplished by undertaking field work at Lake Untersee in Nov–Dec 2019 where the lake water column, microbial mats and lake sediments were sampled and analyzed using a trace carbon chemistry and isotope systematics approach. In addition to Lake Untersee, a series of small perennially ice–covered ponds located on the lateral moraine on the western flank of the Anuchin glacier were also sampled for comparison to Lake Untersee; the bottom these ponds are also covered by microbial mats; however, these could not be sampled at the time.

Specifically, the main objectives of the thesis are to:

1. Characterize the lake water geochemical composition (*e.g.*, temperature, pH, dissolved oxygen, major and trace ions);

2. Investigate the potential development of summer moating during recent time from tritium and radioiodine (^{129}I) analyses;
3. Determine the amount of carbon stored in the water column from total inorganic and organic carbon (TIC–TOC) measurements;
4. Determine the amount of carbon sequestered by the microbial mats by characterizing the organic–carbon abundance;
5. Based on a mass balance approach, determine the C–content and $\delta^{13}\text{C}$ of waters recharging Lake Untersee; and
6. Determine the source of carbon used by the phototrophic mats and potential cycling from their $\delta^{15}\text{N}$ – $\delta^{13}\text{C}$ composition and ^{14}C activity.

Secondary objectives are to:

1. Determine the role of anorthosite weathering on lake water geochemistry from $^{87}\text{Sr}/^{86}\text{Sr}$ measurements; and
2. Determine the source of SO_4^{2-} and NO_3^- in the lake water from $\delta^{34}\text{S}$ and $\delta^{15}\text{N}$ – $\delta^{18}\text{O}$ measurements.

Given that Lake Untersee is thought to be a terrestrial analogue to Gale Crater, which may have once been an ice–covered lake on ancient Mars fed by melting surrounding glaciers (Kling et al., 2019), the findings may help assess the metabolic pathways of life near the limits of habitability in ice–covered crater lakes on early Mars or the icy moon Enceladus (McKay, Andersen and Davila, 2017).

2 Study Area

2.1 Site Location and Climate

Large ice- and snow-free areas in Antarctica are referred to as an *oasis* or a *dry valley*; the McMurdo Dry Valleys (MDV) are amongst the most extensively investigated with studies focusing on the hydrology and limnology of the lakes and the microbial mats they support (Spigel and Priscu, 1998; Moorhead, Schmeling and Hawes, 2005; Gooseff *et al.*, 2006; Hawes *et al.*, 2011). The Sôya Coast (eastern Lützow-Holm Bay) near Syowa station is another region that hosts many ice-covered lakes with active microbial mats (Tanabe *et al.*, 2019).

This study focuses on the Untersee Oasis located in the Otto-von-Guber-Gebirge (Gruber Mountains) at 71°20'S 13°45'E, approximately 90 km southwest of the Schirmacher Oasis (Bormann and Fritzsche, 1995). The oasis contains two large perennially ice-covered lakes: Lake Untersee and Lake Obersee, and a series of small perennially ice-covered ponds (**Figure 2-1**). Measuring 6.5 km long and 1.5 km wide, Lake Untersee is one of the largest perennially ice-covered lakes in Dronning Maud Land, East Antarctica (Hermichen, Kowski and Wand, 1985; Kaup *et al.*, 1988; Wand *et al.*, 1997).

The climate of the Untersee Oasis is part of a polar desert regime. Ten years of climate data (2008–2017) collected by an automated weather station along the shore of Lake Untersee (71.34°S, 13.45°E, 612 m a.s.l.) shows a mean insolation of $99 \pm 7 \text{ W m}^{-2}$, mean annual air temperature (MAAT) of $-9.5 \pm 0.7^\circ\text{C}$, thawing degree-days ranging from 7 to 51 degree-days, and a mean relative humidity of $42 \pm 5\%$ (Andersen, McKay and Lagun, 2015). The mean annual air temperature showed little to no change over the past decade (Andersen, McKay and Lagun, 2015). The average wind speed was 5.4 m s^{-1} , with strong south wind speed descending the polar plateau and sweeping across the southern section of the lake and also strong east wind descending from the Aurkjosen Cirque and flowing across the snout of the Anuchin Glacier (Andersen, McKay and Lagun, 2015). Despite having a relatively warm MAAT for Antarctica, the local climate is

dominated by intense ablation which limits surface melt features due to cooling associated with latent heat of sublimation (*e.g.*, Hoffman, Fountain and Liston, 2008).

2.2 Glacial History

Knowledge about the glacial history of the Untersee Oasis is rather limited and is based on geomorphological evidence (Bormann and Fritzsche, 1995) and ice-sheet elevation inferred from radiocarbon dating of subfossil stomach oil (mumiyo) deposited by the snow petrels that lived in the slopes and moraine deposits in the Untersee Valley (Hiller *et al.*, 1988; Hiller, Hermichen and Wand, 1995).

Bormann and Fritzsche (1995) and Schwab (1998) summarize the glacial history in four stages (**Figure 2–2**). During the late Pleistocene, the region was glaciated by the thick inland ice sheet flowing south to north; the steep U-shaped valley of the Untersee Oasis was carved out during this event (Stage 1). During Stage 2 (~58,000 to 13,000 yrs BP), the ice-flow conditions changed drastically due to lowering of the glacier ice-level. Ice streams flowing north along the eastern and western flanks of the Wohlthat Massif turned back south like an eddy, united at the northern flank of the massif and flowed south into the valley. Ice levels were likely 1200 m and filled most of the valley during this time before further subsiding during Stage 3 to about 300 m. The south-flowing valley glacier formed the tongue-shaped peninsula and terminal moraines during this time (Stage 3), before retreating several hundred metres to the north where the glacier and northern extent of the lake meet today (Stage 4). Schwab (1998) suggested that Lake Untersee likely formed between 12 and 10 kyr BP when the Anuchin Glacier retreated to near its present location.

2.3 Geology and Surface Deposits

Lake Untersee is located in a steep-sided valley in the Gruber Mountains, one the southernmost valleys ending in the eastern Wohlthat Massif. The Wohlthat Massif is a large Precambrian anorthosite complex, comprising an area over 900 km² in central Dronning Maud Land (Ravich

and Solo'vev, 1969; Kämpf and Stackebrandt, 1985). The mountains are comprised of the Eliseev Anorthosite Complex (of the Wohlthat Massif), one of the largest known anorthosite intrusions in Antarctica (Bormann and Fritzsche, 1995). The exposed intrusion in the Oasis is characterized by anorthosite, norite and norite–anorthosite alteration, and is occasionally cut by mafic (e.g., dolerite) to ultra mafic (e.g., lamprophyre) dykes (Singh et al., 1988; Ravikant et al., 2011). Ferromonzodiorite and ferromonzonite have also been observed, however the dominant rock type in the area is undoubtedly the plagioclase rich anorthosite (Bormann and Fritzsche, 1995; Ravikant et al., 2011). Plagioclase in the anorthosite has a composition of $An_{55\pm 5}$ (Bormann and Fritzsche, 1995; Ravikant et al., 2011).

German studies described by Bormann and Fritzsche (1995) worked to infer the rock assemblages under the ice sheet between the ice-free Schirmacher and Untersee oases. The geology under the ice is key to understanding subglacial weathering processes, which may contribute solutes and biological material via subglacial melt to Lake Untersee. Boulder and till samples were collected during the 1985/86 and 1986/87 German expeditions from Schirmacher Oasis, adjacent nunataks and the area of the Untersee Oasis for geochemical characterization and to make inferences on the subglacial geology (Bormann and Fritzsche, 1995). In general, the boulder and till analysis results suggest that the area underlying the ice is a silicate terrain, consisting of igneous and meta-igneous rock types. Rock and boulder analysis of material from in and near the Untersee Oasis found the main rock group in all moraine sample sites to be anorthosite. Migmatites, calc-silicates, amphibole–biotite gneiss, biotite gneiss, sillimanite gneiss and basalt were also observed in the till and moraine material surrounding the lake (Bormann and Fritzsche, 1995; Levitan *et al.*, 2011). Moraines also flank the Anuchin glacier, and a tongue-shaped push moraine extends from the western-side of the valley, a distinct feature visible in satellite imagery (**Figure 2–1**).

2.4 Lake Untersee

Lake Untersee is located in a closed basin at ~ 610 m a.s.l. and is dammed at its northern end by the Anuchin Glacier where a pressure-ridge forms at the lake-glacier interface (**Figure 2–3**). The lake is 2.5 km wide and 6.5 km long, making it the largest freshwater lake in central Dronning Maud Land (Hermichen, Kowski and Wand, 1985). The lake is divided into two basins by a sill that cuts across the lake at 50 m depth (Wand *et al.*, 1997). The larger oxic water basin occupies the north and central section to a maximum observed depth of 169 m, and the shallower anoxic water basin occupies its southern section to a depth of 100 m.

Measurements of the ice cover thickness range from 1.96 to 3.96 m with thicker ice cover in the north-west sector and thinner ice in the southern and north-east sectors (Faucher *et al.*, 2019). The thickness of the ice cover shows a strong relation with sublimation rates ($40 \pm 1.1 \text{ cm yr}^{-1}$ in the northern end to $75 \pm 4.2 \text{ cm yr}^{-1}$ in the southern end). Variations in sublimation rates across the ice cover are largely determined by wind-driven turbulent heat fluxes and the number of snow-covered days (Faucher *et al.*, 2019). The total volume of the lake is $5.21 \times 10^8 \text{ m}^3$ and based on the average sublimation rate, the lake is losing ~1% of water annually (Faucher *et al.*, 2019). Ephemeral streams, runoff, or surface melt at the ice surface have not been observed in the oasis, and the lake does not develop a moat during the austral summer even when air temperatures rise above freezing (Andersen, McKay and Lagun, 2015). Therefore, to maintain the water mass balance in equilibrium, Faucher *et al.* (2019) suggested that 40–45% of the lake water volume is recharged by subaqueous melting of the Anuchin Glacier at the lake-glacier interface with subglacial meltwater providing the remaining 55–60%.

2.5 Lake Water Chemistry

The lake has two sub-basins: 1) a large basin occupies the northern and central section to a maximum depth of 169 m; and 2) a shallower basin occupies its southern section to depth of 100 m depth (Wand *et al.*, 1997). The water in the larger and deeper basin, as well as that above the sill in the shallower basin is well-mixed, has a temperature near 0.5°C, pH near 10.6, dissolved

oxygen near 150% and a specific conductivity near $505 \mu\text{S cm}^{-1}$ (Wand *et al.*, 1997; Andersen *et al.*, 2011). The prevailing ions are Na–Ca–SO₄ with elevated levels of silica (Wand *et al.*, 1997). However, in the southern basin, the water below the sill (60–100 m) is stratified with temperature ranging between 0°C at the ice–water interface to a maximum of 5°C, with lower pH (~7), higher specific conductivity (1100–1300 $\mu\text{S cm}^{-1}$), dissolved oxygen levels near 0% and with methane reported up to 21,800 $\mu\text{mol L}^{-1}$ near the lake bottom (Wand *et al.*, 2006). The north basin, as well as the waters above the sill in the shallower southern basin, are well–mixed due to a thermal gradient and convection caused by melting of the ice–wall at the glacier–lake interface (Wand *et al.*, 1997; Steel, McKay and Andersen, 2015). However, the water below the sill in the southern basin is chemically and physically stratified and its higher density prevents mixing with the overlying oxic water column (Bevington *et al.*, 2018).

2.6 Lake Ecosystem

The floor of the oxic basin in Lake Untersee is covered by photosynthetic microbial mats with the transparency of the lake ice to photosynthetically active radiation (PAR) being $4.9 \pm 0.9\%$ and decreasing to $< 1\%$ at the lake bottom (Andersen *et al.*, 2011). The lake supports exclusively a microbial ecosystem with no higher plants, invertebrates, fish or diatoms (Levitan *et al.*, 2011; Pikuta *et al.*, 2017; Pikuta and Hoover, 2019). The microbial mats are thought to be well–developed as they are protected from physical perturbation (wind and wave forcing) by the perennial ice cover and the lack of bioturbating organisms in the underlying lacustrine sediments.

Early limnological research showed the water column to be clear, ultra–oligotrophic, with remarkably low primary production, represented by low chlorophyll *a* concentrations ($< 3 \text{ mg/m}^3$) (Kaup *et al.*, 1988; Wand *et al.*, 1997; Haendel *et al.*, 2011). The biochemical studies by Wand *et al.* (1997, 2006) were the first to detect microbially produced methane in the anoxic basin and attributed the high abundance to microbial production in the surficial lake sediments and minor contributions from activity in the lake water column. To date, methanogens have not been found

in the water column (Pikuta *et al.*, 2017; Pikuta and Hoover, 2019) but bacterial and archaea methanogen DNA has been detected in the lake sediments (Wagner *et al.*, 2019; Weisleitner *et al.*, 2019) supporting these interpretations.

The next major step in understanding the biology in the lake came with the discovery of photosynthetic mats observed as prostrate, pinnacle and large conical structures on the lake floor (**Figure 2–5**) (Andersen *et al.*, 2011). These structures are unique to Lake Untersee and are described as decimeter scale, non–calcareous, organo–sedimentary structures, morphologically similar to Archaean and Proterozoic conical stromatolites (Andersen *et al.*, 2011). The cones and mats are often pink in colour as a result of high concentrations of the light–capturing pigment phycoerythrin, a characteristic observed in the cyanobacteria communities in Arctic and Antarctic lakes (Vincent and Quesada, 2012). Pigmented benthic microbial mats have been observed at the greatest observed depths of Lake Untersee (169 m) and the conical structures have been observed up to 100 m (Andersen *et al.*, 2011; Weisleitner *et al.*, 2019). Imagery of the lake bottom has been collected using submersible action–cameras lowered through holes drilled in the ice. Personal observations by Dale Andersen were recorded from several scuba–dives under the ice cover during the 2015–2018 expeditions, estimating nearly 100% of the lake bottom is covered by the benthic mats to ~100 m depth, and 20–30% in the deepest sections below 100 m depth.

Metagenomic analysis (16S rRNA sequencing) has been performed on the top three layers of a photosynthetic mat (Koo *et al.*, 2017), as well as the bacterioplankton communities in the aerobic and anaerobic waters (Filippova *et al.*, 2013; Fomenkov *et al.*, 2017; Pikuta *et al.*, 2017). Findings on bacterioplankton include identification of psychrophilic homo–acetogenic bacteria in the bottom layers of the anoxic basin, and sequencing of heterotrophic aerobic bacteria from concentrated oxic water samples. Microbial viruses (bacteriophages) have also been found with aerobic heterotrophic bacteria and are known to play a key role in recycling organic compounds in ice–covered Antarctic lakes with extremely low nutrient concentrations (Sävström *et al.*, 2008; Filippova *et al.*, 2013).

For the conical stromatolites, the microbial taxa identified in the top laminae are predominantly from phylum *Cyanobacteria*, and the predicted metabolic functions showed the bacterial community capable of producing nutrients by photosynthesis (Koo *et al.*, 2017). In contrast, just millimetres below the sediment–water interface the laminae are dominated by heterotrophic bacterial taxa such as *Actinobacteria* and *Verrucomicrobia* (Koo *et al.*, 2017). The predicted metabolic functions (*e.g.*, carbohydrate metabolism, amino acid metabolism) of the heterotrophic bacteria are likely involved in the decomposition of organics and metabolites (Koo *et al.*, 2017). Bulk genomic analysis of deep dredged material from the north basin identified *Bacteroidetes*, *Proteobacteria*, *Cyanobacteria*, *Actinobacteria* and *Planctomycetes* as the main phyla whereas *Proteobacteria*, *Chlorobi*, *Actinobacteria*, *Planctomycetes*, and *Armatimonadetes* were found as the dominating phyla in the dredged anoxic sediments from the south basin (Weisleitner *et al.*, 2019).

Recent metagenomic study of cryoconite holes on the surface of the lake ice–cover and Anuchin glacier attempted to link the lake ecosystem with that of the surrounding soils and/or the Anuchin Glacier (Weisleitner *et al.*, 2019). The study concluded that cryoconite microbial assemblages were a potential source of organisms, particularly to the benthic mat communities in the lake, but that the major biotic sources for the lake ecosystem remain unknown (Weisleitner *et al.*, 2019).

2.7 Lacustrine Sediments

Studies on the lake sediments are limited (*e.g.*, (Schwab, 1998; Levitan *et al.*, 2011), however two deep cores from the north and south basin are described by Schwab (1998). The Schwab dissertation reports that the deepest sediments to be comprised of moraine material, overlain by a layer of gravel to clay sized lacustrine sediments, and the top layer is comprised of silt to clay sized particles and organics. Clays are dominantly illite, with fractions of chlorite, smectite and kaolinite.

Chapter 2 Figures

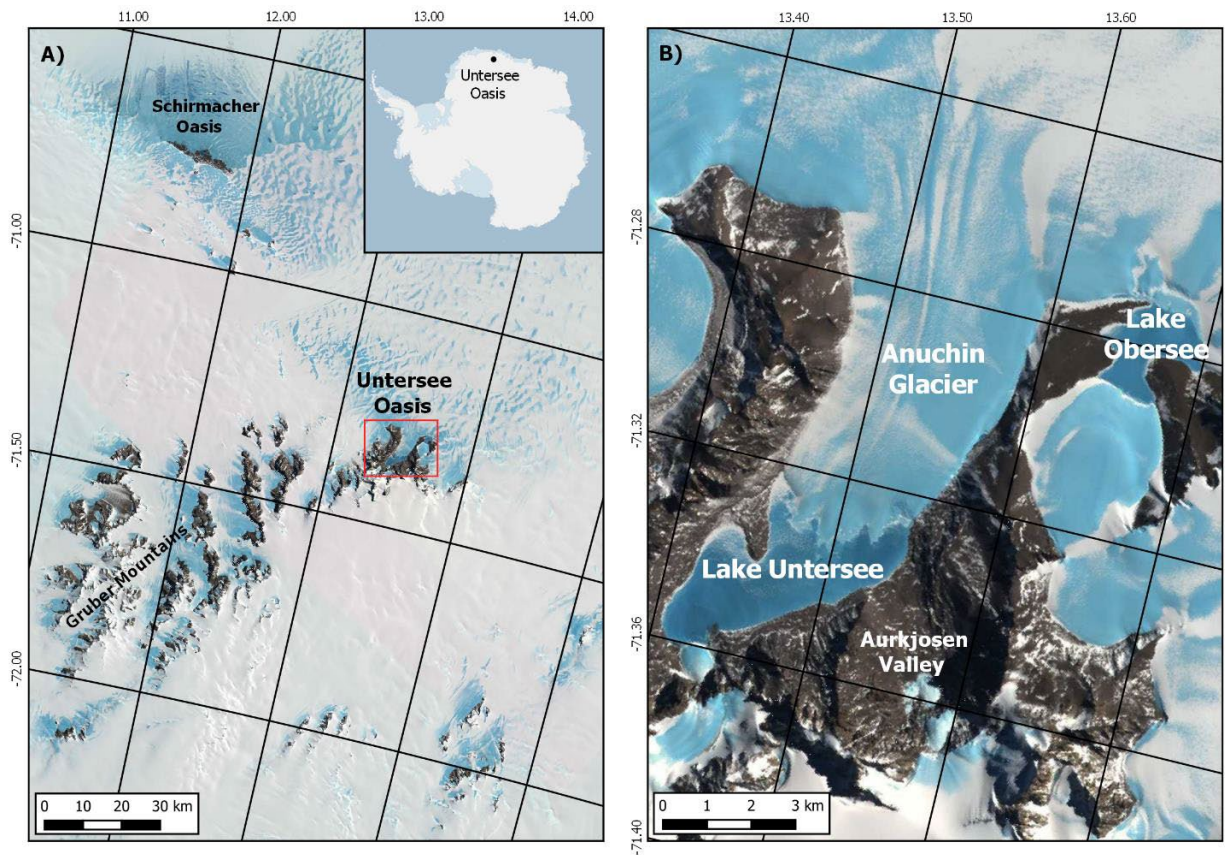
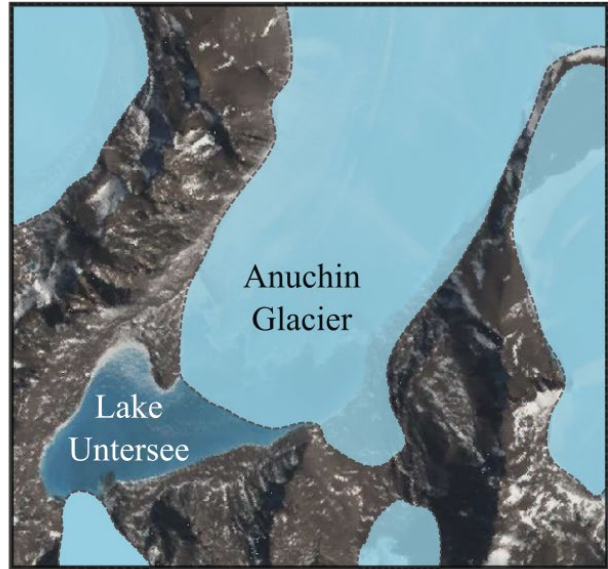


Figure 2–1 Satellite imagery of Dronning Maud Land, East Antarctica (left) and Untersee Oasis (right). The image was captured by the Landsat 8 satellite (download via LIMA database from United States Geographical Survey).

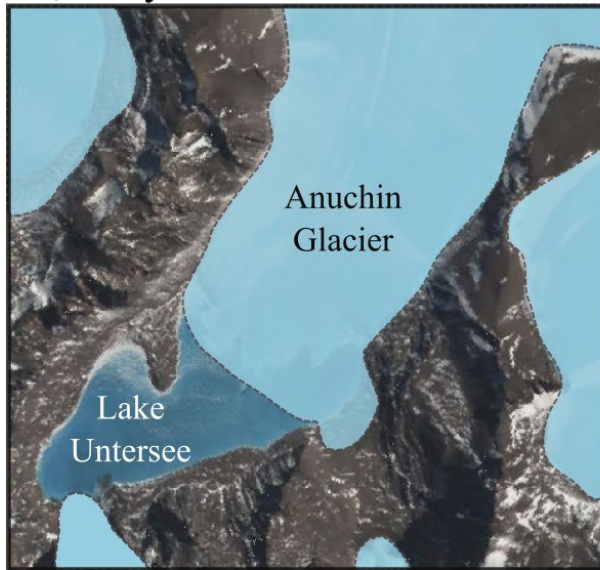
~14,000 years BP



~13,000 – 11,000 years BP



~7,000 years BP



Present-day

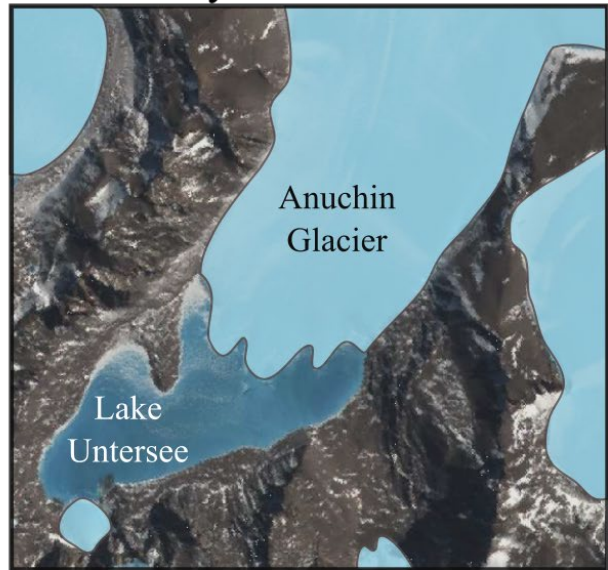


Figure 2-2 Schematic of the glacial history of the Untersee Oasis. Modified from Schwab et al. (1998). Stage 1: valley is filled by advancing glacier. Stage 2 and Stage 3: glacier retreat to indicated positions. Stage 4: present position of the glacier.



Figure 2–3 Pressure ridge at the intersect of the Anuchin Glacier (left) and Lake Untersee (right). Photograph by Benoit Faucher.

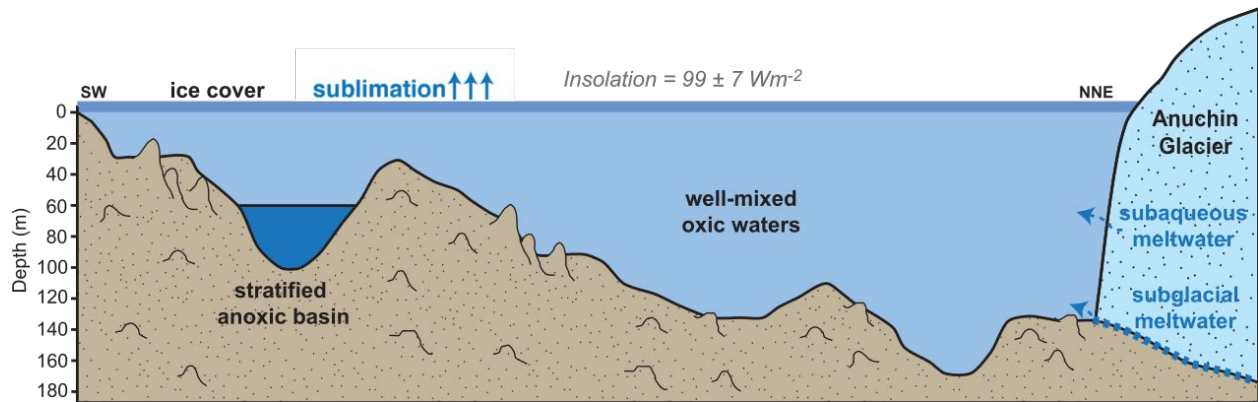


Figure 2–4 Schematic cross-section of Lake Untersee, showing hydrological inputs (subaqueous melt and potential subglacial melt and/or groundwater) and loss by sublimation of the ice cover. Figure modified from Faucher *et al.* (2019).

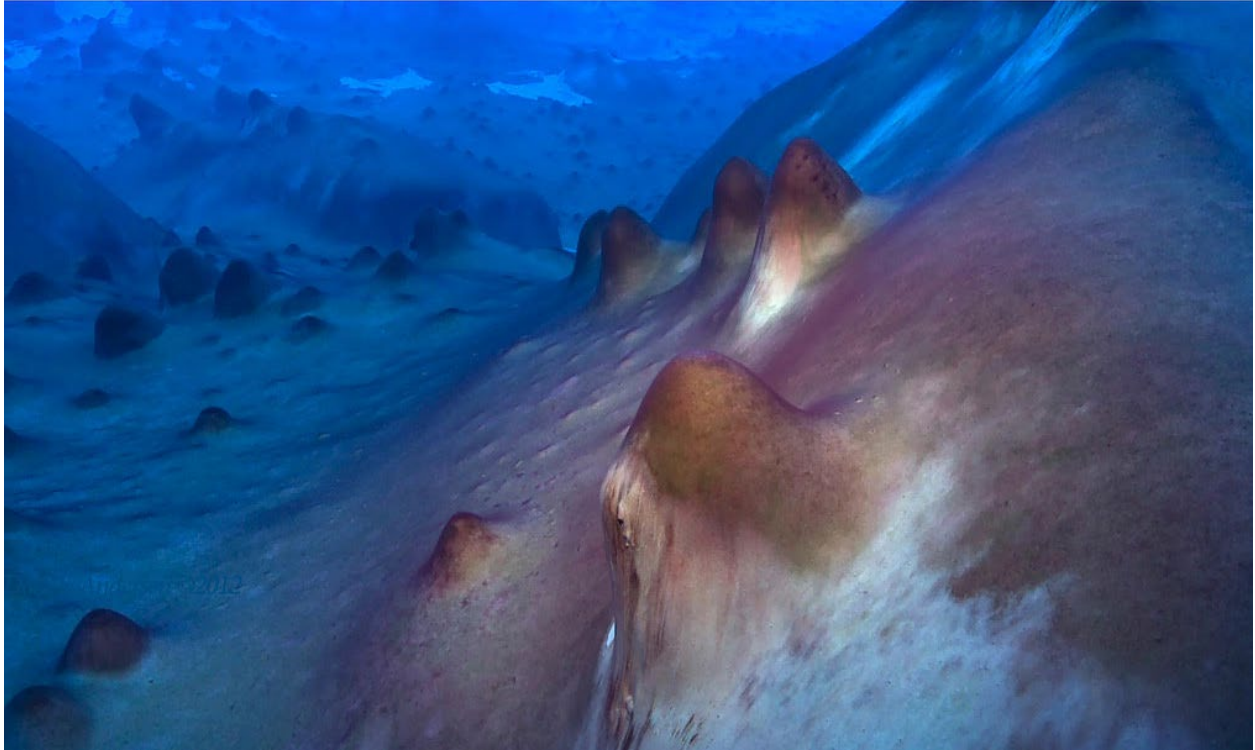


Figure 2–5 Underwater photograph of microbial mats on the lake bottom, including prostrate mats and conical structures (Andersen et *al.*, 2011).

3 Methodology

3.1 Field Logistics

Samples for this study were collected during the 2017 Tawani Expedition to Lake Untersee, an international collaboration with the RAE and researchers from the United States, Canada, Russia and Australia: George Shamilishvily (St. Petersburg State University), Denis Lacelle (University of Ottawa), Benoit Faucher (University of Ottawa), Elliot Steel (University of Queensland) and Dale Andersen (*Expedition Lead*, Carl Sagan Center, SETI Institute) and the author.

Lake Untersee is a very remote and logistically challenging field location, which required support from the Antarctic Logistics Centre International (ALCI), including transportation to the Antarctic continent and access to the field site. The expedition team flew from Cape Town, South Africa on November 1, 2017 to the ice-field landing strip servicing the Novolazarevskaya Station Antarctic Research Station. The Russian research base is located in the Schirmacher Oasis, near the Lazarev Ice Shelf. The team was stationed near the research base in the ALCI facilities until a weather window was safe for transportation across the ice sheet to the field site. The team was deployed from the Schirmacher Oasis on November 11, 2017 and traversed the 125 km to the Untersee Oasis aboard snowmobiles and supply-sleds pulled by the Everest, a large tracked vehicle designed for transport over crevasses and the Antarctic landscape.

The field camp was mobilized on the northern flank of the push-moraine where there was some protection from the katabatic winds sweeping across the lake from the overhanging valley glaciers to the south. Sturdy WeatherPort structures were installed on the lake ice for the kitchen tent, a dry-tent for the scuba-diving gear and to act as emergency shelter in the case of severe weather. Mountain Hardware Stronghold tents were installed on the moraine and lake ice for a science tent and living space for the team members (**Figure 3-1**). The utmost care was taken to limit the footprint of the camp and anthropogenic influence on the environment, including collecting and transporting all waste back to Novolazarevskaya Station following the field program.

3.2 Field Measurements and Sampling

Samples for this study were collected by the author and the expedition team members. Over the course of the field season, areas of interest on the lake and in the oasis were accessed by snowmobile and by foot. Heavier supplies, such as drilling equipment, were pulled on sleds by snowmobile.

Two locations on the lake were selected for sonde profiling and to sample the water. One site is located in northern basin and reaches the deepest section of the lake (169 m), here named the *North Basin Hole* (NB). The second sampling site accesses the deepest section of the southern basin (95 m), here named the *South Basin Hole* (SB). The NB and SB sampling locations are shown in **Figure 3–2**, and coordinates are reported in **Table 3–1**.

The lake water was accessed through holes drilled through the 2–4 m permanent ice–cover using a Jiffy Ice Drill. Field measurements of pH, temperature, specific conductivity, total dissolved solids (TDS), dissolved oxygen (DO) and chlorophyll were measured using a calibrated YSI 6600 V2–4 Multi–Parameter Water Quality Sonde. Multiple water–column profiles were measured at the NB and SB locations between November 15 and November 27, 2018.

Following the sonde measurements, over 40 water samples were collected for high–resolution (5–10 m) sampling of the water column at the NB and SB locations for analyses of major and trace ions, carbon (TIC and $\delta^{13}\text{C}_{\text{TIC}}$, TOC and $\delta^{13}\text{C}_{\text{TOC}}$) and radiogenic isotopes (^{14}C of TIC and TOC, tritium, ^{129}I). Lake water was sampled at 5–10 m intervals at NB and SB from November 26–28. Waters were collected at a specific depth using an acrylic Niskin 2.5 L water sampling bottle (**Figure 3–3**). Several analyte–specific samples bottles were filled per interval for the range of analytes required. On occasion the Niskin bottle had to be deployed twice to the same interval to collect sufficient volume. Clean lab–quality plastic or glass bottles were used, depending on the analyte(s) (**Table 3–2**). The glass radiocarbon bottles were sterilized by baking at 500°C for 3 hours at the University of Ottawa prior to the field program, and cation sample bottles were acid

cleaned using trace–metal grade nitric acid. In the field, bottles were rinsed 2–3 times with sample before filling.

Lake water samples were collected unfiltered due to the ultra–clear and low–particulate content in the waters (<0.3 ppm total dissolved solids) and sensitivity of the high pH waters to absorption of atmospheric CO₂. Filtering of high pH waters in the field would affect water parameters such as DIC, as the alkaline waters would be aerated during the filtering process.

During the 2017 expedition, Lacelle and Faucher explored the lateral moraines west of the Anuchin glacier. They identified an ice–covered pond previously discovered by Russian investigations during the 1980’s and named *Pond Burevestniksee* (Kaup *et al.*, 1988). Over twenty additional ponds were identified by drone aerial photography during the 2017 expedition. Water samples were collected from *Pond Burevestniksee* and a second smaller pond, named here as *Pond 2*, for comparison to Lake Untersee. The same sampling methods and materials were used for the ponds as for the lake waters.

Samples of the microbial mats and lake bottom sediments were collected for carbon content, stable carbon isotopes and radiocarbon dating. Three (3) cores were collected near the eastern edge of the push–moraine (**Figure 3–2**) by a scuba–diver (Andersen) driving a 44 mm diameter polycarbonate tube into the lake floor. Three cores were collected from an area of approximately 30 m diameter and at depths 18.5 m (Core 1), 13 m (Core 2) and 17 m (Core 3). Sodium polyacrylate, a non–toxic gel forming agent, was added to the waters in the tube to form a gel seal prior to sealing the collection tube with a rubber stopper. The gel seal preservation method is an alternative to freezing, minimizes disturbances to sediment cores, and shows no detectable effects on measurements of total organic carbon or total nitrogen values in sediments (Tomkins *et al.*, 2008).

Sample bottles and cores were stored in coolers at Lake Untersee, and later at the airstrip near Novolazarevskaya Station before transport to the Antarctic Logistics Centre International (ACLI)

facility in Cape Town, South Africa. Samples requiring time sensitive analysis (*i.e.*, TIC, TOC) were flown with the University of Ottawa research team back to Ottawa in December 2017. All other samples were stored at 4°C at the ACLI facility before shipment to the University of Ottawa. All samples were received at the university in February 2018 and stored at 4°C until processing and analyses.

3.3 Laboratory Analyses

3.3.1 Major Ions, Rare Earth Elements and Trace Metals in Waters

Major ions and trace metals concentrations in Lake Untersee and the ponds were measured at the Geochemistry Laboratory at the University of Ottawa. Cation and anion samples were collected in separate bottles in the field, with cation samples acidified using 2 mL of trace metal grade 10% nitric acid (HNO₃). Major cations (Na, Ca, Mg, Ca, Sr, Si) were measured by an Agilent 4200 inductively coupled plasma atomic emission spectrometer (ICP–AES). The reported major cations concentrations are the average of three measurements on the ICP–AES, where the reported uncertainty is the (2σ) standard deviation of the three measurements. Major anions (SO₄, NO₂, NO₃, Cl) were measured by ion–chromatography (IC) using a DIONEX IC system, where the reported analytical uncertainty is the maximum (2σ) standard deviation of three sample duplicates. For trace anions (Br, Cl and I), aliquots of unacidified sample were spiked with NH₃[–] prior to analysis by inductively coupled mass spectrometry (ICP–MS) on an Aligent Triple Quad ICP–MS (Model 8800). Unaltered and undiluted samples were analyzed by ICP–MS on the triple quad ICP–MS for rare earth elements (REE) and trace metal concentrations. Instrumental uncertainty for ICP–MS is reported as the (2σ) standard deviation measured from three measurements, where the reported concentration is the average of the three measurements.

The REE measurements were normalized to chondrite [C1] values from McDonough and Sun (1995) for plotting REE diagrams and calculation of europium anomalies. Plagioclase

preferentially incorporates europium into the crystal lattice during mineral crystallization, which results in elevated europium relative to samarium and gadolinium in many plagioclase-bearing rocks. In some cases, waters may reflect positive europium anomalies due to weathering of europium rich plagioclase. The europium anomaly (Eu/Eu^*) is calculated from Worrall and Pearson (2001) using the [C1] normalized values:

$$\frac{Eu}{Eu^*} = \frac{[Eu_{Normalized}]}{\sqrt{[Sm_{Normalized}] \times [Gd_{Normalized}]}}$$

3.3.2 Carbon Content and $\delta^{13}C$ in Waters

Total organic and inorganic carbon (TOC and TIC) and their stable isotope ratios ($^{13}C/^{12}C$) in lake waters and pond were measured at the Ján Veizer Stable Isotope Laboratory, University Ottawa. The and TOC concentrations and their isotopic ratios ($\delta^{13}C_{TIC}$, $\delta^{13}C_{TOC}$) were measured by a wet TOC analyzer interfaced with a Thermo DeltaPlus XP isotope-ratio mass spectrometer (IRMS), using methods described by St-Jean (2003). The 2σ analytical precision is ± 0.5 ppm for TOC and TIC concentrations and $\pm 0.2\%$ for the isotopes. The detection limit of TIC and TOC analyses is <0.3 ppm.

3.3.3 Radiocarbon Analysis of TIC and TOC in Waters

The TIC and TOC in the waters were measured for ^{14}C to constrain the source and age of carbon in Lake Untersee and the ponds. Due to the low particulate content in the waters (<0.3 g/L TDS) and the sensitivity of high pH waters to absorption of CO_2 , water samples were not filtered in the field. Due to the low particulate content in the oxic waters, the TIC and TOC are assumed to be representative of dissolved inorganic carbon (DIC) and dissolved organic carbon (DOC).

Radiocarbon analysis of waters was performed at the A.E. Lalonde Accelerator Mass Spectrometry (AMS) Laboratory at the University of Ottawa. Methods for sample preparation and extraction of inorganic and organic carbon from waters are based on methods by (Murseli *et al.*, 2019). First,

the appropriate sample volume was selected to target 1 mg C depending on the concentration of [DIC] or [DOC]. For DIC extraction, the sample was added to a baked and pre-cleaned round-bottom borosilicate glass reaction bottle with 85% phosphoric acid. The bottle was heated to 60°C for minimum 1 hour, the headspace was sparged with helium, and the gas was then transferred to a vacuum line for cryogenically purification. The DOC was extracted by wet oxidation (Zhou *et al.*, 2015; Lang *et al.*, 2016; Murseli *et al.*, 2019). Approximately 8 mL of sodium persulfate oxidant solution (400g/L) was added to the DIC sparged water along with 1 mL of 0.5N AgNO₃ catalyst, and the vessel was heated to 95°C for minimum 60 minutes. Once the sample was cooled, the headspace was sparged with helium. The CO₂ from DIC or DOC was cryogenically purified on a vacuum extraction line and sealed in a pre-baked 6 mm OD Pyrex breakseal containing a few grains of silver cobaltous (previously baked at 500°C for two hours) to remove S-bearing species or halogens, and baked overnight at 200°C (Palstra and Meijer, 2014).

The CO₂ extracted from the waters (in breakseals) was converted to elemental carbon in the presence of iron and hydrogen using semi-automated graphitization lines which were designed and built in the AEL-AMS Laboratory. This system is described in extensive detail elsewhere (St-Jean *et al.*, 2017). Radiocarbon analysis was performed on a 3MV tandem accelerator mass spectrometer built by High Voltage Engineering (HVE), described in (Kieser *et al.*, 2015). The fraction modern carbon, F¹⁴C, was calculated according to (Reimer, Brown and Reimer, 2004) as the ratio of the sample ¹⁴C/¹²C ratio to the standard ¹⁴C/¹²C ratio (Ox-II) measured in the same data block. Both ¹⁴C/¹²C ratios were background-corrected and the result is corrected for spectrometer and preparation fractionation using the AMS measured ¹³C/¹²C ratio normalized to δ¹³C (VPDB). Radiocarbon ages are calculated as $-8033\ln(F^{14}C)$ and reported in ¹⁴C yr BP (BP=AD1950) as described by (Stuiver and Polach, 1977) The 2σ errors are <0.013 F¹⁴C or <190 years.

The TOC levels are very low in the oxic lake water samples, and were below the 0.3 ppm detection limit for the methods described in **Section 3.3.2**. Two sets of 2 x 1 L samples were composited to

extract sufficient carbon from the oxic waters for radiocarbon analyses of TOC. Samples NB-10 and NB-40 were composited, as well as NB-60 with NB-120.

3.3.4 Strontium ($^{87}\text{Sr}/^{86}\text{Sr}$) Isotopes in Waters

Strontium isotope sample were prepared at the University of Ottawa, column separations were performed at Carleton University, and isotope ratios were measured at Queen's Facility for Isotope Research (QFIR) at the Queens University (Kingston, Ontario). Strontium isotope ratios ($^{86}\text{Sr}/^{87}\text{Sr}$) were measured in lake and pond waters to investigate potential sources of weathering in the lake water. A valuable component of the Sr-Rb system and isotopic tracing is that Sr derived from any mineral through weathering reactions will retain the same $^{87}\text{Sr}/^{86}\text{Sr}$ as the mineral.

Following trace element analysis and determination of strontium concentrations (**Section 3.3.1**), nine (9) sample aliquots (including 1 replicate) were collected from acidified (HNO_3) 250 mL HDPE sample bottles to target 200 ng for strontium isotope analysis. All sample preparation and handling were performed in a laminar flow hood. Eight 11 mL aliquots were dried down in 15 mL Teflon Savillex screw-cap vials overnight, cooled, and redissolved in 400 μL of 7 N trace-level HNO_3^- acid.

Column separations were performed by Sarina Cotroneo. For ion exchange chemistry, 125 mL of Eichron Sr-resin was added to acid-cleaned (6N HCL) teflon columns and rinsed twice with 800 μL of DI water. The resin was conditioned with 400 μL of 7N HNO_3 , then loaded with the full 400 μL sample. Columns were loaded with 800 μL 7N HNO_3 twice, and the leachate discarded. Separated strontium fraction was collected by loading the column with 800 μL DI water and collecting the leachate in 15 mL Savillex vials. Samples were dried down on a hotplate and redissolved in 3% HNO_3 . A 20 μL aliquot was diluted to 1000 ppb Sr with 3% HNO_3 for isotope ratio measurement by multi-collector ICP-MS (MC-ICP-MS).

The Sr isotope ratios were measured using a ThermoFinnigan Neptune MC-ICP-MS with all ratios normalized to $^{86}\text{Sr}/^{88}\text{Sr}$ ratio of 0.1194 to account for mass fractionation. Results are reported

as the mean of 150 consecutive measurements and corrected to internally normalized NIST standard NBS 987 ($^{88}\text{Sr}/^{86}\text{Sr} = 0.710291$). Multiple standards were measured at the beginning and end of each run, and for 1–2 standards between every 10 samples (NIST 987 average = $0.710290 \pm (2\sigma) 0.000023$). The standard error ($\text{SE} = \text{SD}/\sqrt{n}$ where $n = 150$) ranges from 0.00000671 to 0.0000195. The replicate samples were within the analytical uncertainty.

3.3.5 Sulfur Isotopes of Sulfate and Sulfide in Waters

Barium sulfate (BaSO_4) was precipitated from the oxic lake and pond water samples for stable sulfur isotope ($^{34}\text{S}/^{32}\text{S}$) analysis of total and dissolved sulfate to investigate provenance of the high sulfate concentrations in the lake waters. Sulfate was not in high enough concentrations in the deep anoxic basin waters to extract sufficient BaSO_4 for $\delta^{34}\text{S}_{\text{SO}_4}$ analysis, however sulphide (HS^-) was precipitated out of solution as Zn–sulphide and extracted from the anoxic samples for measurement of $\delta^{34}\text{S}_{\text{Sulphide}}$.

Sulfide precipitate was extracted from anoxic water samples (SB–70, SB–75, SB–80, SB–85 and SB–95) using a filtration method modified from (Zhang, 2019). Sample bottles were pre–treated with zinc acetate to facilitate immediate precipitation of solid Zn–sulphide upon sample collection in the field. In the laboratory, the Zn–sulfide was deposited on a nitrocellulose 0.45 μm filter by filtration using a 50 mL plastic syringe. The filtered waters were set aside for other analyses (*i.e.*, $\delta^{34}\text{S}_{\text{SO}_4}$), and the filter with Zn–sulphide sample was dried in an aluminum tray at 60°C . Using a stainless–steel hole–puncher, 6.2 mm diameter circles were cut from the dried filter and weighed in tin capsule with glucose (~1 mg), silica (~1 mg) and tungsten oxide (~1 mg) as a combustion aid. Samples were combusted and analyzed for sulfur abundance per filter hole–punch on an Isotope Cube (Elementar) elemental analyzer (EA) at the Ján Veizer Stable Isotope Laboratory.

Barium sulfate was extracted from oxic water samples for $\delta^{34}\text{S}_{\text{SO}_4}$ analysis, as well as the anoxic waters with the Zn–sulphide component removed. The general method for BaSO_4 precipitation was obtained from the Ján Veizer Stable Isotope Laboratory. For the oxic waters, sample bottles

were sonicated in original 125 mL collection bottles for 30 min before pouring ~12 mL aliquots into 50 mL Corning™ Falcon 50mL centrifuge tubes. Sample aliquots were acidified to a pH of 3–4 with a 5% HCl solution and treated with ~10 mL 0.25M to precipitate BaSO₄. The solutions were mixed and left overnight for the precipitate to form and settle. The following day the solutions were centrifuged, and the supernatant discarded. The remaining precipitate was rinsed twice with de-ionized water (DI) and dried at 60°C. For the filtered anoxic waters, the remaining sample volume after sulphide removal (~200–250 mL) was acidified to pH 3–4 with 5% HCL, treated with 50 mL of the BaCl₂ solution in a 250 mL borosilicate beaker and left over night. The following day the solutions were transferred to centrifuge tubes, centrifuged, DI rinsed and dried in the same manner as the oxic samples. The dried and rinsed precipitates were weighed (~0.5 mg) into tin capsules with ~1 mg of WO₃, loaded into the Isotope Cube EA to be flash combusted at 1800°C. The released gases were carried by helium through the EA to be cleaned, then separated. The resulting SO₂ gas was carried into the Delta Plus XP isotope ratio mass spectrometer (ThermoFinnigan, Germany) via a conflo IV interface for ³⁴S/³²S determination.

All δ³⁴S results are reported as ‰ vs. VCDT (Vienna Canyon Diablo Troilite) and normalized to internal standards calibrated to international standards. International standards for δ³⁴S_{SO₄} were IAEA–NBS–127 (20.3‰), T–124 (–0.22‰), HSA–1 (24.5‰); δ³⁴S_{Sulphide} standards were IAEA–S1 (–0.3‰), IAEA–S2 (22.7‰), AG–2 (–0.71‰). Analytical uncertainty is ± 0.4‰, based on internal standards T–123 and AG–2.

3.3.6 Nitrogen and Oxygen Isotopes of Nitrate in Waters

Stable nitrogen and oxygen isotopes of nitrate were measured to investigate the provenance of nitrogen and potential role of microbes in nitrogen cycling in the lake waters. Lake and pond water samples were sent to an external laboratory (IT2 Isotope Tracer Technologies, Waterloo, Ontario) for nitrate precipitation and δ¹⁵N_{NO₃} and δ¹⁸O_{NO₃} analysis by isotope ratio mass spectrometry. The

analytical precision for $\delta^{15}\text{N}_{\text{NO}_3}$ and $\delta^{18}\text{O}_{\text{NO}_3}$ is $\pm 0.3\text{‰}$ and $\pm 0.5\text{‰}$, respectively. The detailed IT2 methodology report is included in **Appendix A**.

3.3.7 Tritium (^3H) in Waters

Tritium was measured to determine if Lake Untersee and the ponds receive a detectable input of modern water. Tritium (^3H) sample preparation and measurement were performed by the A.E. Lalonde Tritium and Radiohalide laboratories at the University of Ottawa. Tritium values were measured by electrolytic enrichment and liquid scintillation counting. Samples were pretreated prior to enrichment by de-ionizing the waters using an ion-exchange resin and shaken vigorously for 4 hours. The de-ionized waters were mixed with sodium peroxide (Na_2O_2) and electrolytically enriched in metal cells designed by Taylor (1977). Samples were enriched at ~ 5.8 amps for 5 days, reducing the volume from 250 mL to approximately 13 mL. The enriched samples were then decay counted on a low-background Quantilus liquid scintillation counter. Results are reported in tritium units (TU), where $\text{TU} = 1 \text{ } ^3\text{H} \text{ per } 10^{18} \text{ } ^1\text{H}$, or 0.11919Bq/L . Of the six samples, one sample reported values above the >0.8 TU detection limit, with a 2σ analytical precision of 0.8 TU. The sample was calibrated using the certified ^3H radioactivity standard SRM-4926E.

3.3.8 Radioiodine (^{129}I) in Waters

Radioiodine was measured to investigate if Lake Untersee and ponds were potentially moated in contemporary time (post nuclear bomb testing and fallout) and received atmospherically deposited ^{129}I ; if that is the case, then the lake water likely exchange with atmospheric CO_2 in recent history (post 1963). Radioiodine (^{129}I) sample preparation and measurement were performed by the A.E. Lalonde AMS Laboratory at the University of Ottawa. For ^{129}I analysis, a carrier-addition method was used to extract I during a series of redox transformations. First, samples were acidified with concentrated HNO_3 to $\text{pH} \sim 1$, and 1M NSBSO₃ was added to reduce iodine ($\text{IO}_4^-/\text{IO}_3^-$) to iodide (I^-). The I-carrier (2 mg NaI) was added to a 200 mL sample aliquot, vigorously shaken for 30 minutes and left to stand for 16 hours. The following day, I was extracted into hexane by oxidizing

it from I^- to I_2 using 6M $NaNO_2$. This extraction step was repeated 3 times to ensure maximal collection of iodine. The iodine was then back-extracted into distilled water. The resulting solution was acidified again using HNO_3 and heated to $\sim 90^\circ C$ on a hot plate. Silver nitrate was added to precipitate the I as AgI, which was then dried overnight at $50^\circ C$. Targets were prepared by mixing 1 to 2 mg of AgI with high-purity niobium powder, and pneumatically pressed into a stainless-steel cathode for analysis of ^{129}I using an HVE 3MV Tandetron. Measurements were normalized with respect to the ISO-6II reference material for which $^{129}I/^{127}I = (5.72 \pm 0.08) \times 10^{-12}$, by calibration with the NIST 3230 I and II standard reference material.

Results are reported as the measured $^{129}I/^{127}I$ ratio 10^{-14} (with carrier), the calculated ratio (without carrier) and the calculated sample ^{129}I concentration (atoms/L). The ^{129}I concentrations without carrier are calculated based on total iodine measured by ICP-MS (see **Section 3.3.1**) the exact amount of I-carrier added, and the AMS measured $^{129}I/^{127}I$ ratio. Measured and calculated sample and NaI blank values are reported with 2σ analytical precision in **Appendix B**.

A detection limit of 7.5×10^5 atoms/L was obtained for ^{129}I . The limit of detection value is based on three measurements of the NaI blank carried out during the same run as the lake and pond samples. A hypothetical process blank was calculated from the average $^{129}I/^{127}I$ ratio (1.57×10^{-14}), amount of carrier added, and sample size for the three runs, and assuming 0.001 ppb total I per blank. Background counts are typical of radioiodine analyses (Xing *et al.*, 2015), however exceptionally low background was achieved for this study as demonstrated by the NaI blank.

3.3.9 Microbial Mats Sample Preparation

The three cores of microbial mats from Lake Untersee were extruded from the polycarbonate tube onto a clean surface for sampling microbial mat laminae and underlying lacustrine sediments. The core was divided in half lengthwise using a stainless-steel spatula, and the microbial mat laminae were carefully peeled from the core using stainless steel tweezers (**Figure 3-4**). Each sample consisted of one to several laminae, before laminae transitioned to clay, sand and pebble sized

sediments. Intervals of 0.5–2 cm were collected of the lacustrine sediments underlying the mats. Samples were dried in aluminum trays at 40–55°C. Dried samples were crushed using a mortar and pestle. Weights were measured to three decimal precision before and after drying.

An aliquot of 100–300 mg was weighed and acid-treated to remove inorganic carbon for organic-carbon abundances and stable isotopes of the microbial mats (**Section 3.3.2**). Dried material was acidified by treating with 5 mL of 10% HCl in an open 15 mL falcon tube overnight, discarding the supernatant. The acidification step was repeated once, then samples was rinsed 2–3 times with ~8 mL of de-ionized (DI) water. The acid-treated sample was dried at 40–55°C.

3.3.10 Organic-Carbon Content and $\delta^{13}\text{C}$ of Microbial Mats

Elemental abundance and stable isotope ratios of nitrogen and organic carbon in the microbial mats were measured at the Ján Veizer Stable Isotope Laboratory, University Ottawa. All three cores (Core 1, Core 2 and Core 3) were characterized for organic carbon abundance, $\delta^{13}\text{C}$ and ^{14}C , however only samples from Core 3 were additionally analyzed for total-N abundance and $\delta^{15}\text{N}$. To target the organic-carbon component of the mats, the samples were acidified prior to analysis to remove potential inorganic carbon (see **Section 3.3.9**). For organic-carbon concentrations and isotope ratios ($^{13}\text{C}/^{12}\text{C}$) the acid-treated samples were weighed into tin capsules to target 300 ug of C per capsule, plus 50–100 ug of WO_3 to aid combustion. Nitrogen can be mobilized during the acidification step, therefore for nitrogen concentrations and isotope ratios ($^{15}\text{N}/^{14}\text{N}$), ~10 mg of untreated samples were weighed into tin capsules with 20–30 ug of WO_3 . The weighed samples were analyzed by purge and trap chromatography on an elemental analyzer (Vario Isotope Cube, Elementar) coupled via a ConFlo III interface to an isotope ratio mass spectrometry (IRMS) (Thermo DeltaPlus Advantage). All $\delta^{13}\text{C}$ values are reported as ‰ vs. VPDB using internal standards calibrated to International standards IAEA-CH-6 (-10.4‰), NBS-22 (-29.91‰), USGS-40 (-26.24‰), and USGS-41 (37.76‰). All $\delta^{15}\text{N}$ is reported as ‰ vs. AIR and normalized to internal standards calibrated to international standards IAEA-N1 (+0.4‰), IAEA-N2

(+20.3‰), USGS–40 (–4.52‰), and USGS–41 (+47.57‰). The analytical precision of $\delta^{13}\text{C}$ and $\delta^{15}\text{N}$ is based on an internal standard (C–55), which is not used for calibration and is usually better than 0.2‰. Duplicate sample results were within the analytical uncertainty.

The total organic carbon mass (mg) of each microbial mat laminae sample core was calculated using the dry weight and measured carbon abundance (C_{Org} w.t. %). Since each core was split prior to sampling, the mass is doubled to estimate the total carbon mass per core:

$$\text{Organic Carbon Mass of Core} = 2 * \sum_i^n X_i W_i$$

Where X is the fraction organic carbon in sample i , and W is the dry weight of the sample in mg. Dry and wet weights were measured to three decimal precision (mg) for Cores 1 and Core 2 immediately after sampling, however, there was an error weighing the dry weights of the Core 3 samples. The dry weight of Core 3 was estimated from the wet weights using the average fraction water content from the other two cores (56%):

$$\text{Dry Weight for Core 3 Samples} = \text{Sample Wet Weight} * 0.56$$

The calculated organic carbon mass of each sample are reported with the measured carbon abundance and stable isotopes in **Appendix C**. The carbon content (kg m^{-2}) of the microbial mats was calculated using the average total organic carbon mass of the three cores (Core 1, Core 2 and Core 3) and inner core tube diameter (4.445 cm):

$$\begin{aligned} & \text{Microbial Mats Organic Carbon Content (kg m}^{-2}\text{)} \\ &= \frac{\text{Average Organic Carbon Mass of Core (mg)}}{\Pi(0.5d \text{ (cm)})^2} \times \frac{(100 \text{ cm})^2}{1 \text{ m}^2} \times \frac{1 \text{ kg}}{10^6 \text{ mg}} \end{aligned}$$

3.3.11 Radiocarbon Measurements of Microbial Mats

Sub-samples of microbial mats were submitted to the AMS laboratory for ^{14}C analysis where the samples were pretreated (*e.g.*, freeze-dried, acid-treated to remove inorganic-C) according to

methods described by Crann *et al.* (2017). For organic-C extraction, the pretreated and dried sediments were combusted using a Thermo Flash 1112 elemental analyzer (EA) in CN mode interfaced with an extraction line to remove non-condensable gases and trap the pure CO₂ in a prebaked 6mm Pyrex breakseal (Crann *et al.*, 2017). The trapped sample (in breakseal) was graphitized and measured for ¹⁴C by accelerated mass spectrometry using the same methods described for the lake water samples (**Section 3.3.3**). The fraction modern carbon, F¹⁴C, was calculated according to (Reimer, Brown and Reimer, 2004) as the ratio of the sample ¹⁴C/¹²C ratio to the standard ¹⁴C/¹²C ratio (Ox-II) measured in the same data block. Both ¹⁴C/¹²C ratios were background-corrected and the result is corrected for spectrometer and preparation fractionation using the AMS measured ¹³C/¹²C ratio normalized to δ¹³C (VPDB). Radiocarbon ages are calculated as $-8033\ln(F^{14}C)$ and reported in ¹⁴C yr BP (BP = AD1950) as described by (Stuiver and Polach, 1977).

3.4 Carbon Budget

The carbon budget builds on the water mass balance by Faucher *et al.* (2019), by assigning carbon concentrations to the input and outputs of water in Lake Untersee. Lake Untersee is a closed-basin lake dammed at its northern end by the Anuchin Glacier, as such the water mass balance of the lake can be determined from:

$$\Delta V = P + I_s + I_e + I_g - O_s - O_g$$

Where ΔV is the change in the volume of water, P is the annual precipitation, I_s, I_e and I_g are the inflows of surface water, subaqueous melting of Anuchin terminus ice (originating from the melting of submerged Anuchin glacier at the ice-lake interface) and groundwater (subglacial meltwater or other sources), and O_s and O_g are the outflows of surface and groundwater.

Due to the sealed nature of the lake, precipitation (P) is not contributing to the water mass balance. The outflow of surface water (O_s) is representative of the amount of ice loss by ablation. No

groundwater outflows are known for Lake Untersee. According to these observations, the water mass balance can be simplified to:

$$\Delta V = Ie + Ig - Os$$

The two varieties of carbon species must be considered to assign concentrations to the water inputs and outflows: (1) dissolved inorganic carbon (DIC), and (2) dissolved organic carbon (DOC), where ΔC is the change in carbon in the lake system:

$$\Delta C = Ie_{DIC} + Ie_{DOC} + Ig_{DIC} + Ig_{DOC} - Os_{DIC} - Os_{DOC}$$

The final components that must be considered for the carbon budget is dissolved carbon in the lake-waters, and carbon sequestered in the lake sediments. Carbon resides in the lake water column as DIC (L_{IC}) and DOC (L_{OC}), and is sequestered in the lake sediments through carbonate precipitation (S_{IC}) and/or fixation by photosynthetic bacteria (S_{OC}). Thus, the balanced carbon budget can be summarized as follows:

$$S_{IC} + S_{OC} + L_{IC} + L_{OC} = Ie_{DIC} + Ie_{DOC} + Ig_{DIC} + Ig_{DOC} - Os_{DIC} - Os_{DOC}$$

Chapter 3 Tables

Table 3–1 Field sampling locations

Location ID	Latitude	Longitude
North Basin (NB)	71° 20.212' S	13° 28.533' E
South Basin (SB)	71° 21.365' S	13° 25.612' E
Core sampling dive hole	71° 20.520' S	13° 27.277' E
Pond Burevestniksee	71° 19.176' S	13° 27.300' E
Pond 2	71° 18.974' S	13° 27.504' E

Table 3–2 Water sample summary

Analyte(s)	Bottle Volume	Bottle Material	SAMPLING LOCATION			
			North Basin	South Basin	Pond Bure.	Pond 2
Major cations (ppm), trace metals (ppb), $^{87}\text{Sr}/^{86}\text{Sr}$	250 mL	HDPE	18(<i>1</i>)	14(<i>2</i>)	1	1
Major anions (ppm)	125 mL	HDPE	18(<i>1</i>)	14(<i>2</i>)	1	1
TOC, TIC (ppm)	40 mL	Borosilicate glass, amber	18(<i>1</i>)	14(<i>2</i>)	1	1
$\delta^{13}\text{C}_{\text{TIC}}$, $\delta^{13}\text{C}_{\text{TOC}}$	40 mL	Borosilicate glass, amber	18(<i>1</i>)	14(<i>2</i>)	1	1
$\text{F}^{14}\text{C}_{\text{TIC}}$, $\text{F}^{14}\text{C}_{\text{TOC}}$	1 L	Borosilicate glass, amber	4	6(<i>1</i>)	1	1
$\delta^{34}\text{S}_{\text{SO}_4}$ & $\delta^{34}\text{S}_{\text{Sulphide}}$	125 mL	HDPE	9(<i>2</i>)	11(<i>1</i>)	1	1
^3H , ^{129}I	1 L	HDPE	4	6	1	1
$\delta^{15}\text{N}_{\text{NO}_3}$	1 L	HDPE	4	4	1	1

Italicized number in brackets are field duplicates collected for QA–QC

HDPE = High density polyethylene

Bond Bure. = Pond Burevestniksee

Chapter 3 Figures



Figure 3–1 Lake Untersee field camp (top). Red WeatherHaven and orange Stronghold tents on the lake ice (bottom).

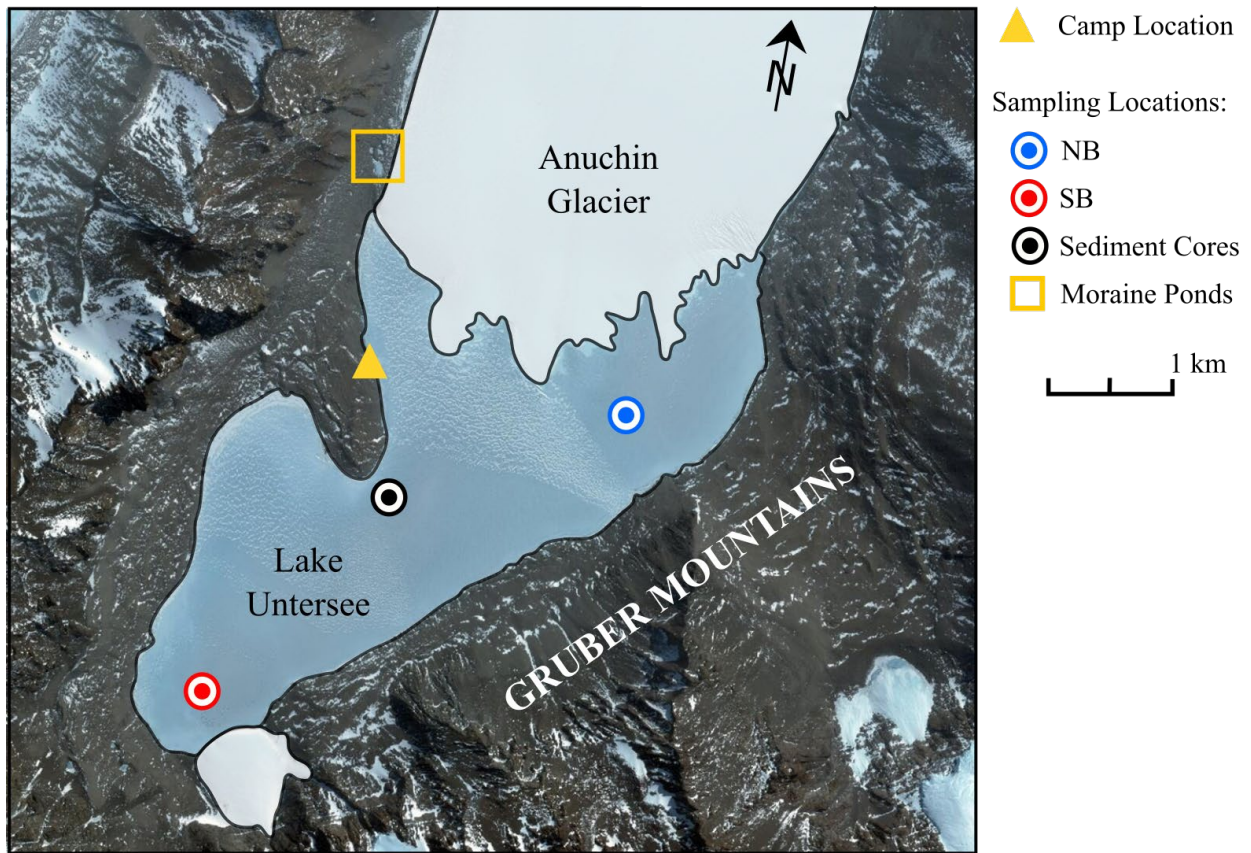


Figure 3–2 Lake water and sediment core sampling sites at Lake Untersee. The image was captured by the Landsat 8 satellite (download via LIMA database from United States Geographical Survey).



Figure 3–3 Niskin water sampling bottle.



Figure 3–4 Split Core 3 prior to sampling (left), and sampling of the microbial mat laminae (right) at the Department of Geography laboratory facilities at the University of Ottawa.

4 Results

Results are divided into four subsections based on location and sample type (water and microbial mats). The first subsection presents results for the *North Basin*, aerobic water column at the deepest section of the basin. The second subsection reports data from waters collected at the *Southern Basin* (SB) sampling location and includes data from the upper oxic layer and the stratified layers in the bottom of the basin. Aqueous chemistry for the two lateral moraine ponds, Pond Burevestniksee and Pond 2 are reported together in the *Moraine Ponds* subsection. Nitrogen and carbon abundance and isotopes for the mats and underlying sediments are reported in the final *Microbial Mats* subsection. All data is available in the appendix.

4.1 North Basin Water Column

The north basin is characterized by well-mixed oxic waters, with analytes generally showing consistent values throughout the water column. This is demonstrated by the 2015–17 sonde data which shows that temperature, pH, specific conductivity, DO and chlorophyll are stable from the just below the ice cover to the bottom at 169 m (**Figure 4–1**). The water is near 0.5°C, alkaline (pH 10.6–11.0), low conductivity (500–545 $\mu\text{S}/\text{cm}$), supersaturated in DO (~150% saturation) with low chlorophyll concentrations (<0.2 g/L). The waters are a Na(Ca)–SO₄ type (**Figure 4–2**) with average SO₄, Na, Ca, Cl and NO₃ concentrations of 166 ppm, 62 ppm, 46 ppm, 39 ppm and 0.50 ppm, respectively (**Table 4–1**). Charge balance error was <2.1% when calculated using measured cations (Al³⁺, Ca²⁺, Mg²⁺, K⁺, and Na⁺), anion concentrations (SO₄²⁻, NO₂⁻, NO₃⁻, F⁻, Br⁻ and I), and [H⁺] and [OH⁻] for an average pH of 10.6.

The TIC in the lake waters was near or at detection (0.3 to 0.4 ppm) of the elemental analyzer. The $\delta^{13}\text{C}_{\text{TIC}}$ values were consistent with depth, ranging from –8.4 to –9.8‰ (average= –9.1‰, 1σ =0.3‰, n=19; **Figure 4–3**). The TOC was below detection for the elemental analyzer (<0.3 ppm) in all samples. However, two 2 L composite samples were analyzed for radiocarbon analysis with 0.27 mg (NB–10 and NB–40) and 0.22 mg (NB–80 and NB–120) of carbon extracted and

graphitized per each 2 L sample. These measurements suggest that TOC is very low in the lake, at approximately 0.1 ppm.

Radiocarbon results for TIC and TOC in the water column is reported as fraction modern carbon ($F^{14}C$) and ages (^{14}C years BP) (**Table 4–2**). Radiocarbon analysis of TIC was successful for three of the four samples (NB–80 was lost during analysis due to sample loading error). The NB–10 and NB–120 samples had very similar $F^{14}C$ values of 0.456 and 0.431, which is equivalent to apparent ages of 6,666 and 6,766 years BP. The third NB–40 sample reported a higher $F^{14}C$ (0.60), however it's possible this sample was subjected to some degree of modern atmospheric contamination, resulting in a younger measured age. To yield sufficient carbon for $F^{14}C$ of the TOC component, two pairs of samples were composited (NB–10 with NB–40, and NB–60 with NB–120); these samples yielded radiocarbon ages of $6,906 \pm 610$ years ($F^{14}C = 0.42 \pm 0.02$) and 4734 ± 606 years BP ($F^{14}C = 0.55 \pm 0.02$).

Tritium (3H) and radioiodine (^{129}I) measurements were below detection in the water column (<0.8 TU and $<7.5 \times 10^5$ atoms L^{-1} , respectively). Decay counts for ^{129}I were higher in the NaI blank than counts for the lake water samples, thus any ^{129}I detected is attributed to instrument background. These 3H and ^{129}I measurements are consistent with $F^{14}C$ that suggest no input of modern water to the lake.

In the water column, the $\delta^{18}O_{NO_3}$ are uniformly close to 16‰ but decrease to 11.2‰ at 120 m depth (Tables 4–4, 4–5). Values for $\delta^{15}N_{NO_3}$ ranged from 5.1‰ to 9.4‰. Measurements of ^{34}S in dissolved sulfate ($\delta^{34}S_{SO_4}$) in the water column ranged from 7.6 to 8.7‰ (**Figure 4–4**). Strontium concentrations were consistently measured at 0.018 ppm. The $^{87}Sr/^{86}Sr$ ratios, reflecting the radiogenic Rb–Sr system, ranged from 0.71804–0.71832 ($n = 6$). The REE data is presented as a chondrite normalized REE diagram in **Figure 4–5** with local anorthosite whole rock data. Whole rock samples (anorthosite, mafic dykes, charnockitoids) and till samples from the Untersee Oasis are enriched in heavy rare earth elements (HREE) relative to the light rare earth elements (LREE; Bormann and Fritzsche, 1995; Ravikant *et al.*, 2011). Chondrite normalized values in the water

column exhibit a flat REE pattern, showing no relative enrichment in LREE or HREE's, and a positive europium anomaly (Eu/Eu^*) of 1.1 to 4.0.

4.2 South Basin Water Column

The upper water column (0–65 m) at the SB sampling location exhibits the same physical characteristics (temperature, specific conductivity, DO) and chemistry (pH, solutes, isotopes) as the NB profile, as water circulate and mixes with the northern basin. Below the sill which separates the two basins, a thermocline, oxycline and chemocline develops with depth. Chemical and physical stratification in the south basin was first reported by Wand *et al.* (1997) and is clear in the SB profiles.

From beneath the ice to ~65 m, the waters are supersaturated with DO (150%), followed by a suboxic zone from 65–80 m, and complete anoxia from 80 m to bottom (**Figure 4–6**). Within the stratified suboxic to anoxic basin, the pH decreases markedly with depth from 10.7 to 6.6 at the bottom. Additionally, temperature, specific conductivity and chlorophyll increases with depth in the layered waters. The sharp chlorophyll spike at 70 m, shown in **Figure 4–6**, is attributed to a visible cloudy mass interpreted as a community of planktonic phototrophic bacteria just above where the waters transition from suboxia to anoxia (D.T. Andersen, personal communication, Sept 4, 2019).

Waters in the upper oxic layer at SB are consistent with major ion concentrations observed in the northern basin, exhibiting a $\text{Na}(\text{Ca})\text{-SO}_4$ type water chemistry. Waters in the suboxic to anoxic layers deviate from the $\text{Na}(\text{Ca})\text{-SO}_4$ facies with increasing depth and anoxia, as sulfate is transformed to HS^- (**Figure 4–2**). The increasing anoxia is also manifested by increases in redox-sensitive metals with depth, such as Fe and Mg. Non-redox-sensitive elements (*e.g.*, Ca, Na and Si) are also higher in the bottom anoxic layer, including REE. The four deepest samples reflect increasing REE concentrations with depth and an enrichment in HREE relative to LREE. Samples

in the upper oxic water show flat chondrite normalized REE patterns similar to waters from NB (**Figure 4–5**).

Concentrations of TIC in the upper water column are low (0.3–0.4 ppm) but increase with depth below 65 m to a maximum of 160 ppm near bottom at 95 m (**Figure 4–7**). The $\delta^{13}\text{C}$ of TIC in the upper oxic layer (0–60 m) range from -6.8‰ to -8.5‰ . Below 65 m depth, ratios are increasingly heavier with depth to a maximum of $+25.6\text{‰}$ $\delta^{13}\text{C}_{\text{TIC}}$ at 95 m (bottom). The TOC was detected in two samples in the upper oxic water column (0.3 ppm and 0.4 ppm) with $\delta^{13}\text{C}_{\text{TOC}}$ of -26.7‰ and -27.5‰ . Concentrations of TOC were consistently above detection starting at 65 m and increased with depth up to 11 ppm; $\delta^{13}\text{C}_{\text{TOC}}$ ranged from -18‰ to -26‰ . While the unique chemistry in the anoxic waters is not the primary focus of this study, these trends are consistent with those described in earlier studies on physical limnology and stable carbon isotopes of the anoxic basin (Wand et al., 1997; Wand et al., 2006).

Radiocarbon analysis of TIC and TOC in the upper oxic water ($F^{14}\text{C} = 0.41\text{--}0.42$) were similar to those in the NB. In the deeper anoxic water (**Table 4–2**). In the deeper anoxic waters, the $F^{14}\text{C}_{\text{TOC}}$ and $F^{14}\text{C}_{\text{TIC}}$ are similar and both lower than the oxic water, ranging from $0.18\text{--}0.26 F^{14}\text{C}$ (apparent age = 10,974 to 13,633 years BP).

Sulfur isotopes of SO_4 in the oxic upper layer fall in a narrow range from 7.7 to 8.5‰ , similar to the NB water column (**Figure 4–4** and **Table 4–5**). Sulfur isotope ratios shift to heavier $\delta^{34}\text{S}_{\text{SO}_4}$ at $80\text{--}85$ m ($10.1\text{--}11.1\text{‰}$). Due to the low SO_4 concentrations in the deepest anoxic waters (90 m to bottom), little or no barium sulfate was precipitated from the solutions for $\delta^{34}\text{S}_{\text{SO}_4}$ analysis (see **Section 3.3.5** for methods). Sulphide was successfully precipitated from sample solution beginning at 80 m depth to bottom (95 m). The sulfur isotopes of sulphide exhibit an increasing trend from -27.9‰ at 80 m to positive values in the deepest waters (1.9 to 5.2‰), correlating with an increase in sulphide and decrease in sulfate with depth as sulfate is reduced to sulphide.

No clear trend is observed in $\delta^{15}\text{N}_{\text{NO}_3}$ and $\delta^{18}\text{O}_{\text{NO}_3}$ from the south basin, however only three samples were analyzed. The shallowest sample (10 m) from the upper oxic layer in the south basin is within the range observed for $\delta^{15}\text{N}_{\text{NO}_3}$ and $\delta^{18}\text{O}_{\text{NO}_3}$ in the northern basin (**Table 4-4**). However, samples at 40 m and 70 m depth show strongly depleted $\delta^{15}\text{N}_{\text{NO}_3}$. The reason for this shift in isotopic composition may be related to the existence of the anoxic zone and the associated cloud of phototropic bacteria above that zone.

4.3 Moraine Ponds

Pond Burevestniksee is ~7 m deep with near zero temperatures throughout the water column (**Figure 4-8**). The pond is alkaline (pH 10.4–11.8), supersaturated in DO (263–281 % sat.) and shows consistent specific conductivity (291–300 μS) with depth. Chlorophyll levels range from 0.27–0.39 $\mu\text{g/l}$. Unlike the oxic water in Lake Untersee, Pond Burevestniksee has a Na(Ca)–Cl geochemical facies with Na, Ca, Cl, SO_4 and NO_3 concentrations of 97 ppm, 83 ppm, 185 ppm, 114 ppm and 8.3 ppm, respectively (**Figure 4-2**). The $\delta^{34}\text{S}_{\text{SO}_4}$ is 11.1‰, while $\delta^{15}\text{N}_{\text{NO}_3}$ and $\delta^{18}\text{O}_{\text{NO}_3}$ are 22.6‰ and 5.5‰, respectively. Concentrations of strontium were 0.22 ppm with an $^{87}\text{Sr}/^{86}\text{Sr}$ ratio of 0.72289 (**Table 4-3**). The chondrite normalized REE patterns for Pond Burevestniksee are similar to the flat pattern observed for the oxic lake waters, with a positive chondrite normalized europium anomaly (Eu/Eu^*) of 7.5 (**Figure 4-5**). The TIC and TOC in the water column is 1.0–1.2 ppm carbon, with $\delta^{13}\text{C}_{\text{TIC}}$ of –3.7‰, and $\delta^{13}\text{C}_{\text{TOC}}$ of –7.8‰ (**Figure 4-3** and **Figure 4-7**). Radiocarbon analyses of TIC and TOC yielded modern ages of 198 ± 50 years BP (0.98 F^{14}C) for TIC, 697 ± 90 years BP (0.92 F^{14}C) for TOC. While no ^{129}I was detected in Lake Untersee ($<7.45 \times 10^5$ atoms L^{-1}), 9.6×10^6 atoms L^{-1} ($\pm 0.3 \times 10^6$) were measured in Pond Burevestniksee (**Table 4-7**).

Pond 2 is smaller and shallower (~2 m) than Pond Burevestniksee, is alkaline (pH 10.4–10.6), supersaturated in DO (263–284 % sat.), and has low chlorophyll levels (0.18 $\mu\text{g/l}$). The upper water (0–1 m) have temperature near 0°C which transition to slightly warmer water in the bottom

layer (1–2.2 m), up to 1.3°C (**Figure 4–8**). Specific conductivity is 850–900 $\mu\text{S}/\text{cm}$ and shows an increase at the bottom potentially from disturbing the sediments with the sonde. Pond 2 is distinguished from Lake Untersee and Pond Burevestniksee by lower SO_4 concentrations (43 ppm) and is a mixed water type of $\text{Ca}(\text{Na})\text{--SO}_4(\text{Cl})$ with Na, Ca, Cl, SO_4 and NO_3 concentrations of 31 ppm, 24 ppm, 32 ppm, 43 ppm and 0.19 ppm (**Table 4–1**). The $\delta^{34}\text{S}_{\text{SO}_4}$ and $\delta^{18}\text{O}_{\text{NO}_3}$ of the water yielded values of 11.4‰ and 17.0‰, respectively; Pond 2 waters had low nitrate concentrations (0.19 ppm) and did not have sufficient nitrate for both $\delta^{18}\text{O}_{\text{NO}_3}$ and $\delta^{15}\text{N}_{\text{NO}_3}$ analysis. The TIC and TOC in the water column is 1.0–1.4 ppm carbon with $\delta^{13}\text{C}_{\text{TIC}}$ and $\delta^{13}\text{C}_{\text{TOC}}$ values of -3.4‰ and -7.6‰ , respectively (**Figure 4–3** and **Figure 4–7**). Radiocarbon analyses of TIC report modern ages of 43 ± 46 years BP ($0.98 \text{ F}^{14}\text{C}$) for TIC. Unfortunately, $^{14}\text{C}_{\text{TOC}}$ was not analyzed for Pond 2 since the sample was lost during the graphitization step during analysis. While ^3H was not detected in Pond 2, ^{129}I was detected at concentrations of 2.29×10^6 atoms L^{-1} (**Table 4–7**).

4.4 Microbial Mats

The organic carbon content and their stable carbon isotopes were measured in 1–10 mm intervals from Core 1 (17.5 cm length), Core 2 (14.5 cm length) and Core 3 (14.3 cm length). Select intervals were radiocarbon dated in Core 2 and Core 3. Sample from Core 3 were also measured for total-N abundance and $\delta^{15}\text{N}$. The majority of the core material consists of the laminated microbial mats that sharply transition to clay to sand sized sediments at the base of the core.

Total N abundance measured in the laminated mats in Core 3 range from 0.1–0.7 w.t.% with $\delta^{15}\text{N}$ ranging from 12.0–28.8‰. Abundances and $\delta^{15}\text{N}$ exhibit a general trend towards lower abundances and heavier isotopic composition with depth (**Figure 4–9**). The organic C abundance of the laminated microbial mats ranges from 1.0–2.8 w.t. % (average = 1.6 w.t. %) in Core 1, 1.2–3.7 w.t. % (average = 2.1 w.t. %) in Core 2, and 0.73–5.8 w.t. % (average = 2.3 w.t. %) in Core 3 (**Table 4–8**). The average organic C abundances of the microbial mats are similar to the 2.5 w.t. % reported by Andersen *et al.*, (2011) from a site near the southern edge of the push moraine. The

total sum of organic C mass from the microbial mats was used to calculate organic carbon content in the mats (kg m^{-2}) in each core. The sum of organic-carbon from the microbial mats samples ranged from 0.996–1.537 g per core (average = 1.329 g). The estimated organic C content of the microbial mats is thus 8.57 kg m^{-2} (**Table 4–9**).

The $\delta^{13}\text{C}_{\text{Org}}$ of the microbial mats range from -18.1 to -6.9 ‰. The top laminae report a $\delta^{13}\text{C}_{\text{Org}}$ value of -11.5 ‰ (Core 1), -9.2 ‰ (Core 2) and -9.2 ‰ (Core 3), similar to the average $\delta^{13}\text{C}_{\text{TIC}}$ measured in the oxic lake waters (9.1 ‰). Some variability is observed in the stable isotope data, but there is a general trend of decreasing $\delta^{13}\text{C}$ values with depth, especially following the transition from microbial mats to the underlying sediments at 11 cm (Core 1), 10 cm (Core 2) and 6 cm (Core 3) (**Figure 4–10**).

Several mat laminae from Core 2 and Core 3 were radiocarbon dated, and the top laminae report radiocarbon ages of $10,052 \pm 56$ years BP (Core 2) and $9,524 \pm 48$ years BP (Core 3) (**Table 4–10**). These apparent age of the top mat layer are comparable to radiocarbon ages reported by Andersen *et al.* (2011) from surficial mats from Lake Untersee ($10,050$ years BP) but all younger than what was reported by Schwab (1998), $11,290$ years BP (**Figure 4–11**). The deepest laminations of microbial mats were dated at $12,031 \pm 68$ years (Core 2) and $13,049 \pm 90$ years (Core 3).

The organic C abundance in the underlying sediments is much lower than in the microbial mats. Organic carbon is ≤ 1 w.t.% (0.01 – 0.96 %) in the sediments, with the exception of the transition immediately below the mats which may contain fragments of the overlying mats. The $\delta^{13}\text{C}_{\text{Org}}$ values in the sediments ranged from -18.4 to -14.5 ‰, and averaged -15.0 ‰ (Core 1), -15.6 ‰ (Core 2), and -14.5 ‰ (Core 3). Generally, $\delta^{13}\text{C}$ is lower in the sediments than the overlying microbial mats (**Figure 4–10**). Total nitrogen abundances in the sediments range from Core 3 range from 0.05 – 0.12 w.t.% and have an isotopic composition of -14.5 to -18.0 ‰ $\delta^{15}\text{N}$ (**Figure 4–9**). The apparent age of the organic C in the sediments are considerably older ($19,370$ years BP) than those measured in the mats.

Chapter 4 Tables

Table 4–1 Major ion summary

Parameter	Unit	NB Oxidic Waters Average (n=27)	SB Oxidic Waters Average (n=6)*	SB Anoxic Waters Range (n=9)**	Pond Bure.	Pond 2
SO ₄	ppm	166	166	3.82–167	114	43.1
Na	ppm	61.2	64.2	60.9–127	96.7	24.2
Ca	ppm	45.7	47.8	45.1–123	82.5	31.2
Cl	ppm	38.6	38.6	38.5–72.4	185	32.4
K	ppm	3.48	3.60	3.37–11.1	11.7	4.43
Si	ppm	2.25	2.24	2.26–11.7	2.34	2.35
NO ₃	ppm	0.499	0.504	0.0004–0.495	8.32	0.187
NO ₂	ppm	0.191	0.199	0.204–10.0	0.378	0.551
Mg	ppm	0.149	0.132	0.110–18.2	2.25	0.186
Al	ppm	0.079	0.080	0.004–0.079	0.0658	0.142
Sr	ppm	0.018	0.018	0.018–0.079	0.219	0.055

*SB samples above 60 m depth

**SB samples at and below 60 m depth

Pond Bure. = Pond Burevestniksee

Table 4–2 Radiocarbon results of lake and pond waters

Sample ID	Depth (m)	Total Inorganic Carbon				Total Organic Carbon			
		F ¹⁴ C	± 2σ	¹⁴ C yr BP	± 2σ	F ¹⁴ C	± 2σ	¹⁴ C yr BP	± 2σ
North Basin									
NB–10	10	0.4361	0.0054	6666	98	*0.4233	*0.0161	*6906	*610
NB–40	40	0.5989	0.0132	4119	176				
NB–80	80	<i>FA</i>	<i>FA</i>	<i>FA</i>	<i>FA</i>	*0.5547	*0.0209	*4734	*610
NB–120	120	0.4307	0.0040	6766	76				
South Basin									
SB–10	10	0.4156	0.0046	7054	88	<i>NA</i>	<i>NA</i>	<i>NA</i>	<i>NA</i>
SB–40	40	0.4143	0.0038	7079	76	<i>NA</i>	<i>NA</i>	<i>NA</i>	<i>NA</i>
SB–70	70	0.2603	0.0028	10811	86	0.2551	0.0057	109`74	358
SB–80	80	0.2542	0.0028	11002	86	0.2264	0.0033	11934	230
SB–80 Duplicate	80	0.2472	0.0026	11228	84	<i>NA</i>	<i>NA</i>	<i>NA</i>	<i>NA</i>
SB–85	85	0.2432	0.0030	11358	96	0.1832	0.0037	13633	324
SB–90	90	0.2427	0.0032	11374	102	<i>NA</i>	<i>NA</i>	<i>NA</i>	<i>NA</i>
Moraine Ponds									
Pond Burevestniksee	2	0.9757	0.006	198	50	0.9169	0.0052	697	90
P2 Pond	1	0.9947	0.0058	43	46	<i>FA</i>	<i>FA</i>	<i>FA</i>	<i>FA</i>

*Composite sample

F¹⁴C = fraction modern carbon

¹⁴C yr BP = years before 1950

FA = failed analysis

NA = no analysis

Table 4–3 Strontium isotopes in lake and pond waters

Sample ID	Depth (m)	⁸⁷Sr/⁸⁶Sr	± SE
North Basin			
NB–10	10	0.718311	0.000007
NB–80	80	0.718296	0.000009
NB–155	155	0.718294	0.000007
South Basin			
SB–10	10	0.718319	0.000007
SB–80	80	0.718218	0.000007
SB–95	95	0.718041	0.000008
Moraine Ponds			
Pond Burevestniksee	1	0.722894	0.000019
Pond Burevestniksee Replicate	1	0.722914	0.000007
Pond 2	1	0.722011	0.000007

Standard error (SE) = standard deviation/sqrt(n) where n=150

Table 4–4 Nitrogen and oxygen isotopes of nitrate in pond and lake waters

Sample ID	Depth (m)	NO ₃ (ppm)	δ ¹⁵ N _{NO₃} (‰) AIR	δ ¹⁸ O _{NO₃} (‰) VSMOW
North Basin				
NB–10	10	0.503	5.1	16.8
NB–40	40	0.507	9.4	16.2
NB–40R	40		9.5	15.8
NB–80	80	0.504	7.3	18.7
NB–120	120	0.509	9.2	11.2
NB–120R	120		9.0	
South Basin				
SB–10	10	0.509	8.8	18.3
SB–40	40	0.491	11.9	–12.1
SB–70	70	0.107	9.8	–2.0
Lateral Moraine Ponds				
Pond Burevestniksee	2	8.32	22.6	5.5
Pond BurevestnikseeR	2		22.3	
P2 Pond	1	0.187	<i>NEP</i>	17.0

NEP = Not enough precipitate

¹⁸O/¹⁶O results are normalized to Vienna Standard Mean Ocean Water (VSMOW) for reporting δ¹⁸O

¹⁵N/¹⁴N results are normalized to air for reporting δ¹⁵N

Analytical precision (2σ STD) of δ¹⁸O is ±1‰ and δ¹⁵N is ±0.6‰

Table 4–5 Sulfur isotopes of sulfate and sulphide in pond and lake waters

Sample ID	Depth (m)	$\delta^{34}\text{S}_{\text{SO}_4}$ VCDT (‰)	$\delta^{34}\text{S}_{\text{Sulfide}}$ VCDT (‰)
North Basin			
NB–5	5	7.61	
NB–20	20	8.65	
NB–40	40	8.52	
NB–40 Duplicate	40	8.51	
NB–60	60	8.68	
NB–80	80	8.74	
NB–120	120	8.74	
NB–120 Duplicate	120	8.35	
NB–140	140	8.61	
NB–155	155	8.56	
South Basin			
SB–5	5	8.44	
SB–20	20	8.42	
SB–40	40	8.45	
SB–60	60	8.41	
SB–70	70	7.69	<i>NP</i>
SB–75	75	8.14	<i>NP</i>
SB–80	80	10.56	–27.9
SB–80 Duplicate	80	11.09	–33.2
SB–85	85	10.09	–7.4
SB–85 Replicate	85	<i>NP</i>	–6.7
SB–90	90	<i>NP</i>	1.9
SB–95	90	<i>NP</i>	5.2
Lateral Moraine Ponds			
Pond Burevestniksee	2	11.11	
Pond2	1	11.42	
Pond2 Replicate	1	11.49	

NP = no/insufficient precipitate

$^{34}\text{S}/^{32}\text{S}$ is normalized to Vienna–Canyon Diablo Troilite (VCTB) for reporting $\delta^{34}\text{S}$

Analytical precision (2σ) of $\delta^{34}\text{S}$ is $\pm 0.2\text{‰}$

Table 4-6 Tritium (³H) results for lake and pond water samples

Sample ID	Depth (m)	³ H (TU)	± 2σ
NB-10	10	<0.8	
NB-40	80	<0.8	
NB-120	120	<0.8	
Pond Burevestniksee	1	1.5	0.8
P2 Pond	1	<0.8	

TU = Tritium Units where 1TU = 0.11919 Bq/L

Table 4-7 Radioiodine results for lake and pond water samples

Sample ID	Total Iodine Concentration (ppb)	Measured ¹²⁹ I/ ¹²⁷ I Ratio (x10 ⁻¹⁴)*		Calculated ¹²⁹ I (atoms/g)**	
		Ratio	Error	Concentration	Error
NaI Blank average (n=3)	0.0005	1.57	0.05	7.45E+05	2.37E+01
NB-40	27.3	0.9	0.11	<750	
NB-120	26	0.8	0.10	<750	
SB-70	30.7	1	0.11	<750	
SB-95	173	1.1	0.13	<750	
Pond Burevestniksee	13.6	18.6	0.52	9.62E+06	2.68E+05
P2 Pond	2.3	4.6	0.22	2.29E+06	1.10E+05

¹* ¹²⁹I/¹²⁷I Measured includes both sample and carrier added

²**Calculated value without carrier

Table 4–8 Lake core organic carbon abundance and stable isotope summary

Statistics	Core 1		Core 2		Core 3	
	wt %	$\delta^{13}\text{C}_{\text{org}}$ VPBD (‰)	wt%	$\delta^{13}\text{C}_{\text{org}}$ VPBD (‰)	wt%	$\delta^{13}\text{C}_{\text{org}}$ VPBD (‰)
Microbial Mats						
Min	1.00	-18.1	1.21	-18.3	0.73	-13.6
Max	2.80	-9.0	3.65	-8.1	5.84	-6.9
Average	1.64	-12.1	2.12	-10.3	2.28	-9.8
n	37	37	30	30	39	39
Sediments						
Min	0.14	-17.2	0.14	-18.4	0.01	-18.0
Max	0.96	-15.0	1.32	-15.6	0.96	-14.5
Average	0.42	-16.1	0.63	-16.6	0.59	-15.9
n	5	5	5	5	7	7

Table 4–9 Core microbial mat organic carbon mass and content

Core	Total Organic Carbon Mass (g)	Calculated Carbon Content (kg m ⁻²)
Core 1	1.455	0.938
Core 2	0.996	0.642
Core 3	1.537	0.991
<i>Average</i>	<i>1.329</i>	<i>0.857</i>

Table 4–10 Radiocarbon results of the organic carbon component from Core 1 and Core 3

Sample ID	Depth (mm)	Sample Material	¹⁴ C yr BP	± 2σ	F ¹⁴ C	± 2σ
Core 2						
C2–1	1	Microbial Mats	10052	56	0.2861	0.0020
C2–5	9	Microbial Mats	10882	70	0.2580	0.0022
C2–8	14	Microbial Mats	9510	64	0.3061	0.0024
C2–9	16	Microbial Mats	11268	104	0.2459	0.0032
C2–12	22	Microbial Mats	11113	58	0.2507	0.0018
C2–19	37	Microbial Mats	11481	60	0.2395	0.0018
C2–24	52	Microbial Mats	16567	80	0.1271	0.0012
C2–29	66	Microbial Mats	13040	76	0.1973	0.0018
C2–30	70	Microbial Mats	12031	68	0.2237	0.0018
Core 3						
C3–1	1	Microbial Mats	9524	48	0.3055	0.0018
C3–2	3	Microbial Mats	10945	82	0.2560	0.0026
C3–8	11	Microbial Mats	9791	58	0.2293	0.0016
C3–10	14	Microbial Mats	9419	76	0.3096	0.0030
C3–13	17	Microbial Mats	11832	58	0.2293	0.0016
C3–20	30	Microbial Mats	11285	80	0.2454	0.0024
C3–30	42	Microbial Mats	12917	78	0.2003	0.0020
C3–40	53	Microbial Mats	13049	90	0.1970	0.0022
C3–49	81	Sediments	19370	156	0.0009	0.0018

F¹⁴C = fraction modern carbon

¹⁴C yr BP = radiocarbon age, years before 1950

Chapter 4 Figures

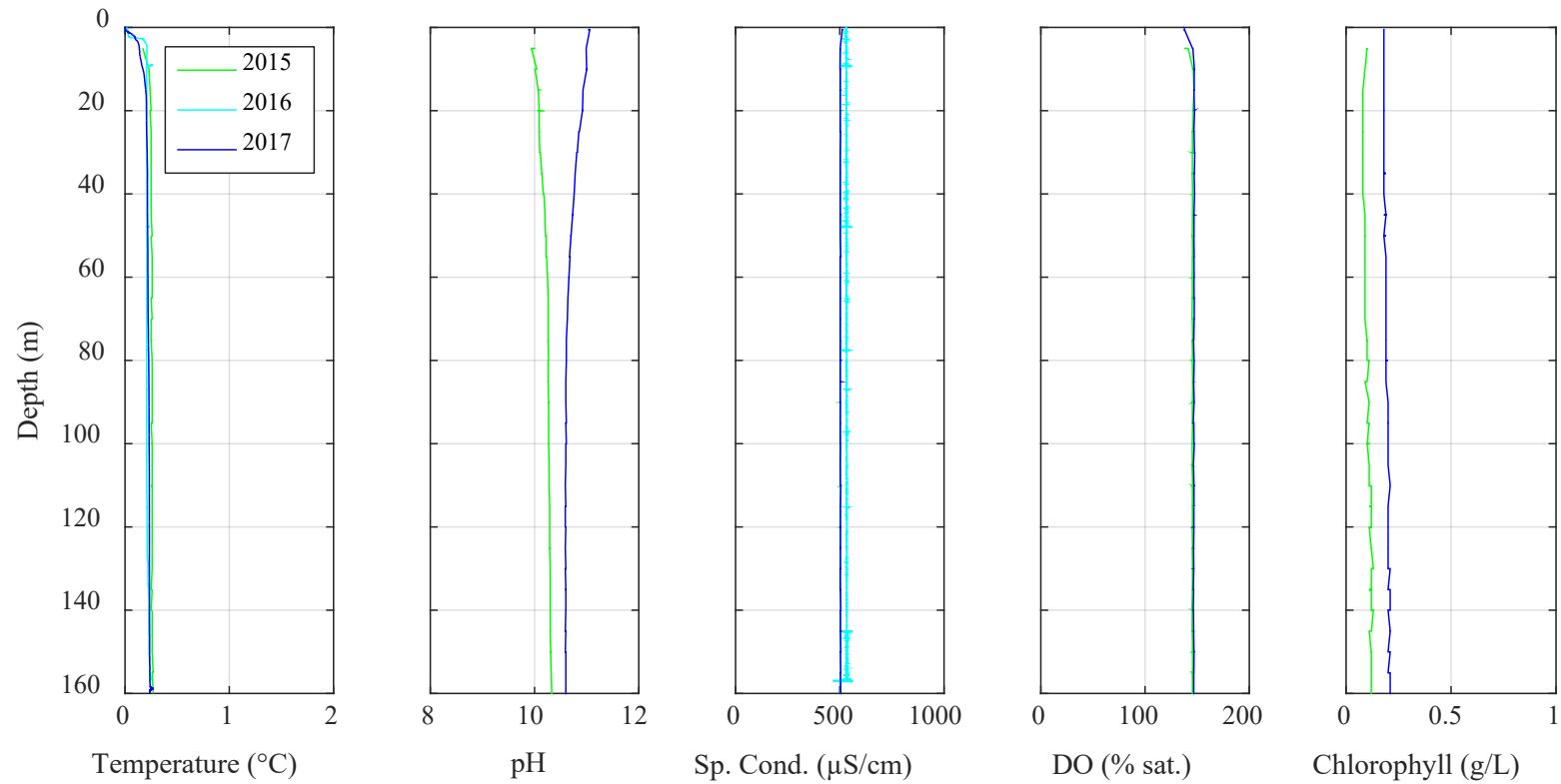


Figure 4–1 Temperature, pH, specific conductivity (Sp. Cond.), dissolved oxygen (DO) and chlorophyll profiles of the northern basin at location NB. Data from previous expeditions (2015, 2016) were collected by Benoit Faucher.

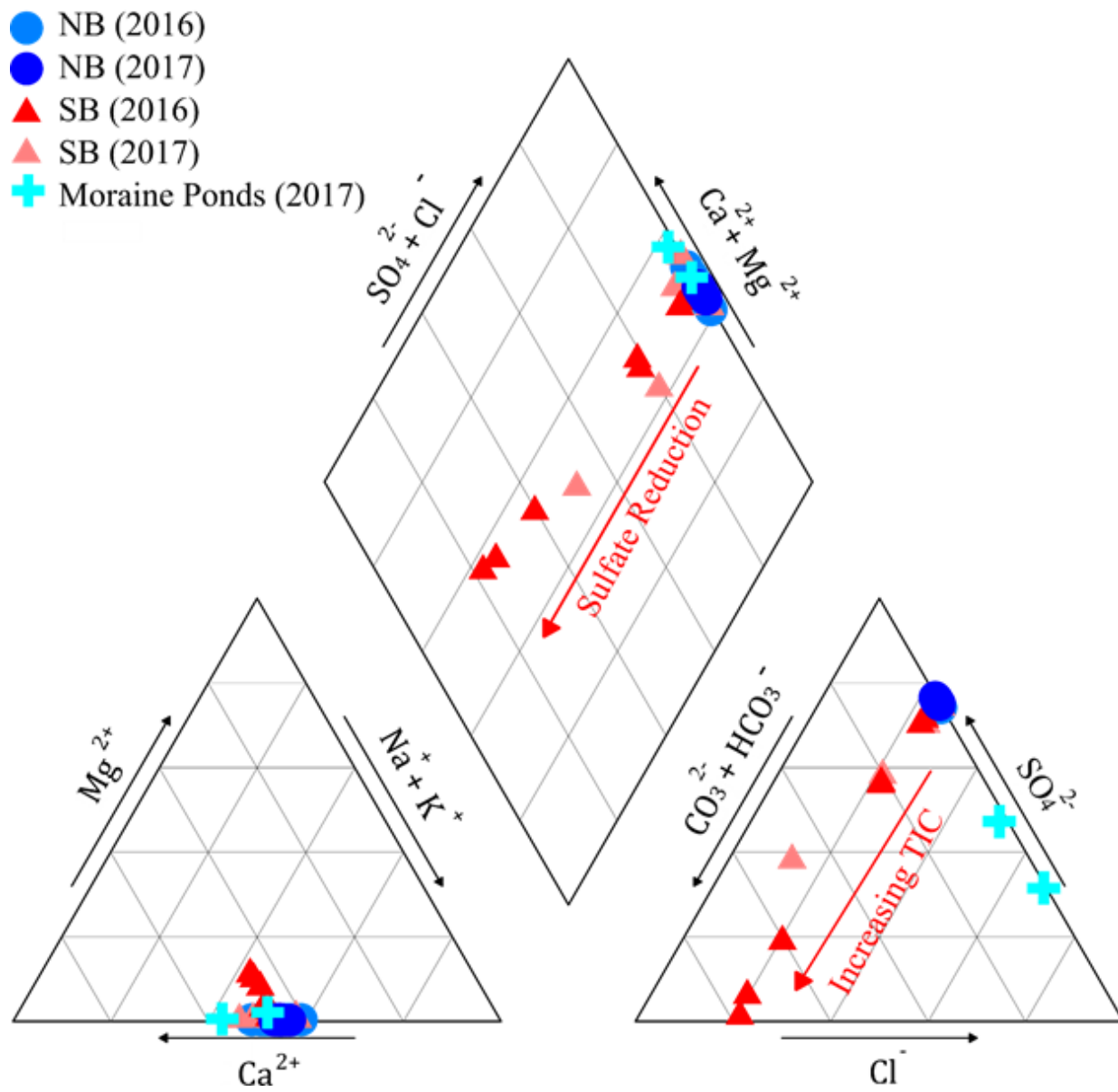


Figure 4-2 Piper plot of lake and moraine pond major ion data.

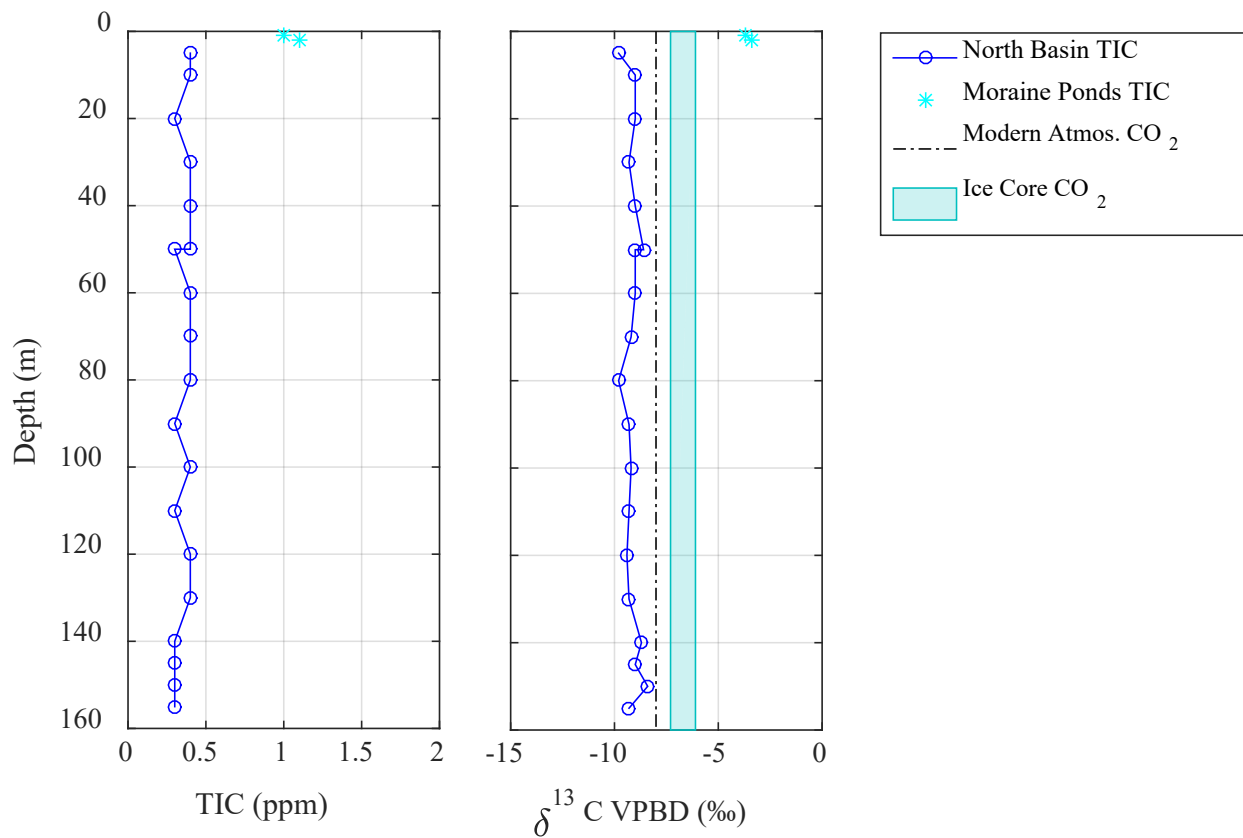


Figure 4–3 North Basin (NB) profiles of total inorganic carbon (TIC) concentrations (left) and $\delta^{13}\text{C}_{\text{TIC}}$ VPBD (right). Stable carbon values for modern atmospheric CO₂ from (Clark, 2015a), and East Antarctica ice core CO₂ compilation data from Eggleston et al. (2016).

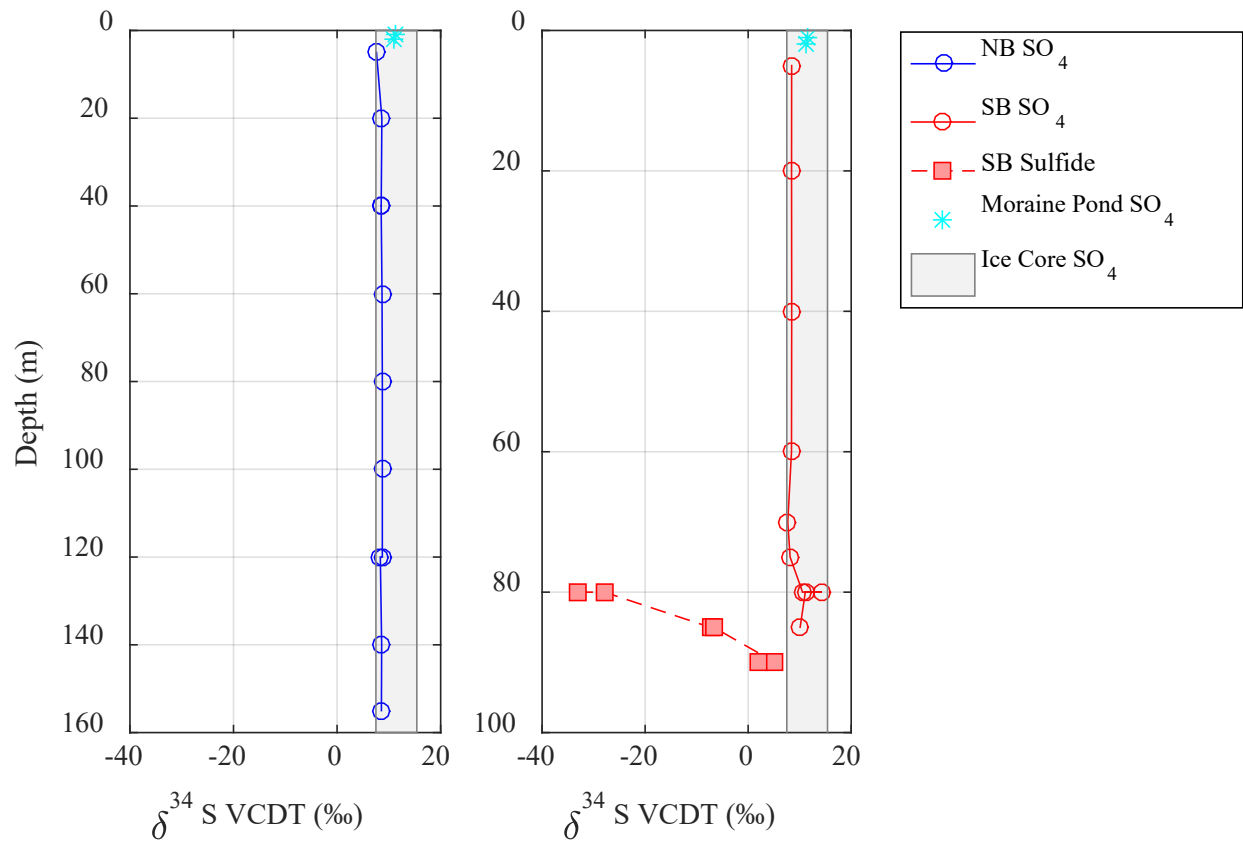


Figure 4-4 North basin (NB) and south basin (SB) profiles of sulfur isotope ratios of sulfate (solid lines) and sulfide (dashed line) with lateral moraine pond $\delta^{34}\text{S}_{\text{SO}_4}$ results (cyan asterisk). Grey shaded area is the range of $\delta^{34}\text{S}_{\text{SO}_4}$ (total) and $\delta^{34}\text{S}_{\text{SO}_4}$ (no sea salt) values published for Dome C and Vostok ice cores spanning ages from 2.5–130 kya (Alexander *et al.*, 2003).

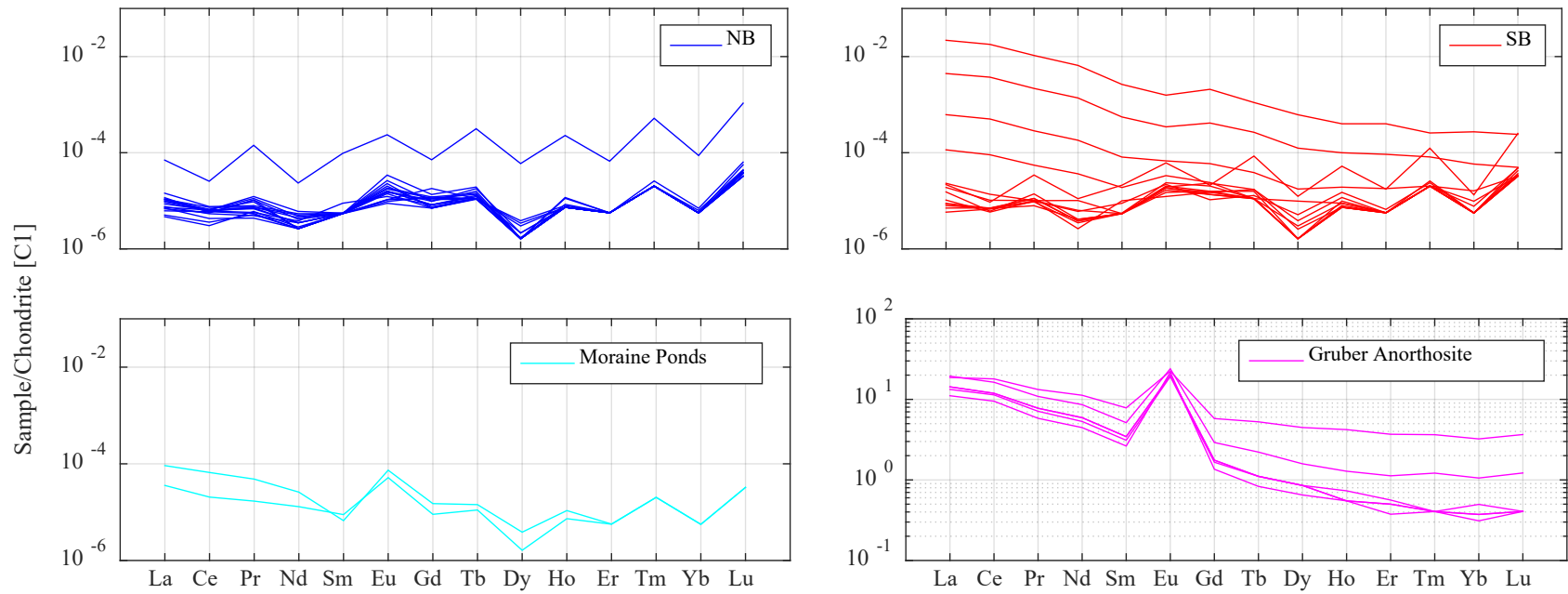


Figure 4–5 Chondrite normalized (C1, after McDonough and Sun, 1995) REE pattern for lake waters (NB, SB) and lateral moraine pond waters (Moraine Ponds). Gruber Anorthosite whole rock sample REE data from Ravikant et al. (2011). Note y-axis change for water results versus whole rock anorthosite data.

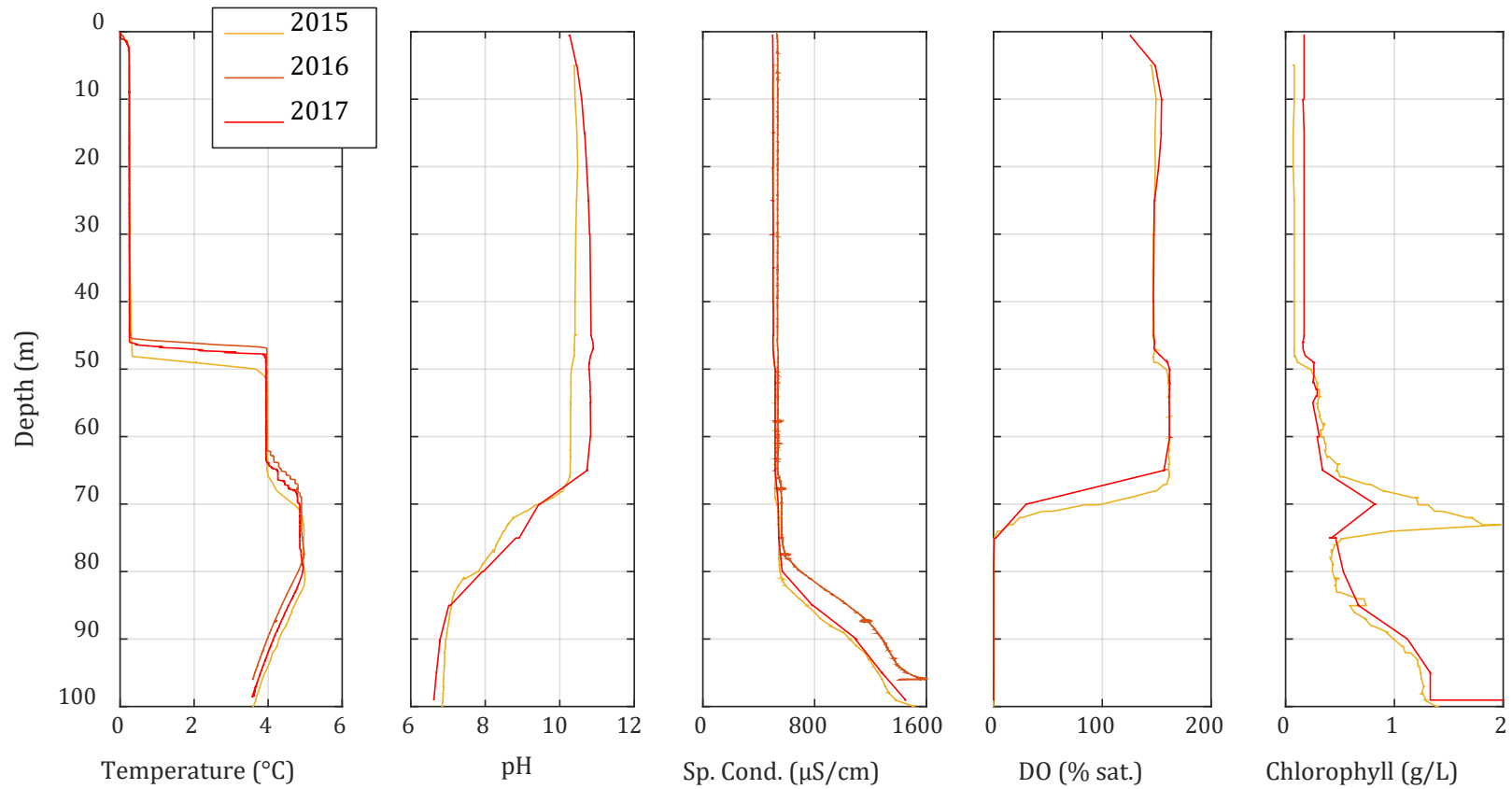


Figure 4–6 Temperature, pH, specific conductivity (Sp. Cond.), dissolved oxygen (DO) and chlorophyll profiles of the southern basin (SB). Data from previous expeditions (2015, 2016) were collected by Benoit Faucher.

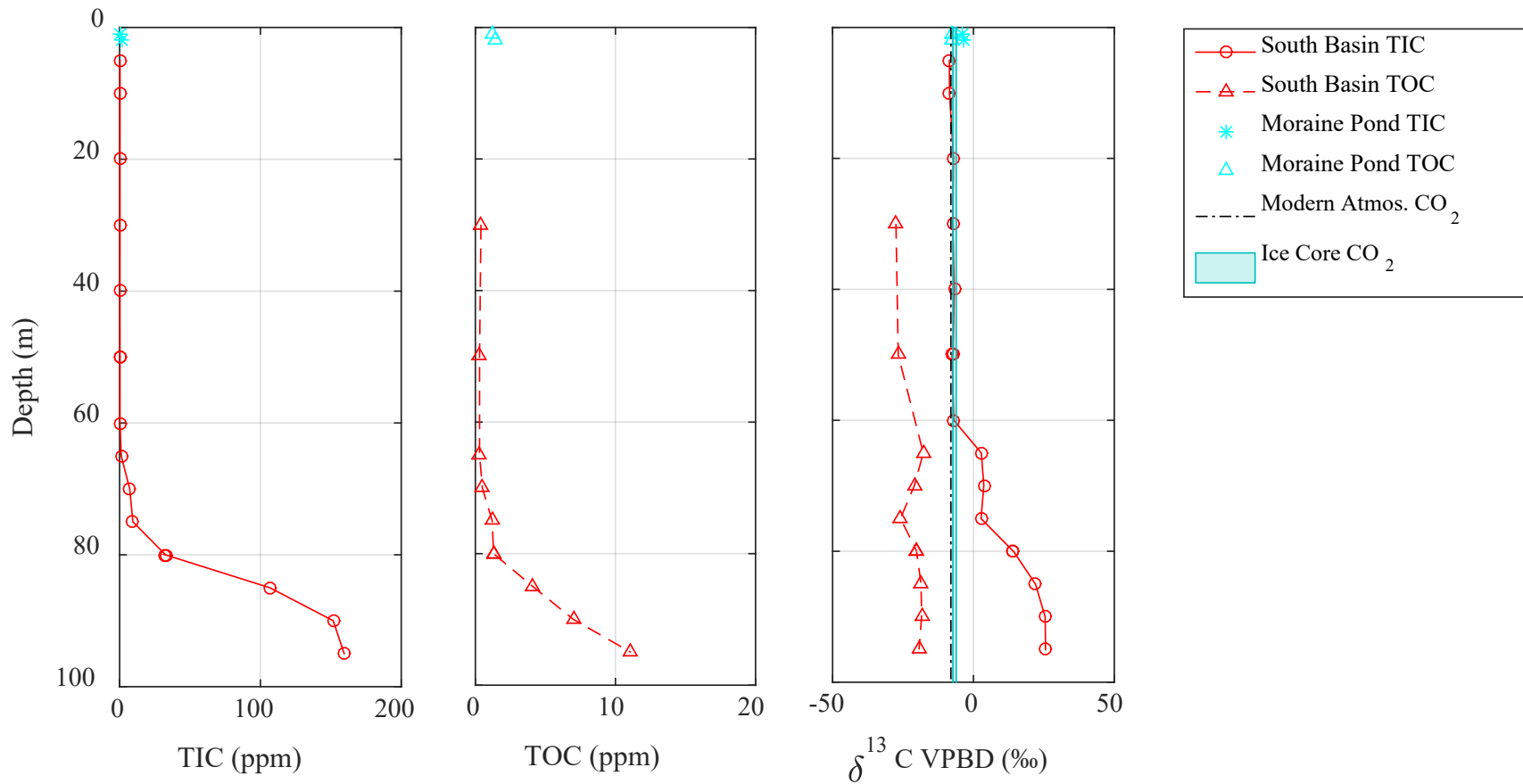


Figure 4–7 South Basin (SB) total inorganic carbon (TIC) concentrations (left), total organic carbon (TIC) concentrations and $\delta^{13}\text{C}_{\text{TIC}}$ and $\delta^{13}\text{C}_{\text{TOC}}$ (right). Stable carbon values for modern atmospheric CO_2 from Clark, (2015a), East Antarctica ice core $\delta^{13}\text{C}-\text{CO}_{2(\text{g})}$ compilation data from Eggleston et al. (2016).

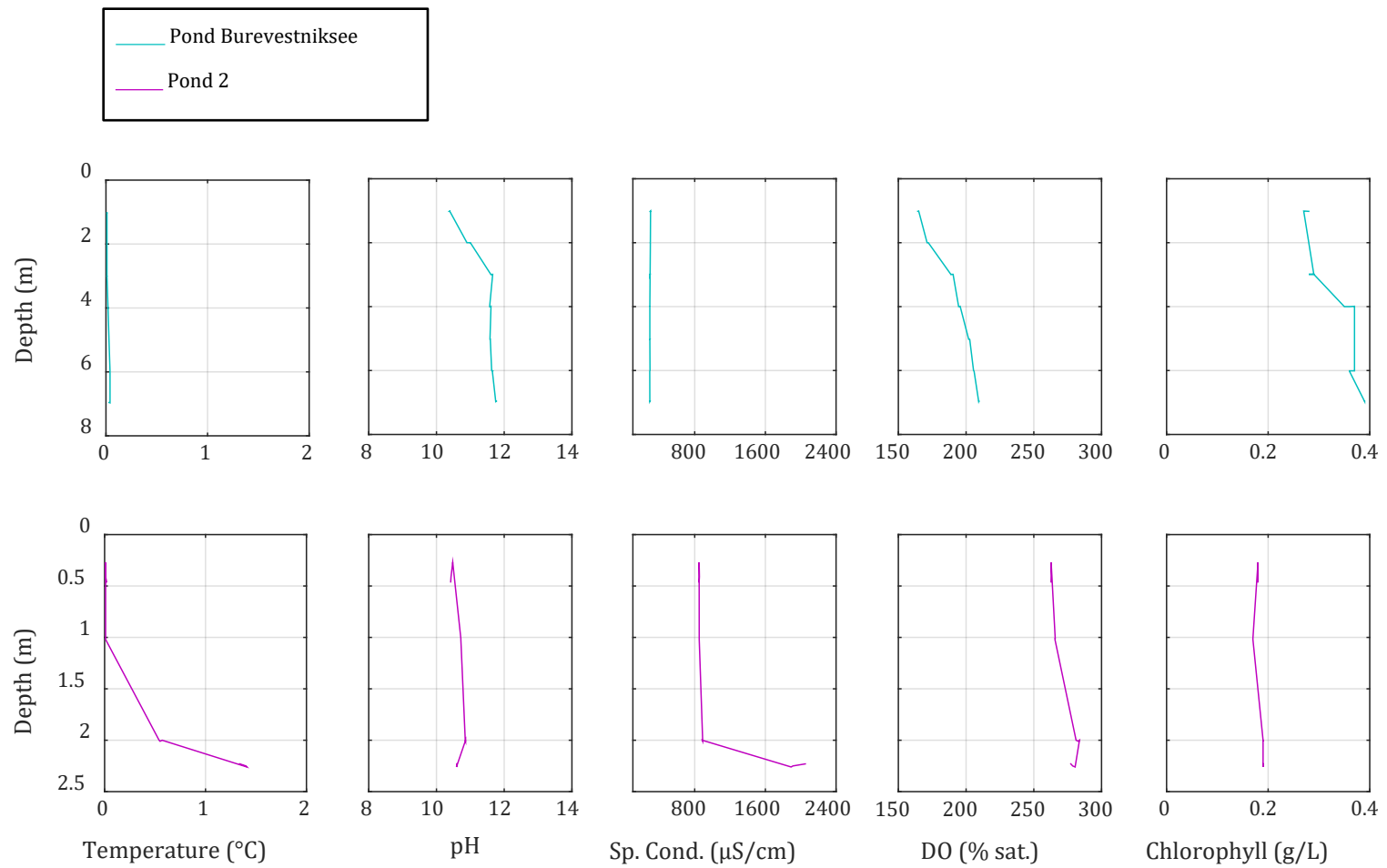


Figure 4–8 Temperature, pH, specific conductivity (Sp. Cond.), dissolved oxygen (DO) and chlorophyll profiles of the lateral moraine ponds.

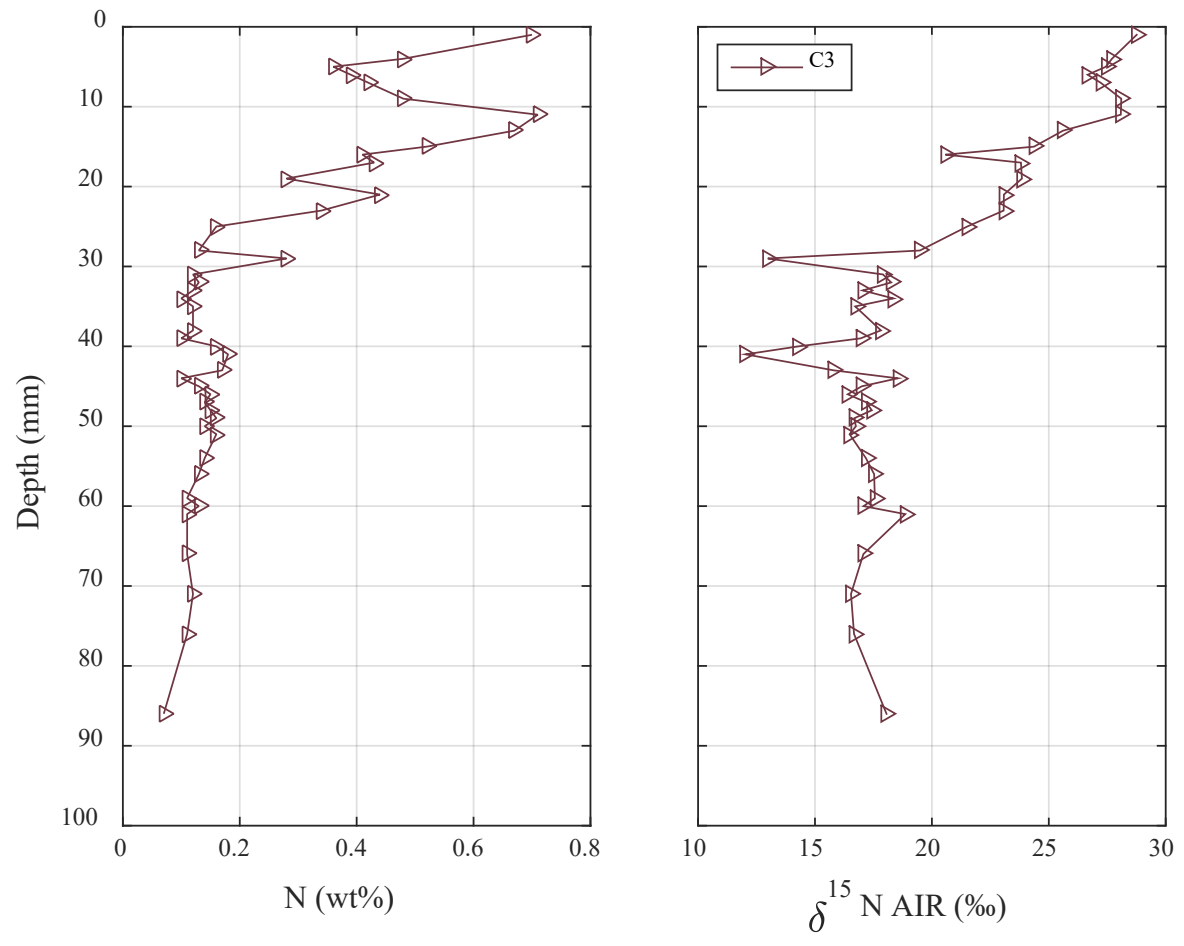


Figure 4-9 Core 3 microbial mat nitrogen abundance and isotope ratios. The ¹⁵N/¹⁴N ratios are normalized to air and reported as δ¹⁵N.

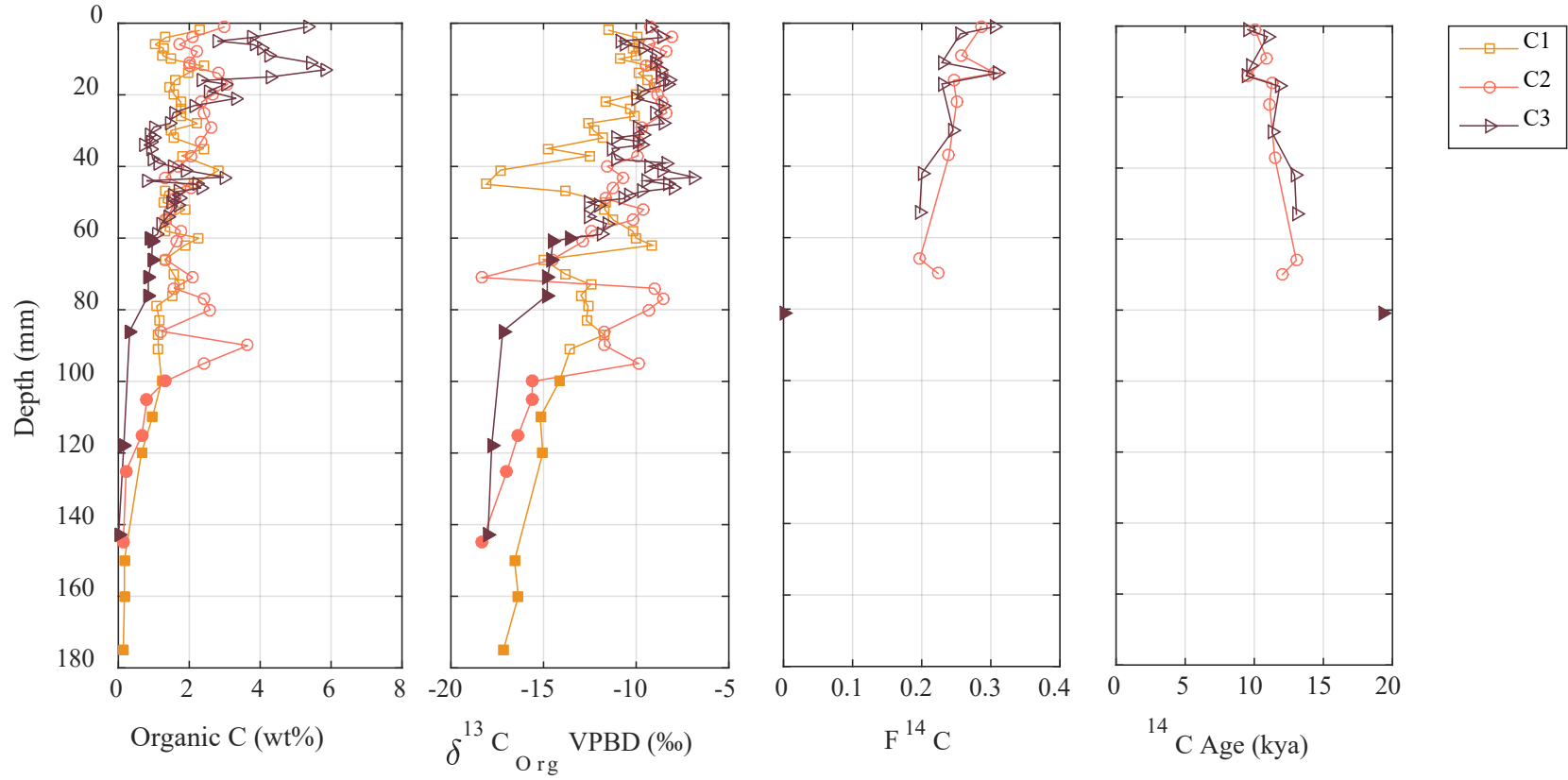


Figure 4–10 Core microbial mat organic carbon abundance, stable isotopes ($\delta^{13}\text{C}$) and radiocarbon results reported as fraction modern carbon ($F^{14}\text{C}$).

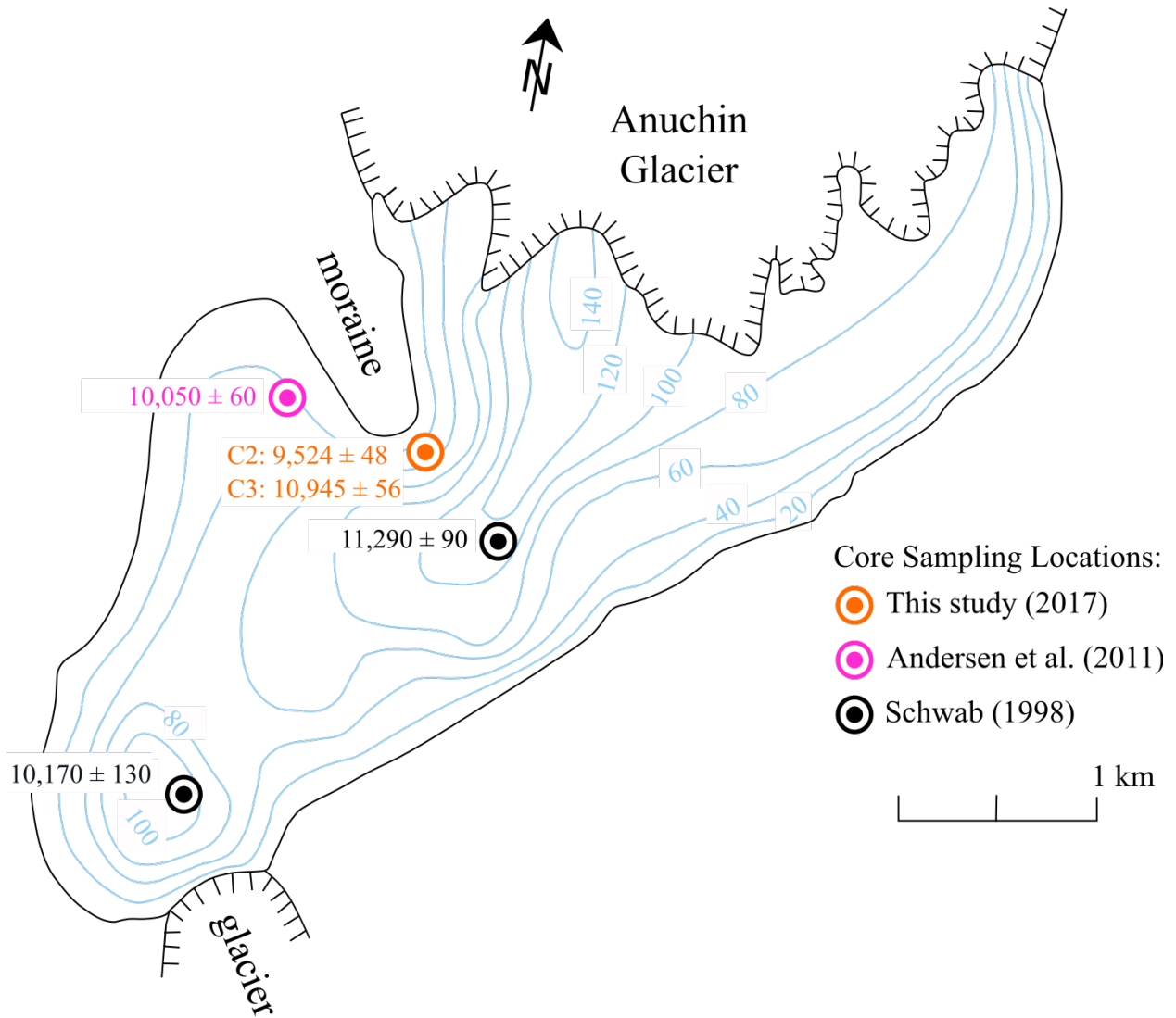


Figure 4–11 Bathymetry map (modified from Kaup, 1988) showing core sampling locations and radiocarbon ages of top laminae reported for each core (years before 1950). Cores from this study (Core 2 and Core 3) were collected within a 30 m radius of the diving hole. Radiocarbon dates in pink from Andersen *et al.*, (2011) and radiocarbon dates in black from Schwab (1998).

5 Discussion

5.1 Lake and Pond Chemistry

Lake Untersee is a closed-basin lake, where a permanent ice-cover has been present for at least 500 years (Wand and Perlt, 1999). Although neither surface waters nor significant moating has been observed at the lake, tritium (^3H) and radioiodine (^{129}I) were measured to determine if Lake Untersee and the lateral moraine ponds receive an input of modern water. These radionuclides are produced naturally cosmogenically, however atmospheric nuclear testing and fallout in the 1940's to 1960's resulted in high levels of ^{129}I and ^3H in modern precipitation, with peak concentrations occurring around 1963 (Clark, 2015b). The high levels of radionuclides produced by thermonuclear testing allows ^3H and ^{129}I to be used as anthropogenic tracers of modern waters (Clark, 2015b). Both radionuclides were below detection in all lake water samples, which is consistent with results from the study by Hermichen and Wand (1985) where the ^3H content in waters was also below detection (<0.5 TU). The absence of ^3H and ^{129}I in lake waters supports that Lake Untersee has been permanently sealed in recent history (post-bomb testing) with negligible interaction with modern waters.

Both ^3H and ^{129}I were detected in Pond Burevestiniskee, and low levels of ^{129}I in the smaller Pond 2, suggesting some degree of interaction with modern waters. While ^{129}I data are sparse in Antarctic literature, the ^{129}I concentration measured in Pond Burevestniksee are comparable to concentrations reported for fresh Antarctic snow ($2.0\text{--}7.6 \times 10^6$ atoms L^{-1}) (Xing *et al.*, 2015). The radiocarbon age for the TIC and TOC in the ponds are modern (0.92–0.99 F^{14}C), and coupled with the radionuclide data, is compelling evidence that the two ponds are sourced from modern ice and/or snow melt.

The sealed nature of Lake Untersee has key effects on major ion and carbon chemistry. Since hydrological inputs are only entering from beneath the ice-cover, and water-loss is by sublimation of the ice-cover, conservative solutes accumulate in the waters over time as annual glacial melt contributes additional solutes and gases to the lake. Solutes are known to segregate out of freezing ice and concentrate in the parent waters (Killawee *et al.*, 1998), these ions are not lost through the ice-cover. The ice-cover also cuts off interaction with the atmosphere, so the carbon stores in the waters are not replenished by exchange with atmosphere as photosynthetic bacteria sequester DIC through carbon-fixation. The microbial activity may be limited by the amount of carbon flux from glacial meltwater. This study was not able to determine if the microbial activity is limited by light, carbon or potentially from other trace nutrients (*e.g.*, P, Fe), however light and genomic studies are currently underway at Lake Untersee and a focused investigation should be completed to determine the limiting factor for the growth of Lake Untersee's benthic phototrophic microbial communities.

The major ion chemistry ($\text{SO}_4 > \text{Na} > \text{Ca} > \text{Cl}$) in Lake Untersee is due to a combination of (1) evaporative concentrating effects; (2) glacial input; (3) weathering processes; and potential input from (4) groundwater and/or subglacial waters. Aerosols trapped in the glacier ice is undoubtedly an important source of solutes to the lake (Kaup *et al.*, 1988; Faucher *et al.*, 2019), and ice-core data from the EPICA Dronning Maud Land (EDML) and deep EPICA DOME C (EDC) cores in Dronning Maud Land may provide the best analogues for the chemical composition of melt from the Anuchin glacier.

Sulfate is the dominant ion in Antarctic ice-cores (Isaksson *et al.*, 1996; Röthlisberger *et al.*, 2000, 2003; Wolff *et al.*, 2006; Rhodes *et al.*, 2012). Sulfate concentrations in the EDC core ranges from 57 to 399 ppb (Wolff *et al.*, 2006). Sulfate concentrations in the EDML range from 15 to 267 ppb with typical $\text{SO}_4:\text{Cl}$ molar ratios of 0.71–1.20 (25th to 75th percentile), and averaging 0.93 ($n = 347$, $\text{std } (1\sigma) = 0.65$). (Isaksson *et al.*, 1996). Similarly, sulfate concentrations are very high in Lake

Untersee (166 ppm) relative to the other major ions (Na, Ca, and Cl) with SO₄:Cl molar ratios of 1.58–1.59 in the oxic waters.

The three major sources of sulfate in pre-industrial Antarctic snow is marine biogenic, sea-salt and continental (including mineral dust, continental biogenic, and volcanic) with marine biogenic generally the dominant source (Alexander *et al.*, 2003). Stable sulfur isotopes of sulfate in the deep Vostok and Dome C Ice cores range from 9.5 to 15.4‰ for 2–130 kya (Alexander *et al.*, 2003) and 14.4–15.0‰ for shallow cores from the EDML site (Jonsell *et al.*, 2005). Ice core $\delta^{34}\text{S}_{\text{SO}_4}$ corrected to remove the sea-salt component is slightly depleted (by 0.3 to 1.7‰) relative to the total sulfate value in the ice cores. The $\delta^{34}\text{S}_{\text{SO}_4}$ in the Lake Untersee's oxic waters fall outside the range of the total sulfate values, but within the 7.5–15.1‰ range of the non-sea-salt component (Alexander *et al.*, 2003; Jonsell *et al.*, 2005).

Subglacial weathering of the sulphide-bearing meta-volcanic rock may account for the lake waters $\delta^{34}\text{S}$ signature sitting just outside the range of the total-sulfate values and a higher SO₄:Cl ratio relative to the average EDML core molar ratios. Sub-ice sheet environments are highly geochemically reactive, where microbial activity and anoxic conditions can drive closed-system weathering (Wadham *et al.*, 2010; Boyd *et al.*, 2014). Where weathering or dissolution of limestone or marine evaporites would result in a signature enriched in the heavier isotope, S-weathering products of sulphide should reflect a depleted $\delta^{34}\text{S}$ signature (**Figure 5–1**). Sulphides have been observed in the Schirmacher oasis and the nunataks between the Schirmacher and Untersee Oasis, including pyrrhotite, pyrite and chalcopyrite (Bormann and Fritzsche, 1995). While sulphides have not been observed in the Eliseev basement complex surrounding Untersee, it is not unreasonable that the crystalline basement under the ice-sheet may contain sufficient sulphide to influence the subglacial water chemistry. Any dissolved sulfur-species entering the lake would ultimately oxidize to SO₄ in Lake Untersee's highly oxidizing conditions. These sulfur

isotope results suggest that the primary input of sulfate to the lake is glacial melt, but that another ^{34}S depleted component is derived elsewhere, such as from subglacial weathering of sulphides.

Glacial melt and subglacial waters are also a source of Ca, Na, Mg, Cl, NO_3 and other ions. The geochemical facies of the Dronning Maud Land ice-cores are similar to that of Lake Untersee's oxic waters. The EDML and EDC cores are characterized as a Na- $\text{SO}_4(\text{Cl})$ and Na- SO_4 types, relative to Na(Ca)- SO_4 type for Lake Untersee. Thousands of years of input from glacial melt, coupled by concentrating effects of the sublimating ice-cover, likely built up these elements in the waters over time. The elevated Ca relative to conservative elements (*e.g.*, Cl) may be due to subglacial or in-situ weathering of plagioclase-rich glacial flour derived from the anorthosite and meta-volcanic crustal bedrock. Kaup (1988) first hypothesized that the unusually high pH, and the high levels of silica and calcium in the lake was due to weathering of plagioclase. Geochemical modelling by Andersen *et al.* (2011) demonstrated that closed-system weathering of plagioclase would consume carbonic acid, driving up the pH as well as $[\text{Ca}^+]$ and $[\text{Na}^+]$ towards calcite saturation. The geochemical modelling exercise was replicated for this study, showing that indeed, incongruent weathering of plagioclase to kaolinite by fresh glacial meltwater composition would increase the pH of the waters to >11 pH. Alternatively, if the system were open but no weathering was occurring, carbonate buffering would neutralize the pH of the waters. This phenomenon was observed when sample bottles are opened to atmosphere, causing waters to shift from 10.6 to a neutral pH. The pH changes for various modelling scenarios are summarized in **Table 5-1**. The conclusion of closed-system weathering is supported by the absence of radionuclides (^3H and ^{129}I) and high pH in the lake waters.

In-lake weathering of the glacial flour and sediments was proposed by Andersen *et al.* (2011), who identified plagioclase and other silicate minerals in the lake sediments using x-ray diffraction. This chemical weathering mechanism would require an acid source, potentially from carbonic acid produced from hydrolyzation of CO_2 when glacier atmospheric gases dissolve in the melt at the

lake–glacier interface. Sub–glacial weathering is another plausible weathering scenario, with the weathering products transported to the lake at the base of the Anuchin glacier. Regardless of where the process is dominantly occurring, weathering of plagioclase and other silicate minerals under the glacier and/or in the lake is an important contributor of Ca^+ and Na^+ ions to the lake waters. Chemical weathering almost certainly is occurring in the ice–covered lateral moraine ponds as well, as evidenced by high $[\text{Ca}^+]$, $[\text{Na}^+]$ and $[\text{OH}^-]$.

Weathering of plagioclase is reflected in the pond and lake water REE data by the presence of positive europium anomalies. Europium is strongly held in plagioclase, and preferentially is incorporated into plagioclase over other minerals during crystallization in the magma chamber (White, 2013). It is unsurprising the plagioclase–rich anorthosites in the Untersee Oasis have inherited europium anomalies, as well as the local ferro–monzonites and –monzodiorites studied by Ravikant *et al.* (2011). Positive anomalies are typical of granulites and other plagioclase rich crystalline rocks, while negative anomalies are observed in sea–water and continental rocks such as shales (Cox *et al.*, 1979; Elderfield and Greaves, 1982). Dust measured in the EDC ice–core exhibits flat normalized REE patterns (*i.e.*, no europium anomaly) (Grousset *et al.*, 1992; Gabrielli *et al.*, 2010). Lake Untersee and moraine pond waters reflect positive europium anomalies in the trace–level REE data, arguably due to the weathering of plagioclase. Europium anomalies were calculated using different normalization schemes to check for calculation error, and positive anomalies of ≥ 1 were observed whether measured REE values were normalized to chondrite (*e.g.*, McDonough and Sun, 1995), bulk continental crust or upper continental crust (*e.g.* Rudnick and Gao, 2013).

The effects of silicate weathering are also reflected in the Sr–isotope data in the lake and pond waters in the Untersee Oasis. Continental crustal rocks have a wide range of Sr isotopic composition, ranging from 0.702 and 0.750 and a mean of ~ 0.720 (Bentley, 2006; Lyons *et al.*, 2016). For reference, MDV rocks range from about 0.705–0.750, while anorthosites and norites

local to the Untersee Oasis range from 0.7079–0.7118 (Bormann and Fritzsche, 1995; Lyons *et al.*, 2002). In general, felsic rocks are enriched in K^+ and Rb^+ , and therefore, have more radiogenic ^{87}Sr from the decay of ^{87}Rb (Lyons *et al.*, 2016). Strontium in lake and moraine ponds in the Untersee Oasis have higher $^{87}Sr/^{86}Sr$ ratios than the regional rock samples, and are considerably more radiogenic than modern sea–water, Antarctic and Greenland ice–cores, and MDV lake waters (**Table 5–2**). Blum and Erel (1995) have demonstrated elevated ^{87}Sr in early stages of weathering of glacial deposits relative to bulk $^{87}Sr/^{86}Sr$ composition, therefore chemical weathering of fine glacial material may account for the higher $^{87}Sr/^{86}Sr$ ratios in the lake waters relative to the regional basement rocks surrounding Lake Untersee. The $^{87}Sr/^{86}Sr$ data supports that felsic mineral components are a major source of Sr to the lake and ponds, and that silicate mineral weathering is an important source of solutes to the waters as initially suggested by Kaup *et al.* (1988). With respect to the lake–environment, it is still unclear whether weathering occurs primarily in the lake sediments or in the subglacial environment. Future work should involve leaching experiments and/or pore–water characterization to investigate the weathering potential of the lake sediments.

Lake Untersee has been described as an ultra–oligotrophic lake due to the low nutrient concentrations of phosphorous in the waters (Kaup *et al.*, 1988; Weisleitner *et al.*, 2019), although nitrate concentrations are high for ice–covered Arctic and Antarctic lakes (Vincent, 1981; Canfield and Green, 1985; Spaulding *et al.*, 1994; Gibson *et al.*, 2002). Early limnological studies by Kaup (1988) observed that Lake Untersee, as compared to the lakes of the Schirmacher Oasis, showed very high nitrate and nitrite values. This study reports average concentrations of 0.5 ppm nitrite ($n=18$, $2\sigma=0.02$) and 0.2 ppm nitrite ($n=18$, $2\sigma=0.01$), with $\delta^{15}N_{NO_3}$ values of 5.1–9.5‰ in the Lake Untersee’s oxic waters. Nitrate concentrations in the EDC and EDML range from 6 to 150 ppb. The West Antarctica ice–sheet may not be as representative as the EDC and EDML core in East Antarctica but includes $\delta^{15}N$ data with the nitrate concentrations in the core; values range from 28–45 ppb NO_3 and 1.5–9.9‰ $\delta^{15}N_{NO_3}$ in the 564 m ice–core. These isotope values are very

similar to what's observed in Lake Untersee and support that nitrate is sourced from melting glacier ice.

The $\delta^{15}\text{N}_{\text{NO}_3}$ in the ponds (22.3–22.6‰) is much higher than what is observed in the lake waters due to the activity of snow petrels in the valley. The sea-birds feed on krill at the coast and make the long journey back to the oasis to breed and roost in moraine material on the slopes of the valley. The presence of nesting petrels has been shown to dramatically increase the $\delta^{15}\text{N}$ in the soils on nunataks (ice-free *glacial islands*) in Dronning Maud Land (Cocks, Balfour and Stock, 1998). Soils where petrels were present reported $\delta^{15}\text{N}$ values of (13.1–25.9‰, $n = 7$) relative to negative to near zero values observed on nunataks where no birds were present (Cocks, Balfour and Stock, 1998). Data from this study suggests that the ponds are fed by modern-snow melt, and that excreta leach and/or leak into the ponds, resulting in the heavy $\delta^{15}\text{N}_{\text{NO}_3}$ signature observed in the lateral moraine ponds.

Thus far, solute sources and controls have been described for the lateral moraine ponds and general lake chemistry, showing that glacial melt and silicate weathering are major controls on the overall lake chemistry. The stratified waters in the bottom of the southern basin is a special case, where reducing conditions drastically effect the concentrations and isotopic composition of the major ions, trace elements, and nutrients. The inorganic and carbon chemistry of the anoxic waters in the south basin is not the focus of this study as it has been described in detail elsewhere (*i.e.*, Wand *et al.*, 2006), however new data for trace elements, $\delta^{15}\text{N}_{\text{NO}_3}$, $\delta^{34}\text{S}_{\text{SO}_4}$ and $\delta^{34}\text{S}_{\text{Sulphide}}$ are contributed from this study to compliment future research on the chemistry and microbial communities in the anoxic waters.

Carbon chemistry and description of sources are described in detail in the subsequent section, however it is important to note here that lake concentrations of DIC and DOC reported in this study (DIC = 0.3–0.4 ppm, DOC = ~0.1 ppm) are much lower than published values, which report higher concentrations (2–8 mg L⁻¹ DIC, 0.58–0.78 mg L⁻¹ DOC) and heavier signatures of $\delta^{13}\text{C}_{\text{DIC}}$

(4.29‰) in oxic water samples (Wand *et al.*, 2006). However, the elevated concentrations and $\delta^{13}\text{C}$ is arguably due to atmospheric contamination of these samples. The $^{13}\text{C}/^{12}\text{C}$ composition of alkaline (pH 10.6) waters in equilibrium with atmospheric CO_2 at 0.1°C would have positive $\delta^{13}\text{C}_{\text{DIC}}$ signatures of ~3‰, and PHREEQC modelling calculates concentrations of 1.4 ppm DIC for an equilibrated sample. The Wand *et al.*, (2006) samples were filtered and poisoned in the field, and therefore at higher risk of atmospheric contamination than the unfiltered samples collected for this study. The results reported here are distinctly depleted in ^{13}C relative to modern atmospheric values, and do not reflect atmospheric influence.

5.2 Lake Carbon Model and Budget

A carbon budget model was developed to estimate the carbon reservoirs and annual inputs to the lake in order to better understand the carbon sources, cycling and fate in Lake Untersee. The carbon model builds on the hydrological model by Faucher *et al.* (2019) using carbon abundance data from this study and Antarctic ice-core data from literature to estimate carbon reservoirs and flux (**Table 5–3** and **Table 5–4**).

Some simplifications were made for the carbon budget calculations while preserving the objective of the study. The complexities of the anoxic basin are not included in the carbon model and therefore the entire lake volume will be comprised of homogenous, well-mixed waters with the typical oxic and alkaline chemistry for the purpose of the calculations.

As described in the methods section (**Section 3.4**), the balanced carbon budget for the lake is:

$$S_{IC} + S_{OC} + L_{IC} + L_{OC} = Ie_{DIC} + Ie_{DOC} + Ig_{DIC} + Ig_{DOC} - Os_{DIC} - Os_{DOC}$$

Where Ie is carbon input by subaqueous melting of the glacier wall at the lake-glacier interface (*i.e.*, englacial melting), Ig is carbon input by subglacial and/or groundwater, and Os is carbon loss by sublimation of the ice-cover. Reservoirs on the left side of the equation include dissolved

carbon in the lake–water (L), and sequestration of carbon in the lake sediments (S). Organic and inorganic components are denoted by OC and IC subscripts, respectively.

5.2.1 Carbon Reservoirs

The carbon reservoirs include (1) inorganic carbon and organic carbon dissolved in the lake water column (L_{OC} and L_{IC}), (2) organic–carbon sequestered by microbial mats by photosynthetic carbon–fixation (S_{OC}) and (3) carbonate spherules found in the sediments. In the oxic and alkaline water column, carbon occurs primarily as inorganic species HCO_3^- and CO_3^{2-} . To estimate the TIC pool in the lake waters, the median total inorganic carbon (TIC) concentration of oxic lake water samples from this study (0.3 mg L^{-1} , $n = 27$) were applied to the lake volume ($5.21 \times 10^{11} \text{ L}$) reported by Faucher *et al.* (2019):

$$\begin{aligned} L_{IC} &= \text{Lake Volume (L)} \times \text{TIC (mg L}^{-1}\text{)} \times \frac{1g}{1000 \text{ mg}} \\ &= 5.21 \cdot 10^{11} \text{ L} \times 0.3 \text{ mgC L}^{-1} \times \frac{1g}{1000 \text{ mg}} \\ &= 1.56 \cdot 10^8 \text{ g C} \end{aligned}$$

The TOC pool was estimated using the 0.1 mg L^{-1} concentration and the water volume:

$$\begin{aligned} L_{OC} &= \text{Lake Volume (L)} \times \text{TOC (mg L}^{-1}\text{)} \times \frac{1g}{1000 \text{ mg}} \\ &= 5.21 \cdot 10^{11} \text{ L} \times 0.1 \text{ mgC L}^{-1} \times \frac{1g}{1000 \text{ mg}} \\ &= 5.21 \cdot 10^7 \text{ g C} \end{aligned}$$

Carbon in the lake bottom is stored primarily as organic carbon fixed by the photosynthetic microbial mats. Inorganic carbon is generally very sparse (Andersen *et al.*, 2011). Sampling of acid–soluble carbon in the sediment cores is also complicated by carbonate precipitation promoted by atmospheric CO_2 diffusing through the core casing and interacting with potentially alkaline pore–waters. For this reason, and due to the rarity of carbonates in the sediments, the inorganic

carbon component was excluded from the lake sediment carbon reservoir estimate ($S_{IC} = 0$) and therefore calculations may be a conservative estimate of the total carbon stored in the lake–bed. The organic–carbon component consists of the active and buried mats, as well as the heterotrophic community recycling biomass below the sediment–water interface (Koo *et al.*, 2017).

The organic carbon reservoir (S_{OC}) in the lake–bed is estimated using the carbon mass measurements from the three sediment cores and the average calculated carbon content (0.857 kg m^{-2}) of the microbial mats (**Table 4–9**). The organic–carbon content calculations included only the microbial mat component and not the sediments collected at the base of the core. The trace organic carbon in the sediments underlying the microbial mats was radiocarbon dated at $>19,000$ years, likely represents organic material deposited prior to the formation of Lake Untersee and are therefore excluded from the mass calculations.

Cores were collected in an area with near 100% microbial mat coverage of the lake–bed. Field observations from the 2015–2019 expeditions estimate that nearly 100% of the lake bottom is covered by the pigmented photosynthetic mats until $\sim 100\text{m}$ depths, but coverage is patchy in the deepest sections (D.T. Andersen, personal communication, Sept 4, 2019). To consider areas where mat coverage is $<100\%$ and/or irradiance to the lake bottom and biomass accumulation might be lower than the core collection site (*e.g.*, deep sections of the lake), three scenarios are considered for the microbial mat carbon reservoir: (1) 100% mat coverage (2) 75% coverage, and (3) 50% coverage. To estimate the total organic–C reservoir in the microbial mats, the microbial mats carbon content (0.855 kg m^{-2}) was used to scale up the total area of the lake bottom ($SA_{\text{Lake Bottom}} = 8.91 \text{ km}^2$) and then multiplied by a scaling factor (SF) for incomplete mat coverage:

$$S_{OC} = \text{Microbial Mats Organic Carbon Content (kg m}^{-2}\text{)} \times SA_{\text{Lake Bottom}} \times SF$$

For example, the carbon sequestered by the microbial mats in a 75% mat coverage scenario using a scaling factor of 0.75 equals:

$$\begin{aligned}
S_{OC (100\% \text{ coverage})} &= 8.91 \text{ km}^2 \times 0.857 \text{ kg m}^{-2} \times 0.75 \\
&= 5.7 \cdot 10^6 \text{ kg C} \\
&= 5.7 \cdot 10^9 \text{ g C}
\end{aligned}$$

The estimated organic-carbon reservoir is 3.8 to 7.6×10^9 g C, one to one and a half orders of magnitude higher than the pool of dissolved carbon in the lake water column. Biomass accumulation and burial has accrued a significant carbon reservoir in Lake Untersee. The laminations observed in the sediment cores are not seasonal varves typically observed in open-water lakes, but microbial mats layered on top of one another mixed with fine to sand sized sediments. Radiocarbon dating of the microbial mats at the sediment-water interface reports radiocarbon ages of 9,520 yrs (Core 2) and 10,050 yrs BP (Core 3), and ages of 12,030 yrs (Core 2) and 13,050 (Core 3) yrs BP where the microbial mats end in the cores. The radiocarbon ages are not necessarily representative of the date of carbon fixation since ages are complicated by a reservoir effect in the lake waters, which carries the signature of old atmospheric carbon from the glacier melt. For instance, oxic lake waters today have a radiocarbon age of $\sim 7,000$ years BP (0.4 F¹⁴C) because the TIC pool is a mix of aging carbon trapped in the ice-covered lake, and the annual flux of Holocene CO₂ from glacial melt.

5.2.2 Glacial CO₂ Input

A key input of carbon to Lake Untersee is atmospheric CO₂ trapped in the bubbles of the Anuchin glacier released by melting under the ice-cover at the lake-glacier interface (I_{eIC}) and contributed by the sub-glacial meltwater component proposed by Faucher *et al.* (2019). The atmospheric CO₂ dissolves in the meltwater and hydrates to carbonic acid, which then deprotonates to HCO₃⁻ and CO₃²⁻ in the high pH lake waters to contribute to the pool of TIC. Concentrations of inorganic carbon in the glacial meltwater can be predicted from gas volumes, the paleorecord of CO₂ concentrations in Antarctic ice-cores and firn porosity at the depth of closure. Ice-cores have not been collected to date of the Anuchin glacier, however inferences can be made from Antarctic

cores. Based on the reported radiocarbon and gas ages for the paleorecord of the nearest ice core, EDML, a glacier of <200 m thickness would host atmospheric gas ages ranging from modern to ~2,000 year old ice, and atmospheric compositions ranging from 267 to 290 ppmv CO₂ and averaging 280 ppmv (n=95), excluding post-industrial values (<200 years BP) which have higher partial pressures of CO₂ due to anthropogenic activity (Monnin *et al.*, 2004; Sievert *et al.*, 2005). Gas volumes in Antarctic ice-cores are 0.10–0.12 cm³ per gram of ice at standard temperature and pressures (STP), regardless of depth into the ice-core (Gow and Williamson, 1975; Samyn, Fitzsimons and Lorrain, 2005). Assuming an average gas volume of 0.11 cm³ g⁻¹ at closure and an average CO₂ concentration of 280 mg L⁻¹ for gas ages ranging from pre-industrial (>200 years) to 2,000 years BP, this translates to a TIC of concentration of 0.0165 mg L⁻¹ (0.00137 mmol C L⁻¹) in the resulting melt:

$$280 \text{ ppmv } CO_2 = \frac{280 \text{ cc } CO_2}{10^6 \text{ cc air}}$$

$$\begin{aligned} [C]_{melt} &= \frac{280 \text{ cc } CO_2}{10^6 \text{ cc air}} \times \frac{11.5 \text{ cc air}}{100 \text{ g melt}} \times \frac{1 \text{ mol } CO_2}{22,414 \text{ cc } CO_2} \times \frac{1 \text{ mol C}}{1 \text{ mol } CO_2} \times \frac{12 \text{ g C}}{1 \text{ mol C}} \times \frac{10^6 \text{ cc}}{1 \text{ m}^3} \\ &= 1.65 \cdot 10^5 \text{ gC m}^{-3} \text{ melt} \\ &= 0.0165 \text{ mg L}^{-1} \end{aligned}$$

Subaqueous melting of terminus ice is the only known water and carbon input, however the hydrological model proposed by Faucher *et al.* (2019) requires a second hydrological input to balance the water mass budget (where $\Delta V = 0$). Since there is no evidence of surface water flowing into the lake, the lake must be connected to a subglacial and/or groundwater system (Faucher *et al.*, 2019). It is unlikely that groundwater recharge occurs in Antarctica's ice-free regions, however geophysical studies have demonstrated there are substantial volumes of subglacial meltwater stored and flowing under the ice-sheet (Mikucki *et al.*, 2015). A subglacial input to Lake Untersee is a potential flux of water, dissolved gases, and solutes to the lake. The subglacial component (*I_g*) would similarly contain inorganic carbon originating from atmospheric gases liberated from basal

melting of the ice, but subject to losses due to consumption of H_2CO_2 in silicate weathering reactions.

Stable carbon isotope results of TIC in the lake waters are very similar to the $\delta^{13}\text{C}$ measurements of atmospheric CO_2 in Antarctic ice cores for the last glacial and interglacial period (Schneider, 2011; Schmitt *et al.*, 2012; Schneider *et al.*, 2013; Eggleston *et al.*, 2016). Compiled CO_2 gas concentration and $\delta^{13}\text{C}$ data from the EPICA, DOME C, and Talos Dome ice cores, and reports $\delta^{13}\text{C}_{\text{CO}_2}$ values from -7.3 to -6.3 (n=129) for gas ages of 390 years to 150 ka before present (Schmitt *et al.*, 2012; Eggleston *et al.*, 2016) relative to -8.4 to -9.8‰ observed in the oxic lake water samples.

While there is a comprehensive paleorecord of CO_2 in Antarctic ice-cores, data on the organic-carbon content of ice sheets and basal ice is limited for East Antarctica. Englacial samples from the McMurdo Dry Valley report average DOC concentrations of 0.4 mg C L^{-1} (Hood *et al.*, 2015), and DOC measured in the Vostok ice-core ranges $0.02\text{--}0.32 \text{ mg C L}^{-1}$ (Priscu *et al.*, 2013). Hood *et al.* (2015) highlights that the MDV samples are in a large ice-free region with an abundance of dry soils and is not representative of the Antarctic ice sheet as a whole. Soils and other environments which would promote increased microbial activity were not observed in the region surrounding Lake Untersee, therefore comparison with MDV data may overestimate the organic material in regional ice. The organic carbon content of the Anuchin glacier flowing over the crystalline basement and into the valley may be more similar to the Vostok ice core which is a deep ice-core from the interior of the continental ice sheet.

Trace carbon and isotope results from this study suggest that organic-carbon flux from the glacier must be low. First, the water column TOC for nearly all samples is below the 0.3 mg L^{-1} limit of detection for the TOC-analyzer (**Section 3.3.2**) and the two samples analyzed for radiocarbon analysis extracted carbon masses equivalent to 0.1 mg L^{-1} (**Section 3.3.3**). Only two oxic water samples from the south basin had detectable TOC (0.3 and 0.4 mg L^{-1}), with measured $\delta^{13}\text{C}_{\text{TOC}}$ of

–26.7 and –27.5‰. The $\delta^{13}\text{C}$ values for TIC in the water column are very similar to $\delta^{13}\text{C}_{\text{CO}_2}$ in East Antarctica ice–cores. If substantial TOC was converted to TIC through aerobic respiration, the resulting combined pool of TIC would show a strong depletion in ^{13}C relative to ancient atmospheric CO_2 . The $\delta^{13}\text{C}_{\text{TIC}}$ in the lake waters is depleted only ~1 permil relative to ice–core $\delta^{13}\text{C}_{\text{CO}_2}$. It's possible that a small amount of TOC is being oxidized to inorganic carbon and contributing to the isotopic signature observed in the lake waters, however isotope data supports that the carbon input to the lake is primarily CO_2 sourced from the glacier, fed to the lake by a combination of subaqueous melt and subglacial waters.

5.2.3 Carbon Output

Lake Untersee is a closed basin lake and is sealed by the permanent ice–cover, therefore there are no carbon losses by outflowing water. Minor amounts of TOC and CO_2 may be lost through the ice cover as ice freezes at the base of the cover and lost through sublimation at the surface. Based on geochemical modelling of the lake–waters (**Appendix D**), PCO_2 is very low and undersaturated in the lake waters ($\text{PCO}_2 = 4.5 \times 10^{-12}$ atm) and therefore gaseous CO_2 incorporated into ice–bubbles during ice–freezing is negligible. Using the modelled CO_2 concentration of 1.33×10^{-10} M in the lake waters, and the annual water loss by sublimation (4.90×10^9 L), loss through the ice–cover equals <10 g of carbon per year ($O_s \text{ IC} \approx 0$).

While solutes (*e.g.*, Mg, Na, Cl) are known to segregate out of freezing lake ice and concentrate in the parent waters, experiments have demonstrated that TOC is incorporated in freezing ice (Killawee *et al.*, 1998; Santibáñez *et al.*, 2019). It is difficult to discern if TOC is in equilibrium (TOC input = TOC output) in the waters given the uncertainty of organic carbon concentrations in the glacial melt and low concentrations measured in the lake waters. Potential TOC loss through the ice–cover is negligible and not incorporated into the carbon budget.

5.2.4 Carbon Mass Balance and Implications

The estimated carbon budget demonstrates that most carbon resides in the sediments ($3.8\text{--}7.6\times 10^9$ gC), with $\leq 5\%$ in the water column (2.1×10^8 gC). Further, melting of the Anuchin glacier (basal melt and subaqueous melting of the glacier face) contributes a relatively small flux of only 8.1×10^4 gC carbon to the lake annually. For the current lake configuration and rate of melting of the Anuchin glacier, and with the sediment carbon model, it would take over 50,000 years to build up the carbon reservoir with glacially derived CO_2 alone (**Table 5–5**). Considering that the amount of melt feeding the lake may have waxed and waned over time, If the glacier CO_2 were the sole source of carbon to the system, the mass balance requires the 4–8x the melt and carbon flux over the predicted 10–13 kyr lifespan of the lake for minimal model of mat coverage at $\geq 50\%$ (**Figure 5–2**). These calculations demonstrate that other sources of carbon are required to complete the mass balance. Two inputs are considered to account for the missing carbon and evaluated using isotope chemistry: (1) higher carbon concentrations in subglacial waters relative to calculate melt concentrations, and (2) CO_2 dissolution in lake waters due to atmospheric exchange during an open–lake event(s).

Source 1: Carbon in Subglacial Waters

The hydrological and chemical conditions beneath the Anuchin glacier have not been studied. Petrological investigations of till, Nunataks and exposed bedrock infer that the ice sheet is underlain by crystalline basement (Bormann and Fritzsche, 1995; Jacobs *et al.*, 2017), but the presence or connectivity of subglacial lakes, aquifers and rivers in the region is unknown. The closest identified subglacial lakes (M–310 and M–2710) are ~ 1000 km from Lake Untersee (Popov and Masolov, 2003; Siegert *et al.*, 2005). The inventory of subglacial lakes in Antarctica is constantly growing with continued exploration of the continent and subglacial environment, and aqueous environments near the oasis and/or connectivity to Lake Untersee is possible and warrants further investigation.

To complete the carbon mass balance, an additional $4.2\text{--}8.2 \times 10^9$ g C of input must be added to the system. In the current lake configuration and steady state conditions (hydrological loss equals hydrological input), ~13,000 years of hydrological input with CO₂ solely sourced from atmospheric gas in the ice would only account for 13–26% of the estimated carbon budget. If higher levels of DIC in the subglacial waters is considered to account for the missing carbon, concentrations of 0.1 to 0.2 mgC L⁻¹ in the subglacial input is required to complete the mass balance using the timescale of 13,000 years and annual hydrological input of 2.8×10^9 L year⁻¹.

Wadham *et al.* (2010) and Wynn, Hodson and Heaton (2006) describe potential sources of carbon in closed-weathering subglacial environment as: (1) ancient CO₂ dissolved in basal melt; (2) microbially respired CO₂ from degradation of organic matter; and (3) carbonate dissolution. Melt with DIC sourced solely from ancient atmospheric CO₂ liberated from melting basal ice is estimated to have a concentration of ~0.0165 mg L⁻¹, and while it's possible (2) and (3) could increase the concentrations to 0.1 or 0.2 mg L⁻¹, the $\delta^{13}\text{C}_{\text{TIC}}$ and $F^{14}\text{C}_{\text{TIC}}$ results do not support an input from ancient organic matter or carbonate dissolution at such high concentrations.

The basement complexes underlying the ice sheet in DML are of Precambrian to Paleozoic age, and the continent has been covered by ice for over 35 million years (Jacobs *et al.*, 2017). Carbonates or ancient organic carbon (*e.g.*, coal, shales) stored under the ice-sheet in East Antarctica are therefore radiocarbon (¹⁴C) dead, and carbon sourced from these ancient deposits would have a $F^{14}\text{C}$ signature of zero. If the dominant source of carbon in the lake waters was ¹⁴C dead, the radiocarbon ages of the lake water would be expected to be much older than the 7,000 years observed today. For instance, if the glacier CO₂ brought into the lake by melting of the Anuchin is ~1,000 years on average and represents 20% of the carbon input, and the remaining 80% input is dead carbon, the resulting carbon pool would be <0.18 $F^{14}\text{C}$ (~14,000 years BP); however, radiocarbon analysis of the TIC reports a more modern signature of 0.41 to 0.60 $F^{14}\text{C}$ in

the oxic lake waters. Thus, a major input of dead carbon cannot account for the missing carbon without considerably aging the TIC pool.

Stable isotope chemistry is another line of evidence against a major input of carbonate or organically derived carbon. The $\delta^{13}\text{C}_{\text{TIC}}$ in the oxic waters samples from the well mixed north basin is -9.1‰ on average, very similar to ice-core $\delta^{13}\text{C}_{\text{CO}_2}$. Organic material is typically strongly depleted in ^{13}C relative to ^{12}C , and carbonates $\delta^{13}\text{C}$ are near zero (Clark, 2015b). Significant contribution from organics would drive the isotope ratios to strongly depleted $\delta^{13}\text{C}$ values, whereas carbonates would be expected to enrich the waters in ^{13}C to near zero $\delta^{13}\text{C}$ values. While it is possible that subglacial waters carry some carbon sourced from ancient carbonates or organics, these results suggest that the input must be minor relative to contribution from Holocene atmospheric CO_2 .

Source 2: Atmospheric CO_2

The second potential source of the missing carbon is uptake of atmospheric CO_2 during a period of atmospheric exchange. While the lake has been permanently sealed in observed history, the lake may have partly or completely lost its ice cover since its formation $\sim 10\text{--}13$ kya. Moating is common in other ice-covered lakes (*e.g.*, MDV lakes), and Schwab (1998) predicted that the lake was periodically ice-free early in the lake history and may have had minor interruptions of permanent ice-cover until recently.

Here we present a scenario where during or shortly after formation, the lake was ice-free or had an open zone around the margin to allow for atmospheric exchange. Ice-core data shows during this time in the early Holocene, average temperatures were climbing (Ciais *et al.*, 1994), and as the Anuchin glacier was retreating in the valley and the proglacial lake was forming, microbial mats were utilizing DIC in the air-equilibrated waters. DIC sequestered by carbon-fixation would then have been replenished from the atmosphere. During such an open-exchange period, a significant carbon reservoir would likely have been sequestered by phototrophic activity. Once the

permanent ice-cover developed, the DIC in the waters would then have been depleted to low levels.

An open-lake event around the time of lake formation is supported by the presence of calcite at a sediment core interval corresponding to $12,490 \pm 60$ in a sediment core from Lake Untersee from a study by Andersen *et al.* (2011). Geochemical modelling of lake and glacier waters demonstrates that open-system weathering of plagioclase rich rocks (*e.g.*, anorthosite) produce waters at or above saturation for calcite, and therefore an open lake would likely have some degree of calcite precipitation in the sediments. This calcite occurrence, relative to the paucity of carbonate in the rest of the core, suggests that the lake may have been open at this time.

The microbial mats at the base of the sediment cores have radiocarbon ages of 12,031–13,049 years BP which corresponds with the predicted timing of lake formation. The radiocarbon ages of the deepest microbial mats are likely a representative age of when the lake was open to atmospheric exchange and dominant source of carbon for the mats was modern CO₂. While some noise is observed in the radiocarbon data, a general trend of aging carbon is observed with depth into core. Accumulation rates are higher in the deep microbial mats relative to the upper mats, shown by the steepening of the Radiocarbon Age vs. Depth plot in **Figure 4–10**, supporting an early high biomass accumulation event.

Once the permanent ice-cover developed and the lake was sealed off from atmosphere, DIC continued to be sequestered by phototrophs, carbon in the waters continued to age, and waters also received input of older CO₂ from the glacier. The waters we measure today have a ¹⁴C_{TIC} signature of ~7,000 years, due to build up of old (~1,000 years) carbon from the glacier and the aging carbon in the water column. If the lake were open today, we would expect a modern ¹⁴C_{TIC} signature, while input of ¹⁴C dead carbon from carbonates or organic material from the subglacial environment would impart a much older ¹⁴C signature on the waters. These results suggest that the missing carbon for the carbon mass balance is derived from atmospheric CO₂ during a high–

biomass accumulation event around 12,000–13,000 years BP, and not from subglacial derived organics or carbonates.

5.2.5 Carbon Cycling in the Sediment Microbiome

Radiocarbon and stable carbon isotope data for the lake waters and sediments provide insight into carbon sources for phototrophic carbon fixation, and carbon cycling in the sediment microbiome. Stable isotope data demonstrates that microbial mats are isotopically indiscriminate in the carbon-starved system, while radiocarbon data supports utilization of two carbon sources for phototrophic carbon fixation.

The average $\delta^{13}\text{C}_{\text{TIC}}$ in the north basin oxic lake waters (-9.1‰) and $\delta^{13}\text{C}_{\text{Org-C}}$ is similar to the microbial mats in the top laminae of the sediment cores (Core 1 = -11.5‰ , Core 2 = -9.2‰ and Core 3 = -9.2‰). Assuming that measured TIC is representative of DIC in the lake-waters, these results demonstrate that there is no isotopic fractionation occurring between the DIC pool and the microbial mats during carbon fixation. In more typical lacustrine environments where $\text{CO}_{2(\text{aq})}$ is in higher concentrations and is available for carbon fixation by the Rubisco enzyme during photosynthesis, isotope effects associated with fixation are observed (Hayes, 1993). Maximum isotope fractionation by cyanobacteria ranges from -23 to -18‰ (Calder and Parker, 1973; Pardue *et al.*, 1976). Hayes (1993) reports that low concentrations of $\text{CO}_{2(\text{aq})}$ are commonly associated with low enrichment factors (ϵ). Fractionation is likely negligible in Lake Untersee's carbon-starved waters, where phototrophs use any carbon available and do not discriminate against the heavier isotope.

Lake Untersee's oxic waters are highly alkaline (~ 10.6 pH) and the dominant DIC species are HCO_3^- and CO_3^{2-} . Geochemical modelling of the lake waters predicts $\text{CO}_{2(\text{aq})}$ concentrations near zero ($< 1 \times 10^{-10}$ M), therefore the phototrophs are fixing HCO_3^- as an alternate carbon source. It is known that numerous algal species actively “pump” bicarbonate into their cells, where carbonic

anhydrase subsequently catalyzes production of dissolved CO₂ that is used for carbon fixation (Badger, 1987; Hayes 1993).

The radiocarbon results provide evidence that phototrophs are also fixing respired CO₂ from heterotrophic metabolism of the buried microbial mats beneath the sediment surface, in addition to HCO₃⁻ in the water column. The top microbial mat samples that best represent active photosynthetic mats in contact with the overlying water column are radiocarbon dated at 10,052 years BP (Core 1) and 9,524 years BP (Core 3), while the TIC pool in the lake waters are dated at ~7,000 years BP. Assuming that TIC is representative of DIC in the lake waters, a reservoir effect of this magnitude might be expected if the active microbial mats were drawing solely from the DIC pool for carbon fixation; however, the top microbial mats are radiocarbon dated >2,500 years older than TIC in Lake Untersee. This phenomenon is likely attributed to the phototrophs fixing carbon from two sources: (1) the HCO₃⁻ with a “young” signature, and (2) heterotrophically respired CO₂ from the decomposition of “old” buried organics (**Figure 5–3**). Alternatively, the greater radiocarbon age of the top lamination may reflect a very low rate of phototrophic activity beneath the ice cover.

Genomic sequencing of the 16S RNA gene of the microbial communities in the top laminae of a conical microbial mat from Lake Untersee identified phototrophic cyanobacteria as the bacterial species in the top–most layer, but heterotrophic bacteria dominated just mm below the sediment–water interface (Koo *et al.*, 2017). Metagenomic (PICRUSt) analysis for predictive metabolic functions predicted with high confidence that the heterotrophic communities were capable of metabolic functions typical of recycling of organic material, such as amino–acid metabolism and carbohydrate metabolism (Koo *et al.*, 2017). Radiocarbon dating of the mats show that they generally age with depth in the sediments (**Figure 4–10** and **Table 4–10**), thus the CO₂ respired by the heterotrophic bacteria consuming the buried microbial–mats would carry an older ¹⁴C

signature. The combined effect is a radiocarbon age of ~9,500–10,000 years in the top microbial mat laminae.

Chapter 5 Tables

Table 5–1 Geochemical modelling (PHREEQC) summary

Modelling Scenario	Starting Solution		Final Solution					
	pH	SI_Calcite	pH	SI_Calcite	$\Delta M_{\text{Alibite}}$	$\Delta M_{\text{Anorthite}}$	$\Delta M_{\text{Kaolinite}}$	M_C
<i>Glacial Water</i>								
Closed–system weathering	5.6	–10.0	11.9	–0.92	–1.76E–03	–1.43E–03	2.30E–03	1.40E–06
Open–system weathering			10.6	6.67	–4.85E–04	–9.89E+00	9.89E+00	1.56E+01
Open–system, no weathering			5.4	–9.13	<i>N/A</i>	<i>N/A</i>	<i>N/A</i>	3.07E–05
<i>Lake Water (North Basin)</i>								
Closed–system weathering	10.6	–0.6	11.8	–0.34	–1.13E–03	–1.04E–03	1.59E–03	4.92E–06
Open–system weathering			10.6	6.68	–1.84E–04	–9.88E+00	9.88E+00	1.56E+01
Open–system, no weathering			7.1	–2.34	<i>N/A</i>	<i>N/A</i>	<i>N/A</i>	1.26E–04

Modelled glacial meltwater concentrations are averages from the Dome C core (Röthlisberger *et al.*, 2003; Wolff *et al.*, 2006)

Modelled pH of glacial meltwater (5.6) based on ice–core acidity data of 2–3 ueq/L from 8 ice–cores in Dronning Maud Land (Pasteris *et al.*, 2014)

Modelled lake water concentrations are average concentrations (n=18) from the north basin (NB) samples

Atmospheric CO₂ and O₂ partial pressures used for atmospheric equilibration from Clark *et al.* (2015a)

SI = saturation indices

ΔM = change in moles in modelled (1 L) solution

M_C = mols of carbon in modelled (1 L) solution

N/A = not applicable

Table 5–2 Radiogenic strontium isotope summary

Sample	Reference	Sample Type	⁸⁷Sr/⁸⁶Sr
Modern seawater	1	Water	0.70918
Mean Continental crust	1	Rock	~0.720
Lake Untersee, Untersee Oasis			
NB–10	This study	Water	0.71831
NB–80	This study	Water	0.71830
NB–155	This study	Water	0.71829
NB–10	This study	Water	0.71832
NB–80	This study	Water	0.71822
NB–95	This study	Water	0.71804
Lateral Moraine Ponds, Untersee Oasis			
Pond Bure.	This study	Water	0.72290
Pond 2	This study	Water	0.72201
Eliseev Anorthosite Complex Main Rock Types, Untersee Oasis			
W74 Norite	2	Rock	0.7119
W20 Noritic Anorthosite	2	Rock	0.7091
W94 Anorthosite	2	Rock	0.7079
W100–1 Anorthosite	2	Rock	0.7107
W100–2 Anorthositic gabbro(?)	2	Rock	0.7102
W100–3 Anorthosite	2	Rock	0.7085
Antarctica Ice Core Data			
Dome C Ice–Core Dust (18 ky)	3	Dust	0.708707
Dome C Ice (7.5–23 ky)	4	Ice	0.7068–0.7097
Law Dome EH (65 ky)	4	Ice	0.0793–0.7097
Aeolian dust in meteoric ice, Vostok	1	Dust	0.708047–0.711254
Greenland Ice Core Data			
Greenland, Summit (GRIP CORE) (7.8 ky)	4	Ice	0.71160–0.7118

1: Lyons *et al.* (2016)

2: Bormann and Fritzsche (1995)

3: Grousset *et al.*, (1992)

4: Burton *et al.* (2002)

Table 5–3 Data from literature used in the carbon mass–balance calculations

Parameter	Value	Source
Lake volume	$5.21 \times 10^8 \text{ m}^3$	Hydrological model (Faucher <i>et al.</i> , 2019)
Annual water loss	$4.90 \times 10^6 \text{ m}^3 \text{ yr}^{-1}$	
Annual englacial melt hydrological input	1.98×10^6 to $2.23 \times 10^6 \text{ m}^3 \text{ yr}^{-1}$	
Annual subglacial melt and/or groundwater hydrological input	2.68×10^6 to $2.92 \times 10^6 \text{ m}^3 \text{ yr}^{-1}$	
Lake bottom surface area	8.91 km^2	Byrd ice–core (Antarctica) gas study (Gow and Williamson, 1975)
Entrapped gas volume in polar ice	10.5 to 12.5 cm^3 air per 100 g ice (STP)	
Glacier bubble atmospheric CO_2 concentrations	271 to 287 mg L^{-1} CO_2 (n=120, average and median = 279)	

Table 5–4 Measured data from this study used in the carbon mass–balance calculations

Parameter	Value	Note
TIC	0.3 mg L^{-1}	Average total inorganic carbon concentration in oxic lake waters
TOC	0.1 mg L^{-1}	Total organic carbon concentration in oxic lake waters from two samples
Organic carbon content in core	1.39 g C per 4.44 cm diameter core	Average organic carbon content of cores C1, C2 and C3
Surface area of lake bottom	8.91 km^2	Determined from the bathymetry map of Wand <i>et al.</i> (2006) which was digitized using ArcMap 10.4.1.

Table 5–5 Carbon budget and mass balance

CARBON RESERVOIR			
<i>Scenario</i>	<i>1</i>	<i>2</i>	<i>3</i>
<i>Mat Coverage</i>	<i>50%</i>	<i>75%</i>	<i>100%</i>
Oxic waters (gC)	2.1E+08	2.1E+08	2.1E+08
Mats (gC)	3.8E+09	5.7E+09	7.6E+09
Total Carbon Reservoir (gC)	4.0E+09	5.9E+09	7.8E+09
GLACIAL CO₂ INPUT			
Subaqueous meltwater (gC/year)	3.4E+04	3.4E+04	3.4E+04
Subglacial meltwater (gC/year)	4.7E+04	4.7E+04	4.7E+04
Annual glacial input (gC/year)	8.1E+04	8.1E+04	8.1E+04
Contribution over 13 ky	1.1E+09	1.1E+09	1.1E+09
% Contribution to carbon in mats	28%	18%	14%
% Contribution to total carbon reservoir	26%	18%	13%

Chapter 5 Figures

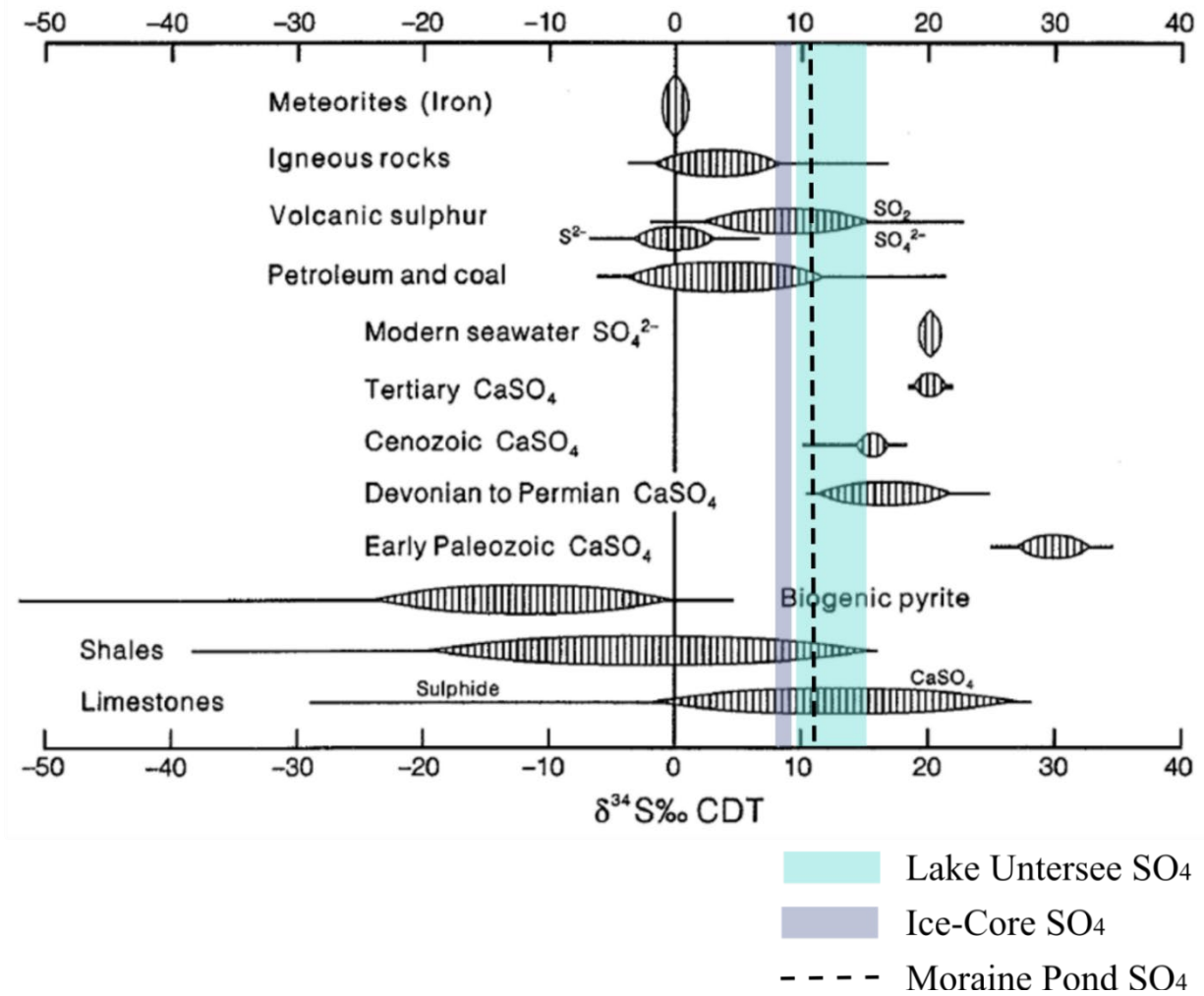


Figure 5-1 Ranges in $\delta^{34}\text{S}$ contents of sulphur and sulphur compounds in different materials and environments. Figure modified from (Krouse, 1980).

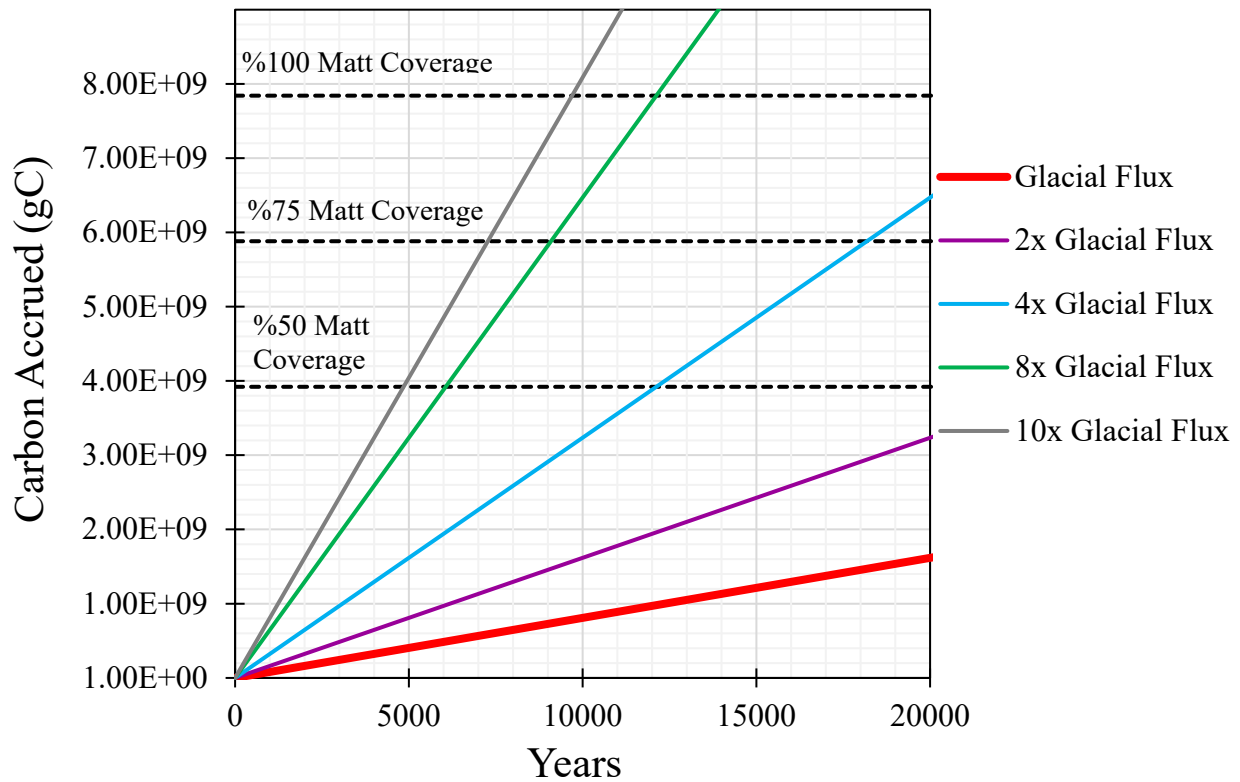


Figure 5–2 Accrued carbon input to the lake by glacial input of CO₂ by combined glacial input of subaqueous melting of the glacial wall and subglacial melt (using [C]_{melt} = 0.0165 gC L⁻¹). Mass of estimated total carbon reservoirs for 50%, 75% and 100% mott coverage scenarios denoted by black dashed lines.

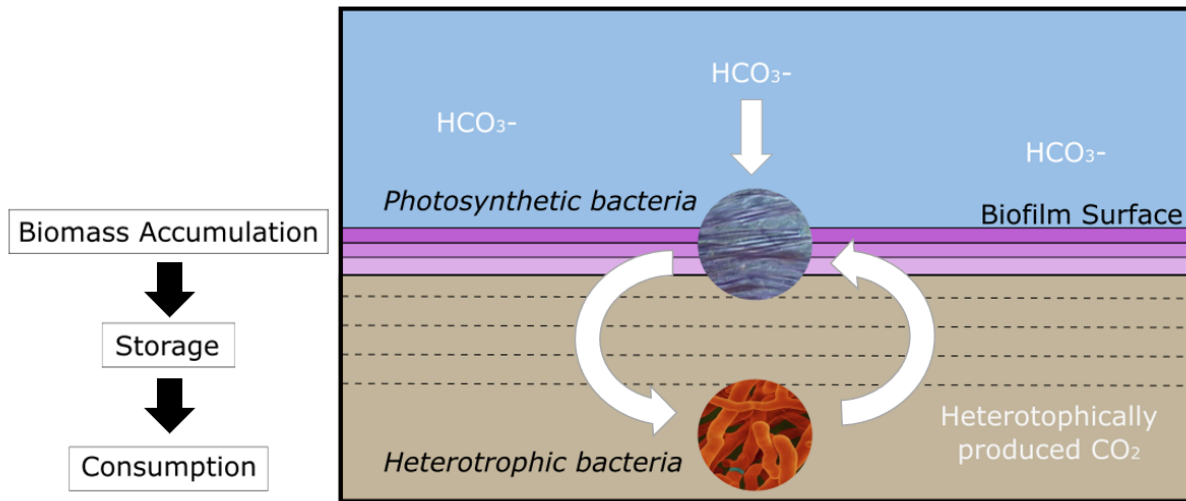


Figure 5–3 Carbon cycling in the sediment microbiome. Image of photosynthetic bacteria (Cyanobacteria) from Andersen et al., (2011) and stock heterotrophic bacteria image by Denis Kunkel (<http://www.denniskunkel.com/>).

6 Conclusions

The results of this thesis have led to the following conclusions:

1. The carbon budget demonstrates that glacial CO₂ input is not sufficient to account for the estimated mass of organic carbon sequestered in the lake sediments by the benthic microbial mats;
2. Radiocarbon and ¹³C analysis of the lake waters and sediments suggests that the missing carbon source is not bedrock carbonate or old organics carried by sub-glacial waters, but rather an early period when the lake was moated or ice-free which allowed higher photosynthetic rates and biomass accumulation leading to a significant sequestration of carbon;
3. Once a permanent ice-cover was established, the concentration of TIC of the water column was depleted by continued phototrophic carbon fixation, and the lake shifted from open- to closed-system weathering;
4. Closed-system incongruent weathering of plagioclase, likely in subglacial meltwater, contributed Ca⁺, Na⁺ and OH⁻ to the lake waters and increased the pH, as previously described by Kaup (1998) and Andersen et al., (2011). This interpretation is further supported by ⁸⁷Sr/⁸⁶Sr and REE results from this study. Positive europium anomalies in the lake waters are indicative of plagioclase weathering, and high ⁸⁷Sr/⁸⁶Sr values support silicate weathering as a source of ions to the lake waters;
5. Stable and radiocarbon analysis of the organic carbon content of the microbial mats and the TIC in the oxic lake waters show no biological fractionation due to non-discriminating photosynthetic fixation of HCO₃⁻ in the alkaline and carbon-starved lake waters;
6. Discrepancies in radiocarbon ages between the top photosynthetic mats with the overlying water column is may be attributed to mixed sources of carbon for biomass production. The mats are likely fixing DIC ($F^{14}C_{DIC} = 0.41-0.60$) as well as respired CO₂ from the degradation of older buried microbial mats ($F^{14}C = 0.12-0.31$) to build biomass; the

combined effect is a radiocarbon age of ~9,500–10,000 years in the top microbial mats. Alternatively, the greater radiocarbon age of the top mats may reflect a very low rate of phototrophic activity beneath the ice cover; and

In summary, this work supports a model for carbon sources, cycling and sequestration in Lake Untersee for the duration of its existence since the late Pleistocene, according to the following chronology:

Late Pleistocene (~13,000 yrs BP): Lake Development

Late Pleistocene–early Holocene (~13,000–10,000 yrs BP): Ice-free or moated conditions with access to atmospheric CO₂ leading to high rates of organic mat development, with high micronutrients from subglacial melt water weathering.

Early Holocene to today: Development of well-sealed perennial ice cover conditions and isolation of lake water from atmospheric CO₂.

Continued supply of meltwater from glacial melting at terminus in lake and glacial meltwater, increase in pH of lake water, depletion of TIC in water column, reduced rate of mat growth.

6.1 Future Work

Additional work which may provide further insight into the carbon systematics of lacustrine system include a focused analysis of microbial mat coverage throughout the lake, as well as increased spatial coverage of sediment cores. Sediment coring for this study was limited by safe SCUBA diving depths, however gravity or percussion coring could be implemented to extract cores at depths greater than 30 m. Biological samples and/or sediment cores should also be sampled

from the lateral moraine ponds for genomic sequencing, radiocarbon dating and stable isotope analysis to compare to Lake Untersee.

Finally, light-studies and further genomic work should be coupled with the carbon data-set presented here to determine if the microbes in the lake are light-, carbon- or nutrient-limited. Understanding adaptations and limitations of life in this extreme aquatic environment may help access the potential for life in other cold extreme environments, such as ancient lakes in Gale Crater on Mars or the icy the icy moon Enceladus (McKay, Andersen and Davila, 2017).

References

- Alexander, B. *et al.* (2003) 'East Antarctic ice core sulfur isotope measurements over a complete glacial–interglacial cycle', *Journal of Geophysical Research: Atmospheres*. doi: 10.1029/2003jd003513.
- Andersen, D. T. *et al.* (2011) 'Discovery of large conical stromatolites in Lake Untersee, Antarctica', *Geobiology*, 9(3), pp. 280–293. doi: 10.1111/j.1472–4669.2011.00279.x.
- Andersen, D. T., McKay, C. P. and Lagun, V. (2015) 'Climate conditions at perennially ice–covered Lake Untersee, East Antarctica', *Journal of Applied Meteorology and Climatology*, 54(7), pp. 1393–1412. doi: 10.1175/JAMC–D–14–0251.1.
- Bentley, R. A. (2006) 'Strontium isotopes from the earth to the archaeological skeleton: A review', *Journal of Archaeological Method and Theory*. doi: 10.1007/s10816–006–9009–x.
- Bereiter, B. *et al.* (2015) 'Revision of the EPICA Dome C CO₂ record from 800 to 600–kyr before present', *Geophysical Research Letters*. doi: 10.1002/2014GL061957.
- Bevington, J. *et al.* (2018) 'The thermal structure of the anoxic trough in Lake Untersee, Antarctica', *Antarctic Science*. doi: 10.1017/S0954102018000354.
- Blum, J. D. and Erel, Y. (1995) 'A silicate weathering mechanism linking increases in marine ⁸⁷Sr/⁸⁶Sr with global glaciation', *Nature*. doi: 10.1038/373415a0.
- Bormann, P. and Fritzsche, D. (eds) (1995) *The Schirmacher Oasis, Queen Maud Land, East Antarctica, and its surroundings*. Gotha, Germany: Justus Perthes Verlag.
- Boyd, E. S. *et al.* (2014) 'Chemolithotrophic primary production in a subglacial ecosystem', *Applied and Environmental Microbiology*, 80(19), pp. 6146–6153. doi: 10.1128/AEM.01956–14.
- Burton, G. R. *et al.* (2002) 'High–sensitivity measurements of strontium isotopes in polar ice', *Analytica Chimica Acta*, 469(2), pp. 225–233. doi: 10.1016/S0003–2670(02)00720–1.
- Calder, J. A. and Parker, P. L. (1973) 'Geochemical implications of induced changes in C¹³ fractionation by blue–green algae', *Geochimica et Cosmochimica Acta*, 37(1), pp. 133–140. doi: 10.1016/0016–7037(73)90251–2.
- Canfield, D. E. and Green, W. J. (1985) 'The cycling of nutrients in a closed–basin Antarctic lake: Lake Vanda', *Biogeochemistry*, 1(3), pp. 233–256. doi: 10.1007/BF02187201.
- Ciais, P. *et al.* (1994) 'Holocene temperature variations inferred from six Antarctic ice cores', *Annals of Glaciology*, 20, pp. 427–436.
- Clark, I. (2015a) 'CO₂ and Weathering', in *Groundwater Geochemistry and Isotopes*. doi: 10.1201/b18347–7.

- Clark, I. (2015b) 'Groundwater Dating', in *Groundwater Geochemistry and Isotopes*. doi: 10.1201/b18347-9.
- Cocks, M. P., Balfour, D. A. and Stock, W. D. (1998) 'On the uptake of ornithogenic products by plants on the inland mountains of Dronning Maud Land, Antarctica, using stable isotopes', *Polar Biology*, 20(2), pp. 107–111. doi: 10.1007/s003000050283.
- Cox, K. G. *et al.* (1979) 'Trace elements in igneous processes', in *The Interpretation of Igneous Rocks*. doi: 10.1007/978-94-017-3373-1_14.
- Crann, C. A. *et al.* (2017) 'First status report on radiocarbon sample preparation techniques at the A.E. Lalonde AMS Laboratory (Ottawa, Canada)', *Radiocarbon*, 59(3), pp. 695–704. doi: 10.1017/rdc.2016.55.
- Eggelston, S. *et al.* (2016) 'Evolution of the stable carbon isotope composition of atmospheric CO₂ over the last glacial cycle', *Paleoceanography*, 31(3), pp. 434–452. doi: 10.1002/2015PA002874.
- Elderfield, H. and Greaves, M. J. (1982) 'The rare earth elements in seawater', *Nature*, 296(5854), pp. 214–219. doi: 10.1038/296214a0.
- Faucher, B. *et al.* (2019) 'Energy and water mass balance of Lake Untersee and its perennial ice cover, East Antarctica', *Antarctic Science*. Cambridge University Press (CUP), pp. 1–15. doi: 10.1017/s0954102019000270.
- Filippova, S. N. *et al.* (2013) 'Detection of phage infection in the bacterial population of Lake Untersee (Antarctica)', *Microbiology*, 82(3), pp. 383–386. doi: 10.1134/s0026261713030041.
- Fomenkov, A. *et al.* (2017) 'Complete genome and methylome analysis of psychrotrophic bacterial isolates from Lake Untersee in Antarctica', *Genome Announcements*, 5(11), pp. 5–6. doi: 10.1128/genomea.01753-16.
- Gabrielli, P. *et al.* (2010) 'A major glacial–interglacial change in aeolian dust composition inferred from rare earth elements in Antarctic ice', *Quaternary Science Reviews*. Elsevier Ltd, 29(1–2), pp. 265–273. doi: 10.1016/j.quascirev.2009.09.002.
- Gibson, J. A. E. *et al.* (2002) 'Geochemistry of ice–covered, meromictic Lake A in the Canadian High Arctic', *Aquatic Geochemistry*, 8(2), pp. 97–119. doi: 10.1023/A:1021317010302.
- Gooseff, M. N. *et al.* (2006) 'A stable isotopic investigation of a polar desert hydrologic system, McMurdo Dry Valleys, Antarctica', *Arctic, Antarctic, and Alpine Research*, 38(1), pp. 60–71. doi: <https://doi.org/10.1038/s41559-017-0253-0>.
- Gow, A. J. and Williamson, T. (1975) 'Gas inclusions in the Antarctic ice sheet and their glaciological significance', *Journal of Geophysical Research*, 80(36), pp. 5101–5108. doi: 10.1029/jc080i036p05101.

- Grousset, F. E. *et al.* (1992) ‘Antarctic (Dome C) ice–core dust at 18 k.y. B.P.: Isotopic constraints on origins’, *Earth and Planetary Science Letters*, 111(1), pp. 175–182. doi: 10.1016/0012–821X(92)90177–W.
- Haendel, D. *et al.* (2011) ‘Hydrology of the lakes in Central Wohlthat Massif, East Antarctica: new results’, *Isotopes in Environmental and Health Studies*, 47(4), pp. 402–406. doi: 10.1080/10256016.2011.630464.
- Hawes, I. *et al.* (2011) ‘Legacies of recent environmental change in the benthic communities of Lake Joyce, a perennially ice–covered Antarctic lake’, *Geobiology*, 9(5), pp. 394–410. doi: 10.1111/j.1472–4669.2011.00289.x.
- Hawes, I. *et al.* (2016) ‘Growth dynamics of a laminated microbial mat in response to variable irradiance in an Antarctic lake’, *Freshwater Biology*, 61(4), pp. 396–410. doi: 10.1111/fwb.12715.
- Hayes, J. (1993) ‘Factors Controlling C–13 Contents of Sedimentary Organic–Compounds – Principles and Evidence’, *Marine Geology*, 113.
- Hermichen, W. D., Kowski, P. and Wand, U. (1985) ‘Lake Untersee, a first isotope study of the largest freshwater lake in the interior of East Antarctica’, *Nature*, 315(6015), p. 131.
- Hiller, A. *et al.* (1988) ‘Occupation of the Antarctic continent by petrels during the past 35 000 years: Inferences from a ¹⁴C study of stomach oil deposits’, *Polar Biology*, 9(2), pp. 69–77. doi: 10.1007/BF00442032.
- Hiller, A., Hermichen, W. D. and Wand, U. (1995) ‘Radiocarbon–dated subfossil stomach oil deposits from petrel nesting sites: novel paleoenvironmental records from continental Antarctica’, *Radiocarbon*, 37(2), pp. 171–180. doi: 10.1017/S0033822200030617.
- Hoffman, M. J., Fountain, A. G. and Liston, G. E. (2008) ‘Surface energy balance and melt thresholds over 11 years at Taylor Glacier, Antarctica’, *Journal of Geophysical Research: Earth Surface*, 113(4), pp. 1–12. doi: 10.1029/2008JF001029.
- Hood, E. *et al.* (2015) ‘Storage and release of organic carbon from glaciers and ice sheets’, *Nature Geoscience*. Nature Publishing Group, 8(2), pp. 91–96. doi: 10.1038/ngeo2331.
- Isaksson, E. *et al.* (1996) ‘A century of accumulation and temperature changes in Dronning Maud Land, Antarctica’, *Journal of Geophysical Research Atmospheres*. doi: 10.1029/95JD03232.
- Jacobs, J. *et al.* (2017) ‘Cryptic sub–ice geology revealed by a U–Pb zircon study of glacial till in Dronning Maud Land, East Antarctica’, *Precambrian Research*. Elsevier B.V., 294, pp. 1–14. doi: 10.1016/j.precamres.2017.03.012.
- Jonsell, U. *et al.* (2005) ‘Sulfur isotopic signals in two shallow ice cores from Dronning Maud Land, Antarctica’, *Tellus, Series B: Chemical and Physical Meteorology*, 57(4), pp. 341–350. doi: 10.1111/j.1600–0889.2005.00157.x.

- Kämpf, H. and Stackebrandt, W. (1985) 'Geological investigations in the Eliseev Anorthosite Massif, Central Dronning Maud Land, East Antarctica', *Zeitschrift der Geologischen Wissenschaft*, 13, pp. 321–333.
- Kaup, E. *et al.* (1988) 'Limnological investigations in the Untersee Oasis', pp. 28–42.
- Kieser, W. E. *et al.* (2015) 'The André E. Lalonde AMS Laboratory – The new accelerator mass spectrometry facility at the University of Ottawa', *Nuclear Instruments and Methods in Physics Research, Section B: Beam Interactions with Materials and Atoms*. doi: 10.1016/j.nimb.2015.03.014.
- Killawee, J. A. *et al.* (1998) 'Segregation of solutes and gases in experimental freezing of dilute solutions: Implications for natural glacial systems', *Geochimica et Cosmochimica Acta*. doi: 10.1016/S0016-7037(98)00268-3.
- Koo, H. *et al.* (2017) 'Microbial communities and their predicted metabolic functions in growth laminae of a unique large conical mat from Lake Untersee, East Antarctica', *Frontiers in Microbiology*, 8(AUG), pp. 1–15. doi: 10.3389/fmicb.2017.01347.
- Krouse, H. R. (1980) 'Sulfur isotopes in our environment', in Fritz, P. and Fontes, J. (eds) *Handbook of Environmental Isotope Geochemistry I, The Terrestrial Environment*. Amsterdam, The Netherlands: Elsevier, pp. 435–472.
- Lang, S. Q. *et al.* (2016) 'Rapid ^{14}C analysis of dissolved organic carbon in non-saline waters', *Radiocarbon*. doi: 10.1017/RDC.2016.17.
- Levitan, M. A. *et al.* (2011) 'Modern sedimentation system of Lake Untersee, East Antarctica', *Geochemistry International*, 49(5), pp. 459–481. doi: 10.1134/s0016702911050077.
- Lyons, W. B. *et al.* (2002) 'Strontium isotopic signatures of the streams and lakes of Taylor Valley, Southern Victoria Land, Antarctica: Chemical weathering in a polar climate', *Aquatic Geochemistry*, 8(2), pp. 75–95. doi: 10.1023/A:1021339622515.
- Lyons, W. B. *et al.* (2013) 'The carbon stable isotope biogeochemistry of streams, Taylor Valley, Antarctica', *Applied Geochemistry*. Elsevier Ltd, 32, pp. 26–36. doi: 10.1016/j.apgeochem.2012.08.019.
- Lyons, W. B. *et al.* (2016) 'Source of Lake Vostok cations constrained with strontium isotopes', *Frontiers in Earth Science*, 4. doi: 10.3389/feart.2016.00078.
- Matsumoto, G. I. *et al.* (1992) 'Geochemical characteristics of Antarctic lakes and ponds', *Proc. NIPR Symp. Polar Biol.*, 5, pp. 125–145.
- McDonough, W. F. and Sun, S. s. (1995) 'The composition of the Earth', *Chemical Geology*. doi: 10.1016/0009-2541(94)00140-4.

- McKay, C. P., Andersen, D. and Davila, A. (2017) ‘Antarctic environments as models of planetary habitats: University Valley as a model for modern Mars and Lake Untersee as a model for Enceladus and ancient Mars’, *Polar Journal*. Routledge, 7(2), pp. 303–318. doi: 10.1080/2154896X.2017.1383705.
- Mikucki, J. A. *et al.* (2015) ‘Deep groundwater and potential subsurface habitats beneath an Antarctic dry valley’, *Nature Communications*, 6(May 2014). doi: 10.1038/ncomms7831.
- Monnin, E. *et al.* (2004) ‘Evidence for substantial accumulation rate variability in Antarctica during the Holocene, through synchronization of CO₂ in the Taylor Dome, Dome C and DML ice cores’, *Earth and Planetary Science Letters*. doi: 10.1016/j.epsl.2004.05.007.
- Moorhead, D., Schmeling, J. and Hawes, I. (2005) ‘Modelling the contribution of benthic microbial mats to net primary production in Lake Hoare, McMurdo Dry Valleys’, *Antarctic Science*, 17(1), pp. 33–45. doi: 10.1017/S0954102005002403.
- Murseli, S. *et al.* (2019) ‘The preparation of water (DIC, DOC) and Gas (CO₂, CH₄) samples for radiocarbon analysis at AEL–AMS, Ottawa, Canada’, *Radiocarbon*, 00(00), pp. 1–9. doi: 10.1017/rdc.2019.14.
- Palstra, S. W. L. and Meijer, H. A. J. (2014) ‘Biogenic carbon fraction of biogas and natural gas fuel mixtures determined with ¹⁴C’, *Radiocarbon*. doi: 10.2458/56.16514.
- Pardue, J. W. *et al.* (1976) ‘Maximum carbon isotope fractionation in photosynthesis by blue–green algae and a green alga’, *Geochimica et Cosmochimica Acta*. doi: 10.1016/0016–7037(76)90208–8.
- Pasteris, D. *et al.* (2014) ‘Acidity decline in Antarctic ice cores during the Little Ice Age linked to changes in atmospheric nitrate and sea salt concentrations’, *Journal of Geophysical Research*. doi: 10.1002/2013JD020377.
- Perriss, S. J. and Laybourn–Parry, J. (1997) ‘Microbial communities in saline lakes of the Vestfold hills (eastern Antarctica)’, *Polar Biology*, 18(2), pp. 135–144. doi: 10.1007/s003000050168.
- Pikuta, E. V. *et al.* (2017) ‘Williamwhitmania taraxaci gen. nov., sp. nov., a proteolytic anaerobe with a novel type of cytology from Lake Untersee in Antarctica, description of Williamwhitmaniaceae fam. nov., and emendation of the order Bacteroidales Krieg 2012’, *International Journal of Systematic and Evolutionary Microbiology*, 67(10), pp. 4132–4145. doi: 10.1099/ijsem.0.002266.
- Pikuta, E. V and Hoover, R. B. (2019) ‘Psychrophilic biomass producers in the trophic chain of the microbial community’, p. 2019.

- Popov, S. V. and Masolov, V. N. (2003) 'Novye dannye o podlednikovih ozerah tsentral'noy chasty Vostochnoy Antarktity [New data on subglacial lakes in central part of Eastern Antarctica]', *Materialy Glatsiologicheskikh Issledovaniy*, 95, pp. 161–167.
- Prisco, J. C. *et al.* (2013) 'ICE CORE METHODS | Biological Material', in *Encyclopedia of Quaternary Science*. Elsevier, pp. 288–297. doi: <https://doi.org/10.1016/B978-0-444-53643-3.00308-3>.
- Ravich, M. G. and Solo'vev, D. S. (1969) 'Geology and petrology of the mountains of central Queen Maud Land', *Isreal Programme for Scientific Translations, Jerusalem*.
- Ravikant, V. *et al.* (2011) 'Petrology and geochemistry of the Grubergebirge anorthosite and marginal rocks, central Dronning Maud Land: Further characterization of the Late Neoproterozoic magmatic event in East Antarctica', *Journal of the Geological Society of India*, 78(1), pp. 7–18. doi: [10.1007/s12594-011-0062-z](https://doi.org/10.1007/s12594-011-0062-z).
- Reimer, P. J., Brown, T. A. and Reimer, R. W. (2004) 'Discussion: Reporting and calibration of post-bomb ^{14}C data', *Radiocarbon*. doi: [10.1017/S0033822200033154](https://doi.org/10.1017/S0033822200033154).
- Rhodes, R. H. *et al.* (2012) 'Little Ice Age climate and oceanic conditions of the Ross Sea, Antarctica from a coastal ice core record', *Climate of the Past*. doi: [10.5194/cp-8-1223-2012](https://doi.org/10.5194/cp-8-1223-2012).
- Röthlisberger, R. *et al.* (2000) 'Factors controlling nitrate in ice cores: Evidence from the Dome C deep ice core', *Journal of Geophysical Research Atmospheres*. doi: [10.1029/2000JD900264](https://doi.org/10.1029/2000JD900264).
- Röthlisberger, R. *et al.* (2003) 'Limited dechlorination of sea-salt aerosols during the last glacial period: Evidence from the European Project for Ice Coring in Antarctica (EPICA) Dome C ice core', *Journal of Geophysical Research D: Atmospheres*.
- Rudnick, R. L. and Gao, S. (2013) 'Composition of the Continental Crust', in *Treatise on Geochemistry: Second Edition*. doi: [10.1016/B978-0-08-095975-7.00301-6](https://doi.org/10.1016/B978-0-08-095975-7.00301-6).
- Samyn, D., Fitzsimons, S. J. and Lorrain, R. D. (2005) 'Strain-induced phase changes within cold basal ice from Taylor Glacier, Antarctica, indicated by textural and gas analyses', *Journal of Glaciology*, 51(175), pp. 611–619. doi: [10.3189/172756505781829098](https://doi.org/10.3189/172756505781829098).
- Santibáñez, P. A. *et al.* (2019) 'Differential incorporation of bacteria, organic matter, and inorganic ions into lake ice during ice formation', *Journal of Geophysical Research: Biogeosciences*, 124(3), pp. 585–600. doi: [10.1029/2018JG004825](https://doi.org/10.1029/2018JG004825).
- Sävström, C. *et al.* (2008) 'Bacteriophage in polar inland waters', *Extremophiles*, 12(2), pp. 167–175. doi: [10.1007/s00792-007-0134-6](https://doi.org/10.1007/s00792-007-0134-6).
- Schmitt, J. *et al.* (2012) 'Carbon isotope constraints on the deglacial CO_2 rise from ice cores', *Science*. doi: [10.1126/science.1217161](https://doi.org/10.1126/science.1217161).

- Schneider, R. (2011) *Quantifying past changes of the global carbon cycle based on $\delta^{13}\text{C}$ measurements in Antarctic ice cores*. (Doctoral dissertation, PhD Thesis, University of Bern).
- Schneider, R. *et al.* (2013) 'A reconstruction of atmospheric carbon dioxide and its stable carbon isotopic composition from the penultimate glacial maximum to the last glacial inception', *Climate of the Past*. doi: 10.5194/cp-9-2507-2013.
- Schwab, M. J. (1998) *Reconstruction of the Late Quaternary climatic and environmental history of the Schirmacher Oasis and the Wohlthat Massif (East Antarctica)*, *Berichte zur Polarforschung*.
- Siegert, M. J. *et al.* (2005) 'A revised inventory of Antarctic subglacial lakes', *Antarctic Science*. University of Ottawa – Library Network, 17(3), pp. 453–460. doi: 10.1017/S0954102005002889.
- Singh, R. K. *et al.* (1988) *A Short Account of the Basic and Ultrabasic Rocks Occurring Between Schirmacher Hills and Gruber Massif, Central Queen*.
- Spaulding, S. A. *et al.* (1994) 'Phytoplankton population dynamics in perennially ice-covered Lake Fryxell, Antarctica', *Journal of Plankton Research*, 16(5), pp. 527–541. doi: 10.1093/plankt/16.5.527.
- Spigel, R. H. and Priscu, J. C. (1998) 'Physical Limnology of the McMurdo Dry Valleys Lakes', in Priscu, J. C. (ed.) *Ecosystem dynamics in a polar desert: the McMurdo Dry Valleys, Antarctica*. American Geophysical Union, pp. 153–187. doi: 10.1029/AR072p0153.
- St-Jean, G. (2003) 'Automated quantitative and isotopic (^{13}C) analysis of dissolved inorganic carbon and dissolved organic carbon in continuous-flow using a total organic carbon analyser', *Rapid Communications in Mass Spectrometry*, 17(5), pp. 419–428. doi: 10.1002/rcm.926.
- St-Jean, G. *et al.* (2017) 'Semi-automated equipment for CO_2 purification and graphitization at the A.E. Lalonde AMS Laboratory (Ottawa, Canada)', *Radiocarbon*, 59(3), pp. 941–956. doi: 10.1017/RDC.2016.57.
- Steel, H. C. B., McKay, C. P. and Andersen, D. T. (2015) 'Modeling circulation and seasonal fluctuations in perennially ice-covered and ice-walled Lake Untersee, Antarctica', *Limnology and Oceanography*, 60(4), pp. 1139–1155. doi: 10.1002/lno.10086.
- Stuiver, M. and Polach, H. A. (1977) 'Reporting of ^{14}C data', *Radiocarbon*. doi: 10.1016/j.forsciint.2010.11.013.
- Tanabe, Y. *et al.* (2019) 'Light quality determines primary production in nutrient-poor small lakes', *Scientific reports*, 9(1), p. 4639. doi: 10.1038/s41598-019-41003-9.
- Tomkins, J. D. *et al.* (2008) 'A simple and effective method for preserving the sediment-water interface of sediment cores during transport', *Journal of Paleolimnology*, 40(1), pp. 577–582. doi: 10.1007/s10933-007-9175-1.

- Vincent, W. F. (1981) 'Production strategies in Antarctic inland waters: Phytoplankton eco-physiology in a permanently ice-covered lake', *Ecology*, 62(5), pp. 1215–1224. doi: 10.2307/1937286.
- Vincent, W. F. and Quesada, A. (2012) 'Cyanobacteria in High Latitude Lakes, Rivers and Seas', in Whitton, B. A. (ed.) *Ecology of Cyanobacteria II: Their Diversity in Space and Time*. Dordrecht: Springer, pp. 371–385. doi: 10.1007/978-94-007-3855-3.
- Wadham, J. L. *et al.* (2010) 'Biogeochemical weathering under ice: Size matters', *Global Biogeochemical Cycles*, 24(3). doi: 10.1029/2009GB003688.
- Wagner, N. Y. *et al.* (2019) 'Draft Genome Sequence from a Putative New Genus and Species in the Family Methanoregulaceae Isolated from the Anoxic Basin of Lake Untersee in East Antarctica', *Microbiology Resource Announcements*. doi: 10.1128/mra.00271-19.
- Wand, U. *et al.* (1997) 'Evidence for physical and chemical stratification in Lake Untersee (central Dronning Maud Land, East Antarctica)', *Antarctic Science*, 9(1), pp. 43–45. doi: 10.1017/s0954102097000060.
- Wand, U. *et al.* (2006) 'Biogeochemistry of methane in the permanently ice-covered Lake Untersee, central Dronning Maud Land, East Antarctica', *Limnology and Oceanography*, 51(2), pp. 1180–1194. doi: 10.4319/lo.2006.51.2.1180.
- Wand, U. and Perlt, J. (1999) 'Glacial boulders "floating" on the ice cover of Lake Untersee, East Antarctica', *Antarctic Science*, 11(2), pp. 256–260. doi: 10.1017/s0954102099000310.
- Weisleitner, K. *et al.* (2019) 'Source environments of the microbiome in perennially ice-covered Lake Untersee, Antarctica', *Frontiers in Microbiology*, 10(May), pp. 1–18. doi: 10.3389/fmicb.2019.01019.
- White, W. M. (2013) 'Chapter 7: Trace Elements in Igneous Processes', in *Geochemistry*. John Wiley & Sons, Ltd., pp. 268–318.
- Wolff, E. W. *et al.* (2006) 'Southern Ocean sea-ice extent, productivity and iron flux over the past eight glacial cycles', *Nature*. doi: 10.1038/nature04614.
- Worrall, F. and Pearson, D. G. (2001) 'The development of acidic groundwaters in coal-bearing strata: Part I. Rare earth element fingerprinting', *Applied Geochemistry*. doi: 10.1016/S0883-2927(01)00018-X.
- Wright, A. and Siegert, M. (2012) 'A fourth inventory of Antarctic subglacial lakes', *Antarctic Science*. doi: 10.1017/S095410201200048X.
- Wynn, P. M., Hodson, A. and Heaton, T. (2006) 'Chemical and isotopic switching within the subglacial environment of a High Arctic glacier', *Biogeochemistry*. doi: 10.1007/s10533-005-3832-0.

Xing, S. *et al.* (2015) 'Iodine-129 in snow and seawater in the Antarctic: Level and source', *Environmental Science and Technology*, 49(11), pp. 6691–6700. doi: 10.1021/acs.est.5b01234.

Zhang, J. (2019) *Origin of porewater sulfate in an Ordovician aquiclude of the Michigan Basin, Ontario: Insights from stable isotopes*. (MSc. Thesis, University of Ottawa). doi: <http://dx.doi.org/10.20381/ruor-22994>.

Zhou, Y. *et al.* (2015) 'Analytical methods and application of stable isotopes in dissolved organic carbon and inorganic carbon in groundwater', *Rapid Communications in Mass Spectrometry*. doi: 10.1002/rcm.7280.

Appendix A: External Laboratory (IT2) Methodology for
Analysis of Nitrogen and Oxygen of Nitrate ($\delta^{15}\text{N}$ and $\delta^{18}\text{O}$)

¹⁵N & ¹⁸O ANALYSIS OF NITRATES (NO₃) IN AQUEOUS SAMPLES

Sample preparation:

Nitrate is concentrated and collected in a 5 mL anion exchange column, after the resin has been cleaned and rinsed with acid and deionized water respectively. The volume of water required to collect sufficient nitrate for isotopic analysis is dependent on the concentration, and can range from 10 mL to several litres of water. Nitrate concentration data is required with sample submission. Prior to running samples through the column, sulfate is removed through additions of barium chloride to precipitate barium sulfate, which is then filtered out of the samples. Sulfate removal is required to prevent the column from preferentially binding sulfate over nitrates. Once samples have been collected from the column, chloride removal is required through additions of clean silver oxide. Silver chloride is then filtered from the samples prior to sample freezing. Samples are frozen overnight, freeze dried the following day, and ready for weighing for isotopic analysis.

Sample Analysis:

Dried samples are weighed into tin cups for separate ¹⁸O and ¹⁵N analysis with a replicate every 3 samples. Approximately 0.1 mg of sample is used for ¹⁸O analysis. ¹⁸O samples are combusted at 1455°C, and purified by gas chromatography before continuous flow isotope ratio mass spectrometry. Analysis is carried out on a Finnigan Mat, DeltaPlus XL IRMS coupled with a Thermo Scientific TC/EA. Data is corrected and normalized using four international standards: USGS 32, NBS 127, IAEA SO5, and IAEA SO6, that bracket the samples. Standards are analyzed at the beginning and end of every run.

The analytical precision for analysis is ± 0.5%.

Analysis for ¹⁵N is carried out on a Finnigan Mat DeltaPlus IRMS with ConFlo III Interface coupled with a CE instruments EA 1110 CHN. Data is corrected and normalized using three international standards, IAEA-N1, IAEA-N2, IAEA-C6, and four calibrated internal standards, that bracket the samples. Standards are run at the beginning, middle and end of every run. The results are evaluated and corrected against standards run with the samples, and then reported against the international reference material.

The analytical precision for analysis is ± 0.3%.



#	Sample ID	Date	Sample #	$\delta^{18}\text{O}$	Result	Repeat	$\delta^{15}\text{N}$	Result	Repeat
				NO_3	VSMOW		NO_3	AIR	
1	Pond1	2017-11-24	50745	X	5.5		X	22.6	22.3
2	Pond3	2017-11-24	50746	X	17.0		X	NEP	
3	AH-10	2017-11-27	50747	X	18.3		X	8.8	
4	AH-40	2017-11-27	50748	X	-12.1		X	11.9	
5	AH-70	2017-11-27	50749	X	-2.0		X	10.1	9.8
6	OH-10	2017-11-26	50750	X	16.8		X	5.1	
7	OH-40	2017-11-26	50751	X	16.2	15.8	X	9.4	9.5
8	OH-80	2017-11-26	50752	X	18.7		X	7.3	
9	OH-120	2017-11-26	50753	X	11.2		X	9.2	9.0

Note

NEP: Not enough precipitate

18O NO3 Analyses**Instrument Used:**

Isotope Ratio Mass Spectrometry (IRMS) - Delta^{Plus}, Finnigan MAT, Germany
 Coupled with TC/EA, Thermo Scientific, Germany.

Standard Used:

USGS-32 / NBS-127 / IAEA-SO-5 / IAEA-SO-6

Typical Standard deviation:

±0.5‰

15N NO3 Analyses**Instrument Used:**

Delta^{Plus} Isotope Ratio Mass Spectrometry (IRMS), Finnigan MAT, Germany.
 Coupled with an Elemental Analyzer EA 1110 CHN, CE Instruments, Italy

Standard Used:IT²-601 / IAEA-N1 / IAEA-N2 / Acetanilide (B2000)**Typical Standard deviation:**

±0.3‰

Approved by:

Orfan Shouakar-Stash, PhD**Director**

Isotope Tracer Technologies Inc.

695 Rupert St. Unit B, Waterloo, ON, N2V 1Z5

Tel: 519-886-5555 | Fax: 519-886-5575

Email: orfan@it2isotopes.comWebsite: www.it2isotopes.com

Appendix B: Lake and Pond Water Data

Appendix B.1 Major ions in waters

Sample ID	Depth (m)	Al (ppm)	±	Ca (ppm)	±	K (ppm)	±	Mg (ppm)	±	Na (ppm)	±
North Basin Profile											
NB-5	5	0.0771	0.0066	46.34	1.57	3.156	0.244	0.225	0.010	60.23	1.4
NB-10	10	0.0786	0.0045	43.16	1.93	3.250	0.251	0.151	0.012	59.11	2.4
NB-20	20	0.0752	0.0018	43.84	1.73	3.230	0.358	0.106	0.007	63.98	0.5
NB-30	30	0.0791	0.0053	47.21	0.35	3.517	0.181	0.124	0.030	62.54	2.9
NB-40	40	0.0767	0.0033	46.36	3.22	3.410	0.187	0.114	0.002	63.18	1.4
NB-50	50	0.0752	0.0013	43.10	1.50	3.260	0.064	0.110	0.026	60.65	3.0
NB-50D	50	0.0796	0.0040	45.82	0.64	3.583	0.074	0.135	0.010	62.97	3.9
NB-60	60	0.0789	0.0032	46.76	0.98	3.606	0.018	0.134	0.026	62.77	1.4
NB-70	70	0.0792	0.0031	47.26	0.35	3.516	0.134	0.163	0.015	61.68	4.1
NB-80	80	0.0770	0.0031	45.63	2.14	3.511	0.209	0.140	0.011	61.92	0.9
NB-90	90	0.0785	0.0041	45.62	1.17	3.498	0.149	0.156	0.001	61.81	3.1
NB-100	100	0.0807	0.0023	46.39	1.84	3.612	0.164	0.116	0.029	62.83	1.0
NB-110	110	0.0786	0.0078	46.84	1.81	3.624	0.352	0.165	0.002	60.12	1.8
NB-120	120	0.0797	0.0032	45.28	0.51	3.532	0.128	0.257	0.024	60.60	2.4
NB-130	130	0.0796	0.0054	46.47	1.76	3.704	0.136	0.194	0.007	62.42	2.2
NB-140	140	0.0793	0.0010	46.22	0.61	3.436	0.078	0.137	0.011	61.95	2.6
NB-145	145	0.0795	0.0020	44.96	1.19	3.562	0.266	0.116	0.017	61.22	1.8
NB-150	150	0.0823	0.0028	46.43	2.46	3.625	0.333	0.127	0.030	61.74	6.7
NB-155	155	0.0809	0.0032	46.15	1.66	3.410	0.140	0.171	0.016	63.03	1.5
South Basin Profile											
SB-5	5	0.0809	0.0031	46.32	0.39	3.585	0.424	0.118	0.016	62.04	2.9
SB-10	10	0.0782	0.0068	46.11	2.67	3.577	0.113	0.145	0.019	63.22	2.7
SB-20	20	0.0804	0.0060	46.98	2.50	3.645	0.299	0.201	0.004	62.73	4.5
SB-30	30	0.0802	0.0038	45.60	1.05	3.788	0.187	0.110	0.018	60.16	3.2
SB-40	40	0.0795	0.0015	45.88	0.96	3.560	0.145	0.116	0.019	60.27	0.6
SB-50	50	0.0800	0.0010	44.32	2.07	3.608	0.184	0.109	0.017	60.20	0.1
SB-50D	50	0.0799	0.0050	45.60	2.35	3.455	0.117	0.124	0.003	60.04	4.1
SB-60	60	0.0791	0.0051	45.10	1.02	3.369	0.179	0.110	0.024	60.93	1.8
SB-65	65	0.0497	0.0011	47.86	1.64	3.729	0.196	0.268	0.001	64.21	2.6
SB-70	70	0.0072	0.0027	52.68	2.61	3.777	0.040	0.597	0.015	65.32	3.2
SB-75	75	0.0043	0.0018	52.62	1.46	3.859	0.196	0.640	0.019	64.56	4.0
SB-80	80	0.0045	0.0006	59.77	0.87	4.630	0.135	2.470	0.040	69.15	1.9
SB-80D	80	0.0048	0.0012	57.58	2.50	4.301	0.020	1.943	0.047	71.08	1.1
SB-85	85	0.0070	0.0019	87.16	2.45	7.353	0.133	9.429	0.360	98.70	2.0
SB-90	90	0.0147	0.0014	109.12	3.55	9.733	0.257	14.646	0.095	115.81	3.6
SB-95	95	0.0257	0.0005	123.32	4.32	11.110	0.064	18.225	0.201	126.58	1.8
Lateral Moraine Ponds											
Pond Burevestniksee	2	0.0658	0.0042	82.53	3.09	11.716	0.632	2.254	0.072	96.69	6.2
P2 Pond	1	0.1421	0.0054	31.18	0.42	4.433	0.124	0.186	0.013	24.25	0.2

Al, C, K, Mg and Si measured by ICP-AES

NO₂, NO₃, SO₄, Cl and F measured by ion chromatography

Br and I measured by ICP-MS in basic (NH₄) solution

Sample ID's ending with 'D' are field duplicates

ICP-AES errors are ± (2σ) standard deviation of three measurements by instrument (n=3)

Ion chromatography errors are ± maximum (2σ) standard deviation of duplicate samples per analyte.

BLD = below limit of detection

Appendix B.1 Major ions in waters

Sample ID	Si (ppm)	±	Sr (ppm)	±	NO ₂ (ppm)	±	NO ₃ (ppm)	±	SO ₄ (ppm)	±
North Basin Profile										
NB-5	2.21	0.01	0.0181	0.0004	0.18	0.08	0.494	0.007	166.4	1.8
NB-10	2.25	0.01	0.0181	0.0004	0.19	0.08	0.503	0.007	165.7	1.8
NB-20	2.23	0.14	0.0178	0.0006	0.19	0.08	0.511	0.007	166.0	1.8
NB-30	2.27	0.04	0.0184	0.0002	0.18	0.08	0.507	0.007	168.0	1.8
NB-40	2.26	0.03	0.0177	0.0004	0.18	0.08	0.507	0.007	166.4	1.8
NB-50	2.29	0.02	0.0178	0.0002	0.18	0.08	0.502	0.007	166.3	1.8
NB-50D	2.25	0.02	0.0182	0.0003	0.19	0.08	0.499	0.007	166.1	1.8
NB-60	2.26	0.03	0.0182	0.0002	0.19	0.08	0.454	0.007	165.8	1.8
NB-70	2.29	0.01	0.0182	0.0002	0.19	0.08	0.502	0.007	166.0	1.8
NB-80	2.26	0.02	0.0181	0.0003	0.19	0.08	0.504	0.007	166.6	1.8
NB-90	2.23	0.04	0.0184	0.0003	0.19	0.08	0.498	0.007	166.1	1.8
NB-100	2.20	0.03	0.0181	0.0004	0.20	0.08	0.525	0.007	166.4	1.8
NB-110	2.20	0.01	0.0183	0.0005	0.20	0.08	0.503	0.007	165.6	1.8
NB-120	2.25	0.02	0.0183	0.0001	0.20	0.08	0.509	0.007	165.8	1.8
NB-130	2.26	0.01	0.0183	0.0005	0.20	0.08	0.491	0.007	165.7	1.8
NB-140	2.30	0.00	0.0183	0.0001	0.20	0.08	0.491	0.007	166.0	1.8
NB-145	2.22	0.02	0.0183	0.0002	0.20	0.08	0.503	0.007	165.2	1.8
NB-150	2.25	0.02	0.0182	0.0003	0.19	0.08	0.492	0.007	164.6	1.8
NB-155	2.23	0.03	0.0180	0.0001	0.20	0.08	0.495	0.007	166.7	1.8
South Basin Profile										
SB-5	2.21	0.02	0.0181	0.0004	0.20	0.08	0.507	0.007	166.1	1.8
SB-10	2.28	0.02	0.0185	0.0003	0.20	0.08	0.509	0.007	165.4	1.8
SB-20	2.26	0.03	0.0184	0.0004	0.17	0.08	0.521	0.007	166.4	1.8
SB-30	2.26	0.03	0.0184	0.0002	0.21	0.08	0.509	0.007	165.2	1.8
SB-40	2.24	0.01	0.0188	0.0003	0.21	0.08	0.491	0.007	165.0	1.8
SB-50	2.23	0.03	0.0183	0.0001	0.20	0.08	0.490	0.007	165.6	1.8
SB-50D	2.23	0.00	0.0182	0.0002	0.20	0.08	0.499	0.007	165.8	1.8
SB-60	2.26	0.02	0.0183	0.0001	0.20	0.08	0.495	0.007	165.8	1.8
SB-65	2.31	0.02	0.0199	0.0004	0.36	0.08	0.359	0.007	167.0	1.8
SB-70	2.51	0.01	0.0209	0.0003	0.72	0.08	0.107	0.007	164.6	1.8
SB-75	2.67	0.01	0.0212	0.0005	0.98	0.08	0.226	0.007	163.3	1.8
SB-80	3.77	0.01	0.0260	0.0003	1.52	0.08	0.018	0.007	137.4	1.8
SB-80D	3.64	0.05	0.0251	0.0003	1.68	0.08	<0.010	0.007	133.7	1.8
SB-85	7.95	0.08	0.0484	0.0012	5.40	0.08	0.039	0.007	53.7	1.8
SB-90	10.47	0.04	0.0657	0.0010	7.89	0.08	0.085	0.007	20.0	1.8
SB-95	11.66	0.12	0.0769	0.0002	10.01	0.08	<0.010	0.007	3.8	1.8
Lateral Moraine Ponds										
Pond Burevestniksee	2.34	0.04	0.219	0.004	0.38	0.08	8.321	0.007	113.9	1.8
P2 Pond	2.35	0.01	0.055	0.001	0.55	0.08	0.187	0.007	43.1	1.8

Appendix B.1 Major ions in waters

Sample ID	F (ppm)	±	Cl (ppm)	±	Br (ppb)	±	I (ppb)	±
North Basin Profile								
NB-5	0.177	0.021	38.7	0.1	96.94	3.44	26.48	0.51
NB-10	0.138	0.021	38.5	0.1	97.50	4.91	27.06	1.46
NB-20	0.137	0.021	38.6	0.1	100.16	4.08	27.76	0.98
NB-30	0.139	0.021	39.1	0.1	98.23	7.80	27.44	1.47
NB-40	0.136	0.021	38.7	0.1	98.72	4.88	27.25	2.26
NB-50	0.137	0.021	38.7	0.1	95.63	3.26	26.75	1.34
NB-50D	0.135	0.021	38.6	0.1	102.56	3.82	28.45	1.07
NB-60	0.134	0.021	38.6	0.1	102.38	4.08	28.30	1.06
NB-70	0.134	0.021	38.6	0.1	103.03	1.00	28.66	0.61
NB-80	0.134	0.021	38.7	0.1	97.23	3.55	27.12	0.96
NB-90	0.170	0.021	38.6	0.1	97.05	1.76	27.03	0.43
NB-100	0.137	0.021	38.7	0.1	100.89	5.08	28.52	0.84
NB-110	0.172	0.021	38.5	0.1	103.79	3.87	28.86	0.99
NB-120	0.172	0.021	38.7	0.1	93.38	1.30	25.99	0.49
NB-130	0.172	0.021	38.6	0.1	98.26	2.19	27.20	0.89
NB-140	0.172	0.021	38.6	0.1	103.36	2.37	28.71	0.92
NB-145	0.134	0.021	38.4	0.1	104.66	2.20	29.48	0.18
NB-150	0.134	0.021	38.3	0.1	100.53	3.75	27.84	1.62
NB-155	0.134	0.021	38.7	0.1	101.61	5.96	28.30	1.60
South Basin Profile								
SB-5	0.138	0.021	38.6	0.1	102.79	2.00	29.11	0.74
SB-10	0.135	0.021	38.5	0.1	94.03	3.51	26.23	0.26
SB-20	0.135	0.021	38.7	0.1	97.59	3.19	27.10	1.88
SB-30	0.175	0.021	38.6	0.1	97.04	2.85	27.48	0.37
SB-40	0.135	0.021	38.5	0.1	99.24	3.73	27.55	1.09
SB-50	0.135	0.021	38.5	0.1	102.55	1.15	29.20	0.38
SB-50D	0.133	0.021	38.6	0.1	104.99	2.92	29.75	0.27
SB-60	0.135	0.021	38.6	0.1	102.42	2.63	29.21	0.17
SB-65	0.174	0.021	39.6	0.1	104.78	3.22	29.68	1.27
SB-70	0.180	0.021	72.1	0.1	103.68	3.88	30.72	0.79
SB-75	0.183	0.021	40.4	0.1	104.80	0.76	30.93	0.87
SB-80	0.200	0.021	41.0	0.1	103.91	5.11	40.38	2.45
SB-80D	0.158	0.021	41.2	0.1	101.68	4.58	41.76	1.97
SB-85	0.182	0.021	44.8	0.1	112.96	2.29	75.06	3.14
SB-90	0.184	0.021	48.4	0.1	127.32	8.90	129.93	9.73
SB-95	0.163	0.021	51.2	0.1	135.32	5.59	172.41	9.76
Lateral Moraine Ponds								
Pond Burevestniksee	0.505	0.021	184.5	0.1	108.35	4.63	13.56	0.70
P2 Pond	0.317	0.021	32.4	0.1	26.51	0.96	2.31	0.24

Appendix B.2 Trace elements in waters

Sample ID	Depth (m)	Li (ppb)	RSD (%)	B (ppb)	RSD (%)	P (ppb)	RSD (%)	Sc (ppb)	RSD (%)	Ti (ppb)	RSD (%)
North Basin Profile											
NB-5	5	0.5708	1.8	11.07	1.3	<5		0.8672	0.1	0.5570	3.8
NB-10	10	0.5841	1.0	11.66	0.6	<5		0.9239	0.8	0.6166	5.1
NB-20	20	0.5866	1.5	12.42	1.7	<5		0.9361	4.6	0.5767	2.2
NB-30	30	0.6069	0.3	12.93	2.5	<5		0.9921	1.3	0.5840	6.1
NB-40	40	0.5973	1.1	13.38	0.7	<5		0.9740	3.0	0.4968	6.5
NB-50	50	0.6142	2.2	13.62	0.2	<5		0.9669	0.4	0.5544	2.1
NB-50D	50	0.6207	1.6	13.74	2.4	<5		1.0475	1.0	0.6782	2.6
NB-60	60	0.6166	2.3	14.13	0.3	<5		1.0267	1.7	0.6697	7.0
NB-70	70	0.6021	2.4	14.12	0.7	<5		1.0166	1.5	0.6403	2.1
NB-80	80	0.6178	1.1	14.23	1.1	<5		1.0382	4.3	0.6498	2.5
NB-90	90	0.6123	2.0	14.09	0.6	<5		1.0583	2.3	0.6643	3.5
NB-100	100	0.6191	1.2	14.21	0.2	<5		1.0754	8.4	0.6646	5.9
NB-110	110	0.6137	1.1	14.46	1.3	<5		0.9925	2.8	0.6284	8.6
NB-120	120	0.6105	2.8	14.59	1.0	<5		0.9966	1.0	0.6309	6.7
NB-130	130	0.6139	0.2	14.79	1.3	<5		1.0287	0.9	0.6556	4.6
NB-140	140	0.5943	1.1	14.91	1.5	<5		1.0198	2.5	0.6349	2.9
NB-145	145	0.6133	2.6	15.11	1.3	<5		1.0206	2.2	0.6537	9.0
NB-150	150	0.6046	2.8	15.12	1.4	<5		1.0155	2.1	0.6380	2.1
NB-155	155	0.6082	0.8	15.32	0.6	<5		1.0374	1.7	0.6851	1.4
South Basin Profile											
SB-5	5	0.6178	3.0	15.16	0.9	<5		1.0557	3.5	0.6670	4.9
SB-10	10	0.6064	0.8	14.98	0.8	<5		1.0682	3.0	0.6505	3.6
SB-20	20	0.6135	1.7	15.07	0.4	<5		1.0461	0.8	0.6706	2.9
SB-30	30	0.6238	2.2	15.48	2.3	<5		1.0287	1.6	0.6818	2.8
SB-40	40	0.6215	0.8	16.18	1.3	<5		1.5552	2.2	1.2436	3.2
SB-50	50	0.6088	0.8	15.50	2.3	<5		1.0500	2.7	0.6563	4.0
SB-50D	50	0.6149	1.6	15.15	2.3	<5		1.0226	2.0	0.6407	3.1
SB-60	60	0.6272	0.2	15.28	0.5	<5		1.0482	1.2	0.6909	0.9
SB-65	65	0.7313	2.2	16.05	2.0	<5		1.0397	1.7	0.6130	6.1
SB-70	70	0.8176	0.6	14.97	2.3	<5		1.1230	1.6	0.6655	3.3
SB-75	75	0.8317	1.4	15.13	1.2	<5		1.1721	3.3	0.6398	3.1

Appendix B.2 Trace elements in waters

Sample ID	Depth (m)	V (ppb)	RSD (%)	Cr (ppb)	RSD (%)	Mn (ppb)	RSD (%)	Fe (ppb)	RSD (%)	Co (ppb)	RSD (%)
North Basin Profile											
NB-5	5	14.69	0.6	0.105	7.4	0.0362	20.0	1.181	6.4	0.0925	3.3
NB-10	10	15.67	2.6	0.131	2.3	0.0508	14.6	3.749	0.8	0.0973	4.0
NB-20	20	16.13	1.4	0.130	6.0	0.0374	4.0	0.587	22.1	0.0983	0.9
NB-30	30	16.81	1.7	0.201	4.7	0.0752	9.0	1.497	5.7	0.1064	0.6
NB-40	40	16.93	0.9	0.162	2.8	0.0233	26.1	<0.14		0.0996	1.8
NB-50	50	17.16	1.8	0.171	2.6	0.0280	12.2	<0.14		0.1001	2.2
NB-50D	50	17.62	1.7	0.184	5.0	0.0515	11.9	1.516	41.1	0.1098	1.8
NB-60	60	17.52	0.4	0.172	3.6	0.0554	1.2	1.098	8.8	0.1102	1.9
NB-70	70	17.58	1.3	0.181	0.4	0.0455	8.1	0.402	29.4	0.1092	2.1
NB-80	80	17.70	0.4	0.181	2.6	0.0486	14.2	0.900	10.0	0.1065	2.4
NB-90	90	17.52	2.6	0.205	3.0	0.0750	5.3	0.776	12.1	0.1311	1.9
NB-100	100	17.83	0.4	0.212	12.3	0.0846	26.6	0.746	6.6	0.1310	19.0
NB-110	110	18.06	2.5	0.209	3.4	0.0515	0.7	0.401	30.7	0.1170	3.4
NB-120	120	18.11	2.1	0.205	4.7	0.0681	3.3	0.435	15.3	0.1174	3.6
NB-130	130	18.26	2.4	0.214	2.5	0.0648	4.5	0.566	11.2	0.1145	2.5
NB-140	140	18.07	2.3	0.230	5.2	0.0552	15.5	0.466	23.0	0.1135	2.0
NB-145	145	17.81	1.3	0.217	2.6	0.0600	5.7	0.615	8.5	0.1142	5.4
NB-150	150	18.34	2.0	0.215	2.6	0.0616	5.0	0.359	65.7	0.1157	1.7
NB-155	155	18.12	1.4	0.229	4.4	0.0774	2.5	1.037	9.9	0.1141	0.7
South Basin Profile											
SB-5	5	18.22	1.5	0.252	1.0	0.0671	9.6	0.712	1.4	0.1153	0.7
SB-10	10	17.71	2.7	0.250	4.3	0.0926	3.4	0.197	32.7	0.1181	2.4
SB-20	20	18.45	3.4	0.216	1.7	0.0725	4.1	0.568	27.7	0.1156	3.2
SB-30	30	18.70	1.1	0.218	3.9	0.0632	12.6	0.545	14.8	0.1164	2.1
SB-40	40	18.94	3.6	0.785	1.3	0.6111	2.4	1.135	11.8	0.6519	0.7
SB-50	50	18.57	0.8	0.221	7.0	0.0611	10.5	0.553	8.4	0.1104	4.4
SB-50D	50	18.51	1.6	0.216	3.7	0.0533	0.4	0.214	37.9	0.1089	1.2
SB-60	60	18.48	0.6	0.236	3.0	0.0710	6.0	0.446	4.8	0.1159	4.4
SB-65	65	13.50	0.8	0.173	3.7	0.5527	0.8	0.570	4.7	0.1276	3.0
SB-70	70	4.44	0.8	0.066	8.3	5.5011	2.1	1.082	6.6	0.1262	3.5
SB-75	75	3.05	0.9	0.066	9.1	8.3536	1.2	4.325	0.4	0.1270	2.6

Appendix B.2 Trace elements in waters

Sample ID	Depth (m)	Ni (ppb)	RSD (%)	Cu (ppb)	RSD (%)	Zn (ppb)	RSD (%)	As (ppb)	RSD (%)	Rb (ppb)	RSD (%)
North Basin Profile											
NB-5	5	0.6734	2.4	0.549	2.1	1.3441	2.0	4.17	1.0	0.163	1.0
NB-10	10	0.7989	4.3	1.013	1.2	2.1681	0.5	4.43	0.6	0.172	1.1
NB-20	20	0.7838	5.6	0.766	2.3	0.9972	1.4	4.57	1.1	0.173	1.9
NB-30	30	0.8257	4.9	0.469	1.2	0.9366	3.7	4.67	0.1	0.183	2.7
NB-40	40	0.8026	1.4	0.223	5.0	0.8500	1.5	4.77	0.9	0.171	0.2
NB-50	50	0.8549	2.7	0.159	4.6	0.5896	2.5	4.80	0.4	0.179	1.2
NB-50D	50	0.8858	3.1	0.290	4.3	0.7393	2.0	4.76	1.3	0.188	2.2
NB-60	60	0.8887	6.2	0.319	1.3	0.8175	4.1	4.80	0.6	0.187	1.2
NB-70	70	0.8869	3.9	0.247	5.4	0.6155	3.2	4.91	1.3	0.189	0.6
NB-80	80	0.8739	2.0	0.180	7.2	0.6156	1.9	4.90	1.1	0.190	3.0
NB-90	90	0.9189	2.4	0.748	2.2	1.0371	2.8	4.83	0.8	0.189	2.0
NB-100	100	0.9363	5.1	0.225	6.3	0.5904	4.9	4.96	0.3	0.201	4.4
NB-110	110	0.8885	0.6	0.247	5.0	0.5614	2.9	4.94	1.2	0.191	1.9
NB-120	120	1.0629	0.6	12.882	1.0	11.6417	1.2	5.03	0.3	0.192	1.0
NB-130	130	0.8914	3.7	0.358	2.9	0.6967	3.1	5.11	1.9	0.192	0.9
NB-140	140	0.8784	5.2	0.833	0.5	0.9612	2.0	5.10	1.4	0.187	0.6
NB-145	145	0.9265	1.3	1.448	1.3	1.6564	1.0	5.03	2.1	0.191	0.5
NB-150	150	0.8740	3.7	0.355	4.4	0.6514	4.2	5.18	0.2	0.189	1.3
NB-155	155	0.8873	4.2	0.714	2.2	1.0019	2.4	5.11	1.0	0.192	1.7
South Basin Profile											
SB-5	5	0.9114	3.1	1.346	0.5	1.4905	1.0	5.17	1.1	0.196	1.9
SB-10	10	0.9204	2.5	1.908	0.4	2.1559	0.6	5.05	0.5	0.188	1.4
SB-20	20	0.8971	2.3	0.258	3.9	0.5737	1.8	5.18	0.2	0.193	3.1
SB-30	30	0.9034	4.6	0.265	3.4	0.5260	2.6	5.19	0.6	0.200	2.0
SB-40	40	1.4426	3.7	0.942	0.8	1.4069	1.9	5.83	2.1	0.194	2.4
SB-50	50	0.9052	1.8	0.298	1.7	0.5194	0.4	5.23	0.7	0.200	1.5
SB-50D	50	0.8784	2.4	0.332	2.7	0.5309	1.2	5.16	0.8	0.192	0.5
SB-60	60	0.8950	4.2	0.344	0.9	0.5249	0.8	5.20	0.7	0.195	0.7
SB-65	65	0.9548	2.6	0.563	0.6	0.5983	2.0	4.56	1.2	0.208	2.2
SB-70	70	1.0065	1.6	0.345	1.3	6.2599	1.3	3.78	1.8	0.220	3.8
SB-75	75	1.0133	4.0	0.286	6.4	2.1535	1.7	3.74	2.3	0.227	2.4

Appendix B.2 Trace elements in waters

Sample ID	Depth (m)	Y (ppb)	RSD (%)	Zr (ppb)	RSD (%)	Nb (ppb)	RSD (%)	Mo (ppb)	RSD (%)	Ag (ppb)	RSD (%)
North Basin Profile											
NB-5	5	0.0018	32.3	0.0016	40.6	<0.0033		10.16	0.8	0.0007	54.5
NB-10	10	0.0013	38.8	0.0012	14.2	<0.0033		10.54	1.4	0.0012	47.3
NB-20	20	0.0014	46.8	<0.0006		<0.0033		10.76	0.7	<0.0007	
NB-30	30	0.0013	25.5	0.0007	17.7	<0.0033		10.98	1.8	0.0026	44.7
NB-40	40	0.0014	18.0	0.0006	55.7	<0.0033		10.82	1.3	0.0007	17.0
NB-50	50	0.0015	59.1	<0.0006		<0.0033		10.96	0.2	0.0007	24.0
NB-50D	50	0.0012	84.6	0.0013	32.4	<0.0033		11.17	0.4	0.0009	10.5
NB-60	60	0.0017	50.1	0.0007	10.2	<0.0033		11.24	0.9	0.0007	17.0
NB-70	70	0.0017	27.1	0.0006	31.5	<0.0033		11.22	0.5	<0.0007	
NB-80	80	0.0022	19.5	<0.0006		<0.0033		11.30	1.7	0.0020	39.4
NB-90	90	0.0012	35.8	0.0010	5.8	<0.0033		11.07	0.4	0.0009	78.6
NB-100	100	0.0247	117.7	0.0141	123.3	0.0124	118.9	11.24	1.6	0.0119	126.6
NB-110	110	0.0016	73.6	0.0007	92.9	<0.0033		11.40	0.5	<0.0007	
NB-120	120	0.0013	37.1	<0.0006		<0.0033		11.28	0.7	0.0036	16.0
NB-130	130	0.0015	11.3	0.0006	35.3	<0.0033		11.17	0.3	0.0009	31.8
NB-140	140	0.0013	16.9	<0.0006		<0.0033		11.17	1.6	0.0011	36.3
NB-145	145	0.0010	51.4	<0.0006		<0.0033		11.45	1.8	0.0008	65.2
NB-150	150	0.0009	10.5	<0.0006		<0.0033		11.33	1.9	<0.0007	
NB-155	155	0.0009	43.0	<0.0006		<0.0033		11.49	1.4	0.0008	26.0
South Basin Profile											
SB-5	5	0.0009	44.8	<0.0006		<0.0033		11.43	0.3	0.0009	70.0
SB-10	10	0.0015	11.4	0.0008	53.7	<0.0033		11.26	1.2	0.0009	17.6
SB-20	20	0.0018	45.3	<0.0006		<0.0033		11.62	1.1	<0.0007	
SB-30	30	0.0022	10.3	<0.0006		<0.0033		11.55	0.3	0.0010	40.5
SB-40	40	0.0015	48.5	0.0008	25.8	<0.0033		11.99	1.0	<0.0007	
SB-50	50	0.0010	37.4	0.0006	60.9	<0.0033		11.63	0.3	0.0008	30.5
SB-50D	50	0.0015	79.2	<0.0006		<0.0033		11.44	1.3	<0.0007	
SB-60	60	0.0077	56.9	0.0030	80.2	0.0035	57.5	11.54	0.1	0.0028	40.1
SB-65	65	0.0022	17.9	<0.0006		<0.0033		10.29	1.9	0.0007	46.6
SB-70	70	0.0018	28.6	<0.0006		<0.0033		7.45	2.1	<0.0007	
SB-75	75	0.0019	11.3	<0.0006		<0.0033		6.84	0.7	<0.0007	

Appendix B.2 Trace elements in waters

Sample ID	Depth (m)	Cd (ppb)	RSD (%)	Sb (ppb)	RSD (%)	Cs (ppb)	RSD (%)	Ba (ppb)	RSD (%)	La (ppb)	RSD (%)
North Basin Profile											
NB-5	5	0.0324	7.1	0.0751	4.2	0.0013	14.3	2.35	2.1	0.0026	28.9
NB-10	10	0.0348	9.7	0.0771	6.0	0.0018	7.8	1.04	0.8	0.0034	23.6
NB-20	20	0.0322	2.1	0.0763	1.4	0.0021	21.1	0.88	1.8	0.0015	31.4
NB-30	30	0.0373	5.5	0.0837	3.7	0.0030	8.9	0.97	2.3	0.0018	33.3
NB-40	40	0.0320	14.3	0.0775	1.4	0.0030	2.4	0.89	1.4	0.0012	54.3
NB-50	50	0.0319	2.1	0.0799	2.5	0.0027	11.8	0.80	2.1	0.0011	12.4
NB-50D	50	0.0349	9.4	0.0766	3.8	0.0029	2.2	1.52	1.1	0.0029	23.9
NB-60	60	0.0326	3.5	0.0777	3.2	0.0021	5.0	0.94	2.1	0.0024	25.3
NB-70	70	0.0349	13.4	0.0768	3.2	0.0023	13.1	0.77	2.4	0.0022	28.1
NB-80	80	0.0323	30.3	0.0800	2.1	0.0023	7.9	1.04	0.2	0.0024	44.0
NB-90	90	0.0615	13.5	0.0791	8.0	0.0020	6.3	0.91	1.4	0.0020	46.7
NB-100	100	0.0693	42.1	0.0878	16.9	0.0133	109.9	0.79	5.4	0.0166	112.6
NB-110	110	0.0398	3.1	0.0817	5.3	0.0022	22.8	0.77	0.6	0.0025	33.2
NB-120	120	0.0471	11.5	0.0853	1.6	0.0021	16.0	0.72	0.1	0.0017	35.2
NB-130	130	0.0421	13.6	0.0768	3.6	0.0023	18.7	1.32	0.7	0.0028	25.5
NB-140	140	0.0409	4.3	0.0798	3.6	0.0023	17.7	0.77	1.2	0.0017	28.3
NB-145	145	0.0440	15.0	0.0815	3.7	0.0019	17.7	0.69	0.6	0.0014	11.1
NB-150	150	0.0375	11.2	0.0824	1.4	0.0023	6.9	0.81	3.1	0.0016	17.0
NB-155	155	0.0386	8.1	0.0823	2.8	0.0023	9.1	0.75	4.0	0.0025	10.8
South Basin Profile											
SB-5	5	0.0391	12.9	0.0796	3.4	0.0023	11.6	1.24	0.9	0.0020	20.2
SB-10	10	0.0489	10.3	0.0826	3.8	0.0020	7.5	0.78	4.9	0.0025	24.9
SB-20	20	0.0420	12.0	0.0793	3.2	0.0025	5.8	1.07	1.7	0.0017	32.6
SB-30	30	0.0431	6.2	0.0830	2.0	0.0027	9.0	0.72	2.2	0.0021	21.1
SB-40	40	0.5929	1.1	0.0876	3.1	0.0024	3.8	1.55	1.2	0.0014	81.0
SB-50	50	0.0412	8.8	0.0868	4.2	0.0023	3.9	0.62	2.8	0.0019	5.5
SB-50D	50	0.0392	6.1	0.0858	2.7	0.0026	7.0	0.62	1.5	0.0014	21.9
SB-60	60	0.0420	11.4	0.0837	5.1	0.0047	30.9	0.66	0.6	0.0051	49.5
SB-65	65	0.0402	20.1	0.0731	4.5	0.0024	15.2	0.97	1.5	0.0036	18.3
SB-70	70	0.0247	15.2	0.0508	2.8	0.0025	10.0	1.11	1.9	0.0045	12.9
SB-75	75	0.0194	5.4	0.0462	6.2	0.0024	17.7	1.23	1.2	0.0055	24.7

Appendix B.2 Trace elements in waters

Sample ID	Depth (m)	Ce (ppb)	RSD (%)	Pr (ppb)	RSD (%)	Nd (ppb)	RSD (%)	Sm (ppb)	RSD (%)	Eu (ppb)	RSD (%)
North Basin Profile											
NB-5	5	0.0040	5.3	0.0010	26.4	0.0022	75.7	<0.0008		0.0019	11.7
NB-10	10	0.0046	9.9	0.0007	45.1	0.0025	46.7	<0.0008		0.0013	11.5
NB-20	20	0.0036	11.0	0.0005	39.7	<0.0012		<0.0008		0.0008	10.8
NB-30	30	0.0033	28.0	0.0005	9.6	0.0016	72.2	<0.0008		0.0010	65.4
NB-40	40	0.0022	9.6	0.0005	48.2	<0.0012		0.0008	173.2	0.0011	39.1
NB-50	50	0.0019	7.5	0.0006	67.3	0.0013	50.9	<0.0008		0.0009	9.6
NB-50D	50	0.0044	15.8	0.0012	64.8	<0.0012		<0.0008		0.0012	25.0
NB-60	60	0.0039	24.2	0.0007	17.0	0.0023	43.3	0.0008	86.6	0.0010	29.7
NB-70	70	0.0037	21.4	0.0007	11.5	0.0016	72.2	<0.0008		0.0006	128.3
NB-80	80	0.0041	10.3	0.0009	22.7	<0.0012		<0.0008		0.0006	76.4
NB-90	90	0.0039	5.9	0.0011	26.9	0.0027	39.7	0.0008	114.6	0.0009	34.7
NB-100	100	0.0156	97.0	0.0132	128.4	0.0107	111.1	0.0143	0.0	0.0133	112.1
NB-110	110	0.0038	8.6	0.0005	43.6	0.0017	76.4	0.0013	24.7	0.0007	37.1
NB-120	120	0.0039	21.6	0.0006	66.1	0.0016	81.8	<0.0008		0.0005	72.2
NB-130	130	0.0035	12.9	0.0010	20.9	0.0019	48.0	<0.0008		<0.0005	
NB-140	140	0.0026	34.9	0.0004	57.3	<0.0012		<0.0008		0.0008	88.2
NB-145	145	0.0035	10.3	0.0008	20.8	0.0013	19.3	<0.0008		0.0007	115.5
NB-150	150	0.0034	5.6	0.0010	28.5	<0.0012		<0.0008		0.0015	35.1
NB-155	155	0.0045	24.3	0.0007	50.1	0.0020	21.4	<0.0008		0.0009	41.9
South Basin Profile											
SB-5	5	0.0042	36.5	0.0007	27.4	0.0019	26.6	<0.0008	124.9	0.0008	61.1
SB-10	10	0.0036	9.7	0.0009	33.7	0.0027	32.9	0.0013	N/A	0.0012	42.1
SB-20	20	0.0043	30.8	0.0010	43.9	0.0017	144.3	<0.0008		0.0011	47.0
SB-30	30	0.0043	26.3	0.0009	4.8	<0.0012		0.0015	N/A	0.0007	21.4
SB-40	40	0.0041	1.3	0.0009	22.7	0.0016	47.2	<0.0008		0.0010	45.9
SB-50	50	0.0042	14.0	0.0010	31.9	0.0017	14.4	0.0008	173.2	0.0013	32.1
SB-50D	50	0.0032	36.1	0.0008	20.8	0.0026	53.6	<0.0008		0.0015	55.1
SB-60	60	0.0057	23.5	0.0032	47.7	0.0051	53.5	0.0031	34.7	0.0035	38.9
SB-65	65	0.0037	17.0	0.0013	3.4	0.0019	93.3	<0.0008		0.0011	15.7
SB-70	70	0.0063	9.1	0.0009	26.1	0.0046	61.5	<0.0008		0.0010	64.4
SB-75	75	0.0084	13.9	0.0009	12.4	0.0029	39.7	<0.0008		0.0009	48.2

Appendix B.2 Trace elements in waters

Sample ID	Depth (m)	Gd (ppb)	RSD (%)	Tb (ppb)	RSD (%)	Dy (ppb)	RSD (%)	Ho (ppb)	RSD (%)	Er (ppb)	RSD (%)
North Basin Profile											
NB-5	5	0.0027	25.5	0.0007	25.7	<0.0004		0.0006	42.1	<0.0009	
NB-10	10	<0.0014		0.0004	127.0	0.0009	100.0	0.0004	88.8	<0.0009	
NB-20	20	<0.0014		<0.0004		0.0004	114.6	<0.0004		0.0009	50.0
NB-30	30	0.0022	102.6	<0.0004		0.0008	142.0	<0.0004		<0.0009	
NB-40	40	0.0015	108.2	<0.0004		<0.0004		<0.0004		<0.0009	
NB-50	50	0.0016	68.6	0.0005	67.4	<0.0004		<0.0004		<0.0009	
NB-50D	50	<0.0014		<0.0004		0.0009	0.0	0.0006	56.7	<0.0009	
NB-60	60	0.0024	32.5	0.0005	91.7	<0.0004		0.0006	21.6	<0.0009	
NB-70	70	0.0022	181.5	0.0005	83.6	<0.0004		0.0005	50.0	<0.0009	
NB-80	80	0.0036	26.0	<0.0004		<0.0004		<0.0004		<0.0009	
NB-90	90	0.0019	69.2	0.0006	82.9	<0.0004		<0.0004		<0.0009	
NB-100	100	0.0142	105.7	0.0114	129.6	0.0146	116.8	0.0125	131.7	0.0107	133.8
NB-110	110	0.0016	181.6	<0.0004		<0.0004		<0.0004		0.0009	66.2
NB-120	120	0.0024	67.6	<0.0004		0.0007	65.5	<0.0004		<0.0009	
NB-130	130	<0.0014		<0.0004		<0.0004		<0.0004		<0.0009	
NB-140	140	0.0021	86.6	<0.0004		<0.0004		<0.0004		<0.0009	
NB-145	145	0.0036	26.0	<0.0004		0.0004	86.6	<0.0004		<0.0009	
NB-150	150	0.0019	40.0	0.0006	31.8	0.0005	124.9	<0.0004		<0.0009	
NB-155	155	0.0016	95.8	0.0004	44.4	0.0005	91.7	<0.0004		<0.0009	
South Basin Profile											
SB-5	5	0.0031	16.5	<0.0004		0.0007	24.7	0.0005	107.5	<0.0009	
SB-10	10	0.0021	68.9	0.0005	58.5	0.0013	0.0	0.0008	57.3	0.0011	68.9
SB-20	20	0.0031	16.5	0.0006	47.2	<0.0004		<0.0004		<0.0009	
SB-30	30	0.0030	43.3	0.0006	38.2	0.0009	33.3	0.0006	54.1	<0.0009	
SB-40	40	0.0030	75.5	<0.0004		<0.0004		0.0004	36.7	<0.0009	
SB-50	50	0.0040	17.0	<0.0004		<0.0004		0.0005	37.8	<0.0009	
SB-50D	50	0.0021	24.7	<0.0004		<0.0004		0.0005	44.1	<0.0009	
SB-60	60	0.0042	0.0	0.0031	86.8	0.0031	33.3	0.0029	67.8	0.0028	38.3
SB-65	65	0.0046	50.3	0.0006	19.1	0.0006	50.0	<0.0004		<0.0009	
SB-70	70	0.0027	75.2	<0.0004		<0.0004		<0.0004		<0.0009	
SB-75	75	0.0027	67.4	<0.0004		<0.0004		<0.0004		<0.0009	

Appendix B.2 Trace elements in waters

Sample ID	Depth (m)	Tm (ppb)	RSD (%)	Yb (ppb)	RSD (%)	Lu (ppb)	RSD (%)	Hf (ppb)	RSD (%)	Hg (ppb)	RSD (%)
North Basin Profile											
NB-5	5	0.0006	50.0	0.0011	75.5	0.0016	20.5	0.0015	13.4	0.0168	33.3
NB-10	10	<0.0005		0.0010	33.3	0.0011	27.7	0.0017	10.8	0.0224	43.3
NB-20	20	<0.0005		<0.0009		<0.0008		0.0013	15.7	0.0177	24.1
NB-30	30	<0.0005		0.0009	86.6	0.0014	33.8	0.0012	24.4	0.0205	55.1
NB-40	40	<0.0005		0.0009	86.6	0.0010	44.1	<0.0004		0.0261	44.6
NB-50	50	<0.0005		<0.0009		0.0009	57.1	0.0010	17.6	<0.0140	
NB-50D	50	<0.0005		<0.0009		0.0012	30.6	0.0009	10.0	<0.0140	
NB-60	60	<0.0005		<0.0009		0.0009	17.8	0.0010	23.3	0.0187	60.6
NB-70	70	<0.0005		<0.0009		0.0010	48.0	0.0007	25.4	<0.0140	
NB-80	80	<0.0005		<0.0009		0.0009	19.8	0.0008	17.2	0.0196	37.8
NB-90	90	<0.0005		<0.0009		0.0010	15.4	0.0008	33.0	<0.0140	
NB-100	100	0.0129	128.9	0.0141	123.8	0.0264	117.9	0.0103	112.2	0.0196	65.5
NB-110	110	<0.0005		<0.0009		0.0009	32.5	0.0006	39.6	<0.0140	
NB-120	120	<0.0005		<0.0009		<0.0008		0.0006	44.3	<0.0140	
NB-130	130	<0.0005		<0.0009		0.0009	39.8	0.0008	8.4	<0.0140	
NB-140	140	<0.0005		<0.0009		<0.0008		0.0005	43.3	<0.0140	
NB-145	145	<0.0005		<0.0009		<0.0008		0.0005	21.5	<0.0140	
NB-150	150	<0.0005		<0.0009		<0.0008		0.0004	28.4	<0.0140	
NB-155	155	<0.0005		<0.0009		<0.0008		0.0006	29.6	0.0168	60.1
South Basin Profile											
SB-5	5	<0.0005		<0.0009		<0.0008		0.0007	32.5	<0.0140	
SB-10	10	0.0006	59.8	<0.0009		0.0010	40.0	0.0007	29.9	<0.0140	
SB-20	20	<0.0005		<0.0009		0.0012	17.6	0.0005	77.8	<0.0140	
SB-30	30	<0.0005		0.0012	41.7	0.0012	20.8	0.0006	5.1	<0.0140	
SB-40	40	0.0006	34.6	<0.0009		0.0008	23.6	0.0005	61.9	<0.0140	
SB-50	50	<0.0005		<0.0009		0.0009	35.7	0.0005	54.1	<0.0140	
SB-50D	50	<0.0005		<0.0009		0.0008	44.7	<0.0004		<0.0140	
SB-60	60	0.0031	55.7	0.0021	65.7	0.0062	54.0	0.0025	41.4	<0.0140	
SB-65	65	<0.0005		0.0009	94.4	<0.0008		0.0005	55.0	<0.0140	
SB-70	70	<0.0005		<0.0009		<0.0008		<0.0004		<0.0140	
SB-75	75	<0.0005		<0.0009		<0.0008		<0.0004		<0.0140	

Appendix B.2 Trace elements in waters

Sample ID	Depth (m)	Pb (ppb)	RSD (%)	Bi (ppb)	RSD (%)	Th (ppb)	RSD (%)	U (ppb)	RSD (%)
North Basin Profile									
NB-5	5	0.0646	4.5	0.0005	56.3	0.0037	10.4	0.0229	1.8
NB-10	10	0.0727	1.6	0.0005	53.3	0.0028	16.6	0.0245	8.3
NB-20	20	0.0357	3.5	<0.0003		0.0020	21.9	0.0233	5.8
NB-30	30	0.0317	4.0	0.0005	51.6	0.0025	28.8	0.0249	5.8
NB-40	40	0.0279	12.6	<0.0003		0.0017	24.6	0.0241	3.4
NB-50	50	0.0125	13.2	0.0005	47.7	0.0024	28.1	0.0238	1.1
NB-50D	50	0.0460	5.4	<0.0003		0.0021	18.7	0.0247	3.6
NB-60	60	0.0185	6.2	0.0003	72.1	0.0025	10.4	0.0252	0.7
NB-70	70	0.0117	6.2	<0.0003		0.0023	23.9	0.0241	5.7
NB-80	80	0.0133	9.0	<0.0003		0.0020	5.6	0.0247	7.0
NB-90	90	0.0570	5.2	<0.0003		0.0030	10.6	0.0245	0.4
NB-100	100	0.0439	66.5	0.0097	127.7	0.0485	123.1	0.0484	65.9
NB-110	110	0.0216	8.1	<0.0003		0.0022	12.7	0.0237	5.0
NB-120	120	0.5947	1.8	0.0006	13.8	0.0017	20.8	0.0248	6.4
NB-130	130	0.0633	5.4	<0.0003		0.0022	13.1	0.0244	5.6
NB-140	140	0.0329	2.1	<0.0003		0.0013	24.9	0.0229	0.7
NB-145	145	0.0707	1.7	<0.0003		0.0016	40.0	0.0253	2.3
NB-150	150	0.0249	1.6	<0.0003		0.0016	39.3	0.0236	5.3
NB-155	155	0.0480	5.6	<0.0003		0.0014	39.7	0.0241	2.6
South Basin Profile									
SB-5	5	0.0908	2.2	<0.0003		0.0014	26.3	0.0257	4.6
SB-10	10	0.0933	1.6	<0.0003		0.0036	1.7	0.0243	3.7
SB-20	20	0.0433	4.1	0.0004	24.5	0.0025	10.7	0.0246	5.4
SB-30	30	0.0180	1.7	<0.0003		0.0026	5.8	0.0255	4.1
SB-40	40	0.5652	0.4	0.0004	22.9	0.0020	16.7	0.0240	4.0
SB-50	50	0.0106	21.7	0.0004	37.8	0.0020	3.8	0.0247	2.2
SB-50D	50	0.0087	14.3	<0.0003		0.0014	20.7	0.0239	0.7
SB-60	60	0.0244	11.8	0.0020	60.0	0.0121	57.9	0.0295	10.1
SB-65	65	0.0222	8.4	<0.0003		0.0018	28.4	0.1445	2.8
SB-70	70	0.0105	10.6	<0.0003		<0.0003		0.1094	2.3
SB-75	75	0.0105	8.2	<0.0003		<0.0003		0.0920	3.1

Appendix B.2 Trace elements in waters

Sample ID	Depth (m)	Li (ppb)	RSD (%)	B (ppb)	RSD (%)	P (ppb)	RSD (%)	Sc (ppb)	RSD (%)	Ti (ppb)	RSD (%)
South Basin Profile (cont.)											
SB-80	80	1.3806	2.3	14.56	1.7	<5		1.5936	5.1	0.9646	2.9
SB-80D	80	1.3122	0.5	14.82	0.7	<5		1.5858	5.4	0.9407	5.5
SB-85	85	4.3646	0.3	16.73	1.0	699.4	1.9	3.5799	3.1	4.1208	0.7
SB-90	90	6.6318	0.3	18.79	0.9	1530.1	2.9	4.7050	0.8	7.1698	1.7
SB-95	95	8.0445	1.1	21.29	1.3	1925.4	1.3	5.2157	0.2	9.1204	2.9
Lateral Moraine Ponds											
Pond Burevestniksee	2	3.9104	0.6	8.81	1.9	<5.3		1.0999	0.7	1.9604	3.4
P2 Pond	1	0.2589	2.5	5.74	0.4	<5.3		1.1241	0.2	0.8118	5.3

Values below detection are italicized

RSD is calculated and output by instrument from three measurements (n=3)

Sample ID's ending with 'D' are field duplicates

Appendix B.2 Trace elements in waters

Sample ID	Depth (m)	V (ppb)	RSD (%)	Cr (ppb)	RSD (%)	Mn (ppb)	RSD (%)	Fe (ppb)	RSD (%)	Co (ppb)	RSD (%)
South Basin Profile (cont.)											
SB-80	80	7.95	1.7	0.106	9.4	18.8799	2.7	49.454	1.2	0.2039	2.3
SB-80D	80	7.49	0.2	0.108	4.0	17.9036	2.9	52.586	1.0	0.1901	3.4
SB-85	85	13.57	1.0	0.240	3.4	78.6800	1.3	31.000	0.3	0.7369	0.6
SB-90	90	12.47	0.7	0.279	2.9	173.4676	1.3	99.536	1.4	1.0714	1.7
SB-95	95	10.91	0.7	0.252	5.7	224.2627	1.6	408.938	0.3	1.2717	4.0
Lateral Moraine Ponds											
Pond Burevestniksee	2	5.64	0.6	0.268	3.8	0.4159	2.2	19.507	1.8	0.2514	2.5
P2 Pond	1	6.99	0.3	0.120	2.8	0.1284	5.9	3.355	3.5	0.1705	1.3

Values below detection are italicized

RSD is calculated and output by instrument from three measurements (n=3)

Sample ID's ending with 'D' are field duplicates

Appendix B.2 Trace elements in waters

Sample ID	Depth (m)	Ni (ppb)	RSD (%)	Cu (ppb)	RSD (%)	Zn (ppb)	RSD (%)	As (ppb)	RSD (%)	Rb (ppb)	RSD (%)
South Basin Profile (cont.)											
SB-80	80	1.2380	4.1	0.428	2.7	0.3335	4.4	5.16	2.2	0.281	0.3
SB-80D	80	1.1905	2.2	1.405	1.1	1.2162	1.7	5.35	1.3	0.278	0.5
SB-85	85	2.6102	0.5	0.796	1.1	0.3866	9.0	4.32	0.1	0.543	2.2
SB-90	90	3.8388	0.5	1.630	1.4	0.8434	1.9	4.18	2.1	0.745	1.0
SB-95	95	5.1716	1.2	4.804	12.9	2.9331	1.7	6.13	0.8	0.916	1.5
Lateral Moraine Ponds											
Pond Burevestniksee	2	1.4675	2.1	1.553	2.6	1.9733	1.9	4.15	1.2	0.579	0.6
P2 Pond	1	0.6666	3.5	1.099	0.8	2.6617	0.8	4.31	0.6	0.265	1.7

Values below detection are italicized

RSD is calculated and output by instrument from three measurements (n=3)

Sample ID's ending with 'D' are field duplicates

Appendix B.2 Trace elements in waters

Sample ID	Depth (m)	Y (ppb)	RSD (%)	Zr (ppb)	RSD (%)	Nb (ppb)	RSD (%)	Mo (ppb)	RSD (%)	Ag (ppb)	RSD (%)
South Basin Profile (cont.)											
SB-80	80	0.0115	8.2	<i><0.0006</i>		0.0074	16.3	2.67	1.7	0.0012	10.2
SB-80D	80	0.0099	4.5	<i><0.0006</i>		0.0072	14.8	2.81	0.2	0.0011	45.4
SB-85	85	0.0354	4.1	0.0051	9.6	0.0458	4.1	4.94	0.2	0.0011	19.8
SB-90	90	0.1543	1.1	0.0094	3.4	0.0666	2.2	8.78	1.0	0.0023	19.2
SB-95	95	0.6428	3.7	0.0311	20.6	0.1215	6.4	15.71	5.2	0.0241	71.3
Lateral Moraine Ponds											
Pond Burevestniksee	2	0.0066	25.1	0.0023	9.4	<i><0.0033</i>		4.99	0.4	0.0022	9.4
P2 Pond	1	0.0022	11.8	<i><0.0006</i>		<i><0.0033</i>		3.97	0.7	<i><0.0007</i>	

Values below detection are italicized

RSD is calculated and output by instrument from three measurements (n=3)

Sample ID's ending with 'D' are field duplicates

Appendix B.2 Trace elements in waters

Sample ID	Depth (m)	Cd (ppb)	RSD (%)	Sb (ppb)	RSD (%)	Cs (ppb)	RSD (%)	Ba (ppb)	RSD (%)	La (ppb)	RSD (%)
South Basin Profile (cont.)											
SB-80	80	0.0145	8.0	0.0311	6.9	0.0028	17.2	1.78	2.6	0.0272	15.1
SB-80D	80	0.0158	22.9	0.0312	7.7	0.0026	7.6	1.66	1.6	0.0255	10.8
SB-85	85	0.0200	7.4	0.0306	3.4	0.0035	5.8	4.37	0.8	0.1465	0.0
SB-90	90	0.0439	11.0	0.0403	3.6	0.0050	2.7	6.80	0.7	1.0517	2.1
SB-95	95	0.0951	2.8	0.0820	3.1	0.0064	6.4	7.29	2.2	5.1691	1.4
Lateral Moraine Ponds											
Pond Burevestniksee	2	0.0172	17.5	0.1594	1.2	0.0052	19.3	10.45	1.0	0.0218	3.0
P2 Pond	1	0.0155	19.8	0.0869	2.9	0.0021	6.4	5.07	1.9	0.0085	10.9

Values below detection are italicized

RSD is calculated and output by instrument from three measurements (n=3)

Sample ID's ending with 'D' are field duplicates

Appendix B.2 Trace elements in waters

Sample ID	Depth (m)	Ce (ppb)	RSD (%)	Pr (ppb)	RSD (%)	Nd (ppb)	RSD (%)	Sm (ppb)	RSD (%)	Eu (ppb)	RSD (%)
South Basin Profile (cont.)											
SB-80	80	0.0555	2.4	0.0051	19.2	0.0166	4.0	0.0028	25.0	0.0019	13.7
SB-80D	80	0.0530	0.7	0.0038	16.7	0.0159	2.7	0.0023	21.6	0.0016	31.9
SB-85	85	0.3079	0.9	0.0265	11.4	0.0830	2.0	0.0120	28.9	0.0038	11.7
SB-90	90	2.2825	1.1	0.2017	2.8	0.6294	6.2	0.0819	7.2	0.0194	9.8
SB-95	95	10.9872	1.5	0.9789	0.7	2.9910	1.6	0.3901	5.4	0.0886	3.9
Lateral Moraine Ponds											
Pond Burevestniksee	2	0.0405	11.7	0.0045	16.3	0.0119	17.3	0.0010	21.6	0.0042	8.2
P2 Pond	1	0.0126	5.3	0.0016	53.2	0.0059	14.6	0.0013	173.2	0.0029	35.6

Values below detection are italicized

RSD is calculated and output by instrument from three measurements (n=3)

Sample ID's ending with 'D' are field duplicates

Appendix B.2 Trace elements in waters

Sample ID	Depth (m)	Gd (ppb)	RSD (%)	Tb (ppb)	RSD (%)	Dy (ppb)	RSD (%)	Ho (ppb)	RSD (%)	Er (ppb)	RSD (%)
South Basin Profile (cont.)											
SB-80	80	0.0048	32.9	<i><0.0004</i>		0.0024	27.1	0.0005	18.2	0.0009	50.0
SB-80D	80	0.0024	65.0	<i><0.0004</i>		0.0023	43.8	<i><0.0004</i>		<i><0.0009</i>	
SB-85	85	0.0118	3.8	0.0014	3.2	0.0043	27.7	0.0010	34.6	0.0029	19.9
SB-90	90	0.0825	3.0	0.0096	3.3	0.0306	13.5	0.0054	9.9	0.0148	10.4
SB-95	95	0.4145	3.0	0.0400	3.2	0.1517	6.8	0.0218	5.3	0.0640	6.4
Lateral Moraine Ponds											
Pond Burevestniksee	2	0.0030	91.7	0.0005	105.4	0.0009	57.7	0.0006	39.8	0.0009	75.0
P2 Pond	1	0.0018	28.9	<i><0.0004</i>		<i><0.0004</i>		<i><0.0004</i>		<i><0.0009</i>	

Values below detection are italicized

RSD is calculated and output by instrument from three measurements (n=3)

Sample ID's ending with 'D' are field duplicates

Appendix B.2 Trace elements in waters

Sample ID	Depth (m)	Tm (ppb)	RSD (%)	Yb (ppb)	RSD (%)	Lu (ppb)	RSD (%)	Hf (ppb)	RSD (%)	Hg (ppb)	RSD (%)
South Basin Profile (cont.)											
SB-80	80	<i><0.0005</i>		0.0016	99.0	<i><0.0008</i>		<i><0.0004</i>		0.0187	34.6
SB-80D	80	<i><0.0005</i>		<i><0.0009</i>		<i><0.0008</i>		<i><0.0004</i>		0.0196	0.0
SB-85	85	<i><0.0005</i>		0.0026	7.5	<i><0.0008</i>		0.0005	43.7	0.0252	29.4
SB-90	90	0.0020	7.9	0.0093	33.6	0.0012	21.0	0.0005	56.7	0.0373	72.8
SB-95	95	0.0064	19.9	0.0438	13.7	0.0059	16.7	0.0018	19.3	0.0233	50.0
Lateral Moraine Ponds											
Pond Burevestniksee	2	<i><0.0005</i>		<i><0.0009</i>		<i><0.0008</i>		0.0004	58.8	0.0149	28.6
P2 Pond	1	<i><0.0005</i>		<i><0.0009</i>		<i><0.0008</i>		<i><0.0004</i>		<i><0.0140</i>	

Values below detection are italicized

RSD is calculated and output by instrument from three measurements (n=3)

Sample ID's ending with 'D' are field duplicates

Appendix B.2 Trace elements in waters

Sample ID	Depth (m)	Pb (ppb)	RSD (%)	Bi (ppb)	RSD (%)	Th (ppb)	RSD (%)	U (ppb)	RSD (%)
South Basin Profile (cont.)									
SB-80	80	0.0250	3.9	0.0014	12.0	0.0046	14.0	0.0610	3.0
SB-80D	80	0.0714	1.7	0.0014	15.2	0.0030	18.5	0.0591	2.8
SB-85	85	0.0364	3.8	0.0033	12.8	0.0284	2.8	0.0583	1.6
SB-90	90	0.1065	2.1	0.0101	5.5	0.1984	7.5	0.2383	0.8
SB-95	95	0.2633	2.2	0.0318	8.2	1.5097	55.5	1.2213	8.9
Lateral Moraine Ponds									
Pond Burevestniksee	2	0.0300	2.8	0.0003	48.0	0.0203	3.7	0.2628	0.9
P2 Pond	1	0.0886	1.0	<i><0.0003</i>		0.0067	14.4	0.1261	1.9

Values below detection are italicized

RSD is calculated and output by instrument from three measurements (n=3)

Sample ID's ending with 'D' are field duplicates

Appendix B.3 Unpublished major and trace element data from 2016 expedition to Lake Untersee

Sample ID	Depth (m)	Ba (ppm)	Ca (ppm)	K (ppm)	Mg (ppm)	Na (ppm)	Sr (ppm)	Cl (ppm)	SO ₄ (ppm)	NO ₃ (ppm)	Fe (ppm)
North Basin Profile											
NB-10	10	0.030	43.6	1.76	1.22	61.1	0.030	38.0	156.9	0.186	0.36
NB-20	20	0.018	55.2	2.73	0.22	72.7	0.024	1.4	149.2	0.399	0.24
NB-30	30	0.016	52.9	1.89	0.23	61.6	0.024	38.5	153.9	0.238	0.17
NB-40	40	0.018	43.9	2.27	0.23	57.2	0.021	39.3	157.0	0.270	0.18
NB-50	50	0.018	46.2	2.70	0.22	67.1	0.023	38.6	155.5	0.145	0.22
NB-60	60	0.015	46.6	2.19	0.21	57.2	0.023	40.8	163.2	0.279	0.19
NB-70	70	0.018	49.7	2.44	0.22	64.2	0.024	38.2	154.3	0.222	0.23
NB-80	80	0.017	51.8	2.47	0.22	61.6	0.022	38.9	156.3	0.162	0.25
NB-90	90	0.020	42.8	2.76	0.22	61.9	0.020	34.1	134.1	0.267	0.23
NB-100	100	0.022	58.4	3.41	0.22	62.3	0.026	38.7	155.3	0.251	0.33
NB-110	110	0.019	41.7	1.86	0.21	64.1	0.025	38.6	155.3	0.245	0.16
NB-120	120	0.016	40.9	1.69	0.21	67.0	0.021	38.8	155.7	0.294	0.17
NB-130	130	0.020	55.6	2.85	0.22	67.3	0.025	38.8	155.3	0.281	0.27
NB-140	140	0.016	41.3	1.85	0.21	56.5	0.021	38.7	154.9	0.207	0.17
NB-150	150	0.017	52.6	2.70	0.22	65.8	0.025	38.2	153.9	0.223	0.31
South Basin Profile											
SB-10	5	0.017	38.9	1.90	0.22	61.5	0.021	38.2	152.8	0.163	0.22
SB-20	20	0.015	42.6	2.11	0.23	55.5	0.022	37.2	147.4	0.249	0.27
SB-30	30	0.015	38.4	1.92	0.22	60.9	0.021	38.3	152.2	0.238	0.18
SB-40	40	0.018	44.8	2.31	0.20	58.1	0.020	30.2	119.1	0.112	0.38
SB-50	50	0.017	53.4	2.10	0.25	51.9	0.023	38.6	154.4	0.168	0.31
SB-60	60	0.018	53.3	2.63	0.29	68.9	0.025	39.8	158.1	0.101	0.30
SB-70	70	0.019	59.3	3.37	0.44	63.7	0.025	39.7	154.5	0.114	0.37
SB-80	80	0.015	47.9	2.62	0.81	74.8	0.026	41.1	150.1	0.082	0.23
SB-90	90	0.018	53.2	3.03	0.29	65.8	0.024	37.7	149.2	0.260	0.36

Samples collected during 2016 expedition (Nov-Dec) by Benoit Faucher and Denis Lacelle (University of Ottawa)

Samples measured by the University of Ottawa Geochemistry Laboratory (May 2018)

Cl, SO₄ and NO₃ measured by ion chromatography (IC)

Analytical uncertainty of IC is typically better than $\pm (2\sigma)$ 2 ppm for SO₄, $\pm (2\sigma)$ 0.1 ppm for Cl, and $\pm (2\sigma)$ 0.01 ppm for NO₃

Ba, Ca, Fe, K, Mg, Na and Sr measured by ICP-AES

Analytical uncertainty of ICP-AES is $\leq 13\%$ RSD for Ba, Ca, Fe, K and Mg, and $\leq 19\%$ RSD for Na

Appendix B.4 Concentrations and stable carbon isotopes of TIC and TOC in waters

Sample ID	Depth (m)	TIC (ppm)	$\delta^{13}\text{C}_{\text{TIC}}$ VPBD (‰)	TOC (ppm)	$\delta^{13}\text{C}_{\text{TOC}}$ VPBD (‰)
North Basin Profile					
NB-5	5	0.4	-9.8	<0.3	BLD
NB-10	10	0.4	-9.0	<0.3	BLD
NB-20	20	0.3	-9.0	<0.3	BLD
NB-30	30	0.4	-9.3	<0.3	BLD
NB-40	40	0.4	-9.0	<0.3	BLD
NB-50	50	0.3	-8.6	<0.3	BLD
NB-50D	50	0.3	-9.0	<0.3	BLD
NB-60	60	0.4	-9.0	<0.3	BLD
NB-70	70	0.4	-9.2	<0.3	BLD
NB-80	80	0.4	-9.8	<0.3	BLD
NB-90	90	0.3	-9.3	<0.3	BLD
NB-100	100	0.4	-9.2	<0.3	BLD
NB-110	110	0.3	-9.3	<0.3	BLD
NB-120	120	0.4	-9.4	<0.3	BLD
NB-130	130	0.4	-9.3	<0.3	BLD
NB-140	140	0.3	-8.7	<0.3	BLD
NB-145	145	0.3	-9.0	<0.3	BLD
NB-150	150	0.3	-8.4	<0.3	BLD
NB-155	155	0.3	-9.3	<0.3	BLD
South Basin Profile					
SB-5	5	0.3	-8.5	<0.3	BLD
SB-10	10	0.3	-8.5	<0.3	BLD
SB-20	20	0.3	-7.1	<0.3	BLD
SB-30	30	0.3	-7.3	0.4	-27.5
SB-40	40	0.3	-6.8	<0.3	BLD
SB-50	50	0.3	-7.2	0.3	-26.7
SB-50D	50	0.3	-7.6	<0.3	BLD
SB-60	60	0.3	-7.0	<0.3	BLD
SB-65	65	1.2	2.8	0.3	-17.8
SB-70	70	7.2	3.7	0.5	-21.0
SB-75	75	9.4	2.7	1.2	-25.9
SB-80	80	32.7	14.2	1.3	-20.1
SB-80D	80	32.5	14.2	1.3	-20.2
SB-85	85	106.8	22.0	4.1	-18.6
SB-90	90	151.7	25.5	7.0	-18.4
SB-95	95	159.5	25.6	11.1	-19.3
Lateral Moraine Ponds					
Pond Burevestniksee	2	1.1	-3.7	1.2	-7.8
P2 Pond	1	1	-3.4	1.4	-7.6

BLD = below limit of detection

$^{13}\text{C}/^{12}\text{C}$ results are normalized to Vienna Pee Dee Belemnite (VPBD) for reporting $\delta^{13}\text{C}$

Sample ID's ending with 'D' are field duplicates

Analytical precision (2σ) of TIC and TOC concentrations are ± 0.5 (ppm)

Analytical precision (2σ) of $\delta^{13}\text{C}$ is $\pm 0.2\text{‰}$

Appendix B.5 Radiocarbon analysis of TIC and TOC in waters

Sample ID	Depth (m)	Total Inorganic Carbon				Total Organic Carbon			
		F ¹⁴ C	± 2σ	¹⁴ C yr BP	± 2σ	F ¹⁴ C	± 2σ	¹⁴ C yr BP	± 2σ
North Basin Profile									
NB-10	10	0.4361	0.0054	6666	98	*0.4233	0.0322	*6906	610
NB-40	40	0.5989	0.0132	4119	176				
NB-80	80	<i>FA</i>	<i>FA</i>	<i>FA</i>	<i>FA</i>	*0.5547	0.0418	*4734	610
NB-120	120	0.4307	0.004	6766	76				
South Basin Profile									
SB-10	10	0.4156	0.0046	7054	88	<i>NA</i>	<i>NA</i>	<i>NA</i>	<i>NA</i>
SB-40	40	0.4143	0.0038	7079	76	<i>NA</i>	<i>NA</i>	<i>NA</i>	<i>NA</i>
SB-70	70	0.2603	0.0028	10811	86	0.2551	0.0114	10974	358
SB-80	80	0.2542	0.0028	11002	86	0.2264	0.0066	11934	230
SB-80D	80	0.2472	0.0026	11228	84	<i>NA</i>	<i>NA</i>	<i>NA</i>	<i>NA</i>
SB-85	85	0.2432	0.0030	11358	96	0.1832	0.0074	13633	324
SB-90	90	0.2427	0.0032	11374	102	<i>NA</i>	<i>NA</i>	<i>NA</i>	<i>NA</i>
Lateral Moraine Ponds									
Pond Burevestniksee	2	0.9757	0.006	198	50	0.9169	0.0104	697	90
P2 Pond	1	0.9947	0.0058	43	46	<i>FA</i>	<i>FA</i>	<i>FA</i>	<i>FA</i>

TIC = total inorganic carbon

TOC = total organic carbon

F¹⁴C = fraction modern carbon

¹⁴C yr BP = radiocarbon age, years before 1950

FA = failed analysis

NA = no analysis

* Two samples composited to extract sufficient carbon for analysis

Appendix B.6 Stable sulfur isotopes of sulfate and sulfide

Sample ID	Depth (m)	$\delta^{34}\text{S}_{\text{SO}_4}$ VCPT (‰)	$\delta^{34}\text{S}_{\text{Sulfide}}$ VCPT (‰)
North Basin Profile			
NB-5	5	7.6	
NB-20	20	8.7	
NB-40	40	8.5	
NB-40D	40	8.5	
NB-60	60	8.7	
NB-80	80	8.7	
NB-80D	80		
NB-100	100	8.7	
NB-120	120	8.7	
NB-120R	120	8.4	
NB-140	140	8.6	
NB-155	155	8.6	
South Basin Profile			
SB-5	5	8.4	
SB-20	20	8.4	
SB-40	40	8.5	
SB-60	60	8.4	
SB-70	70	7.7	<i>NP</i>
SB-75	75	8.1	<i>NP</i>
SB-80	80	10.6	-27.9
SB-80R	80	14.3	
SB-80D	80	11.1	-33.2
SB-85	85	10.1	-7.4
SB-85R	85	<i>NP</i>	-6.7
SB-90	90	<i>NP</i>	1.9
SB-95	95	<i>NP</i>	5.2
Lateral Moraine Ponds			
Pond Burevestniksee	2	11.1	
Pond2 Pond	1	11.4	
Pond2 PondD	1	11.5	

NP = no/insufficient precipitate

Sample ID's ending with 'D' are field duplicates

Sample ID's ending with 'R' are laboratory replicates

$\delta^{34}\text{S}$ -SO₄ measured from barite precipitate

$\delta^{34}\text{S}$ -Sulfide measured from Zn-sulfide precipitate

³⁴S/³²S is normalized to Vienna-Canyon Diablo Troilite (VCTB) for reporting $\delta^{34}\text{S}$

Analytical precision (2 σ) of $\delta^{34}\text{S}$ is $\pm 0.2\text{‰}$

Appendix B.7 Nitrogen and oxygen isotopes of nitrate in waters

Sample ID	Depth (m)	NO ₃ (ppm)	$\delta^{18}\text{O-NO}_3$ vsmow (‰)	$\delta^{15}\text{N-NO}_3$ air (‰)
North Basin Profile				
NB-10	10	0.5026	16.8	5.1
NB-40	40	0.5068	16.2	9.4
NB-40R	40		15.8	9.5
NB-80	80	0.5042	18.7	7.3
NB-120	120	0.5090	11.2	9.2
NB-120R	120			9.0
South Basin Profile				
SB-10	10	0.5089	18.3	8.8
SB-40	40	0.4913	-12.1	11.9
SB-70	70	0.1073	-2.0	9.8
Lateral Moraine Ponds				
Pond Burevestniksee	2	8.321	5.5	22.6
Pond BurevestnikseeR	2			22.3
P2 Pond	1	0.1871	17.0	

Sample ID's ending with 'R' are laboratory replicates

¹⁸O/¹⁶O results are normalized to Vienna Standard Mean Ocean Water (VSMOW) for reporting $\delta^{18}\text{O}$

¹⁵N/¹⁴N results are normalized to air for reporting $\delta^{15}\text{N}$

Analytical precision of $\delta^{18}\text{O}$ is $\pm (2\sigma)$ 1‰

Analytical precision of $\delta^{15}\text{N}$ is $\pm (2\sigma)$ 0.6‰

Appendix B.8 Strontium isotopes in waters

Sample ID	Depth (m)	$^{87}\text{Sr}/^{86}\text{Sr}$	\pm SE
North Basin			
NB-10	10	0.718311	0.000007
NB-80	80	0.718296	0.000009
NB-155	155	0.718294	0.000007
South Basin			
SB-10	10	0.718319	0.000007
SB-80	80	0.718218	0.000007
SB-95	95	0.718041	0.000008
Moraine Ponds			
Pond Burevestniksee	1	0.722894	0.000019
Pond Burevestniksee R	1	0.722914	0.000007
Pond 2	1	0.722011	0.000007

Standard error (SE) = standard deviation/sqrt(n) where n=150

Sample ID's ending with 'R' are laboratory replicates

Appendix B.9 Tritium and radioiodine in waters

Sample ID	Depth (m)	Weight of Water Used (g)	Total Iodine Concentration (ppb)	Mass of Iodide Carrier Added (mg)	Measured ¹²⁹ I/ ¹²⁷ I Ratio (x10 ⁻¹⁴)*		Calculated ¹²⁹ I (atoms/g)	
					Ratio	Error	Concentration	Error
NaI Blank Average (n=3)		200	0.0005	2.00	1.57	0.05	7.45E+02	2.37E+01
NB-40	40	199.98	27	2.10	0.9	0.1	<750	-
NB-120	120	200.69	26	2.10	0.8	0.1	<750	-
SB-70	70	199.18	31	2.26	1	0.1	<750	-
SB-95	95	199.64	173	2.23	1.1	0.1	<750	-
Pond Burevestniksee	2	201.61	14	2.19	18.6	0.5	9.62E+03	2.68E+02
P2 Pond	1	201.01	2	2.12	4.6	0.2	2.29E+03	1.10E+02

Total iodine concentration measured by ICP-MS. Analytical uncertainty of 5% is based on maximum instrument RSD (n=3) of run

* ¹²⁹I/¹²⁷I Ratio Measured includes both sample and carrier added

** Calculated value without carrier

Sample ID	Depth (m)	³ H (TU)	± 2σ
NB-10	10	<0.8	
NB-40	80	<0.8	
NB-120	120	<0.8	
Pond Burevestniksee	2	1.5	0.8
P2 Pond	1	<0.8	

TU = Tritium Units where 1TU = 0.11919 Bq/L

Appendix B.10 North basin 2015 sonde data

Location: North Basin Hole (NB)

Instrument: YSI 6600

Date / Time	Depth (m)	Temp. (°C)	pH	ORP (mV)	Sp. Cond. (µS/cm)	TDS (g/L)	LDO% (% Saturation)	LDO (mg/L)	Chlorophyll (µg/L)
2015-12-02 10:56:26	5.04	0.17	10.00	94	504	0.3	138.1	18.08	0.10
2015-12-02 10:56:27	5.02	0.17	9.99	94	502	0.3	138.9	18.17	0.10
2015-12-02 10:56:28	5.02	0.17	9.99	94	502	0.3	138.9	18.17	0.10
2015-12-02 10:56:29	5.03	0.17	9.98	94	502	0.3	139.7	18.28	0.10
2015-12-02 10:56:30	5.03	0.17	9.98	94	502	0.3	139.7	18.28	0.10
2015-12-02 10:56:31	5.04	0.17	9.97	95	502	0.3	140.6	18.40	0.10
2015-12-02 10:56:32	5.04	0.17	9.97	95	502	0.3	140.6	18.40	0.10
2015-12-02 10:56:33	5.03	0.17	9.95	95	502	0.3	141.1	18.46	0.10
2015-12-02 10:56:34	5.03	0.17	9.94	95	502	0.3	141.4	18.50	0.10
2015-12-02 10:56:35	5.03	0.17	9.94	95	502	0.3	141.4	18.50	0.10
2015-12-02 10:57:37	10.01	0.23	10.04	96	502	0.3	145.9	19.05	0.09
2015-12-02 10:57:38	10.01	0.23	10.04	96	502	0.3	145.9	19.05	0.09
2015-12-02 10:57:39	10.01	0.23	10.03	96	503	0.3	145.9	19.06	0.09
2015-12-02 10:57:40	10.01	0.23	10.03	96	503	0.3	145.9	19.06	0.09
2015-12-02 10:57:41	10.02	0.23	10.02	96	503	0.3	146.1	19.09	0.09
2015-12-02 10:57:42	10.02	0.23	10.02	96	503	0.3	146.1	19.09	0.09
2015-12-02 10:57:43	10.02	0.23	10.02	96	505	0.3	146.2	19.10	0.09
2015-12-02 10:57:44	10.02	0.23	10.02	96	502	0.3	146.2	19.10	0.09
2015-12-02 10:57:45	10.02	0.23	10.02	96	502	0.3	146.2	19.10	0.09
2015-12-02 10:57:46	10.02	0.23	10.01	96	503	0.3	146.2	19.09	0.09
2015-12-02 10:59:15	15.05	0.24	10.07	98	503	0.3	146.9	19.17	0.08
2015-12-02 10:59:16	15.05	0.24	10.07	98	503	0.3	146.9	19.17	0.08
2015-12-02 10:59:17	15.06	0.24	10.08	98	502	0.3	147.0	19.19	0.08
2015-12-02 10:59:18	15.06	0.24	10.08	98	502	0.3	147.0	19.19	0.08
2015-12-02 10:59:19	15.09	0.24	10.07	98	503	0.3	146.9	19.19	0.08
2015-12-02 10:59:20	15.09	0.24	10.07	98	503	0.3	146.9	19.19	0.08
2015-12-02 10:59:21	15.09	0.24	10.07	98	503	0.3	146.8	19.17	0.08
2015-12-02 10:59:22	15.09	0.24	10.07	98	502	0.3	147.0	19.20	0.08
2015-12-02 10:59:23	15.09	0.24	10.07	98	502	0.3	147.0	19.20	0.08
2015-12-02 10:59:24	15.09	0.24	10.07	98	503	0.3	147.0	19.19	0.08
2015-12-02 11:00:13	19.99	0.25	10.09	99	502	0.3	146.0	19.06	0.08
2015-12-02 11:00:14	19.99	0.25	10.09	99	502	0.3	146.0	19.06	0.08

Appendix B.10 North basin 2015 sonde data

Location: North Basin Hole (NB)

Instrument: YSI 6600

Date / Time	Depth (m)	Temp. (°C)	pH	ORP (mV)	Sp. Cond. (µS/cm)	TDS (g/L)	LDO% (% Saturation)	LDO (mg/L)	Chlorophyll (µg/L)
2015-12-02 11:00:15	19.95	0.25	10.07	99	502	0.3	146.0	19.06	0.08
2015-12-02 11:00:16	19.95	0.25	10.07	99	502	0.3	146.0	19.06	0.08
2015-12-02 11:00:17	19.97	0.24	10.10	99	505	0.3	146.0	19.07	0.08
2015-12-02 11:00:18	20.00	0.25	10.09	99	502	0.3	146.1	19.07	0.08
2015-12-02 11:00:19	20.00	0.25	10.09	99	502	0.3	146.1	19.07	0.08
2015-12-02 11:00:20	20.03	0.24	10.10	99	502	0.3	146.2	19.09	0.08
2015-12-02 11:00:21	20.03	0.24	10.10	99	502	0.3	146.2	19.09	0.08
2015-12-02 11:00:22	20.03	0.24	10.09	100	503	0.3	146.3	19.10	0.08
2015-12-02 11:01:01	25.06	0.25	10.09	100	503	0.3	145.8	19.03	0.08
2015-12-02 11:01:02	25.06	0.25	10.09	100	503	0.3	145.7	19.01	0.08
2015-12-02 11:01:03	25.06	0.25	10.09	100	503	0.3	145.7	19.01	0.08
2015-12-02 11:01:04	25.07	0.25	10.09	100	503	0.3	145.6	19.00	0.08
2015-12-02 11:01:05	25.07	0.25	10.09	100	503	0.3	145.6	19.00	0.08
2015-12-02 11:01:06	25.08	0.25	10.09	100	503	0.3	145.6	19.01	0.08
2015-12-02 11:01:07	25.07	0.25	10.09	100	503	0.3	145.6	19.00	0.08
2015-12-02 11:01:08	25.07	0.25	10.09	100	503	0.3	145.6	19.00	0.08
2015-12-02 11:01:09	25.08	0.25	10.09	100	503	0.3	145.4	18.98	0.08
2015-12-02 11:01:10	25.08	0.25	10.09	100	503	0.3	145.4	18.98	0.08
2015-12-02 11:02:09	30.10	0.25	10.10	102	503	0.3	145.6	19.01	0.08
2015-12-02 11:02:10	30.09	0.25	10.10	102	503	0.3	145.3	18.97	0.08
2015-12-02 11:02:11	30.09	0.25	10.10	102	503	0.3	145.3	18.97	0.08
2015-12-02 11:02:12	30.10	0.25	10.11	102	503	0.3	145.4	18.98	0.08
2015-12-02 11:02:13	30.10	0.25	10.11	102	503	0.3	145.4	18.98	0.08
2015-12-02 11:02:14	30.09	0.25	10.10	102	503	0.3	145.3	18.97	0.08
2015-12-02 11:02:15	30.10	0.25	10.11	102	503	0.3	145.4	18.98	0.08
2015-12-02 11:02:16	30.10	0.25	10.11	102	503	0.3	145.4	18.98	0.08
2015-12-02 11:02:17	30.10	0.25	10.11	102	503	0.3	145.4	18.97	0.08
2015-12-02 11:02:18	30.10	0.25	10.11	102	503	0.3	145.4	18.97	0.08
2015-12-02 11:03:16	35.09	0.25	10.14	103	503	0.3	145.4	18.98	0.08
2015-12-02 11:03:17	35.09	0.25	10.14	103	503	0.3	145.4	18.98	0.08
2015-12-02 11:03:18	35.11	0.25	10.13	103	503	0.3	145.4	18.98	0.08
2015-12-02 11:03:19	35.11	0.25	10.13	103	503	0.3	145.4	18.98	0.08

Appendix B.10 North basin 2015 sonde data

Location: North Basin Hole (NB)

Instrument: YSI 6600

Date / Time	Depth (m)	Temp. (°C)	pH	ORP (mV)	Sp. Cond. (µS/cm)	TDS (g/L)	LDO% (% Saturation)	LDO (mg/L)	Chlorophyll (µg/L)
2015-12-02 11:03:20	35.11	0.25	10.14	103	505	0.3	145.3	18.97	0.08
2015-12-02 11:03:21	35.12	0.25	10.14	103	503	0.3	145.3	18.97	0.08
2015-12-02 11:03:22	35.12	0.25	10.14	103	503	0.3	145.3	18.97	0.08
2015-12-02 11:03:23	35.12	0.25	10.14	103	503	0.3	145.2	18.96	0.08
2015-12-02 11:03:24	35.12	0.25	10.14	103	503	0.3	145.2	18.96	0.08
2015-12-02 11:03:25	35.13	0.25	10.14	103	503	0.3	145.2	18.96	0.08
2015-12-02 11:04:11	40.07	0.25	10.17	104	503	0.3	145.8	19.03	0.08
2015-12-02 11:04:12	40.08	0.25	10.17	104	503	0.3	145.6	19.01	0.08
2015-12-02 11:04:13	40.08	0.25	10.17	104	503	0.3	145.6	19.01	0.08
2015-12-02 11:04:14	40.08	0.25	10.17	104	503	0.3	145.6	19.00	0.08
2015-12-02 11:04:15	40.08	0.25	10.17	104	503	0.3	145.6	19.00	0.08
2015-12-02 11:04:16	40.09	0.25	10.17	104	505	0.3	145.5	18.99	0.08
2015-12-02 11:04:17	40.09	0.25	10.17	104	503	0.3	145.7	19.02	0.08
2015-12-02 11:04:18	40.09	0.25	10.17	104	503	0.3	145.7	19.02	0.08
2015-12-02 11:04:19	40.10	0.25	10.18	104	503	0.3	145.6	19.01	0.08
2015-12-02 11:04:20	40.10	0.25	10.18	104	503	0.3	145.6	19.01	0.08
2015-12-02 11:05:03	44.97	0.25	10.20	105	503	0.3	145.7	19.01	0.09
2015-12-02 11:05:04	44.97	0.25	10.20	105	503	0.3	145.7	19.01	0.09
2015-12-02 11:05:05	44.97	0.25	10.20	105	505	0.3	145.7	19.02	0.09
2015-12-02 11:05:06	44.98	0.25	10.20	105	503	0.3	145.8	19.03	0.09
2015-12-02 11:05:07	44.98	0.25	10.20	105	503	0.3	145.8	19.03	0.09
2015-12-02 11:05:08	44.98	0.25	10.20	105	503	0.3	145.7	19.02	0.09
2015-12-02 11:05:09	44.98	0.25	10.20	105	503	0.3	145.7	19.02	0.09
2015-12-02 11:05:10	44.98	0.25	10.20	105	503	0.3	145.8	19.03	0.09
2015-12-02 11:05:11	44.98	0.25	10.20	105	503	0.3	145.8	19.03	0.09
2015-12-02 11:05:12	44.98	0.25	10.20	105	506	0.3	145.6	19.01	0.09
2015-12-02 11:05:58	50.16	0.26	10.21	105	503	0.3	145.3	18.96	0.09
2015-12-02 11:05:59	50.16	0.26	10.21	105	503	0.3	145.3	18.96	0.09
2015-12-02 11:06:00	50.16	0.26	10.21	105	503	0.3	145.3	18.96	0.09
2015-12-02 11:06:01	50.16	0.26	10.21	105	506	0.3	145.3	18.97	0.09
2015-12-02 11:06:02	50.17	0.26	10.21	105	503	0.3	145.4	18.98	0.09
2015-12-02 11:06:03	50.17	0.26	10.21	105	503	0.3	145.4	18.98	0.09

Appendix B.10 North basin 2015 sonde data

Location: North Basin Hole (NB)

Instrument: YSI 6600

Date / Time	Depth (m)	Temp. (°C)	pH	ORP (mV)	Sp. Cond. (µS/cm)	TDS (g/L)	LDO% (% Saturation)	LDO (mg/L)	Chlorophyll (µg/L)
2015-12-02 11:06:04	50.17	0.25	10.22	105	503	0.3	145.5	18.99	0.09
2015-12-02 11:06:05	50.17	0.25	10.22	105	503	0.3	145.5	18.99	0.09
2015-12-02 11:06:06	50.17	0.25	10.22	105	503	0.3	145.4	18.98	0.09
2015-12-02 11:06:07	50.17	0.25	10.22	105	503	0.3	145.4	18.98	0.09
2015-12-02 11:07:06	55.02	0.26	10.22	106	503	0.3	145.7	19.02	0.09
2015-12-02 11:07:07	55.03	0.26	10.22	106	503	0.3	145.5	18.99	0.09
2015-12-02 11:07:08	55.03	0.26	10.22	106	503	0.3	145.5	18.99	0.09
2015-12-02 11:07:09	55.03	0.26	10.22	106	503	0.3	145.6	19.01	0.09
2015-12-02 11:07:10	55.03	0.26	10.22	106	503	0.3	145.6	19.01	0.09
2015-12-02 11:07:11	55.02	0.26	10.23	106	506	0.3	145.6	19.00	0.09
2015-12-02 11:07:12	55.03	0.26	10.23	106	503	0.3	145.5	18.99	0.09
2015-12-02 11:07:13	55.03	0.26	10.23	106	503	0.3	145.5	18.99	0.09
2015-12-02 11:07:14	55.03	0.26	10.23	106	503	0.3	145.4	18.97	0.09
2015-12-02 11:07:15	55.03	0.26	10.23	106	503	0.3	145.4	18.97	0.09
2015-12-02 11:08:13	60.08	0.26	10.25	107	503	0.3	145.3	18.96	0.09
2015-12-02 11:08:14	60.08	0.26	10.25	107	503	0.3	145.4	18.97	0.09
2015-12-02 11:08:15	60.08	0.26	10.25	107	503	0.3	145.3	18.96	0.09
2015-12-02 11:08:16	60.08	0.26	10.25	107	503	0.3	145.3	18.96	0.09
2015-12-02 11:08:17	60.09	0.26	10.25	107	503	0.3	145.2	18.95	0.09
2015-12-02 11:08:18	60.09	0.26	10.25	107	503	0.3	145.2	18.95	0.09
2015-12-02 11:08:19	60.09	0.26	10.25	107	503	0.3	145.3	18.96	0.09
2015-12-02 11:08:20	60.09	0.26	10.25	107	503	0.3	145.3	18.96	0.09
2015-12-02 11:08:21	60.09	0.26	10.25	107	505	0.3	145.3	18.97	0.09
2015-12-02 11:08:22	60.10	0.26	10.25	107	503	0.3	145.3	18.96	0.09
2015-12-02 11:09:18	65.01	0.26	10.26	108	503	0.3	145.4	18.97	0.09
2015-12-02 11:09:19	65.01	0.26	10.26	108	503	0.3	145.4	18.97	0.09
2015-12-02 11:09:20	65.02	0.25	10.26	108	503	0.3	145.5	18.99	0.09
2015-12-02 11:09:21	65.02	0.25	10.26	108	503	0.3	145.5	18.99	0.09
2015-12-02 11:09:22	65.02	0.25	10.26	108	503	0.3	145.5	18.98	0.09
2015-12-02 11:09:23	65.02	0.25	10.26	108	503	0.3	145.5	18.98	0.09
2015-12-02 11:09:24	65.02	0.26	10.26	108	506	0.3	145.4	18.98	0.09
2015-12-02 11:09:25	65.02	0.26	10.26	108	503	0.3	145.4	18.98	0.09

Appendix B.10 North basin 2015 sonde data

Location: North Basin Hole (NB)

Instrument: YSI 6600

Date / Time	Depth (m)	Temp. (°C)	pH	ORP (mV)	Sp. Cond. (µS/cm)	TDS (g/L)	LDO% (% Saturation)	LDO (mg/L)	Chlorophyll (µg/L)
2015-12-02 11:09:26	65.02	0.26	10.26	108	503	0.3	145.4	18.98	0.09
2015-12-02 11:09:27	65.02	0.25	10.26	108	503	0.3	145.3	18.97	0.09
2015-12-02 11:10:11	70.05	0.26	10.26	109	503	0.3	145.1	18.94	0.09
2015-12-02 11:10:12	70.05	0.26	10.26	109	503	0.3	145.1	18.94	0.09
2015-12-02 11:10:13	70.06	0.26	10.26	109	506	0.3	145.2	18.95	0.09
2015-12-02 11:10:14	70.07	0.26	10.26	109	504	0.3	145.3	18.96	0.09
2015-12-02 11:10:15	70.07	0.26	10.26	109	504	0.3	145.3	18.96	0.09
2015-12-02 11:10:16	70.06	0.26	10.26	109	503	0.3	145.1	18.94	0.09
2015-12-02 11:10:17	70.06	0.26	10.26	109	503	0.3	145.1	18.94	0.09
2015-12-02 11:10:18	70.07	0.25	10.26	109	503	0.3	145.3	18.96	0.09
2015-12-02 11:10:19	70.07	0.25	10.26	109	503	0.3	145.3	18.96	0.09
2015-12-02 11:10:20	70.07	0.25	10.26	109	503	0.3	145.3	18.97	0.09
2015-12-02 11:11:28	75.17	0.25	10.26	110	504	0.3	145.8	19.03	0.10
2015-12-02 11:11:29	75.17	0.25	10.26	110	504	0.3	145.8	19.03	0.10
2015-12-02 11:11:30	75.15	0.25	10.26	110	506	0.3	145.8	19.03	0.10
2015-12-02 11:11:31	75.15	0.26	10.26	110	503	0.3	145.6	19.00	0.10
2015-12-02 11:11:32	75.15	0.26	10.26	110	503	0.3	145.6	19.00	0.10
2015-12-02 11:11:33	75.15	0.26	10.26	110	503	0.3	145.5	18.99	0.10
2015-12-02 11:11:34	75.15	0.26	10.26	110	503	0.3	145.5	18.99	0.10
2015-12-02 11:11:35	75.16	0.26	10.26	110	503	0.3	145.2	18.95	0.10
2015-12-02 11:11:36	75.16	0.26	10.26	110	503	0.3	145.2	18.95	0.10
2015-12-02 11:11:37	75.15	0.25	10.26	110	506	0.3	145.2	18.95	0.10
2015-12-02 11:12:29	79.96	0.26	10.27	110	503	0.3	145.6	19.00	0.10
2015-12-02 11:12:30	79.96	0.26	10.27	110	503	0.3	145.6	19.00	0.10
2015-12-02 11:12:31	79.96	0.26	10.26	110	503	0.3	145.6	19.00	0.10
2015-12-02 11:12:32	79.96	0.26	10.26	110	503	0.3	145.6	19.00	0.10
2015-12-02 11:12:33	79.96	0.26	10.26	110	506	0.3	145.4	18.97	0.10
2015-12-02 11:12:34	79.97	0.26	10.26	110	503	0.3	145.5	18.99	0.10
2015-12-02 11:12:35	79.97	0.26	10.26	110	503	0.3	145.5	18.99	0.10
2015-12-02 11:12:36	79.97	0.26	10.26	110	503	0.3	145.4	18.98	0.11
2015-12-02 11:12:37	79.97	0.26	10.26	110	503	0.3	145.4	18.98	0.11
2015-12-02 11:12:38	79.96	0.26	10.26	110	504	0.3	145.3	18.96	0.11

Appendix B.10 North basin 2015 sonde data

Location: North Basin Hole (NB)

Instrument: YSI 6600

Date / Time	Depth (m)	Temp. (°C)	pH	ORP (mV)	Sp. Cond. (µS/cm)	TDS (g/L)	LDO% (% Saturation)	LDO (mg/L)	Chlorophyll (µg/L)
2015-12-02 11:13:49	85.07	0.26	10.26	111	503	0.3	145.7	19.02	0.10
2015-12-02 11:13:50	85.07	0.26	10.26	111	506	0.3	145.7	19.02	0.10
2015-12-02 11:13:51	85.07	0.26	10.26	111	503	0.3	145.8	19.03	0.10
2015-12-02 11:13:52	85.07	0.26	10.26	111	503	0.3	145.8	19.03	0.10
2015-12-02 11:13:53	85.08	0.26	10.27	111	503	0.3	145.9	19.04	0.10
2015-12-02 11:13:54	85.08	0.26	10.27	111	503	0.3	145.9	19.04	0.10
2015-12-02 11:13:55	85.08	0.26	10.26	111	503	0.3	145.7	19.02	0.10
2015-12-02 11:13:56	85.08	0.26	10.26	111	503	0.3	145.7	19.02	0.10
2015-12-02 11:13:57	85.08	0.26	10.26	111	506	0.3	145.7	19.02	0.10
2015-12-02 11:13:58	85.09	0.26	10.26	111	503	0.3	145.7	19.01	0.09
2015-12-02 11:15:07	90.05	0.26	10.27	112	503	0.3	145.6	19.00	0.11
2015-12-02 11:15:08	90.05	0.26	10.27	112	504	0.3	145.7	19.01	0.11
2015-12-02 11:15:09	90.05	0.26	10.27	112	504	0.3	145.7	19.01	0.11
2015-12-02 11:15:10	90.06	0.26	10.27	112	503	0.3	145.5	18.99	0.11
2015-12-02 11:15:11	90.06	0.26	10.27	112	503	0.3	145.5	18.99	0.11
2015-12-02 11:15:12	90.06	0.26	10.26	112	503	0.3	145.4	18.98	0.11
2015-12-02 11:15:13	90.06	0.26	10.26	112	503	0.3	145.4	18.98	0.11
2015-12-02 11:15:14	90.07	0.26	10.27	112	506	0.3	145.3	18.96	0.11
2015-12-02 11:15:15	90.05	0.26	10.27	112	503	0.3	145.4	18.98	0.11
2015-12-02 11:15:16	90.05	0.26	10.27	112	503	0.3	145.4	18.98	0.11
2015-12-02 11:16:11	95.05	0.26	10.27	112	503	0.3	145.3	18.97	0.10
2015-12-02 11:16:12	95.05	0.26	10.27	112	503	0.3	145.3	18.97	0.10
2015-12-02 11:16:13	95.06	0.25	10.27	112	503	0.3	145.4	18.98	0.11
2015-12-02 11:16:14	95.06	0.25	10.27	112	503	0.3	145.4	18.98	0.11
2015-12-02 11:16:15	95.06	0.26	10.27	112	503	0.3	145.4	18.98	0.11
2015-12-02 11:16:16	95.06	0.26	10.27	112	503	0.3	145.4	18.98	0.11
2015-12-02 11:16:17	95.06	0.25	10.27	112	504	0.3	145.6	19.00	0.11
2015-12-02 11:16:18	95.05	0.26	10.27	112	504	0.3	145.7	19.01	0.11
2015-12-02 11:16:19	95.05	0.26	10.27	112	504	0.3	145.7	19.01	0.11
2015-12-02 11:16:20	95.06	0.25	10.27	113	503	0.3	145.6	19.01	0.11
2015-12-02 11:17:21	100.01	0.26	10.27	113	504	0.3	145.2	18.95	0.10
2015-12-02 11:17:22	100.01	0.26	10.27	113	504	0.3	145.2	18.95	0.10

Appendix B.10 North basin 2015 sonde data

Location: North Basin Hole (NB)

Instrument: YSI 6600

Date / Time	Depth (m)	Temp. (°C)	pH	ORP (mV)	Sp. Cond. (µS/cm)	TDS (g/L)	LDO% (% Saturation)	LDO (mg/L)	Chlorophyll (µg/L)
2015-12-02 11:17:23	100.02	0.26	10.27	113	503	0.3	145.3	18.97	0.10
2015-12-02 11:17:24	100.02	0.26	10.27	113	503	0.3	145.3	18.97	0.10
2015-12-02 11:17:25	100.01	0.26	10.27	113	504	0.3	145.4	18.98	0.10
2015-12-02 11:17:26	100.01	0.26	10.27	113	504	0.3	145.4	18.98	0.10
2015-12-02 11:17:27	100.02	0.26	10.27	113	503	0.3	145.2	18.96	0.11
2015-12-02 11:17:28	100.03	0.25	10.27	113	503	0.3	145.2	18.95	0.11
2015-12-02 11:17:29	100.03	0.25	10.27	113	503	0.3	145.2	18.95	0.11
2015-12-02 11:17:30	100.03	0.26	10.27	113	504	0.3	145.2	18.95	0.10
2015-12-02 11:18:27	105.03	0.26	10.28	114	503	0.3	145.3	18.96	0.11
2015-12-02 11:18:28	105.04	0.26	10.28	114	503	0.3	145.2	18.95	0.11
2015-12-02 11:18:29	105.04	0.26	10.28	114	503	0.3	145.2	18.95	0.11
2015-12-02 11:18:30	105.04	0.26	10.28	114	506	0.3	145.1	18.94	0.11
2015-12-02 11:18:31	105.05	0.26	10.28	114	504	0.3	145.0	18.92	0.11
2015-12-02 11:18:32	105.05	0.26	10.28	114	504	0.3	145.0	18.92	0.11
2015-12-02 11:18:33	105.06	0.26	10.28	114	504	0.3	145.1	18.94	0.11
2015-12-02 11:18:34	105.06	0.26	10.28	114	504	0.3	145.1	18.94	0.11
2015-12-02 11:18:35	105.04	0.26	10.28	114	503	0.3	145.0	18.93	0.11
2015-12-02 11:18:36	105.04	0.26	10.28	114	503	0.3	145.0	18.93	0.11
2015-12-02 11:19:33	110.13	0.26	10.28	114	503	0.3	145.8	19.02	0.11
2015-12-02 11:19:34	110.13	0.26	10.28	114	504	0.3	145.5	18.99	0.12
2015-12-02 11:19:35	110.13	0.26	10.28	114	504	0.3	145.5	18.99	0.12
2015-12-02 11:19:36	110.16	0.26	10.28	114	503	0.3	145.4	18.97	0.12
2015-12-02 11:19:37	110.16	0.26	10.28	114	503	0.3	145.4	18.97	0.12
2015-12-02 11:19:38	110.15	0.25	10.28	114	504	0.3	145.6	19.00	0.12
2015-12-02 11:19:39	110.15	0.25	10.28	114	504	0.3	145.6	19.00	0.12
2015-12-02 11:19:40	110.14	0.26	10.28	114	506	0.3	145.5	18.99	0.12
2015-12-02 11:19:41	110.16	0.26	10.28	114	504	0.3	145.6	19.00	0.12
2015-12-02 11:19:42	110.16	0.26	10.28	114	504	0.3	145.6	19.00	0.12
2015-12-02 11:20:42	115.09	0.26	10.29	115	504	0.3	145.4	18.97	0.12
2015-12-02 11:20:43	115.10	0.26	10.29	115	503	0.3	145.4	18.97	0.12
2015-12-02 11:20:44	115.10	0.26	10.29	115	504	0.3	145.4	18.97	0.12
2015-12-02 11:20:45	115.10	0.26	10.29	115	504	0.3	145.4	18.97	0.12

Appendix B.10 North basin 2015 sonde data

Location: North Basin Hole (NB)

Instrument: YSI 6600

Date / Time	Depth (m)	Temp. (°C)	pH	ORP (mV)	Sp. Cond. (µS/cm)	TDS (g/L)	LDO% (% Saturation)	LDO (mg/L)	Chlorophyll (µg/L)
2015-12-02 11:20:46	115.10	0.26	10.29	115	503	0.3	145.4	18.98	0.11
2015-12-02 11:20:47	115.10	0.26	10.29	115	503	0.3	145.4	18.98	0.11
2015-12-02 11:20:48	115.10	0.26	10.29	115	504	0.3	145.4	18.98	0.12
2015-12-02 11:20:49	115.10	0.26	10.29	115	504	0.3	145.4	18.98	0.12
2015-12-02 11:20:50	115.10	0.26	10.29	115	506	0.3	145.5	18.99	0.12
2015-12-02 11:20:51	115.10	0.26	10.29	115	503	0.3	145.5	18.99	0.12
2015-12-02 11:21:45	120.02	0.26	10.29	115	504	0.3	145.4	18.98	0.12
2015-12-02 11:21:46	120.03	0.26	10.29	115	506	0.3	145.6	19.01	0.12
2015-12-02 11:21:47	120.03	0.26	10.29	115	504	0.3	145.5	18.98	0.11
2015-12-02 11:21:48	120.03	0.26	10.29	115	504	0.3	145.5	18.98	0.11
2015-12-02 11:21:49	120.02	0.26	10.29	115	504	0.3	145.5	18.99	0.12
2015-12-02 11:21:50	120.02	0.26	10.29	115	504	0.3	145.5	18.99	0.12
2015-12-02 11:21:51	120.04	0.26	10.29	115	503	0.3	145.4	18.98	0.12
2015-12-02 11:21:52	120.04	0.26	10.29	115	503	0.3	145.4	18.98	0.12
2015-12-02 11:21:53	120.04	0.26	10.29	115	506	0.3	145.3	18.96	0.11
2015-12-02 11:21:54	120.05	0.26	10.29	115	504	0.3	145.2	18.95	0.11
2015-12-02 11:22:54	125.09	0.26	10.29	116	504	0.3	145.6	19.00	0.12
2015-12-02 11:22:55	125.09	0.26	10.29	116	504	0.3	145.6	19.00	0.12
2015-12-02 11:22:56	125.09	0.26	10.29	116	504	0.3	145.5	18.99	0.12
2015-12-02 11:22:57	125.09	0.26	10.30	116	504	0.3	145.5	18.99	0.12
2015-12-02 11:22:58	125.09	0.26	10.30	116	504	0.3	145.5	18.99	0.12
2015-12-02 11:22:59	125.09	0.26	10.30	116	504	0.3	145.3	18.97	0.12
2015-12-02 11:23:00	125.09	0.26	10.30	116	504	0.3	145.3	18.97	0.12
2015-12-02 11:23:01	125.10	0.26	10.29	116	504	0.3	145.4	18.97	0.12
2015-12-02 11:23:02	125.10	0.26	10.29	116	503	0.3	145.4	18.97	0.12
2015-12-02 11:23:03	125.10	0.26	10.29	116	503	0.3	145.3	18.96	0.12
2015-12-02 11:23:50	130.01	0.26	10.30	116	504	0.3	145.5	18.99	0.13
2015-12-02 11:23:51	130.01	0.26	10.30	116	504	0.3	145.5	18.99	0.13
2015-12-02 11:23:52	130.02	0.26	10.30	116	504	0.3	145.6	19.00	0.13
2015-12-02 11:23:53	130.02	0.26	10.30	116	504	0.3	145.6	19.00	0.12
2015-12-02 11:23:54	130.02	0.26	10.30	116	504	0.3	145.6	19.00	0.12
2015-12-02 11:23:55	130.02	0.26	10.30	116	504	0.3	145.7	19.02	0.12

Appendix B.10 North basin 2015 sonde data

Location: North Basin Hole (NB)

Instrument: YSI 6600

Date / Time	Depth (m)	Temp. (°C)	pH	ORP (mV)	Sp. Cond. (µS/cm)	TDS (g/L)	LDO% (% Saturation)	LDO (mg/L)	Chlorophyll (µg/L)
2015-12-02 11:23:56	130.02	0.26	10.30	116	504	0.3	145.7	19.02	0.12
2015-12-02 11:23:57	130.02	0.26	10.30	116	504	0.3	145.7	19.02	0.12
2015-12-02 11:23:58	130.02	0.26	10.30	116	504	0.3	145.5	19.00	0.12
2015-12-02 11:23:59	130.02	0.26	10.30	116	504	0.3	145.5	19.00	0.12
2015-12-02 11:24:37	135.08	0.25	10.30	116	504	0.3	145.4	18.98	0.12
2015-12-02 11:24:38	135.08	0.25	10.30	116	504	0.3	145.4	18.98	0.12
2015-12-02 11:24:39	135.08	0.26	10.30	117	503	0.3	145.5	18.99	0.11
2015-12-02 11:24:40	135.08	0.26	10.30	117	504	0.3	145.5	18.99	0.11
2015-12-02 11:24:41	135.08	0.26	10.30	117	504	0.3	145.5	18.99	0.12
2015-12-02 11:24:42	135.08	0.26	10.30	117	503	0.3	145.3	18.97	0.11
2015-12-02 11:24:43	135.08	0.26	10.30	117	503	0.3	145.3	18.97	0.11
2015-12-02 11:24:44	135.08	0.26	10.30	117	504	0.3	145.3	18.96	0.11
2015-12-02 11:24:45	135.08	0.26	10.30	117	504	0.3	145.3	18.96	0.11
2015-12-02 11:24:46	135.08	0.26	10.30	117	504	0.3	145.4	18.97	0.12
2015-12-02 11:25:41	140.02	0.25	10.30	117	504	0.3	145.0	18.93	0.12
2015-12-02 11:25:42	140.04	0.25	10.30	117	504	0.3	145.3	18.96	0.12
2015-12-02 11:25:43	140.05	0.26	10.30	117	504	0.3	145.3	18.96	0.13
2015-12-02 11:25:44	140.05	0.26	10.30	117	504	0.3	145.3	18.96	0.13
2015-12-02 11:25:45	140.04	0.26	10.30	117	504	0.3	145.2	18.95	0.12
2015-12-02 11:25:46	140.04	0.26	10.30	117	504	0.3	145.2	18.95	0.12
2015-12-02 11:25:47	140.06	0.26	10.30	117	504	0.3	145.3	18.96	0.13
2015-12-02 11:25:48	140.06	0.26	10.30	117	504	0.3	145.3	18.96	0.12
2015-12-02 11:25:49	140.06	0.26	10.30	117	504	0.3	145.3	18.96	0.12
2015-12-02 11:25:50	140.06	0.26	10.30	117	504	0.3	145.3	18.96	0.13
2015-12-02 11:26:37	145.05	0.26	10.30	117	504	0.3	145.1	18.94	0.12
2015-12-02 11:26:38	145.05	0.26	10.30	117	504	0.3	145.1	18.94	0.12
2015-12-02 11:26:39	145.06	0.26	10.31	117	504	0.3	145.2	18.94	0.12
2015-12-02 11:26:40	145.06	0.26	10.31	117	504	0.3	145.2	18.94	0.12
2015-12-02 11:26:41	145.06	0.26	10.30	117	504	0.3	145.1	18.94	0.12
2015-12-02 11:26:42	145.06	0.26	10.30	117	504	0.3	145.1	18.94	0.12
2015-12-02 11:26:43	145.06	0.26	10.30	117	504	0.3	145.1	18.94	0.12
2015-12-02 11:26:44	145.06	0.26	10.30	117	504	0.3	145.1	18.94	0.12

Appendix B.10 North basin 2015 sonde data

Location: North Basin Hole (NB)

Instrument: YSI 6600

Date / Time	Depth (m)	Temp. (°C)	pH	ORP (mV)	Sp. Cond. (µS/cm)	TDS (g/L)	LDO% (% Saturation)	LDO (mg/L)	Chlorophyll (µg/L)
2015-12-02 11:26:45	145.06	0.26	10.30	117	504	0.3	145.1	18.94	0.12
2015-12-02 11:26:46	145.06	0.26	10.30	117	504	0.3	145.2	18.95	0.11
2015-12-02 11:29:07	149.98	0.26	10.31	118	504	0.3	145.7	19.02	0.12
2015-12-02 11:29:08	149.98	0.26	10.31	118	504	0.3	145.7	19.02	0.12
2015-12-02 11:29:09	150.00	0.26	10.32	118	504	0.3	145.9	19.03	0.12
2015-12-02 11:29:10	150.00	0.26	10.32	118	504	0.3	145.9	19.03	0.12
2015-12-02 11:29:11	150.00	0.26	10.31	118	504	0.3	145.9	19.04	0.12
2015-12-02 11:29:12	150.00	0.26	10.31	118	504	0.3	145.9	19.04	0.12
2015-12-02 11:29:13	150.00	0.26	10.31	118	506	0.3	145.7	19.02	0.12
2015-12-02 11:29:14	149.99	0.26	10.31	118	504	0.3	145.8	19.02	0.12
2015-12-02 11:29:15	149.99	0.26	10.31	118	504	0.3	145.8	19.02	0.12
2015-12-02 11:29:16	149.99	0.26	10.31	118	504	0.3	145.6	18.99	0.12
2015-12-02 11:30:38	154.98	0.27	10.32	119	504	0.3	145.7	19.01	0.12
2015-12-02 11:30:39	154.98	0.27	10.32	119	504	0.3	145.7	19.01	0.12
2015-12-02 11:30:40	154.97	0.27	10.32	119	504	0.3	145.6	19.00	0.12
2015-12-02 11:30:41	154.97	0.27	10.32	119	504	0.3	145.6	19.00	0.12
2015-12-02 11:30:42	154.97	0.26	10.32	119	507	0.3	145.7	19.02	0.12
2015-12-02 11:30:43	154.98	0.27	10.32	119	504	0.3	145.5	18.99	0.12
2015-12-02 11:30:44	154.98	0.27	10.32	119	504	0.3	145.5	18.99	0.12
2015-12-02 11:30:45	154.97	0.27	10.32	119	504	0.3	145.4	18.97	0.12
2015-12-02 11:30:46	154.97	0.27	10.32	119	504	0.3	145.4	18.97	0.12
2015-12-02 11:30:47	154.98	0.26	10.32	119	504	0.3	145.4	18.97	0.12
2015-12-02 11:31:55	159.99	0.27	10.33	119	504	0.3	145.5	18.99	0.12
2015-12-02 11:31:56	159.99	0.27	10.33	119	504	0.3	145.5	18.98	0.12
2015-12-02 11:31:57	159.99	0.27	10.33	119	504	0.3	145.5	18.98	0.12
2015-12-02 11:31:58	159.99	0.27	10.33	119	504	0.3	145.7	19.00	0.12
2015-12-02 11:31:59	159.99	0.27	10.33	119	504	0.3	145.7	19.00	0.12
2015-12-02 11:32:00	160.00	0.27	10.33	119	504	0.3	145.6	19.00	0.12
2015-12-02 11:32:01	160.00	0.27	10.33	119	504	0.3	145.6	19.00	0.12
2015-12-02 11:32:02	159.99	0.27	10.33	119	504	0.3	145.7	19.01	0.12
2015-12-02 11:32:03	159.99	0.27	10.33	119	504	0.3	145.7	19.01	0.12
2015-12-02 11:32:04	160.00	0.27	10.33	119	504	0.3	145.8	19.02	0.12

Appendix B.10 North basin 2015 sonde data

Location: North Basin Hole (NB)

Instrument: YSI 6600

Date / Time	Depth (m)	Temp. (°C)	pH	ORP (mV)	Sp. Cond. (μ S/cm)	TDS (g/L)	LDO% (% Saturation)	LDO (mg/L)	Chlorophyll (μ g/L)
-------------	--------------	---------------	----	-------------	----------------------------	--------------	------------------------	---------------	-----------------------------

ORP = oxidation-reduction potential

TDS = total dissolved solids

LDO = luminescent dissolved oxygen

Appendix B.11 North basin 2017 sonde data

Location: North Basin Hole (NB)

Instrument: YSI 6600

Date / Time	Depth (m)	Temp. (°C)	pH	ORP (mV)	Sp. Cond. (µS/cm)	LDO% (% Saturation)	LDO (mg/L)	Chlorophyll (µg/L)
2017-11-26 10:38:02	0.52	0.01	11.04	164	512	137.9	19.43	0.18
2017-11-26 10:38:03	0.54	0.02	11.04	164	512	137.8	19.41	0.18
2017-11-26 10:38:04	0.54	0.02	11.04	164	512	137.8	19.41	0.18
2017-11-26 10:38:05	0.53	0.02	11.05	164	514	137.8	19.41	0.18
2017-11-26 10:38:06	0.52	0.02	11.06	164	512	137.8	19.41	0.18
2017-11-26 10:38:54	5.08	0.18	10.99	164	502	145.6	20.42	0.18
2017-11-26 10:38:55	5.08	0.18	10.99	164	502	145.9	20.46	0.18
2017-11-26 10:38:56	5.08	0.18	10.99	164	502	145.9	20.46	0.18
2017-11-26 10:38:57	5.10	0.19	10.99	164	502	145.9	20.46	0.18
2017-11-26 10:38:58	5.10	0.19	10.99	164	502	145.9	20.46	0.18
2017-11-26 10:39:38	10.07	0.20	11.00	163	501	147.3	20.65	0.18
2017-11-26 10:39:39	10.07	0.20	11.01	163	502	147.2	20.63	0.18
2017-11-26 10:39:40	10.07	0.20	11.01	163	502	147.2	20.63	0.18
2017-11-26 10:39:41	10.08	0.19	11.00	163	502	147.2	20.63	0.18
2017-11-26 10:39:42	10.08	0.19	11.00	163	502	147.2	20.63	0.18
2017-11-26 10:40:52	15.00	0.20	10.93	162	502	147.1	20.61	0.18
2017-11-26 10:40:53	15.00	0.20	10.93	162	504	147.0	20.60	0.18
2017-11-26 10:40:54	15.00	0.20	10.93	162	502	146.8	20.57	0.18
2017-11-26 10:40:55	15.00	0.20	10.93	162	502	146.8	20.57	0.18
2017-11-26 10:40:56	15.01	0.20	10.93	162	502	146.8	20.58	0.18
2017-11-26 10:41:55	20.00	0.20	10.92	161	502	147.4	20.65	0.18
2017-11-26 10:41:56	19.95	0.19	10.92	161	502	147.4	20.65	0.18
2017-11-26 10:41:57	19.93	0.20	10.93	161	502	147.6	20.68	0.18
2017-11-26 10:41:58	19.93	0.20	10.93	161	502	147.6	20.68	0.18
2017-11-26 10:41:59	19.95	0.20	10.92	161	502	147.5	20.67	0.18
2017-11-26 10:42:48	25.02	0.19	10.86	160	502	146.8	20.58	0.18
2017-11-26 10:42:49	25.02	0.19	10.86	160	502	146.8	20.58	0.18
2017-11-26 10:42:50	25.03	0.19	10.85	160	502	147.0	20.60	0.18
2017-11-26 10:42:51	25.03	0.19	10.85	160	502	147.0	20.60	0.18
2017-11-26 10:42:52	25.04	0.20	10.85	160	504	147.0	20.60	0.18

Appendix B.11 North basin 2017 sonde data

Location: North Basin Hole (NB)

Instrument: YSI 6600

Date / Time	Depth (m)	Temp. (°C)	pH	ORP (mV)	Sp. Cond. (µS/cm)	LDO% (% Saturation)	LDO (mg/L)	Chlorophyll (µg/L)
2017-11-26 10:43:26	30.09	0.20	10.82	160	502	147.4	20.66	0.18
2017-11-26 10:43:27	30.08	0.19	10.82	160	502	147.5	20.68	0.18
2017-11-26 10:43:28	30.08	0.20	10.82	160	502	147.5	20.67	0.18
2017-11-26 10:43:29	30.08	0.20	10.82	160	502	147.5	20.67	0.18
2017-11-26 10:43:30	30.08	0.19	10.81	160	502	147.7	20.69	0.18
2017-11-26 10:44:07	35.04	0.20	10.78	159	502	147.3	20.64	0.18
2017-11-26 10:44:08	35.04	0.20	10.78	159	502	147.3	20.64	0.18
2017-11-26 10:44:09	35.04	0.20	10.78	159	504	147.3	20.64	0.19
2017-11-26 10:44:10	35.05	0.20	10.78	159	502	147.1	20.61	0.18
2017-11-26 10:44:11	35.05	0.20	10.78	159	502	147.1	20.61	0.18
2017-11-26 10:44:56	40.02	0.20	10.76	159	502	147.5	20.66	0.18
2017-11-26 10:44:57	40.02	0.20	10.76	159	502	147.5	20.66	0.18
2017-11-26 10:44:58	40.02	0.20	10.76	159	502	147.5	20.67	0.18
2017-11-26 10:44:59	40.02	0.20	10.76	159	502	147.5	20.67	0.18
2017-11-26 10:45:00	40.02	0.20	10.76	159	502	147.5	20.67	0.18
2017-11-26 10:45:35	45.06	0.20	10.73	159	502	146.9	20.59	0.19
2017-11-26 10:45:36	45.06	0.20	10.74	159	502	147.1	20.61	0.18
2017-11-26 10:45:37	45.06	0.20	10.74	159	502	147.1	20.61	0.18
2017-11-26 10:45:38	45.05	0.20	10.73	159	502	147.0	20.59	0.19
2017-11-26 10:45:39	45.05	0.20	10.73	159	502	147.0	20.59	0.19
2017-11-26 10:46:16	50.02	0.21	10.70	159	502	146.9	20.58	0.18
2017-11-26 10:46:17	50.02	0.21	10.70	159	502	146.9	20.58	0.18
2017-11-26 10:46:18	50.02	0.20	10.71	159	502	146.9	20.58	0.19
2017-11-26 10:46:19	50.02	0.20	10.71	159	502	146.9	20.58	0.19
2017-11-26 10:46:20	50.02	0.21	10.70	159	502	146.8	20.57	0.18
2017-11-26 10:47:11	55.14	0.21	10.67	159	505	147.1	20.61	0.19
2017-11-26 10:47:12	55.14	0.21	10.68	159	502	147.0	20.60	0.19
2017-11-26 10:47:13	55.14	0.21	10.68	159	502	147.0	20.60	0.19
2017-11-26 10:47:14	55.16	0.21	10.68	159	502	146.9	20.58	0.19
2017-11-26 10:47:15	55.16	0.21	10.68	159	502	146.9	20.58	0.19

Appendix B.11 North basin 2017 sonde data

Location: North Basin Hole (NB)

Instrument: YSI 6600

Date / Time	Depth (m)	Temp. (°C)	pH	ORP (mV)	Sp. Cond. (µS/cm)	LDO% (% Saturation)	LDO (mg/L)	Chlorophyll (µg/L)
2017-11-26 10:47:57	60.02	0.21	10.66	159	502	147.1	20.60	0.19
2017-11-26 10:47:58	60.03	0.21	10.65	158	502	147.0	20.59	0.19
2017-11-26 10:47:59	60.03	0.21	10.65	158	502	147.0	20.59	0.19
2017-11-26 10:48:00	60.03	0.21	10.66	159	504	147.0	20.59	0.19
2017-11-26 10:48:01	60.02	0.22	10.66	159	502	146.9	20.58	0.19
2017-11-26 10:48:43	65.03	0.22	10.64	158	502	147.0	20.59	0.19
2017-11-26 10:48:44	65.03	0.22	10.64	158	502	147.0	20.59	0.19
2017-11-26 10:48:45	65.04	0.21	10.64	158	502	147.2	20.62	0.19
2017-11-26 10:48:46	65.04	0.21	10.64	158	502	147.2	20.62	0.19
2017-11-26 10:48:47	65.04	0.21	10.64	158	502	147.2	20.63	0.19
2017-11-26 10:49:43	69.95	0.22	10.63	158	502	147.2	20.61	0.19
2017-11-26 10:49:44	69.95	0.22	10.63	158	502	147.2	20.61	0.19
2017-11-26 10:49:45	69.95	0.22	10.63	158	504	147.2	20.62	0.19
2017-11-26 10:49:46	69.96	0.22	10.63	158	502	147.1	20.60	0.19
2017-11-26 10:49:47	69.96	0.22	10.63	158	502	147.1	20.60	0.19
2017-11-26 10:50:41	75.06	0.22	10.61	158	502	146.7	20.55	0.19
2017-11-26 10:50:42	75.04	0.22	10.61	158	502	146.7	20.55	0.19
2017-11-26 10:50:43	75.04	0.22	10.61	158	502	146.7	20.55	0.19
2017-11-26 10:50:44	75.06	0.22	10.61	158	502	146.5	20.52	0.19
2017-11-26 10:50:45	75.06	0.22	10.61	158	502	146.5	20.52	0.19
2017-11-26 10:51:31	80.05	0.22	10.61	158	502	147.0	20.58	0.19
2017-11-26 10:51:32	80.05	0.22	10.61	158	502	147.0	20.58	0.19
2017-11-26 10:51:33	80.05	0.22	10.61	158	503	147.0	20.59	0.20
2017-11-26 10:51:34	80.05	0.22	10.61	158	503	147.0	20.59	0.20
2017-11-26 10:51:35	80.08	0.22	10.61	158	502	147.1	20.60	0.19
2017-11-26 10:51:56	85.08	0.22	10.60	158	502	146.7	20.55	0.19
2017-11-26 10:51:57	85.08	0.22	10.60	158	502	146.7	20.55	0.19
2017-11-26 10:51:58	85.11	0.22	10.60	158	505	146.6	20.53	0.19
2017-11-26 10:51:59	85.12	0.22	10.60	158	502	146.6	20.53	0.19
2017-11-26 10:52:00	85.12	0.22	10.60	158	502	146.6	20.53	0.19

Appendix B.11 North basin 2017 sonde data

Location: North Basin Hole (NB)

Instrument: YSI 6600

Date / Time	Depth (m)	Temp. (°C)	pH	ORP (mV)	Sp. Cond. (µS/cm)	LDO% (% Saturation)	LDO (mg/L)	Chlorophyll (µg/L)
2017-11-26 10:52:47	89.99	0.22	10.60	158	502	147.1	20.60	0.20
2017-11-26 10:52:48	89.99	0.22	10.60	158	502	147.0	20.59	0.20
2017-11-26 10:52:49	89.99	0.22	10.60	158	502	147.0	20.59	0.20
2017-11-26 10:52:50	90.00	0.22	10.60	158	503	147.0	20.58	0.20
2017-11-26 10:52:51	90.00	0.22	10.60	158	503	147.0	20.58	0.20
2017-11-26 10:53:54	95.04	0.22	10.61	158	502	146.2	20.47	0.20
2017-11-26 10:53:55	95.04	0.22	10.61	158	502	146.3	20.49	0.20
2017-11-26 10:53:56	95.04	0.22	10.61	158	502	146.3	20.49	0.20
2017-11-26 10:53:57	95.05	0.22	10.60	158	502	146.6	20.53	0.20
2017-11-26 10:53:58	95.07	0.22	10.60	158	502	146.8	20.55	0.20
2017-11-26 10:54:40	100.02	0.22	10.61	158	502	146.9	20.57	0.20
2017-11-26 10:54:41	100.02	0.22	10.61	158	502	146.9	20.57	0.20
2017-11-26 10:54:42	100.03	0.22	10.61	158	503	147.0	20.59	0.20
2017-11-26 10:54:43	100.03	0.22	10.61	158	503	147.0	20.59	0.20
2017-11-26 10:54:44	100.03	0.22	10.60	158	503	147.2	20.61	0.20
2017-11-26 10:55:36	105.05	0.22	10.60	157	502	146.4	20.50	0.20
2017-11-26 10:55:37	105.05	0.22	10.60	157	502	146.4	20.50	0.20
2017-11-26 10:55:38	105.05	0.22	10.60	158	503	146.4	20.51	0.20
2017-11-26 10:55:39	105.05	0.22	10.60	158	503	146.4	20.51	0.20
2017-11-26 10:55:40	105.06	0.22	10.60	158	502	146.4	20.51	0.20
2017-11-26 10:56:41	110.02	0.23	10.59	157	503	146.9	20.57	0.21
2017-11-26 10:56:42	110.02	0.23	10.59	157	503	146.9	20.57	0.21
2017-11-26 10:56:43	110.01	0.22	10.59	157	502	146.8	20.55	0.21
2017-11-26 10:56:44	110.01	0.22	10.59	157	502	146.8	20.55	0.21
2017-11-26 10:56:45	110.02	0.22	10.59	157	505	146.9	20.57	0.21
2017-11-26 10:57:35	115.06	0.22	10.60	157	503	146.9	20.57	0.20
2017-11-26 10:57:36	115.06	0.22	10.60	157	503	146.9	20.57	0.20
2017-11-26 10:57:37	115.05	0.22	10.59	157	503	146.9	20.57	0.20
2017-11-26 10:57:38	115.05	0.22	10.59	157	503	146.9	20.57	0.20
2017-11-26 10:57:39	115.05	0.22	10.59	157	503	146.8	20.56	0.20

Appendix B.11 North basin 2017 sonde data

Location: North Basin Hole (NB)

Instrument: YSI 6600

Date / Time	Depth (m)	Temp. (°C)	pH	ORP (mV)	Sp. Cond. (µS/cm)	LDO% (% Saturation)	LDO (mg/L)	Chlorophyll (µg/L)
2017-11-26 10:58:15	120.01	0.23	10.59	157	503	146.8	20.55	0.20
2017-11-26 10:58:16	120.01	0.23	10.59	157	505	146.6	20.53	0.20
2017-11-26 10:58:17	120.00	0.23	10.59	157	503	146.7	20.54	0.20
2017-11-26 10:58:18	120.00	0.23	10.59	157	503	146.7	20.54	0.20
2017-11-26 10:58:19	120.02	0.23	10.60	157	503	146.8	20.55	0.20
2017-11-26 10:59:10	125.01	0.23	10.59	157	503	146.6	20.52	0.20
2017-11-26 10:59:11	125.01	0.23	10.59	157	503	146.6	20.52	0.20
2017-11-26 10:59:12	125.00	0.23	10.59	157	505	146.5	20.51	0.20
2017-11-26 10:59:13	125.02	0.23	10.59	157	503	146.5	20.51	0.20
2017-11-26 10:59:14	125.02	0.23	10.59	157	503	146.5	20.51	0.20
2017-11-26 10:59:51	130.04	0.23	10.60	157	503	146.7	20.54	0.20
2017-11-26 10:59:52	130.04	0.23	10.60	157	503	146.8	20.55	0.21
2017-11-26 10:59:53	130.04	0.23	10.60	157	503	146.8	20.55	0.21
2017-11-26 10:59:54	130.05	0.23	10.60	157	505	146.6	20.53	0.21
2017-11-26 10:59:55	130.06	0.23	10.59	157	502	146.7	20.54	0.21
2017-11-26 11:00:56	135.05	0.23	10.60	157	502	146.3	20.48	0.20
2017-11-26 11:00:57	135.06	0.23	10.59	157	505	146.5	20.50	0.21
2017-11-26 11:00:58	135.06	0.24	10.60	157	503	146.5	20.51	0.21
2017-11-26 11:00:59	135.06	0.24	10.60	157	503	146.5	20.51	0.21
2017-11-26 11:01:00	135.06	0.23	10.60	157	503	146.6	20.52	0.21
2017-11-26 11:02:14	139.98	0.24	10.60	157	505	146.2	20.47	0.21
2017-11-26 11:02:15	139.99	0.24	10.60	157	503	146.3	20.48	0.21
2017-11-26 11:02:16	139.99	0.24	10.60	157	503	146.3	20.48	0.21
2017-11-26 11:02:17	139.98	0.24	10.60	157	503	146.4	20.49	0.20
2017-11-26 11:02:18	139.98	0.24	10.60	157	503	146.4	20.49	0.20
2017-11-26 11:02:54	145.00	0.24	10.59	157	503	146.6	20.52	0.21
2017-11-26 11:02:55	145.00	0.24	10.59	157	503	146.6	20.52	0.21
2017-11-26 11:02:56	145.00	0.23	10.59	157	506	146.6	20.52	0.21
2017-11-26 11:02:57	145.00	0.24	10.60	157	503	146.6	20.52	0.21
2017-11-26 11:02:58	145.00	0.24	10.60	157	503	146.6	20.52	0.21

Appendix B.11 North basin 2017 sonde data

Location: North Basin Hole (NB)

Instrument: YSI 6600

Date / Time		Depth (m)	Temp. (°C)	pH	ORP (mV)	Sp. Cond. (µS/cm)	LDO% (% Saturation)	LDO (mg/L)	Chlorophyll (µg/L)
2017-11-26	11:03:59	150.01	0.25	10.59	157	505	146.9	20.55	0.20
2017-11-26	11:04:00	150.01	0.26	10.60	157	503	147.0	20.56	0.20
2017-11-26	11:04:01	150.01	0.26	10.60	157	503	147.0	20.56	0.20
2017-11-26	11:04:02	150.01	0.25	10.60	157	503	147.0	20.57	0.21
2017-11-26	11:04:03	150.01	0.25	10.60	157	503	147.0	20.57	0.21
2017-11-26	11:04:55	155.02	0.25	10.60	157	505	146.8	20.54	0.20
2017-11-26	11:04:56	155.04	0.25	10.60	157	503	146.8	20.54	0.20
2017-11-26	11:04:57	155.04	0.25	10.60	157	503	146.8	20.54	0.20
2017-11-26	11:04:58	155.04	0.25	10.60	157	503	146.7	20.52	0.21
2017-11-26	11:04:59	155.04	0.25	10.60	157	503	146.7	20.52	0.21
2017-11-26	11:06:47	160.03	0.25	10.60	157	505	146.7	20.53	0.21
2017-11-26	11:06:48	160.03	0.26	10.61	157	503	146.7	20.53	0.21
2017-11-26	11:06:49	160.03	0.26	10.61	157	503	146.7	20.53	0.22
2017-11-26	11:06:50	160.03	0.26	10.60	157	503	146.8	20.53	0.21
2017-11-26	11:06:51	160.03	0.26	10.60	157	503	146.8	20.53	0.21

ORP = oxidation-reduction potential

TDS = total dissolved solids

LDO = luminescent dissolved oxygen

TDS not measured at NB location in 2017

Appendix B.12 South basin 2015 sonde data

Location: South Basin Hole

Instrument: YSI 6600

Date / Time	Depth (m)	Temp. (°C)	pH	ORP (mV)	Sp. Cond. (µS/cm)	TDS (g/L)	LDO% (% Saturation)	LDO (mg/L)	Chlorophyll (µg/L)
2015-12-01 11:05:49	5.01	0.26	10.39	63	502	0.3	144.4	18.85	0.07
2015-12-01 11:05:50	5.02	0.26	10.39	63	502	0.3	144.4	18.85	0.07
2015-12-01 11:05:51	5.01	0.26	10.39	63	502	0.3	144.6	18.88	0.07
2015-12-01 11:05:52	5.01	0.26	10.39	63	502	0.3	144.6	18.88	0.07
2015-12-01 11:05:53	4.99	0.26	10.39	63	505	0.3	144.9	18.90	0.07
2015-12-01 11:05:54	4.99	0.26	10.39	63	505	0.3	144.9	18.90	0.07
2015-12-01 11:05:55	4.99	0.26	10.39	63	503	0.3	145.0	18.92	0.08
2015-12-01 11:05:56	4.99	0.26	10.39	63	503	0.3	145.0	18.92	0.08
2015-12-01 11:05:57	5.00	0.26	10.39	64	503	0.3	145.2	18.95	0.08
2015-12-01 11:05:58	5.00	0.26	10.39	64	503	0.3	145.2	18.95	0.08
2015-12-01 11:07:17	9.99	0.26	10.41	70	503	0.3	149.5	19.52	0.08
2015-12-01 11:07:18	9.99	0.26	10.41	70	503	0.3	149.5	19.52	0.08
2015-12-01 11:07:19	10.00	0.26	10.41	70	503	0.3	149.7	19.53	0.08
2015-12-01 11:07:20	10.00	0.26	10.41	70	503	0.3	149.7	19.53	0.08
2015-12-01 11:07:21	10.00	0.26	10.41	70	503	0.3	149.5	19.52	0.08
2015-12-01 11:07:22	10.00	0.26	10.41	70	503	0.3	149.5	19.52	0.08
2015-12-01 11:07:23	10.00	0.26	10.41	70	503	0.3	149.5	19.51	0.08
2015-12-01 11:07:24	10.00	0.26	10.41	70	503	0.3	149.5	19.51	0.08
2015-12-01 11:07:25	10.00	0.26	10.41	70	503	0.3	149.5	19.51	0.08
2015-12-01 11:07:26	10.00	0.26	10.41	70	503	0.3	149.5	19.51	0.08
2015-12-01 11:08:46	15.02	0.26	10.46	75	503	0.3	148.5	19.39	0.07
2015-12-01 11:08:47	15.02	0.26	10.46	75	503	0.3	148.7	19.40	0.07
2015-12-01 11:08:48	15.02	0.26	10.46	75	503	0.3	148.5	19.38	0.07
2015-12-01 11:08:49	15.02	0.26	10.46	75	503	0.3	148.5	19.38	0.07
2015-12-01 11:08:50	15.02	0.26	10.46	75	503	0.3	148.5	19.38	0.07
2015-12-01 11:08:51	15.03	0.27	10.46	75	503	0.3	148.5	19.37	0.07
2015-12-01 11:08:52	15.02	0.26	10.46	75	503	0.3	148.5	19.38	0.07
2015-12-01 11:08:56	15.02	0.26	10.46	75	502	0.3	148.4	19.37	0.07
2015-12-01 11:08:57	15.02	0.26	10.47	75	502	0.3	148.4	19.37	0.07
2015-12-01 11:08:58	15.03	0.27	10.46	75	503	0.3	148.4	19.36	0.07
2015-12-01 11:10:03	20.05	0.27	10.48	79	506	0.3	148.7	19.41	0.07
2015-12-01 11:10:04	20.05	0.27	10.48	79	506	0.3	148.7	19.41	0.07

Appendix B.12 South basin 2015 sonde data

Location: South Basin Hole

Instrument: YSI 6600

Date / Time	Depth (m)	Temp. (°C)	pH	ORP (mV)	Sp. Cond. (µS/cm)	TDS (g/L)	LDO% (% Saturation)	LDO (mg/L)	Chlorophyll (µg/L)
2015-12-01 11:10:05	20.03	0.27	10.48	79	503	0.3	148.7	19.41	0.07
2015-12-01 11:10:06	20.03	0.27	10.48	79	503	0.3	148.7	19.41	0.07
2015-12-01 11:10:07	20.04	0.27	10.48	79	503	0.3	148.7	19.40	0.07
2015-12-01 11:10:08	20.04	0.27	10.48	79	503	0.3	148.7	19.40	0.07
2015-12-01 11:10:09	20.03	0.27	10.48	79	503	0.3	148.7	19.40	0.07
2015-12-01 11:10:10	20.04	0.27	10.48	79	503	0.3	148.7	19.40	0.07
2015-12-01 11:10:11	20.04	0.27	10.48	79	503	0.3	148.7	19.39	0.07
2015-12-01 11:10:12	20.04	0.27	10.48	79	503	0.3	148.7	19.39	0.07
2015-12-01 11:11:08	25.09	0.27	10.45	81	503	0.3	147.9	19.30	0.08
2015-12-01 11:11:09	25.09	0.27	10.45	81	503	0.3	147.9	19.30	0.08
2015-12-01 11:11:10	25.09	0.27	10.45	81	503	0.3	148.0	19.30	0.08
2015-12-01 11:11:11	25.09	0.27	10.45	81	503	0.3	148.0	19.30	0.08
2015-12-01 11:11:12	25.09	0.27	10.45	81	503	0.3	148.0	19.31	0.08
2015-12-01 11:11:13	25.09	0.27	10.45	81	503	0.3	148.0	19.31	0.08
2015-12-01 11:11:14	25.10	0.27	10.45	81	503	0.3	148.0	19.31	0.08
2015-12-01 11:11:15	25.09	0.27	10.45	81	503	0.3	148.1	19.31	0.08
2015-12-01 11:11:16	25.09	0.27	10.45	81	503	0.3	148.1	19.31	0.08
2015-12-01 11:11:17	25.09	0.27	10.45	81	503	0.3	147.9	19.29	0.08
2015-12-01 11:12:21	30.03	0.28	10.43	84	503	0.3	147.1	19.20	0.08
2015-12-01 11:12:22	30.03	0.28	10.43	84	503	0.3	147.1	19.20	0.08
2015-12-01 11:12:23	30.04	0.28	10.43	84	503	0.3	147.1	19.18	0.08
2015-12-01 11:12:24	30.04	0.28	10.43	84	503	0.3	147.1	19.18	0.08
2015-12-01 11:12:25	30.05	0.28	10.43	84	503	0.3	146.9	19.17	0.08
2015-12-01 11:12:26	30.05	0.28	10.43	84	503	0.3	146.9	19.17	0.08
2015-12-01 11:12:27	30.03	0.27	10.43	84	505	0.3	146.9	19.16	0.08
2015-12-01 11:12:28	30.04	0.28	10.43	84	503	0.3	146.8	19.15	0.08
2015-12-01 11:12:29	30.04	0.28	10.43	84	503	0.3	146.8	19.15	0.08
2015-12-01 11:12:30	30.05	0.27	10.43	84	503	0.3	147.0	19.17	0.08
2015-12-01 11:13:07	35.03	0.27	10.42	85	503	0.3	146.7	19.14	0.08
2015-12-01 11:13:08	35.03	0.27	10.42	85	503	0.3	146.7	19.14	0.08
2015-12-01 11:13:09	35.02	0.27	10.42	85	506	0.3	146.5	19.11	0.08
2015-12-01 11:13:10	35.03	0.28	10.42	85	503	0.3	146.5	19.10	0.08

Appendix B.12 South basin 2015 sonde data

Location: South Basin Hole

Instrument: YSI 6600

Date / Time	Depth (m)	Temp. (°C)	pH	ORP (mV)	Sp. Cond. (µS/cm)	TDS (g/L)	LDO% (% Saturation)	LDO (mg/L)	Chlorophyll (µg/L)
2015-12-01 11:13:11	35.03	0.28	10.42	85	503	0.3	146.5	19.10	0.08
2015-12-01 11:13:12	35.04	0.28	10.42	85	503	0.3	146.4	19.10	0.08
2015-12-01 11:13:13	35.04	0.28	10.42	85	503	0.3	146.4	19.10	0.08
2015-12-01 11:13:14	35.03	0.28	10.42	85	503	0.3	146.3	19.09	0.08
2015-12-01 11:13:15	35.03	0.28	10.42	85	503	0.3	146.3	19.09	0.08
2015-12-01 11:13:16	35.04	0.27	10.42	85	503	0.3	146.4	19.09	0.08
2015-12-01 11:14:06	40.02	0.29	10.41	87	504	0.3	146.7	19.12	0.08
2015-12-01 11:14:07	40.02	0.29	10.41	87	504	0.3	146.7	19.12	0.08
2015-12-01 11:14:08	40.03	0.29	10.40	87	503	0.3	146.7	19.13	0.08
2015-12-01 11:14:09	40.03	0.29	10.40	87	503	0.3	146.7	19.13	0.08
2015-12-01 11:14:10	40.03	0.29	10.40	87	503	0.3	146.8	19.13	0.08
2015-12-01 11:14:11	40.03	0.29	10.40	87	503	0.3	146.8	19.13	0.08
2015-12-01 11:14:12	40.04	0.29	10.40	87	506	0.3	146.8	19.15	0.08
2015-12-01 11:14:13	40.02	0.29	10.40	87	503	0.3	146.7	19.13	0.08
2015-12-01 11:14:14	40.02	0.29	10.40	87	503	0.3	146.7	19.13	0.08
2015-12-01 11:14:15	40.03	0.29	10.41	87	503	0.3	146.7	19.13	0.08
2015-12-01 11:14:49	44.99	0.30	10.41	88	503	0.3	146.5	19.10	0.08
2015-12-01 11:14:50	44.99	0.30	10.41	88	503	0.3	146.6	19.11	0.08
2015-12-01 11:14:51	44.99	0.30	10.41	88	503	0.3	146.6	19.11	0.08
2015-12-01 11:14:52	44.99	0.29	10.40	88	503	0.3	146.6	19.12	0.08
2015-12-01 11:14:53	44.99	0.29	10.40	88	503	0.3	146.6	19.12	0.08
2015-12-01 11:14:54	44.99	0.29	10.40	88	506	0.3	146.7	19.13	0.08
2015-12-01 11:14:55	44.99	0.30	10.41	88	503	0.3	146.7	19.12	0.08
2015-12-01 11:14:56	44.99	0.30	10.41	88	503	0.3	146.7	19.12	0.08
2015-12-01 11:14:57	45.01	0.30	10.40	88	503	0.3	146.6	19.11	0.08
2015-12-01 11:14:58	45.01	0.30	10.40	88	503	0.3	146.6	19.11	0.08
2015-12-01 11:16:05	47.12	0.33	10.39	90	503	0.3	148.6	19.36	0.08
2015-12-01 11:16:06	47.12	0.33	10.39	90	503	0.3	148.6	19.36	0.08
2015-12-01 11:16:07	47.12	0.32	10.39	90	503	0.3	148.5	19.35	0.08
2015-12-01 11:16:08	47.12	0.32	10.39	90	503	0.3	148.5	19.35	0.08
2015-12-01 11:16:09	47.12	0.31	10.39	90	503	0.3	148.7	19.38	0.08
2015-12-01 11:16:10	47.12	0.31	10.39	90	503	0.3	148.7	19.38	0.08

Appendix B.12 South basin 2015 sonde data

Location: South Basin Hole

Instrument: YSI 6600

Date / Time	Depth (m)	Temp. (°C)	pH	ORP (mV)	Sp. Cond. (µS/cm)	TDS (g/L)	LDO% (% Saturation)	LDO (mg/L)	Chlorophyll (µg/L)
2015-12-01 11:16:11	47.11	0.32	10.39	90	505	0.3	148.4	19.33	0.08
2015-12-01 11:16:12	47.12	0.32	10.39	90	503	0.3	148.3	19.32	0.08
2015-12-01 11:16:13	47.12	0.32	10.39	90	503	0.3	148.3	19.32	0.08
2015-12-01 11:16:14	47.11	0.32	10.39	90	503	0.3	148.3	19.32	0.08
2015-12-01 11:17:03	48.11	0.33	10.39	91	503	0.3	147.1	19.16	0.08
2015-12-01 11:17:04	48.11	0.33	10.39	91	503	0.3	147.1	19.16	0.08
2015-12-01 11:17:05	48.11	0.33	10.39	91	503	0.3	147.1	19.16	0.09
2015-12-01 11:17:06	48.11	0.33	10.39	91	503	0.3	147.1	19.16	0.09
2015-12-01 11:17:07	48.11	0.33	10.39	91	506	0.3	147.2	19.18	0.08
2015-12-01 11:17:08	48.11	0.33	10.39	91	503	0.3	147.1	19.16	0.09
2015-12-01 11:17:09	48.11	0.33	10.39	91	503	0.3	147.1	19.16	0.09
2015-12-01 11:17:10	48.12	0.33	10.39	91	503	0.3	147.1	19.16	0.09
2015-12-01 11:17:11	48.12	0.33	10.39	91	503	0.3	147.1	19.16	0.09
2015-12-01 11:17:12	48.12	0.33	10.38	91	503	0.3	147.0	19.14	0.09
2015-12-01 11:17:28	49.03	1.98	10.35	91	511	0.3	147.5	18.36	0.11
2015-12-01 11:17:29	49.03	2.00	10.35	91	508	0.3	148.3	18.43	0.11
2015-12-01 11:17:30	49.03	2.00	10.35	91	508	0.3	148.3	18.43	0.11
2015-12-01 11:17:31	49.03	2.06	10.35	91	507	0.3	149.0	18.49	0.12
2015-12-01 11:17:32	49.03	2.06	10.35	91	507	0.3	149.0	18.49	0.12
2015-12-01 11:17:33	49.03	2.08	10.35	91	507	0.3	149.7	18.57	0.12
2015-12-01 11:17:34	49.03	2.08	10.35	91	507	0.3	149.7	18.57	0.12
2015-12-01 11:17:35	49.03	2.06	10.35	91	510	0.3	150.3	18.66	0.12
2015-12-01 11:17:36	49.05	2.04	10.35	91	508	0.3	150.8	18.74	0.12
2015-12-01 11:17:37	49.05	2.04	10.35	91	508	0.3	150.8	18.74	0.12
2015-12-01 11:18:05	49.97	3.65	10.31	90	517	0.3	158.0	18.79	0.22
2015-12-01 11:18:06	49.97	3.65	10.31	90	519	0.3	158.3	18.83	0.23
2015-12-01 11:18:07	49.97	3.65	10.31	90	519	0.3	158.3	18.83	0.23
2015-12-01 11:18:08	49.97	3.66	10.31	90	517	0.3	158.4	18.83	0.23
2015-12-01 11:18:09	49.97	3.66	10.31	90	517	0.3	158.4	18.83	0.23
2015-12-01 11:18:10	49.97	3.67	10.31	90	519	0.3	158.5	18.84	0.23
2015-12-01 11:18:11	49.97	3.67	10.31	90	517	0.3	158.6	18.86	0.23
2015-12-01 11:18:12	49.97	3.67	10.31	90	517	0.3	158.6	18.86	0.23

Appendix B.12 South basin 2015 sonde data

Location: South Basin Hole

Instrument: YSI 6600

Date / Time	Depth (m)	Temp. (°C)	pH	ORP (mV)	Sp. Cond. (µS/cm)	TDS (g/L)	LDO% (% Saturation)	LDO (mg/L)	Chlorophyll (µg/L)
2015-12-01 11:18:13	49.98	3.67	10.31	90	517	0.3	158.7	18.87	0.23
2015-12-01 11:18:14	49.98	3.67	10.31	90	517	0.3	158.7	18.87	0.23
2015-12-01 11:18:50	51.11	3.92	10.30	90	518	0.3	160.6	18.97	0.26
2015-12-01 11:18:51	51.11	3.92	10.30	90	518	0.3	160.6	18.97	0.26
2015-12-01 11:18:52	51.13	3.92	10.30	90	518	0.3	160.6	18.97	0.26
2015-12-01 11:18:53	51.11	3.92	10.30	90	518	0.3	160.6	18.96	0.26
2015-12-01 11:18:54	51.11	3.92	10.30	90	518	0.3	160.6	18.96	0.26
2015-12-01 11:18:55	51.13	3.93	10.30	90	518	0.3	160.5	18.95	0.26
2015-12-01 11:18:56	51.13	3.93	10.30	90	518	0.3	160.5	18.95	0.26
2015-12-01 11:18:57	51.13	3.93	10.30	90	518	0.3	160.6	18.97	0.27
2015-12-01 11:18:58	51.13	3.93	10.30	90	518	0.3	160.6	18.97	0.27
2015-12-01 11:18:59	51.13	3.93	10.30	90	521	0.3	160.6	18.96	0.27
2015-12-01 11:19:23	52.09	3.97	10.30	90	518	0.3	160.7	18.95	0.29
2015-12-01 11:19:24	52.09	3.97	10.30	90	518	0.3	160.7	18.95	0.29
2015-12-01 11:19:25	52.08	3.96	10.30	90	519	0.3	160.7	18.96	0.29
2015-12-01 11:19:26	52.08	3.96	10.30	90	519	0.3	160.7	18.96	0.29
2015-12-01 11:19:27	52.08	3.96	10.30	91	521	0.3	160.8	18.97	0.29
2015-12-01 11:19:28	52.09	3.97	10.30	91	519	0.3	160.8	18.97	0.30
2015-12-01 11:19:29	52.09	3.97	10.30	91	519	0.3	160.8	18.97	0.30
2015-12-01 11:19:30	52.08	3.96	10.30	91	518	0.3	161.0	18.99	0.29
2015-12-01 11:19:31	52.08	3.96	10.30	91	518	0.3	161.0	18.99	0.29
2015-12-01 11:19:32	52.09	3.96	10.30	91	518	0.3	160.9	18.98	0.29
2015-12-01 11:19:47	53.07	3.97	10.30	91	519	0.3	161.3	19.02	0.29
2015-12-01 11:19:48	53.06	3.98	10.30	91	521	0.3	161.4	19.03	0.30
2015-12-01 11:19:49	53.06	3.97	10.30	91	519	0.3	161.3	19.03	0.30
2015-12-01 11:19:50	53.06	3.97	10.30	91	519	0.3	161.3	19.03	0.30
2015-12-01 11:19:51	53.06	3.98	10.30	91	519	0.3	161.3	19.02	0.31
2015-12-01 11:19:52	53.06	3.98	10.30	91	519	0.3	161.3	19.02	0.31
2015-12-01 11:19:53	53.06	3.97	10.30	91	519	0.3	161.4	19.04	0.31
2015-12-01 11:19:54	53.06	3.97	10.30	91	519	0.3	161.4	19.04	0.31
2015-12-01 11:19:55	53.06	3.97	10.30	91	521	0.3	161.3	19.02	0.31
2015-12-01 11:19:56	53.07	3.98	10.30	91	518	0.3	161.1	19.00	0.31

Appendix B.12 South basin 2015 sonde data

Location: South Basin Hole

Instrument: YSI 6600

Date / Time	Depth (m)	Temp. (°C)	pH	ORP (mV)	Sp. Cond. (µS/cm)	TDS (g/L)	LDO% (% Saturation)	LDO (mg/L)	Chlorophyll (µg/L)
2015-12-01 11:20:09	54.07	3.97	10.30	91	521	0.3	161.2	19.00	0.31
2015-12-01 11:20:10	54.09	3.98	10.30	91	519	0.3	160.9	18.97	0.31
2015-12-01 11:20:11	54.09	3.98	10.30	91	519	0.3	160.9	18.97	0.31
2015-12-01 11:20:12	54.07	3.98	10.30	91	519	0.3	161.0	18.98	0.31
2015-12-01 11:20:13	54.07	3.98	10.30	91	519	0.3	161.0	18.98	0.31
2015-12-01 11:20:14	54.08	3.98	10.30	91	519	0.3	161.1	19.00	0.32
2015-12-01 11:20:15	54.08	3.98	10.30	91	519	0.3	161.1	19.00	0.32
2015-12-01 11:20:16	54.07	3.98	10.30	91	521	0.3	161.2	19.01	0.32
2015-12-01 11:20:17	54.07	3.98	10.30	91	519	0.3	161.3	19.02	0.31
2015-12-01 11:20:18	54.07	3.98	10.30	91	519	0.3	161.3	19.02	0.31
2015-12-01 11:20:53	55.11	3.98	10.29	92	519	0.3	161.4	19.03	0.29
2015-12-01 11:20:54	55.11	3.98	10.29	92	519	0.3	161.3	19.02	0.29
2015-12-01 11:20:55	55.11	3.98	10.29	92	519	0.3	161.3	19.02	0.29
2015-12-01 11:20:56	55.11	3.97	10.29	92	518	0.3	161.4	19.03	0.29
2015-12-01 11:20:57	55.11	3.97	10.29	92	518	0.3	161.4	19.03	0.29
2015-12-01 11:20:58	55.13	3.97	10.29	92	521	0.3	161.5	19.04	0.30
2015-12-01 11:20:59	55.12	3.98	10.29	92	518	0.3	161.5	19.04	0.29
2015-12-01 11:21:00	55.12	3.98	10.29	92	518	0.3	161.5	19.04	0.29
2015-12-01 11:21:01	55.11	3.97	10.30	92	518	0.3	161.4	19.03	0.29
2015-12-01 11:21:02	55.11	3.97	10.30	92	518	0.3	161.4	19.03	0.29
2015-12-01 11:21:24	56.04	3.97	10.29	93	519	0.3	161.5	19.05	0.30
2015-12-01 11:21:25	56.04	3.97	10.29	93	519	0.3	161.5	19.05	0.30
2015-12-01 11:21:26	56.04	3.97	10.29	93	521	0.3	161.5	19.05	0.30
2015-12-01 11:21:27	56.03	3.98	10.29	93	518	0.3	161.6	19.05	0.30
2015-12-01 11:21:28	56.03	3.98	10.29	93	518	0.3	161.6	19.05	0.30
2015-12-01 11:21:29	56.02	3.97	10.29	93	518	0.3	161.4	19.03	0.30
2015-12-01 11:21:30	56.02	3.97	10.29	93	518	0.3	161.4	19.03	0.30
2015-12-01 11:21:31	56.04	3.97	10.29	93	519	0.3	161.2	19.02	0.30
2015-12-01 11:21:32	56.04	3.97	10.29	93	519	0.3	161.2	19.02	0.30
2015-12-01 11:21:33	56.03	3.97	10.29	93	519	0.3	161.3	19.02	0.30
2015-12-01 11:21:49	56.99	3.97	10.29	93	519	0.3	161.7	19.07	0.32
2015-12-01 11:21:50	57.00	3.97	10.29	93	519	0.3	161.6	19.06	0.32

Appendix B.12 South basin 2015 sonde data

Location: South Basin Hole

Instrument: YSI 6600

Date / Time	Depth (m)	Temp. (°C)	pH	ORP (mV)	Sp. Cond. (µS/cm)	TDS (g/L)	LDO% (% Saturation)	LDO (mg/L)	Chlorophyll (µg/L)
2015-12-01 11:21:51	57.00	3.97	10.29	93	519	0.3	161.6	19.06	0.32
2015-12-01 11:21:52	56.99	3.97	10.29	93	519	0.3	161.8	19.08	0.32
2015-12-01 11:21:53	56.99	3.97	10.29	93	519	0.3	161.8	19.08	0.32
2015-12-01 11:21:54	56.99	3.97	10.29	93	521	0.3	161.7	19.07	0.31
2015-12-01 11:21:55	56.99	3.97	10.29	93	518	0.3	161.5	19.05	0.31
2015-12-01 11:21:56	56.99	3.97	10.29	93	518	0.3	161.5	19.05	0.31
2015-12-01 11:21:57	56.99	3.97	10.29	93	519	0.3	161.6	19.06	0.31
2015-12-01 11:21:58	56.99	3.97	10.29	93	519	0.3	161.6	19.06	0.31
2015-12-01 11:22:20	58.09	3.97	10.29	94	519	0.3	161.5	19.05	0.34
2015-12-01 11:22:21	58.09	3.97	10.29	94	519	0.3	161.5	19.05	0.34
2015-12-01 11:22:22	58.09	3.97	10.29	94	519	0.3	161.5	19.05	0.34
2015-12-01 11:22:23	58.09	3.97	10.29	94	519	0.3	161.6	19.06	0.34
2015-12-01 11:22:24	58.09	3.97	10.29	94	519	0.3	161.6	19.06	0.34
2015-12-01 11:22:25	58.08	3.97	10.29	94	519	0.3	161.6	19.05	0.34
2015-12-01 11:22:26	58.08	3.97	10.29	94	519	0.3	161.6	19.05	0.34
2015-12-01 11:22:27	58.08	3.97	10.29	94	519	0.3	161.6	19.06	0.35
2015-12-01 11:22:28	58.08	3.97	10.29	94	519	0.3	161.6	19.06	0.35
2015-12-01 11:22:29	58.09	3.97	10.29	94	521	0.3	161.6	19.06	0.36
2015-12-01 11:22:43	58.99	3.97	10.29	94	521	0.3	161.4	19.03	0.34
2015-12-01 11:22:44	59.00	3.97	10.29	94	519	0.3	161.3	19.02	0.34
2015-12-01 11:22:45	59.00	3.97	10.29	94	519	0.3	161.3	19.02	0.34
2015-12-01 11:22:46	59.01	3.97	10.29	94	518	0.3	161.4	19.04	0.32
2015-12-01 11:22:47	59.01	3.97	10.29	94	518	0.3	161.4	19.04	0.32
2015-12-01 11:22:48	59.01	3.97	10.29	94	518	0.3	161.5	19.04	0.32
2015-12-01 11:22:49	59.01	3.97	10.29	94	518	0.3	161.5	19.04	0.32
2015-12-01 11:22:50	59.00	3.97	10.29	94	521	0.3	161.5	19.04	0.32
2015-12-01 11:22:51	59.02	3.97	10.29	94	519	0.3	161.5	19.04	0.32
2015-12-01 11:22:52	59.02	3.97	10.29	94	519	0.3	161.5	19.04	0.32
2015-12-01 11:23:12	60.04	3.97	10.29	95	518	0.3	161.7	19.07	0.33
2015-12-01 11:23:13	60.04	3.97	10.29	95	518	0.3	161.7	19.07	0.34
2015-12-01 11:23:14	60.04	3.97	10.29	95	519	0.3	161.6	19.05	0.34
2015-12-01 11:23:15	60.04	3.97	10.29	95	519	0.3	161.6	19.05	0.34

Appendix B.12 South basin 2015 sonde data

Location: South Basin Hole

Instrument: YSI 6600

Date / Time	Depth (m)	Temp. (°C)	pH	ORP (mV)	Sp. Cond. (µS/cm)	TDS (g/L)	LDO% (% Saturation)	LDO (mg/L)	Chlorophyll (µg/L)
2015-12-01 11:23:16	60.05	3.97	10.29	95	519	0.3	161.5	19.04	0.34
2015-12-01 11:23:17	60.05	3.97	10.29	95	519	0.3	161.5	19.04	0.34
2015-12-01 11:23:18	60.04	3.97	10.29	95	521	0.3	161.7	19.07	0.35
2015-12-01 11:23:19	60.05	3.97	10.29	95	519	0.3	161.5	19.05	0.35
2015-12-01 11:23:20	60.05	3.97	10.29	95	519	0.3	161.5	19.05	0.35
2015-12-01 11:23:21	60.06	3.98	10.29	95	519	0.3	161.5	19.04	0.35
2015-12-01 11:23:39	61.00	3.97	10.29	95	519	0.3	161.7	19.06	0.36
2015-12-01 11:23:40	61.00	3.97	10.29	95	518	0.3	161.6	19.06	0.36
2015-12-01 11:23:41	61.00	3.97	10.29	95	518	0.3	161.6	19.06	0.36
2015-12-01 11:23:42	61.01	3.97	10.29	95	519	0.3	161.5	19.04	0.36
2015-12-01 11:23:43	61.01	3.97	10.29	95	519	0.3	161.5	19.04	0.36
2015-12-01 11:23:44	61.00	3.97	10.29	95	519	0.3	161.4	19.03	0.37
2015-12-01 11:23:45	61.00	3.97	10.29	95	519	0.3	161.4	19.03	0.37
2015-12-01 11:23:46	61.00	3.97	10.29	95	521	0.3	161.4	19.03	0.37
2015-12-01 11:23:47	61.01	3.98	10.29	95	519	0.3	161.3	19.01	0.37
2015-12-01 11:23:48	61.01	3.98	10.29	95	519	0.3	161.3	19.01	0.37
2015-12-01 11:24:20	62.02	3.97	10.28	96	519	0.3	161.5	19.04	0.37
2015-12-01 11:24:21	62.02	3.97	10.28	96	521	0.3	161.5	19.05	0.37
2015-12-01 11:24:22	62.01	3.97	10.29	96	519	0.3	161.6	19.06	0.36
2015-12-01 11:24:23	62.01	3.97	10.29	96	519	0.3	161.6	19.06	0.36
2015-12-01 11:24:24	62.05	3.97	10.29	96	519	0.3	161.6	19.06	0.36
2015-12-01 11:24:25	62.05	3.97	10.29	96	519	0.3	161.6	19.06	0.36
2015-12-01 11:24:26	62.06	3.97	10.28	96	519	0.3	161.4	19.04	0.36
2015-12-01 11:24:27	62.06	3.97	10.28	96	519	0.3	161.4	19.04	0.36
2015-12-01 11:24:28	62.06	3.97	10.28	96	521	0.3	161.3	19.02	0.36
2015-12-01 11:24:29	62.07	3.97	10.28	96	519	0.3	161.3	19.01	0.36
2015-12-01 11:24:42	62.99	3.97	10.29	96	519	0.3	160.9	18.97	0.38
2015-12-01 11:24:43	62.98	3.97	10.29	96	519	0.3	161.0	18.99	0.38
2015-12-01 11:24:44	62.98	3.97	10.29	96	519	0.3	161.0	18.99	0.38
2015-12-01 11:24:45	62.98	3.97	10.29	96	519	0.3	161.1	19.00	0.39
2015-12-01 11:24:46	62.98	3.97	10.29	96	519	0.3	161.1	19.00	0.39
2015-12-01 11:24:47	62.99	3.97	10.28	96	519	0.3	161.2	19.01	0.39

Appendix B.12 South basin 2015 sonde data

Location: South Basin Hole

Instrument: YSI 6600

Date / Time	Depth (m)	Temp. (°C)	pH	ORP (mV)	Sp. Cond. (µS/cm)	TDS (g/L)	LDO% (% Saturation)	LDO (mg/L)	Chlorophyll (µg/L)
2015-12-01 11:24:48	62.99	3.97	10.28	96	519	0.3	161.2	19.01	0.39
2015-12-01 11:24:49	62.98	3.97	10.28	96	521	0.3	161.2	19.01	0.39
2015-12-01 11:24:50	62.99	3.98	10.29	96	519	0.3	161.4	19.03	0.40
2015-12-01 11:24:51	62.99	3.98	10.29	96	519	0.3	161.4	19.03	0.40
2015-12-01 11:25:13	64.06	3.98	10.28	97	519	0.3	161.8	19.08	0.47
2015-12-01 11:25:14	64.06	3.98	10.28	97	519	0.3	161.8	19.08	0.47
2015-12-01 11:25:15	64.07	3.97	10.28	97	519	0.3	161.7	19.07	0.48
2015-12-01 11:25:16	64.07	3.97	10.28	97	519	0.3	161.7	19.07	0.48
2015-12-01 11:25:17	64.07	3.97	10.28	97	521	0.3	161.9	19.09	0.49
2015-12-01 11:25:18	64.07	3.98	10.28	97	519	0.3	161.8	19.07	0.49
2015-12-01 11:25:19	64.07	3.98	10.28	97	519	0.3	161.8	19.07	0.49
2015-12-01 11:25:20	64.07	3.97	10.28	97	518	0.3	161.6	19.06	0.50
2015-12-01 11:25:21	64.07	3.97	10.28	97	518	0.3	161.6	19.06	0.50
2015-12-01 11:25:22	64.06	3.97	10.28	97	519	0.3	161.6	19.05	0.48
2015-12-01 11:25:44	65.07	3.97	10.28	97	519	0.3	160.7	18.95	0.47
2015-12-01 11:25:45	65.08	3.97	10.28	97	519	0.3	160.8	18.97	0.46
2015-12-01 11:25:46	65.08	3.97	10.28	97	519	0.3	161.0	18.98	0.46
2015-12-01 11:25:47	65.08	3.97	10.28	97	519	0.3	161.0	18.98	0.46
2015-12-01 11:25:48	65.07	3.97	10.28	97	519	0.3	161.0	18.98	0.47
2015-12-01 11:25:49	65.07	3.97	10.28	97	519	0.3	161.0	18.98	0.47
2015-12-01 11:25:50	65.08	3.97	10.28	97	519	0.3	161.1	18.99	0.47
2015-12-01 11:25:51	65.08	3.97	10.28	97	519	0.3	161.1	18.99	0.47
2015-12-01 11:25:52	65.08	3.97	10.28	97	521	0.3	161.2	19.01	0.48
2015-12-01 11:25:53	65.08	3.98	10.28	97	519	0.3	161.3	19.02	0.48
2015-12-01 11:26:07	65.96	4.00	10.27	98	518	0.3	161.4	19.02	0.50
2015-12-01 11:26:08	65.96	4.00	10.27	98	518	0.3	161.4	19.02	0.50
2015-12-01 11:26:09	65.97	4.00	10.27	98	518	0.3	161.4	19.02	0.50
2015-12-01 11:26:10	65.97	4.00	10.27	98	518	0.3	161.4	19.02	0.50
2015-12-01 11:26:11	65.97	4.00	10.27	98	518	0.3	161.3	19.00	0.51
2015-12-01 11:26:12	65.97	4.00	10.27	98	518	0.3	161.3	19.00	0.51
2015-12-01 11:26:13	65.96	4.00	10.27	98	518	0.3	161.3	19.00	0.53
2015-12-01 11:26:14	65.95	4.01	10.27	98	518	0.3	161.3	19.00	0.53

Appendix B.12 South basin 2015 sonde data

Location: South Basin Hole

Instrument: YSI 6600

Date / Time	Depth (m)	Temp. (°C)	pH	ORP (mV)	Sp. Cond. (µS/cm)	TDS (g/L)	LDO% (% Saturation)	LDO (mg/L)	Chlorophyll (µg/L)
2015-12-01 11:26:15	65.95	4.01	10.27	98	518	0.3	161.3	19.00	0.53
2015-12-01 11:26:16	65.95	4.01	10.27	98	518	0.3	161.3	19.00	0.53
2015-12-01 11:26:38	67.06	4.14	10.18	101	517	0.3	159.4	18.71	0.74
2015-12-01 11:26:39	67.08	4.14	10.18	102	517	0.3	159.0	18.66	0.75
2015-12-01 11:26:40	67.08	4.14	10.18	102	517	0.3	159.0	18.66	0.75
2015-12-01 11:26:41	67.07	4.14	10.18	102	519	0.3	158.6	18.62	0.76
2015-12-01 11:26:42	67.08	4.14	10.18	102	517	0.3	158.1	18.56	0.78
2015-12-01 11:26:43	67.08	4.14	10.18	102	517	0.3	158.1	18.56	0.78
2015-12-01 11:26:44	67.07	4.14	10.18	102	517	0.3	157.4	18.48	0.78
2015-12-01 11:26:45	67.07	4.14	10.18	102	517	0.3	157.4	18.48	0.78
2015-12-01 11:26:46	67.07	4.14	10.17	102	517	0.3	156.9	18.42	0.78
2015-12-01 11:26:47	67.07	4.14	10.17	102	517	0.3	156.9	18.42	0.78
2015-12-01 11:27:17	68.10	4.24	10.07	105	516	0.3	149.4	17.50	0.90
2015-12-01 11:27:18	68.10	4.24	10.07	105	516	0.3	149.4	17.50	0.90
2015-12-01 11:27:19	68.10	4.24	10.07	105	515	0.3	148.9	17.43	0.91
2015-12-01 11:27:20	68.10	4.24	10.07	105	515	0.3	148.9	17.43	0.91
2015-12-01 11:27:21	68.10	4.24	10.06	105	516	0.3	148.5	17.38	0.91
2015-12-01 11:27:22	68.10	4.24	10.06	105	516	0.3	148.5	17.38	0.91
2015-12-01 11:27:23	68.09	4.24	10.06	105	518	0.3	148.0	17.33	0.91
2015-12-01 11:27:24	68.10	4.25	10.06	105	515	0.3	147.6	17.27	0.92
2015-12-01 11:27:25	68.10	4.25	10.06	105	515	0.3	147.6	17.27	0.92
2015-12-01 11:27:26	68.10	4.25	10.06	105	515	0.3	147.0	17.21	0.92
2015-12-01 11:27:48	69.05	4.46	9.81	115	517	0.3	125.3	14.59	1.17
2015-12-01 11:27:49	69.05	4.46	9.80	115	517	0.3	124.8	14.53	1.18
2015-12-01 11:27:50	69.05	4.46	9.80	115	517	0.3	124.8	14.53	1.18
2015-12-01 11:27:51	69.05	4.46	9.80	115	520	0.3	125.1	14.56	1.21
2015-12-01 11:27:52	69.05	4.46	9.80	115	517	0.3	124.8	14.53	1.22
2015-12-01 11:27:53	69.05	4.46	9.80	115	517	0.3	124.8	14.53	1.22
2015-12-01 11:27:54	69.06	4.46	9.80	115	516	0.3	124.5	14.50	1.21
2015-12-01 11:27:55	69.06	4.46	9.80	115	516	0.3	124.5	14.50	1.21
2015-12-01 11:27:56	69.07	4.46	9.79	115	517	0.3	124.2	14.45	1.20
2015-12-01 11:27:57	69.07	4.46	9.79	115	517	0.3	124.2	14.45	1.20

Appendix B.12 South basin 2015 sonde data

Location: South Basin Hole

Instrument: YSI 6600

Date / Time	Depth (m)	Temp. (°C)	pH	ORP (mV)	Sp. Cond. (µS/cm)	TDS (g/L)	LDO% (% Saturation)	LDO (mg/L)	Chlorophyll (µg/L)
2015-12-01 11:28:16	70.11	4.71	9.42	132	530	0.3	97.4	11.27	1.22
2015-12-01 11:28:17	70.11	4.71	9.41	132	531	0.3	88.0	10.17	1.25
2015-12-01 11:28:18	70.11	4.71	9.41	132	531	0.3	88.0	10.17	1.25
2015-12-01 11:28:19	70.11	4.71	9.39	132	535	0.3	87.1	10.07	1.27
2015-12-01 11:28:20	70.13	4.71	9.38	133	531	0.3	86.1	9.96	1.30
2015-12-01 11:28:21	70.13	4.71	9.38	133	531	0.3	86.1	9.96	1.30
2015-12-01 11:28:22	70.11	4.71	9.37	133	531	0.3	85.2	9.85	1.31
2015-12-01 11:28:23	70.11	4.71	9.37	133	531	0.3	85.2	9.85	1.31
2015-12-01 11:28:24	70.11	4.71	9.36	133	533	0.3	84.3	9.75	1.31
2015-12-01 11:28:25	70.11	4.71	9.36	133	533	0.3	84.3	9.75	1.31
2015-12-01 11:28:40	71.08	4.89	9.11	144	540	0.3	54.2	6.24	1.37
2015-12-01 11:28:41	71.07	4.89	9.10	144	539	0.3	52.5	6.04	1.38
2015-12-01 11:28:42	71.07	4.89	9.10	144	539	0.3	52.5	6.04	1.38
2015-12-01 11:28:43	71.07	4.90	9.10	145	537	0.3	51.2	5.90	1.41
2015-12-01 11:28:44	71.07	4.90	9.10	145	537	0.3	51.2	5.90	1.41
2015-12-01 11:28:45	71.07	4.90	9.09	145	537	0.3	50.1	5.77	1.43
2015-12-01 11:28:46	71.07	4.90	9.09	145	537	0.3	50.1	5.77	1.43
2015-12-01 11:28:47	71.08	4.89	9.08	145	541	0.3	45.3	5.21	1.44
2015-12-01 11:28:48	71.09	4.89	9.07	145	538	0.3	44.7	5.14	1.45
2015-12-01 11:28:49	71.09	4.89	9.07	145	538	0.3	44.7	5.14	1.45
2015-12-01 11:29:50	72.03	4.93	8.77	152	543	0.3	25.7	2.95	1.67
2015-12-01 11:29:51	72.03	4.93	8.77	152	540	0.3	25.5	2.93	1.67
2015-12-01 11:29:52	72.03	4.93	8.77	152	540	0.3	25.5	2.93	1.67
2015-12-01 11:29:53	72.03	4.93	8.76	152	540	0.3	25.1	2.88	1.68
2015-12-01 11:29:54	72.03	4.93	8.76	152	540	0.3	25.1	2.88	1.68
2015-12-01 11:29:55	72.03	4.93	8.76	152	541	0.3	24.7	2.84	1.70
2015-12-01 11:29:56	72.03	4.93	8.76	152	541	0.3	24.7	2.84	1.70
2015-12-01 11:29:57	72.03	4.93	8.75	152	543	0.3	24.3	2.80	1.72
2015-12-01 11:29:58	72.02	4.93	8.75	153	541	0.3	24.0	2.76	1.72
2015-12-01 11:29:59	72.02	4.93	8.75	153	541	0.3	24.0	2.76	1.71
2015-12-01 11:30:24	73.07	4.95	8.61	156	541	0.3	17.6	2.02	1.81
2015-12-01 11:30:25	73.07	4.96	8.61	156	544	0.3	17.3	1.98	1.84

Appendix B.12 South basin 2015 sonde data

Location: South Basin Hole

Instrument: YSI 6600

Date / Time	Depth (m)	Temp. (°C)	pH	ORP (mV)	Sp. Cond. (µS/cm)	TDS (g/L)	LDO% (% Saturation)	LDO (mg/L)	Chlorophyll (µg/L)
2015-12-01 11:30:26	73.07	4.96	8.61	156	542	0.3	16.9	1.94	1.86
2015-12-01 11:30:27	73.07	4.96	8.61	156	542	0.3	16.9	1.94	1.86
2015-12-01 11:30:28	73.07	4.96	8.60	156	542	0.3	14.3	1.65	1.89
2015-12-01 11:30:29	73.07	4.96	8.60	156	542	0.3	14.3	1.65	1.89
2015-12-01 11:30:30	73.07	4.96	8.60	156	542	0.3	14.2	1.63	1.91
2015-12-01 11:30:31	73.07	4.96	8.60	156	542	0.3	14.2	1.63	1.91
2015-12-01 11:30:32	73.09	4.96	8.60	156	544	0.3	14.0	1.61	1.95
2015-12-01 11:30:33	73.07	4.96	8.60	156	542	0.3	13.8	1.58	1.98
2015-12-01 11:30:47	74.02	4.97	8.51	157	544	0.3	6.8	0.78	0.98
2015-12-01 11:30:48	74.02	4.97	8.51	157	544	0.3	6.8	0.78	0.98
2015-12-01 11:30:49	74.02	4.97	8.50	157	544	0.3	6.5	0.74	0.97
2015-12-01 11:30:50	74.02	4.97	8.50	157	544	0.3	6.5	0.74	0.97
2015-12-01 11:30:51	74.02	4.97	8.50	156	543	0.3	6.1	0.70	0.97
2015-12-01 11:30:52	74.02	4.97	8.50	156	544	0.3	6.1	0.70	0.97
2015-12-01 11:30:53	74.01	4.97	8.50	156	544	0.3	4.1	0.47	0.97
2015-12-01 11:30:54	74.01	4.97	8.49	156	544	0.3	3.9	0.45	0.96
2015-12-01 11:30:55	74.01	4.97	8.49	156	544	0.3	3.9	0.45	0.96
2015-12-01 11:30:56	74.08	4.97	8.48	156	544	0.3	3.7	0.43	0.95
2015-12-01 11:31:29	75.13	4.96	8.39	126	544	0.3	0.4	0.05	0.52
2015-12-01 11:31:30	75.13	4.96	8.39	126	544	0.3	0.4	0.05	0.52
2015-12-01 11:31:31	75.14	4.96	8.39	124	544	0.3	0.3	0.04	0.52
2015-12-01 11:31:32	75.14	4.96	8.39	124	544	0.3	0.3	0.04	0.52
2015-12-01 11:31:33	75.12	4.96	8.39	122	544	0.3	0.3	0.03	0.52
2015-12-01 11:31:34	75.12	4.96	8.39	122	544	0.3	0.3	0.03	0.52
2015-12-01 11:31:35	75.15	4.96	8.39	121	546	0.3	0.2	0.02	0.51
2015-12-01 11:31:36	75.13	4.97	8.38	119	544	0.3	0.2	0.02	0.51
2015-12-01 11:31:37	75.13	4.97	8.38	119	544	0.3	0.2	0.02	0.51
2015-12-01 11:31:38	75.13	4.96	8.38	117	544	0.3	0.1	0.02	0.52
2015-12-01 11:32:04	76.05	4.95	8.30	67	544	0.3	0	0	0.46
2015-12-01 11:32:05	76.05	4.95	8.30	67	544	0.3	0	0	0.46
2015-12-01 11:32:06	76.06	4.95	8.30	65	544	0.3	0	0	0.45
2015-12-01 11:32:07	76.06	4.95	8.30	65	544	0.3	0	0	0.45

Appendix B.12 South basin 2015 sonde data

Location: South Basin Hole

Instrument: YSI 6600

Date / Time	Depth (m)	Temp. (°C)	pH	ORP (mV)	Sp. Cond. (µS/cm)	TDS (g/L)	LDO% (% Saturation)	LDO (mg/L)	Chlorophyll (µg/L)
2015-12-01 11:32:08	76.05	4.95	8.30	63	544	0.3	0	0	0.45
2015-12-01 11:32:09	76.05	4.95	8.30	63	544	0.3	0	0	0.45
2015-12-01 11:32:10	76.07	4.95	8.29	62	546	0.3	0	0	0.45
2015-12-01 11:32:11	76.06	4.96	8.29	60	544	0.3	0	0	0.44
2015-12-01 11:32:12	76.06	4.96	8.29	60	544	0.3	0	0	0.44
2015-12-01 11:32:13	76.07	4.95	8.29	59	544	0.3	0	0	0.45
2015-12-01 11:32:39	77.11	4.95	8.24	40	544	0.3	0	0	0.43
2015-12-01 11:32:40	77.11	4.95	8.24	40	544	0.3	0	0	0.43
2015-12-01 11:32:41	77.12	4.95	8.24	39	544	0.3	0	0	0.42
2015-12-01 11:32:42	77.12	4.95	8.24	39	544	0.3	0	0	0.42
2015-12-01 11:32:43	76.91	4.95	8.23	38	544	0.3	0	0	0.42
2015-12-01 11:32:44	76.91	4.95	8.23	38	544	0.3	0	0	0.42
2015-12-01 11:32:45	76.78	4.95	8.22	37	547	0.3	0	0	0.42
2015-12-01 11:32:46	76.78	4.95	8.21	36	544	0.3	0	0	0.43
2015-12-01 11:32:47	76.78	4.95	8.21	36	544	0.3	0	0	0.43
2015-12-01 11:32:48	76.93	4.95	8.21	35	544	0.3	0	0	0.43
2015-12-01 11:34:04	78.01	4.95	8.05	5	544	0.3	0	0	0.42
2015-12-01 11:34:05	78.04	4.95	8.05	4	544	0.3	0	0	0.42
2015-12-01 11:34:06	78.04	4.95	8.05	4	544	0.3	0	0	0.42
2015-12-01 11:34:07	78.06	4.95	8.05	3	544	0.3	0	0	0.42
2015-12-01 11:34:08	78.06	4.95	8.05	3	544	0.3	0	0	0.42
2015-12-01 11:34:09	78.06	4.95	8.05	2	547	0.3	0	0	0.41
2015-12-01 11:34:10	78.04	4.95	8.05	1	544	0.3	0	0	0.41
2015-12-01 11:34:11	78.04	4.95	8.05	1	544	0.3	0	0	0.41
2015-12-01 11:34:12	78.04	4.95	8.05	0	544	0.3	0	0	0.41
2015-12-01 11:34:13	78.04	4.95	8.05	0	544	0.3	0	0	0.41
2015-12-01 11:34:46	79.02	4.96	7.92	-32	548	0.4	0	0	0.44
2015-12-01 11:34:47	79.03	4.97	7.92	-33	547	0.4	0	0	0.44
2015-12-01 11:34:48	79.03	4.97	7.92	-33	547	0.4	0	0	0.44
2015-12-01 11:34:49	79.04	4.96	7.92	-34	547	0.4	0	0	0.44
2015-12-01 11:34:50	79.04	4.96	7.92	-34	547	0.4	0	0	0.44
2015-12-01 11:34:51	79.02	4.96	7.92	-35	550	0.4	0	0	0.44

Appendix B.12 South basin 2015 sonde data

Location: South Basin Hole

Instrument: YSI 6600

Date / Time	Depth (m)	Temp. (°C)	pH	ORP (mV)	Sp. Cond. (µS/cm)	TDS (g/L)	LDO% (% Saturation)	LDO (mg/L)	Chlorophyll (µg/L)
2015-12-01 11:34:52	79.02	4.97	7.92	-36	547	0.3	0	0	0.43
2015-12-01 11:34:53	79.02	4.97	7.92	-36	547	0.3	0	0	0.43
2015-12-01 11:34:54	79.02	4.96	7.92	-36	547	0.4	0	0	0.43
2015-12-01 11:34:55	79.02	4.96	7.92	-36	547	0.4	0	0	0.43
2015-12-01 11:35:22	79.99	4.98	7.82	-52	552	0.4	0	0	0.43
2015-12-01 11:35:23	79.99	4.98	7.82	-52	552	0.4	0	0	0.43
2015-12-01 11:35:24	79.99	4.98	7.81	-53	552	0.4	0	0	0.43
2015-12-01 11:35:25	79.99	4.98	7.81	-53	552	0.4	0	0	0.43
2015-12-01 11:35:26	79.98	4.99	7.81	-54	555	0.4	0	0	0.43
2015-12-01 11:35:27	79.99	4.99	7.80	-54	553	0.4	0	0	0.43
2015-12-01 11:35:28	79.99	4.99	7.80	-54	553	0.4	0	0	0.43
2015-12-01 11:35:29	79.99	4.98	7.80	-55	553	0.4	0	0	0.43
2015-12-01 11:35:30	79.99	4.98	7.80	-55	553	0.4	0	0	0.43
2015-12-01 11:35:31	80.01	4.98	7.80	-56	553	0.4	0	0	0.43
2015-12-01 11:37:12	81.02	4.99	7.47	-87	563	0.4	0	0	0.45
2015-12-01 11:37:13	81.02	4.99	7.47	-87	563	0.4	0	0	0.45
2015-12-01 11:37:14	81.01	4.99	7.47	-87	563	0.4	0	0	0.45
2015-12-01 11:37:15	81.01	4.99	7.47	-87	563	0.4	0	0	0.45
2015-12-01 11:37:16	81.01	4.99	7.47	-87	563	0.4	0	0	0.46
2015-12-01 11:37:17	81.01	4.99	7.47	-87	563	0.4	0	0	0.46
2015-12-01 11:37:18	81.03	4.99	7.47	-88	565	0.4	0	0	0.46
2015-12-01 11:37:19	81.02	4.99	7.47	-88	563	0.4	0	0	0.46
2015-12-01 11:37:20	81.02	4.99	7.47	-88	563	0.4	0	0	0.46
2015-12-01 11:37:21	81.02	5.00	7.46	-89	563	0.4	0	0	0.45
2015-12-01 11:37:57	81.02	5.00	7.43	-94	564	0.4	0	0	0.49
2015-12-01 11:37:58	81.03	5.00	7.43	-94	564	0.4	0	0	0.49
2015-12-01 11:37:59	81.03	5.00	7.43	-94	564	0.4	0	0	0.49
2015-12-01 11:38:00	81.02	5.00	7.43	-94	564	0.4	0	0	0.49
2015-12-01 11:38:01	81.02	5.00	7.43	-94	563	0.4	0	0	0.48
2015-12-01 11:38:02	81.02	5.00	7.43	-94	563	0.4	0	0	0.48
2015-12-01 11:38:03	81.03	5.00	7.42	-95	563	0.4	0	0	0.47
2015-12-01 11:38:04	81.03	5.00	7.42	-95	563	0.4	0	0	0.47

Appendix B.12 South basin 2015 sonde data

Location: South Basin Hole

Instrument: YSI 6600

Date / Time	Depth (m)	Temp. (°C)	pH	ORP (mV)	Sp. Cond. (µS/cm)	TDS (g/L)	LDO% (% Saturation)	LDO (mg/L)	Chlorophyll (µg/L)
2015-12-01 11:38:05	81.02	5.00	7.42	-95	563	0.4	0	0	0.46
2015-12-01 11:38:06	81.02	5.00	7.42	-95	563	0.4	0	0	0.46
2015-12-01 11:38:14	81.02	5.00	7.42	-96	563	0.4	0	0	0.45
2015-12-01 11:38:15	81.03	5.00	7.41	-96	564	0.4	0	0	0.45
2015-12-01 11:38:16	81.03	5.00	7.41	-96	564	0.4	0	0	0.45
2015-12-01 11:38:17	81.03	5.00	7.41	-96	563	0.4	0	0	0.45
2015-12-01 11:38:18	81.03	5.00	7.41	-96	563	0.4	0	0	0.45
2015-12-01 11:38:19	81.03	5.00	7.41	-96	563	0.4	0	0	0.46
2015-12-01 11:38:20	81.03	5.00	7.41	-96	563	0.4	0	0	0.46
2015-12-01 11:38:21	81.03	5.00	7.41	-97	565	0.4	0	0	0.46
2015-12-01 11:38:22	81.02	5.00	7.41	-97	564	0.4	0	0	0.47
2015-12-01 11:38:23	81.02	5.00	7.41	-97	564	0.4	0	0	0.47
2015-12-01 11:39:33	82.07	4.97	7.29	-105	591	0.4	0	0	0.46
2015-12-01 11:39:34	82.06	4.97	7.29	-105	587	0.4	0	0	0.45
2015-12-01 11:39:35	82.06	4.97	7.29	-105	587	0.4	0	0	0.45
2015-12-01 11:39:36	82.05	4.97	7.29	-106	589	0.4	0	0	0.45
2015-12-01 11:39:37	82.05	4.97	7.29	-106	589	0.4	0	0	0.45
2015-12-01 11:39:38	82.06	4.97	7.29	-106	589	0.4	0	0	0.46
2015-12-01 11:39:39	82.05	4.97	7.29	-106	589	0.4	0	0	0.46
2015-12-01 11:39:40	82.05	4.97	7.29	-106	589	0.4	0	0	0.46
2015-12-01 11:39:41	82.06	4.97	7.28	-107	590	0.4	0	0	0.46
2015-12-01 11:39:42	82.06	4.97	7.28	-107	590	0.4	0	0	0.46
2015-12-01 11:40:14	83.08	4.89	7.18	-116	642	0.4	0	0	0.47
2015-12-01 11:40:15	83.07	4.88	7.18	-116	644	0.4	0	0	0.47
2015-12-01 11:40:16	83.08	4.88	7.17	-117	642	0.4	0	0	0.48
2015-12-01 11:40:17	83.08	4.88	7.17	-117	642	0.4	0	0	0.48
2015-12-01 11:40:18	83.08	4.88	7.17	-118	642	0.4	0	0	0.49
2015-12-01 11:40:19	83.08	4.88	7.17	-118	642	0.4	0	0	0.49
2015-12-01 11:40:20	83.07	4.88	7.17	-118	642	0.4	0	0	0.50
2015-12-01 11:40:21	83.07	4.88	7.17	-118	642	0.4	0	0	0.50
2015-12-01 11:40:22	83.08	4.87	7.17	-119	646	0.4	0	0	0.50
2015-12-01 11:40:23	83.08	4.88	7.17	-119	644	0.4	0	0	0.50

Appendix B.12 South basin 2015 sonde data

Location: South Basin Hole

Instrument: YSI 6600

Date / Time	Depth (m)	Temp. (°C)	pH	ORP (mV)	Sp. Cond. (µS/cm)	TDS (g/L)	LDO% (% Saturation)	LDO (mg/L)	Chlorophyll (µg/L)
2015-12-01 11:40:53	84.06	4.79	7.12	-127	690	0.4	0	0	0.67
2015-12-01 11:40:54	84.06	4.79	7.12	-127	690	0.4	0	0	0.67
2015-12-01 11:40:55	84.05	4.79	7.12	-127	694	0.4	0	0	0.68
2015-12-01 11:40:56	84.05	4.79	7.12	-128	696	0.4	0	0	0.70
2015-12-01 11:40:57	84.05	4.79	7.12	-128	696	0.4	0	0	0.70
2015-12-01 11:40:58	84.05	4.79	7.12	-128	695	0.4	0	0	0.71
2015-12-01 11:40:59	84.05	4.79	7.12	-128	695	0.4	0	0	0.71
2015-12-01 11:41:00	84.05	4.79	7.12	-129	695	0.4	0	0	0.72
2015-12-01 11:41:01	84.05	4.79	7.12	-129	695	0.4	0	0	0.72
2015-12-01 11:41:02	84.05	4.79	7.12	-129	696	0.4	0	0	0.72
2015-12-01 11:41:20	85.04	4.71	7.09	-131	745	0.5	0	0	0.74
2015-12-01 11:41:21	85.04	4.71	7.09	-132	744	0.5	0	0	0.71
2015-12-01 11:41:22	85.04	4.71	7.09	-132	744	0.5	0	0	0.71
2015-12-01 11:41:23	85.04	4.71	7.09	-132	744	0.5	0	0	0.69
2015-12-01 11:41:24	85.04	4.71	7.09	-132	745	0.5	0	0	0.66
2015-12-01 11:41:25	85.04	4.71	7.09	-132	745	0.5	0	0	0.66
2015-12-01 11:41:26	85.05	4.71	7.09	-133	744	0.5	0	0	0.64
2015-12-01 11:41:27	85.05	4.71	7.09	-133	744	0.5	0	0	0.64
2015-12-01 11:41:28	85.05	4.71	7.09	-133	744	0.5	0	0	0.61
2015-12-01 11:41:29	85.05	4.70	7.09	-133	745	0.5	0	0	0.59
2015-12-01 11:41:58	86.00	4.63	7.06	-136	798	0.5	0	0	0.63
2015-12-01 11:41:59	85.99	4.63	7.06	-136	798	0.5	0	0	0.63
2015-12-01 11:42:00	85.99	4.63	7.06	-136	798	0.5	0	0	0.63
2015-12-01 11:42:01	86.01	4.63	7.06	-136	798	0.5	0	0	0.63
2015-12-01 11:42:02	86.01	4.63	7.06	-136	798	0.5	0	0	0.63
2015-12-01 11:42:03	86.01	4.64	7.06	-137	799	0.5	0	0	0.63
2015-12-01 11:42:06	86.01	4.64	7.06	-137	799	0.5	0	0	0.63
2015-12-01 11:42:07	86.01	4.64	7.06	-137	799	0.5	0	0	0.63
2015-12-01 11:42:08	86.01	4.64	7.06	-137	799	0.5	0	0	0.63
2015-12-01 11:42:09	86.02	4.65	7.06	-137	799	0.5	0	0	0.63
2015-12-01 11:42:37	86.99	4.55	7.03	-138	842	0.5	0	0	0.73
2015-12-01 11:42:38	86.99	4.55	7.03	-138	842	0.5	0	0	0.73

Appendix B.12 South basin 2015 sonde data

Location: South Basin Hole

Instrument: YSI 6600

Date / Time	Depth (m)	Temp. (°C)	pH	ORP (mV)	Sp. Cond. (µS/cm)	TDS (g/L)	LDO% (% Saturation)	LDO (mg/L)	Chlorophyll (µg/L)
2015-12-01 11:42:39	87.01	4.56	7.03	-138	843	0.5	0	0	0.74
2015-12-01 11:42:40	87.01	4.56	7.03	-138	843	0.5	0	0	0.74
2015-12-01 11:42:41	86.99	4.56	7.03	-139	842	0.5	0	0	0.74
2015-12-01 11:42:42	86.99	4.57	7.03	-139	841	0.5	0	0	0.74
2015-12-01 11:42:43	87.01	4.57	7.03	-139	841	0.5	0	0	0.74
2015-12-01 11:42:44	87.00	4.57	7.03	-139	841	0.5	0	0	0.73
2015-12-01 11:42:45	87.00	4.57	7.03	-139	841	0.5	0	0	0.73
2015-12-01 11:42:46	87.00	4.57	7.03	-139	841	0.5	0	0	0.73
2015-12-01 11:43:54	88.10	4.47	7.00	-141	919	0.6	0	0	0.79
2015-12-01 11:43:55	88.09	4.47	7.00	-141	919	0.6	0	0	0.80
2015-12-01 11:43:56	88.10	4.48	7.00	-142	917	0.6	0	0	0.80
2015-12-01 11:43:57	88.10	4.48	7.00	-142	917	0.6	0	0	0.80
2015-12-01 11:43:58	88.10	4.48	7.00	-142	916	0.6	0	0	0.80
2015-12-01 11:43:59	88.09	4.48	7.00	-142	916	0.6	0	0	0.80
2015-12-01 11:44:00	88.10	4.48	7.00	-142	915	0.6	0	0	0.81
2015-12-01 11:44:01	88.10	4.48	7.00	-142	915	0.6	0	0	0.81
2015-12-01 11:44:02	88.10	4.48	7.00	-142	916	0.6	0	0	0.81
2015-12-01 11:44:03	88.10	4.48	7.00	-142	916	0.6	0	0	0.81
2015-12-01 11:44:38	89.04	4.36	6.97	-140	1003	0.6	0	0	0.94
2015-12-01 11:44:39	89.04	4.36	6.97	-140	1003	0.6	0	0	0.94
2015-12-01 11:44:40	89.02	4.36	6.97	-140	1007	0.6	0	0	0.94
2015-12-01 11:44:41	89.02	4.36	6.97	-140	1007	0.6	0	0	0.94
2015-12-01 11:44:42	89.04	4.36	6.97	-140	1008	0.6	0	0	0.93
2015-12-01 11:44:43	89.04	4.36	6.97	-140	1008	0.6	0	0	0.93
2015-12-01 11:44:44	89.04	4.36	6.97	-140	1013	0.6	0	0	0.93
2015-12-01 11:44:45	89.03	4.37	6.97	-140	1008	0.6	0	0	0.93
2015-12-01 11:44:46	89.03	4.37	6.97	-140	1008	0.6	0	0	0.93
2015-12-01 11:44:47	89.05	4.37	6.97	-140	1009	0.6	0	0	0.93
2015-12-01 11:46:30	90.01	4.29	6.95	-141	1050	0.7	0	0	0.99
2015-12-01 11:46:31	90.01	4.29	6.95	-141	1051	0.7	0	0	0.99
2015-12-01 11:46:32	90.02	4.29	6.95	-141	1050	0.7	0	0	0.99
2015-12-01 11:46:33	90.02	4.29	6.95	-141	1050	0.7	0	0	0.99

Appendix B.12 South basin 2015 sonde data

Location: South Basin Hole

Instrument: YSI 6600

Date / Time	Depth (m)	Temp. (°C)	pH	ORP (mV)	Sp. Cond. (µS/cm)	TDS (g/L)	LDO% (% Saturation)	LDO (mg/L)	Chlorophyll (µg/L)
2015-12-01 11:46:34	90.01	4.29	6.95	-141	1050	0.7	0	0	0.99
2015-12-01 11:46:35	90.01	4.29	6.95	-141	1050	0.7	0	0	0.99
2015-12-01 11:46:36	90.02	4.29	6.94	-141	1051	0.7	0	0	0.99
2015-12-01 11:46:37	90.02	4.29	6.94	-141	1050	0.7	0	0	0.99
2015-12-01 11:46:38	90.01	4.29	6.94	-141	1050	0.7	0	0	0.99
2015-12-01 11:46:39	89.99	4.29	6.94	-141	1051	0.7	0	0	0.99
2015-12-01 11:47:04	91.07	4.24	6.93	-140	1099	0.7	0	0	1.07
2015-12-01 11:47:05	91.07	4.23	6.93	-140	1101	0.7	0	0	1.07
2015-12-01 11:47:06	91.09	4.23	6.93	-140	1101	0.7	0	0	1.07
2015-12-01 11:47:07	91.07	4.24	6.93	-140	1101	0.7	0	0	1.08
2015-12-01 11:47:08	91.07	4.24	6.93	-140	1101	0.7	0	0	1.08
2015-12-01 11:47:09	91.10	4.24	6.93	-140	1102	0.7	0	0	1.08
2015-12-01 11:47:10	91.10	4.24	6.93	-140	1102	0.7	0	0	1.08
2015-12-01 11:47:11	91.08	4.24	6.93	-139	1101	0.7	0	0	1.08
2015-12-01 11:47:12	91.08	4.24	6.93	-139	1101	0.7	0	0	1.08
2015-12-01 11:47:13	91.09	4.24	6.93	-139	1101	0.7	0	0	1.08
2015-12-01 11:47:29	92.04	4.13	6.91	-138	1161	0.7	0	0	1.10
2015-12-01 11:47:30	92.03	4.13	6.92	-138	1161	0.7	0	0	1.11
2015-12-01 11:47:31	92.03	4.12	6.92	-138	1162	0.7	0	0	1.11
2015-12-01 11:47:32	92.04	4.12	6.91	-138	1162	0.7	0	0	1.12
2015-12-01 11:47:33	92.05	4.13	6.91	-138	1161	0.7	0	0	1.13
2015-12-01 11:47:34	92.05	4.13	6.91	-138	1161	0.7	0	0	1.13
2015-12-01 11:47:35	92.04	4.12	6.92	-138	1161	0.7	0	0	1.14
2015-12-01 11:47:36	92.04	4.12	6.92	-138	1161	0.7	0	0	1.14
2015-12-01 11:47:37	92.04	4.12	6.91	-138	1162	0.7	0	0	1.15
2015-12-01 11:47:38	92.04	4.12	6.91	-138	1161	0.7	0	0	1.15
2015-12-01 11:48:18	93.03	4.07	6.91	-137	1187	0.8	0	0	1.21
2015-12-01 11:48:19	93.02	4.07	6.91	-137	1187	0.8	0	0	1.21
2015-12-01 11:48:20	93.02	4.07	6.91	-137	1187	0.8	0	0	1.21
2015-12-01 11:48:21	93.02	4.07	6.91	-137	1189	0.8	0	0	1.21
2015-12-01 11:48:22	93.03	4.08	6.91	-137	1189	0.8	0	0	1.21
2015-12-01 11:48:23	93.03	4.08	6.91	-137	1189	0.8	0	0	1.21

Appendix B.12 South basin 2015 sonde data

Location: South Basin Hole

Instrument: YSI 6600

Date / Time	Depth (m)	Temp. (°C)	pH	ORP (mV)	Sp. Cond. (µS/cm)	TDS (g/L)	LDO% (% Saturation)	LDO (mg/L)	Chlorophyll (µg/L)
2015-12-01 11:48:24	93.03	4.07	6.91	-137	1190	0.8	0	0	1.21
2015-12-01 11:48:25	93.03	4.07	6.91	-137	1190	0.8	0	0	1.21
2015-12-01 11:48:26	93.03	4.07	6.91	-137	1194	0.8	0	0	1.21
2015-12-01 11:48:27	93.03	4.07	6.91	-137	1194	0.8	0	0	1.21
2015-12-01 11:48:52	94.05	4.00	6.90	-136	1222	0.8	0	0	1.22
2015-12-01 11:48:53	94.05	4.00	6.90	-136	1222	0.8	0	0	1.22
2015-12-01 11:48:54	94.03	4.00	6.90	-136	1223	0.8	0	0	1.22
2015-12-01 11:48:55	94.06	4.00	6.90	-136	1222	0.8	0	0	1.22
2015-12-01 11:48:56	94.06	4.00	6.90	-136	1222	0.8	0	0	1.22
2015-12-01 11:48:57	94.06	4.00	6.90	-136	1222	0.8	0	0	1.22
2015-12-01 11:48:58	94.06	4.00	6.90	-136	1221	0.8	0	0	1.22
2015-12-01 11:48:59	94.05	4.00	6.90	-136	1222	0.8	0	0	1.22
2015-12-01 11:49:00	94.05	4.00	6.90	-136	1222	0.8	0	0	1.22
2015-12-01 11:49:01	94.05	4.00	6.90	-136	1222	0.8	0	0	1.23
2015-12-01 11:49:24	95.04	3.91	6.89	-135	1253	0.8	0	0	1.24
2015-12-01 11:49:25	95.04	3.91	6.89	-135	1255	0.8	0	0	1.24
2015-12-01 11:49:26	95.05	3.91	6.89	-135	1255	0.8	0	0	1.25
2015-12-01 11:49:27	95.05	3.91	6.89	-135	1255	0.8	0	0	1.25
2015-12-01 11:49:28	95.05	3.91	6.89	-135	1255	0.8	0	0	1.25
2015-12-01 11:49:29	95.05	3.91	6.89	-134	1256	0.8	0	0	1.25
2015-12-01 11:49:30	95.05	3.91	6.89	-134	1256	0.8	0	0	1.25
2015-12-01 11:49:31	95.05	3.91	6.89	-134	1255	0.8	0	0	1.25
2015-12-01 11:49:32	95.05	3.91	6.89	-134	1256	0.8	0	0	1.25
2015-12-01 11:49:33	95.04	3.91	6.89	-135	1256	0.8	0	0	1.24
2015-12-01 11:49:55	95.97	3.84	6.88	-133	1282	0.8	0	0	1.25
2015-12-01 11:49:56	95.98	3.84	6.88	-133	1282	0.8	0	0	1.25
2015-12-01 11:49:57	95.98	3.84	6.88	-133	1283	0.8	0	0	1.25
2015-12-01 11:49:58	95.98	3.84	6.88	-133	1283	0.8	0	0	1.25
2015-12-01 11:49:59	95.97	3.84	6.88	-133	1283	0.8	0	0	1.25
2015-12-01 11:50:00	95.97	3.84	6.88	-133	1283	0.8	0	0	1.25
2015-12-01 11:50:01	95.98	3.84	6.88	-133	1283	0.8	0	0	1.25
2015-12-01 11:50:02	95.98	3.84	6.88	-133	1283	0.8	0	0	1.25

Appendix B.12 South basin 2015 sonde data

Location: South Basin Hole

Instrument: YSI 6600

Date / Time	Depth (m)	Temp. (°C)	pH	ORP (mV)	Sp. Cond. (µS/cm)	TDS (g/L)	LDO% (% Saturation)	LDO (mg/L)	Chlorophyll (µg/L)
2015-12-01 11:50:03	95.97	3.84	6.88	-133	1288	0.8	0	0	1.25
2015-12-01 11:50:04	95.99	3.84	6.88	-133	1283	0.8	0	0	1.25
2015-12-01 11:50:35	97.04	3.78	6.87	-130	1306	0.8	0	0	1.27
2015-12-01 11:50:36	97.05	3.78	6.88	-130	1306	0.8	0	0	1.27
2015-12-01 11:50:37	97.04	3.78	6.88	-130	1306	0.8	0	0	1.27
2015-12-01 11:50:38	97.04	3.78	6.88	-130	1306	0.8	0	0	1.27
2015-12-01 11:50:39	97.05	3.78	6.88	-130	1307	0.8	0	0	1.27
2015-12-01 11:50:40	97.05	3.78	6.88	-130	1307	0.8	0	0	1.27
2015-12-01 11:50:41	97.05	3.78	6.87	-130	1307	0.8	0	0	1.28
2015-12-01 11:50:42	97.06	3.77	6.88	-130	1307	0.8	0	0	1.27
2015-12-01 11:50:43	97.06	3.77	6.88	-130	1307	0.8	0	0	1.27
2015-12-01 11:50:44	97.06	3.78	6.88	-130	1306	0.8	0	0	1.27
2015-12-01 11:51:17	98.05	3.72	6.87	-127	1334	0.9	0	0	1.25
2015-12-01 11:51:18	98.05	3.72	6.87	-127	1334	0.9	0	0	1.26
2015-12-01 11:51:19	98.06	3.72	6.87	-127	1334	0.9	0	0	1.26
2015-12-01 11:51:20	98.06	3.72	6.87	-127	1334	0.9	0	0	1.26
2015-12-01 11:51:21	98.07	3.72	6.87	-127	1334	0.9	0	0	1.25
2015-12-01 11:51:22	98.07	3.72	6.87	-127	1334	0.9	0	0	1.25
2015-12-01 11:51:23	97.98	3.72	6.87	-127	1325	0.8	0	0	1.26
2015-12-01 11:51:24	97.98	3.72	6.87	-127	1333	0.9	0	0	1.26
2015-12-01 11:51:25	98.00	3.72	6.87	-127	1333	0.9	0	0	1.26
2015-12-01 11:51:26	98.04	3.72	6.87	-127	1333	0.9	0	0	1.26
2015-12-01 11:52:02	99.06	3.66	6.86	-124	1384	0.9	0	0	1.29
2015-12-01 11:52:03	99.05	3.66	6.86	-125	1382	0.9	0	0	1.29
2015-12-01 11:52:04	99.05	3.66	6.86	-125	1382	0.9	0	0	1.29
2015-12-01 11:52:05	99.06	3.67	6.86	-124	1379	0.9	0	0	1.29
2015-12-01 11:52:06	99.05	3.67	6.86	-124	1379	0.9	0	0	1.29
2015-12-01 11:52:07	99.05	3.67	6.86	-124	1379	0.9	0	0	1.29
2015-12-01 11:52:08	99.05	3.67	6.86	-124	1379	0.9	0	0	1.29
2015-12-01 11:52:09	99.05	3.67	6.86	-124	1380	0.9	0	0	1.29
2015-12-01 11:52:10	99.06	3.67	6.86	-124	1379	0.9	0	0	1.28
2015-12-01 11:52:11	99.06	3.67	6.86	-124	1379	0.9	0	0	1.28

Appendix B.12 South basin 2015 sonde data

Location: South Basin Hole

Instrument: YSI 6600

Date / Time	Depth (m)	Temp. (°C)	pH	ORP (mV)	Sp. Cond. (µS/cm)	TDS (g/L)	LDO% (% Saturation)	LDO (mg/L)	Chlorophyll (µg/L)
2015-12-01 11:52:39	99.96	3.60	6.84	-121	1506	1	0	0	1.38
2015-12-01 11:52:40	99.97	3.60	6.84	-120	1506	1	0	0	1.39
2015-12-01 11:52:41	99.97	3.59	6.84	-120	1503	1	0	0	1.39
2015-12-01 11:52:42	99.98	3.59	6.84	-120	1503	1	0	0	1.39
2015-12-01 11:52:43	99.97	3.59	6.84	-120	1507	1	0	0	1.40
2015-12-01 11:52:44	99.97	3.59	6.84	-120	1507	1	0	0	1.40
2015-12-01 11:52:45	99.97	3.59	6.84	-120	1506	1	0	0	1.40
2015-12-01 11:52:46	99.97	3.59	6.84	-120	1506	1	0	0	1.40
2015-12-01 11:52:47	99.96	3.59	6.85	-120	1510	1	0	0	1.40
2015-12-01 11:52:48	99.97	3.58	6.85	-120	1509	1	0	0	1.40

ORP = oxidation-reduction potential

TDS = total dissolved solids

LDO = luminescent dissolved oxygen

Appendix B.13 South basin 2017 sonde data

Location: South Basin Hole (SB)

Instrument: YSI 6600

Date / Time	Depth (m)	Temp. (°C)	pH	ORP (mV)	Sp. Cond. (µS/cm)	TDS (g/L)	LDO% (% Saturation)	LDO (mg/L)	Chlorophyll (µg/L)
2017-11-27 10:36:53	0.54	0.02	10.25	131	501	0.3	125.5	17.67	0.17
2017-11-27 10:36:54	0.54	0.02	10.25	131	503	0.3	125.4	17.67	0.17
2017-11-27 10:36:55	0.54	0.02	10.26	131	500	0.3	125.5	17.67	0.17
2017-11-27 10:36:56	0.54	0.02	10.26	131	500	0.3	125.5	17.67	0.17
2017-11-27 10:36:57	0.54	0.02	10.27	131	500	0.3	125.5	17.67	0.17
2017-11-27 10:38:33	5.03	0.15	10.45	129	502	0.3	148.6	20.85	0.17
2017-11-27 10:38:34	5.03	0.15	10.45	129	502	0.3	148.6	20.85	0.17
2017-11-27 10:38:35	5.02	0.14	10.46	129	502	0.3	148.6	20.86	0.17
2017-11-27 10:38:36	5.02	0.14	10.46	129	502	0.3	148.6	20.86	0.17
2017-11-27 10:38:37	5.03	0.14	10.46	129	502	0.3	148.7	20.87	0.17
2017-11-27 10:39:45	10.03	0.24	10.59	129	501	0.3	154.5	21.62	0.17
2017-11-27 10:39:46	10.03	0.24	10.59	129	501	0.3	154.5	21.62	0.17
2017-11-27 10:39:47	10.03	0.24	10.59	128	501	0.3	154.6	21.64	0.16
2017-11-27 10:39:48	10.03	0.24	10.59	128	501	0.3	154.6	21.64	0.16
2017-11-27 10:39:49	10.02	0.24	10.59	128	502	0.3	154.5	21.63	0.16
2017-11-27 10:40:51	15.01	0.23	10.66	128	502	0.3	154.0	21.56	0.17
2017-11-27 10:40:52	15.01	0.23	10.66	128	503	0.3	154.1	21.58	0.17
2017-11-27 10:40:53	15.02	0.24	10.66	128	502	0.3	154.3	21.59	0.17
2017-11-27 10:40:54	15.02	0.24	10.66	128	502	0.3	154.3	21.59	0.17
2017-11-27 10:40:55	15.02	0.23	10.67	128	502	0.3	154.3	21.60	0.17
2017-11-27 10:41:56	20.01	0.24	10.72	128	502	0.3	151.8	21.25	0.17
2017-11-27 10:41:57	20.01	0.24	10.72	128	502	0.3	151.8	21.25	0.17
2017-11-27 10:41:58	20.04	0.24	10.72	128	501	0.3	151.8	21.24	0.17
2017-11-27 10:41:59	20.04	0.24	10.72	128	501	0.3	151.8	21.24	0.17
2017-11-27 10:42:00	20.02	0.24	10.72	128	501	0.3	151.8	21.25	0.17
2017-11-27 10:43:07	25.05	0.24	10.77	127	502	0.3	148.1	20.73	0.17
2017-11-27 10:43:08	25.05	0.25	10.78	127	501	0.3	148.0	20.72	0.17
2017-11-27 10:43:09	25.05	0.25	10.78	127	501	0.3	148.0	20.72	0.17
2017-11-27 10:43:10	25.06	0.25	10.77	127	502	0.3	147.8	20.68	0.17
2017-11-27 10:43:11	25.06	0.25	10.77	127	502	0.3	147.8	20.68	0.17

Appendix B.13 South basin 2017 sonde data

Date / Time	Depth (m)	Temp. (°C)	pH	ORP (mV)	Sp. Cond. (µS/cm)	TDS (g/L)	LDO% (% Saturation)	LDO (mg/L)	Chlorophyll (µg/L)
2017-11-27 10:44:08	30.01	0.25	10.8	127	504	0.3	147.6	20.65	0.17
2017-11-27 10:44:09	30.02	0.25	10.8	127	501	0.3	147.5	20.63	0.17
2017-11-27 10:44:10	30.02	0.25	10.8	127	501	0.3	147.5	20.63	0.17
2017-11-27 10:44:11	30.00	0.25	10.81	127	503	0.3	147.5	20.64	0.17
2017-11-27 10:44:12	30.00	0.25	10.81	127	503	0.3	147.5	20.64	0.17
2017-11-27 10:45:43	35.03	0.26	10.82	127	502	0.3	147.3	20.60	0.17
2017-11-27 10:45:44	35.04	0.26	10.82	127	502	0.3	147.3	20.61	0.17
2017-11-27 10:45:45	35.04	0.26	10.82	127	502	0.3	147.3	20.61	0.17
2017-11-27 10:45:46	35.04	0.26	10.82	127	503	0.3	147.3	20.61	0.17
2017-11-27 10:45:47	35.05	0.25	10.82	127	502	0.3	147.3	20.61	0.17
2017-11-27 10:46:59	40.00	0.26	10.83	127	502	0.3	146.9	20.56	0.17
2017-11-27 10:47:00	40.00	0.26	10.83	127	502	0.3	146.9	20.56	0.17
2017-11-27 10:47:01	40.00	0.26	10.83	127	502	0.3	147.2	20.60	0.17
2017-11-27 10:47:02	40.00	0.26	10.83	127	502	0.3	147.2	20.60	0.17
2017-11-27 10:47:03	40.00	0.26	10.83	127	504	0.3	147.2	20.60	0.17
2017-11-27 10:48:41	45.02	0.26	10.84	127	505	0.3	147.3	20.61	0.17
2017-11-27 10:48:42	45.03	0.26	10.84	127	502	0.3	147.3	20.61	0.17
2017-11-27 10:48:43	45.03	0.26	10.84	127	502	0.3	147.3	20.61	0.17
2017-11-27 10:48:44	45.03	0.27	10.84	127	502	0.3	147.3	20.60	0.17
2017-11-27 10:48:45	45.03	0.27	10.84	127	502	0.3	147.3	20.60	0.17
2017-11-27 10:50:14	50.07	3.96	10.71	125	516	0.3	161.2	20.39	0.26
2017-11-27 10:50:15	50.07	3.97	10.71	125	516	0.3	161.3	20.40	0.26
2017-11-27 10:50:16	50.07	3.97	10.71	125	516	0.3	161.3	20.40	0.26
2017-11-27 10:50:17	50.06	3.96	10.71	125	516	0.3	161.4	20.41	0.27
2017-11-27 10:50:18	50.06	3.96	10.71	125	516	0.3	161.4	20.41	0.27
2017-11-27 10:51:52	46.01	0.29	10.89	126	502	0.3	148.2	20.71	0.16
2017-11-27 10:51:53	46.01	0.29	10.89	126	503	0.3	148.2	20.71	0.17
2017-11-27 10:51:54	46.01	0.29	10.89	126	503	0.3	148.2	20.71	0.17
2017-11-27 10:51:55	46.01	0.29	10.89	126	502	0.3	148.1	20.70	0.16
2017-11-27 10:51:56	46.01	0.29	10.89	126	502	0.3	148.1	20.70	0.16
2017-11-27 10:52:34	47.01	0.29	10.9	126	502	0.3	147.5	20.62	0.16
2017-11-27 10:52:35	47.01	0.29	10.89	126	502	0.3	147.5	20.61	0.16

Appendix B.13 South basin 2017 sonde data

Date / Time	Depth (m)	Temp. (°C)	pH	ORP (mV)	Sp. Cond. (µS/cm)	TDS (g/L)	LDO% (% Saturation)	LDO (mg/L)	Chlorophyll (µg/L)
2017-11-27 10:52:36	47.01	0.29	10.89	126	502	0.3	147.5	20.61	0.16
2017-11-27 10:52:37	47.02	0.29	10.89	126	502	0.3	147.6	20.62	0.16
2017-11-27 10:52:38	47.02	0.29	10.89	126	502	0.3	147.6	20.62	0.16
2017-11-27 10:53:15	48.00	2.44	10.83	125	507	0.3	153.1	20.17	0.18
2017-11-27 10:53:16	48.00	2.44	10.83	125	507	0.3	153.1	20.17	0.18
2017-11-27 10:53:17	48.00	2.44	10.84	125	507	0.3	153.3	20.19	0.18
2017-11-27 10:53:18	48.00	2.44	10.84	125	507	0.3	153.3	20.19	0.18
2017-11-27 10:53:19	48.00	2.44	10.83	125	507	0.3	153.4	20.20	0.18
2017-11-27 10:54:05	49.02	3.71	10.79	124	512	0.3	159.9	20.36	0.26
2017-11-27 10:54:06	49.01	3.71	10.79	124	512	0.3	159.9	20.36	0.25
2017-11-27 10:54:07	49.01	3.71	10.79	124	512	0.3	159.9	20.36	0.25
2017-11-27 10:54:08	49.01	3.71	10.79	124	512	0.3	159.9	20.35	0.26
2017-11-27 10:54:09	49.01	3.71	10.79	124	512	0.3	159.9	20.35	0.26
2017-11-27 10:55:02	50.05	3.95	10.78	124	517	0.3	162.0	20.49	0.26
2017-11-27 10:55:03	50.05	3.95	10.78	124	517	0.3	162.0	20.49	0.26
2017-11-27 10:55:04	50.04	3.96	10.79	124	517	0.3	161.9	20.48	0.26
2017-11-27 10:55:05	50.04	3.96	10.79	124	517	0.3	161.9	20.48	0.26
2017-11-27 10:55:06	50.04	3.95	10.79	124	519	0.3	161.8	20.47	0.26
2017-11-27 10:56:17	51.03	3.98	10.8	123	517	0.3	161.7	20.43	0.26
2017-11-27 10:56:18	51.03	3.98	10.8	123	517	0.3	161.7	20.43	0.26
2017-11-27 10:56:19	51.04	3.98	10.8	123	517	0.3	161.6	20.42	0.26
2017-11-27 10:56:20	51.04	3.98	10.8	123	517	0.3	161.6	20.42	0.26
2017-11-27 10:56:21	51.03	3.98	10.8	123	517	0.3	161.6	20.43	0.26
2017-11-27 10:57:13	52.00	3.98	10.81	123	517	0.3	161.9	20.47	0.25
2017-11-27 10:57:14	52.00	3.98	10.81	123	517	0.3	161.9	20.47	0.25
2017-11-27 10:57:15	52.01	3.98	10.81	123	517	0.3	162.0	20.48	0.25
2017-11-27 10:57:16	52.01	3.98	10.81	123	517	0.3	162.0	20.48	0.25
2017-11-27 10:57:17	51.97	3.98	10.81	123	518	0.3	161.9	20.46	0.26
2017-11-27 10:58:05	53.00	3.97	10.82	123	517	0.3	161.9	20.47	0.28
2017-11-27 10:58:06	53.01	3.98	10.81	123	518	0.3	162.1	20.49	0.28
2017-11-27 10:58:07	53.01	3.98	10.81	123	518	0.3	162.1	20.49	0.28
2017-11-27 10:58:08	53.00	3.97	10.81	123	520	0.3	161.9	20.47	0.29

Appendix B.13 South basin 2017 sonde data

Date / Time	Depth (m)	Temp. (°C)	pH	ORP (mV)	Sp. Cond. (µS/cm)	TDS (g/L)	LDO% (% Saturation)	LDO (mg/L)	Chlorophyll (µg/L)
2017-11-27 10:58:09	53.01	3.98	10.81	123	517	0.3	161.9	20.46	0.29
2017-11-27 10:59:19	54.01	3.99	10.82	123	518	0.3	161.5	20.41	0.29
2017-11-27 10:59:20	54.01	3.99	10.82	123	518	0.3	161.5	20.41	0.29
2017-11-27 10:59:21	53.99	3.99	10.82	123	518	0.3	161.7	20.43	0.28
2017-11-27 10:59:22	53.99	3.99	10.82	123	518	0.3	161.7	20.43	0.28
2017-11-27 10:59:23	53.99	3.99	10.82	123	517	0.3	161.8	20.44	0.28
2017-11-27 11:00:30	55.00	3.99	10.83	123	517	0.3	161.4	20.40	0.25
2017-11-27 11:00:31	55.00	3.99	10.83	123	517	0.3	161.6	20.42	0.25
2017-11-27 11:00:32	55.00	3.99	10.83	123	517	0.3	161.6	20.42	0.25
2017-11-27 11:00:33	55.01	3.99	10.82	123	517	0.3	161.6	20.42	0.25
2017-11-27 11:00:34	55.01	3.99	10.82	123	517	0.3	161.6	20.42	0.25
2017-11-27 11:02:08	60.01	4.00	10.83	123	517	0.3	161.8	20.45	0.31
2017-11-27 11:02:09	60.02	4.00	10.83	123	517	0.3	162.1	20.49	0.30
2017-11-27 11:02:10	60.02	4.00	10.83	123	517	0.3	162.1	20.49	0.30
2017-11-27 11:02:11	60.01	4.00	10.82	123	517	0.3	162.0	20.47	0.29
2017-11-27 11:02:12	60.01	4.00	10.82	123	517	0.3	162.0	20.47	0.29
2017-11-27 11:03:36	65.01	4.07	10.73	124	517	0.3	156.7	19.76	0.34
2017-11-27 11:03:37	65.00	4.06	10.73	124	517	0.3	156.9	19.79	0.34
2017-11-27 11:03:38	65.00	4.06	10.74	124	516	0.3	157.0	19.80	0.34
2017-11-27 11:03:39	65.00	4.06	10.74	124	516	0.3	157.0	19.80	0.34
2017-11-27 11:03:40	64.99	4.06	10.74	124	517	0.3	157.1	19.81	0.34
2017-11-27 11:05:07	70.00	4.81	9.47	169	540	0.3	30.8	3.81	0.82
2017-11-27 11:05:08	70.00	4.81	9.46	170	539	0.3	30.5	3.77	0.81
2017-11-27 11:05:09	70.00	4.81	9.45	170	539	0.3	30.2	3.74	0.81
2017-11-27 11:05:10	70.00	4.81	9.45	170	539	0.3	30.2	3.74	0.81
2017-11-27 11:05:11	70.01	4.81	9.44	170	539	0.3	30.0	3.71	0.82
2017-11-27 11:06:09	75.03	4.89	8.91	179	543	0.3	2.2	0.27	0.42
2017-11-27 11:06:10	75.03	4.89	8.91	179	543	0.3	2.2	0.27	0.42
2017-11-27 11:06:11	75.02	4.89	8.9	179	546	0.3	1.9	0.24	0.41
2017-11-27 11:06:12	75.03	4.89	8.89	180	544	0.3	1.6	0.20	0.40
2017-11-27 11:06:13	75.03	4.89	8.89	180	544	0.3	1.6	0.20	0.40
2017-11-27 11:06:31	75.03	4.90	8.84	181	544	0.3	0.6	0.08	0.47

Appendix B.13 South basin 2017 sonde data

Date / Time	Depth (m)	Temp. (°C)	pH	ORP (mV)	Sp. Cond. (µS/cm)	TDS (g/L)	LDO% (% Saturation)	LDO (mg/L)	Chlorophyll (µg/L)
2017-11-27 11:06:32	75.02	4.89	8.83	181	546	0.3	0.6	0.07	0.45
2017-11-27 11:06:33	75.02	4.90	8.83	181	543	0.3	0.6	0.07	0.45
2017-11-27 11:06:34	75.02	4.90	8.83	181	543	0.3	0.6	0.07	0.45
2017-11-27 11:06:35	75.03	4.89	8.82	181	543	0.3	0.6	0.07	0.46
2017-11-27 11:08:05	80.01	4.97	7.95	-58	568	0.4	0.0	0.00	0.53
2017-11-27 11:08:06	80.01	4.97	7.94	-59	569	0.4	0.1	0.01	0.53
2017-11-27 11:08:07	80.01	4.97	7.94	-59	569	0.4	0.1	0.01	0.53
2017-11-27 11:08:08	80.01	4.97	7.92	-60	570	0.4	0.1	0.01	0.53
2017-11-27 11:08:09	80.01	4.97	7.92	-60	570	0.4	0.1	0.01	0.53
2017-11-27 11:09:43	84.99	4.68	7.07	-121	783	0.5	0.1	0.01	0.67
2017-11-27 11:09:44	85.00	4.68	7.07	-121	782	0.5	0.1	0.01	0.67
2017-11-27 11:09:45	85.00	4.68	7.07	-121	782	0.5	0.1	0.01	0.67
2017-11-27 11:09:46	85.00	4.67	7.06	-122	782	0.5	0.1	0.01	0.66
2017-11-27 11:09:47	85.00	4.67	7.06	-122	782	0.5	0.1	0.01	0.66
2017-11-27 11:10:12	85.02	4.67	7.02	-128	783	0.5	0.1	0.01	0.67
2017-11-27 11:10:13	85.02	4.67	7.02	-128	783	0.5	0.1	0.01	0.67
2017-11-27 11:10:14	85.03	4.67	7.02	-128	785	0.5	0.1	0.01	0.67
2017-11-27 11:10:15	85.03	4.67	7.02	-128	785	0.5	0.1	0.01	0.67
2017-11-27 11:10:16	85.03	4.67	7.02	-128	789	0.5	0.1	0.01	0.67
2017-11-27 11:11:40	90.00	4.25	6.79	-127	1098	0.7	0.1	0.01	1.12
2017-11-27 11:11:41	89.99	4.25	6.79	-127	1093	0.7	0.1	0.01	1.12
2017-11-27 11:11:42	89.99	4.25	6.79	-127	1093	0.7	0.1	0.01	1.12
2017-11-27 11:11:43	90.00	4.25	6.79	-127	1091	0.7	0.1	0.01	1.12
2017-11-27 11:11:44	90.00	4.25	6.79	-127	1091	0.7	0.1	0.01	1.12
2017-11-27 11:13:22	95.01	3.87	6.69	-120	1282	0.8	0.1	0.02	1.33
2017-11-27 11:13:23	95.00	3.86	6.69	-120	1282	0.8	0.1	0.02	1.33
2017-11-27 11:13:24	95.00	3.86	6.69	-120	1282	0.8	0.1	0.02	1.33
2017-11-27 11:13:25	95.01	3.87	6.68	-120	1287	0.8	0.1	0.01	1.33
2017-11-27 11:13:26	95.00	3.87	6.69	-120	1282	0.8	0.1	0.01	1.33

ORP = oxidation-reduction potential

TDS = total dissolved solids

LDO = luminescent dissolved oxygen

Appendix B.14 Pond Burevestniksee sonde data

Location: Pond Burevestniksee

Instrument: YSI 6600

Date / Time	Depth (m)	Temp. (°C)	pH	ORP (mV)	Sp. Cond. (µS/cm)	TDS (g/L)	LDO% (% Saturation)	LDO (mg/L)	Chlorophyll (µg/L)
2017-11-26 14:05:41	1.02	<0.01	10.39	178	298	0.2	164.30	23.17	0.28
2017-11-26 14:05:42	1.02	<0.01	10.39	178	298	0.2	164.30	23.17	0.28
2017-11-26 14:05:43	1.02	<0.01	10.38	177	297	0.2	164.50	23.20	0.28
2017-11-26 14:05:44	1.02	<0.01	10.38	177	297	0.2	164.50	23.20	0.28
2017-11-26 14:05:45	1.01	<0.01	10.39	177	300	0.2	165.00	23.27	0.27
2017-11-26 14:06:19	2.00	<0.01	10.9	175	298	0.2	171.20	24.15	0.28
2017-11-26 14:06:20	2.00	<0.01	10.91	175	300	0.2	171.50	24.20	0.28
2017-11-26 14:06:21	2.00	<0.01	11.01	175	298	0.2	171.80	24.24	0.28
2017-11-26 14:06:22	2.00	<0.01	11.01	175	298	0.2	171.80	24.24	0.28
2017-11-26 14:06:23	2.00	<0.01	11	175	298	0.2	172.10	24.29	0.28
2017-11-26 14:07:01	3.00	<0.01	11.61	172	295	0.2	188.90	26.64	0.29
2017-11-26 14:07:02	2.99	<0.01	11.64	172	296	0.2	189.30	26.70	0.29
2017-11-26 14:07:03	2.99	<0.01	11.66	172	295	0.2	189.90	26.78	0.28
2017-11-26 14:07:04	2.99	<0.01	11.66	172	295	0.2	189.90	26.78	0.28
2017-11-26 14:07:05	2.99	<0.01	11.66	172	295	0.2	190.40	26.85	0.29
2017-11-26 14:07:32	4.00	0.02	11.57	171	292	0.2	194.50	27.41	0.35
2017-11-26 14:07:33	4.00	0.02	11.59	171	292	0.2	195.00	27.48	0.36
2017-11-26 14:07:34	4.00	0.02	11.59	171	292	0.2	195.00	27.48	0.36
2017-11-26 14:07:35	3.99	0.02	11.61	171	292	0.2	195.60	27.57	0.37
2017-11-26 14:07:36	3.99	0.02	11.61	171	292	0.2	195.60	27.57	0.37
2017-11-26 14:08:16	5.02	0.03	11.58	170	292	0.2	201.90	28.45	0.37
2017-11-26 14:08:17	5.02	0.03	11.59	169	292	0.2	202.30	28.50	0.37
2017-11-26 14:08:18	5.02	0.03	11.59	169	292	0.2	202.30	28.50	0.37
2017-11-26 14:08:19	5.02	0.03	11.59	169	294	0.2	202.60	28.54	0.37
2017-11-26 14:08:20	5.03	0.03	11.59	169	292	0.2	202.70	28.56	0.37
2017-11-26 14:09:01	6.00	0.04	11.63	168	294	0.2	205.50	28.96	0.37
2017-11-26 14:09:02	6.01	0.04	11.66	168	292	0.2	205.70	28.98	0.37
2017-11-26 14:09:03	6.01	0.04	11.66	168	292	0.2	205.70	28.98	0.36
2017-11-26 14:09:04	6.02	0.04	11.65	168	291	0.2	205.90	29.00	0.36
2017-11-26 14:09:05	6.02	0.04	11.65	168	291	0.2	205.90	29.00	0.36
2017-11-26 14:10:09	6.97	0.04	11.75	166	292	0.2	209.30	29.49	0.39
2017-11-26 14:10:10	6.97	0.04	11.75	166	292	0.2	209.30	29.49	0.39

Appendix B.14 Pond Burevestniksee sonde data

Location: Pond Burevestniksee

Instrument: YSI 6600

Date / Time	Depth (m)	Temp. (°C)	pH	ORP (mV)	Sp. Cond. (µS/cm)	TDS (g/L)	LDO% (% Saturation)	LDO (mg/L)	Chlorophyll (µg/L)
2017-11-26 14:10:11	6.96	0.03	11.76	166	294	0.2	209.40	29.51	0.39
2017-11-26 14:10:12	6.96	0.03	11.77	166	292	0.2	209.60	29.54	0.39
2017-11-26 14:10:13	6.96	0.03	11.77	166	292	0.2	209.60	29.54	0.39

ORP = oxidation-reduction potential

TDS = total dissolved solids

LDO = luminescent dissolved oxygen

Appendix B.15 Pond 2 sonde data

Location: Pond 2

Instrument: YSI 6600

Date / Time	Depth (m)	Temp. (°C)	pH	ORP (mV)	Sp. Cond. (µS/cm)	TDS (g/L)	LDO% (% Saturation)	LDO (mg/L)	Chlorophyll (µg/L)
2017-11-26 14:46:00	0.27	0.01	10.48	158	850	0.44	262.8	36.97	0.18
2017-11-26 14:46:01	0.27	0.01	10.48	158	850	0.44	262.8	36.97	0.18
2017-11-26 14:45:59	0.41	0.01	10.43	158	853	0.44	262.8	36.97	0.18
2017-11-26 14:45:57	0.46	0.02	10.42	158	850	0.44	262.7	36.95	0.18
2017-11-26 14:45:58	0.46	0.02	10.42	158	850	0.44	262.7	36.95	0.18
2017-11-26 14:47:11	1.01	0.01	10.72	152	851	0.44	265.8	37.39	0.17
2017-11-26 14:47:12	1.01	0.01	10.72	152	851	0.44	265.7	37.39	0.17
2017-11-26 14:47:13	1.01	0.01	10.72	152	851	0.44	265.7	37.39	0.17
2017-11-26 14:47:14	1.02	0.01	10.72	152	851	0.44	265.6	37.37	0.17
2017-11-26 14:47:15	1.02	0.01	10.72	152	851	0.44	265.6	37.37	0.17
2017-11-26 14:48:10	2.00	0.54	10.85	149	890	0.46	281.2	38.98	0.19
2017-11-26 14:48:11	2.00	0.54	10.85	149	890	0.46	281.2	38.98	0.19
2017-11-26 14:48:12	2.01	0.55	10.86	149	890	0.46	282.8	39.19	0.19
2017-11-26 14:48:13	2.00	0.57	10.86	149	885	0.46	283.7	39.29	0.19
2017-11-26 14:48:14	2.00	0.57	10.86	149	885	0.46	283.7	39.29	0.19
2017-11-26 14:48:49	2.26	1.41	10.59	161	1891	1.01	280.5	37.8	0.19
2017-11-26 14:48:50	2.25	1.40	10.60	161	1912	1.02	278.7	37.57	0.19
2017-11-26 14:48:51	2.25	1.40	10.60	161	1912	1.02	278.7	37.57	0.19
2017-11-26 14:48:52	2.23	1.34	10.60	161	2052	1.10	277.3	37.42	0.19
2017-11-26 14:48:53	2.23	1.34	10.60	161	2052	1.10	277.3	37.42	0.19

ORP = oxidation-reduction potential

TDS = total dissolved solids

LDO = luminescent dissolved oxygen

Appendix C: Microbial Mat Data

Appendix C.1 Organic carbon data for microbial mat and sediments (Core 1)

Sample ID	Sample Depth (mm)	Sample Type	Wet Weight (g)	Dry Weight (g)	Water Content (%)
C1-1	2	MM	0.830	0.285	66%
C1-2	4	MM	1.663	0.867	48%
C1-3	6	MM	1.305	0.711	46%
C1-4	7	MM	0.661	0.329	50%
C1-5	9	MM	1.007	0.509	49%
C1-6	10	MM	0.730	0.351	52%
C1-7	12	MM	1.069	0.546	49%
C1-8	14	MM	0.948	0.412	57%
C1-9	16	MM	0.849	0.377	56%
C1-10	18	MM	0.815	0.362	56%
C1-11	20	MM	1.966	0.777	60%
C1-12	22	MM	1.249	0.466	63%
C1-13	24	MM	1.477	0.561	62%
C1-14	26	MM	2.193	0.786	64%
C1-15	28	MM	1.522	0.514	66%
C1-16	30	MM	1.383	0.544	61%
C1-17	32	MM	1.778	0.729	59%
C1-18	35	MM	2.812	0.886	68%
C1-19	37	MM	2.183	0.779	64%
C1-20	41	MM	6.078	2.341	61%
C1-21	45	MM	5.930	2.848	52%
C1-22	47	MM	2.333	0.987	58%
C1-23	50	MM	2.673	1.239	54%
C1-24	52	MM	2.402	0.927	61%
C1-25	55	MM	3.527	1.518	57%
C1-26	58	MM	3.444	1.462	58%
C1-27	60	MM	2.451	0.855	65%
C1-28	62	MM	2.072	0.772	63%
C1-29	66	MM	4.998	2.241	55%
C1-30	70	MM	5.482	2.353	57%
C1-31	73	MM	2.005	0.876	56%
C1-32	76	MM	4.209	1.993	53%
C1-33	79	MM	3.749	1.927	49%
C1-34	83	MM	6.158	3.125	49%
C1-35	87	MM	5.043	2.561	49%
C1-36	91	MM	5.620	3.017	46%
C1-37	100	MM	15.922	5.327	67%
C1-38	110	Sediment	13.4	8.341	38%
C1-39	120	Sediment	13.3	8.859	33%
C1-40	140	Sediment	27.6	21.582	22%
C1-41	150	Sediment	12.6	10.314	18%
C1-42	160	Sediment	13.6	10.409	23%
C1-43	175	Sediment	20.0	15.639	22%

Appendix C.1 Organic carbon data for microbial mat and sediments (Core 1)

Sample ID	Sample Depth (mm)	Measured Organic Carbon (wt %)	Calculated Organic Carbon Mass (g)	$\delta^{13}\text{C}$ VPBD (‰)
C1-1	2	2.3	0.007	-11.5
C1-2	4	1.3	0.011	-10.0
C1-3	6	1.0	0.007	-9.8
C1-4	7	1.3	0.004	-10.2
C1-5	9	1.3	0.007	-10.0
C1-6	10	1.5	0.005	-10.9
C1-7	12	2.4	0.013	-9.2
C1-8	14	2.0	0.008	-9.9
C1-9	16	1.6	0.006	-9.4
C1-10	18	1.5	0.005	-9.0
C1-11	20	1.6	0.012	-10.0
C1-12	22	1.8	0.008	-11.7
C1-13	24	1.8	0.010	-10.3
C1-14	26	1.8	0.014	-10.1
C1-15	28	2.2	0.011	-12.6
C1-16	30	1.5	0.008	-12.3
C1-17	32	1.6	0.012	-11.8
C1-18	35	2.4	0.021	-14.8
C1-19	37	1.8	0.014	-12.5
C1-20	41	2.8	0.066	-17.3
C1-21	45	2.1	0.060	-18.1
C1-22	47	1.3	0.013	-13.8
C1-23	50	1.3	0.016	-11.6
C1-24	52	1.9	0.018	-11.7
C1-25	55	1.4	0.021	-11.2
C1-26	58	1.3	0.019	-10.2
C1-27	60	2.3	0.020	-10.0
C1-28	62	1.9	0.015	-9.1
C1-29	66	1.3	0.029	-15.0
C1-30	70	1.6	0.038	-13.8
C1-31	73	1.7	0.015	-12.5
C1-32	76	1.5	0.030	-13.0
C1-33	79	1.1	0.021	-12.6
C1-34	83	1.2	0.038	-12.7
C1-35	87	1.1	0.028	-11.7
C1-36	91	1.1	0.033	-13.6
C1-37	100	1.2	0.064	-14.2
C1-38	110	1.0	0.080	-15.2
C1-39	120	0.7	0.058	-15.0
C1-40	140	<i>Sample not analyzed</i>		
C1-41	150	0.2	0.018	-16.6
C1-42	160	0.2	0.018	-16.4
C1-43	175	0.1	0.022	-17.2

Appendix C.1 Organic carbon data for microbial mat and sediments (Core 1)

Sample ID	Sample Depth (mm)	Sample Type	Wet Weight (g)	Dry Weight (g)	Water Content (%)
<i>Laboratory Replicates</i>					
<i>C1-4R</i>	-	-	-	-	-
<i>C1-16R</i>	-	-	-	-	-
<i>C1-30R</i>	-	-	-	-	-
<i>C1-39R</i>	-	-	-	-	-

Samples collected from split core

¹³C/¹²C results are normalized to Vienna Pee Dee Belemnite (VPBD)

MM = microbial mats

Appendix C.1 Organic carbon data for microbial mat and sediments (Core 1)

Sample ID	Sample Depth (mm)	Measured Organic Carbon (wt %)	Calculated Organic Carbon Mass (g)	$\delta^{13}\text{C}$ VPBD (‰)
<i>Laboratory Replicates</i>				
<i>C1-4R</i>	-	<i>1.2</i>	-	<i>-10.7</i>
<i>C1-16R</i>	-	<i>1.5</i>	-	<i>-11.9</i>
<i>C1-30R</i>	-	<i>1.7</i>	-	<i>-13.1</i>
<i>C1-39R</i>	-	<i>0.7</i>	-	<i>-15.1</i>

Appendix C.2 Organic carbon data for microbial mat and sediments (Core 2)

Sample ID	Sample Depth (mm)	Sample Type	Wet Weight (g)	Dry Weight (g)	Water Content (%)
C2-1	1	MM	0.462	0.235	49%
C2-2	4	MM	1.522	0.815	46%
C2-3	6	MM	0.624	0.332	47%
C2-4	8	MM	0.648	0.316	51%
C2-5	11	MM	1.076	0.555	48%
C2-6	12	MM	0.367	0.184	50%
C2-7	14	MM	0.835	0.387	54%
C2-8	17	MM	1.001	0.449	55%
C2-9	20	MM	1.300	0.608	53%
C2-10	22	MM	0.731	0.353	52%
C2-11	25	MM	1.451	0.672	54%
C2-12	29	MM	3.061	1.261	59%
C2-13	33	MM	1.697	0.725	57%
C2-14	37	MM	2.659	1.079	59%
C2-15	40	MM	1.161	0.518	55%
C2-16	43	MM	1.324	0.726	45%
C2-17	46	MM	1.384	0.571	59%
C2-18	49	MM	1.408	0.635	55%
C2-19	52	MM	1.075	0.577	46%
C2-20	55	MM	1.330	0.740	44%
C2-21	58	MM	2.279	1.224	46%
C2-22	61	MM	2.485	1.448	42%
C2-23	66	MM	4.201	2.409	43%
C2-24	71	MM	3.965	2.507	37%
C2-25	74	MM	1.493	0.786	47%
C2-26	77	MM	1.273	0.616	52%
C2-27	80	MM	1.460	0.661	55%
C2-28	86	MM	2.870	1.684	41%
C2-29	90	MM	1.713	0.672	61%
C2-30	95	MM	2.668	1.274	52%
C2-31	100	Sediment	7.886	4.726	40%
C2-32	105	Sediment	12.784	9.236	28%
C2-33	115	Sediment	8.697	5.749	34%
C2-34	125	Sediment	11.434	9.003	21%
C2-35	145	Sediment	32.323	27.671	14%
<i>Laboratory Replicates</i>					
C2-3R	-	-	-	-	
C2-17R	-	-	-	-	
C2-34R	-	-	-	-	

Samples collected from split core

¹³C/¹²C results are normalized to Vienna Pee Dee Belemnite (VPBD)

MM = Microbial Mat

Appendix C.2 Organic carbon data for microbial mat and sediments (Core 2)

Sample ID	Sample Depth (mm)	Measured Organic Carbon (wt %)	Calculated Organic Carbon Mass (g)	$\delta^{13}\text{C}$ VPBD (‰)
C2-1	1	3.0	0.007	-9.2
C2-2	4	2.1	0.017	-8.1
C2-3	6	1.7	0.006	-9.3
C2-4	8	2.2	0.007	-8.4
C2-5	11	2.0	0.011	-8.9
C2-6	12	2.0	0.004	-9.5
C2-7	14	2.8	0.011	-8.6
C2-8	17	3.1	0.014	-9.0
C2-9	20	2.7	0.016	-8.9
C2-10	22	2.4	0.008	-8.6
C2-11	25	2.4	0.016	-8.4
C2-12	29	2.6	0.033	-9.7
C2-13	33	2.3	0.017	-9.9
C2-14	37	2.1	0.022	-9.9
C2-15	40	1.7	0.009	-11.5
C2-16	43	1.3	0.010	-10.7
C2-17	46	2.1	0.012	-11.3
C2-18	49	1.6	0.010	-11.7
C2-19	52	1.5	0.009	-9.6
C2-20	55	1.3	0.010	-10.2
C2-21	58	1.8	0.021	-12.4
C2-22	61	1.6	0.024	-12.9
C2-23	66	1.3	0.032	-14.5
C2-24	71	2.1	0.053	-18.3
C2-25	74	1.6	0.012	-9.0
C2-26	77	2.4	0.015	-8.6
C2-27	80	2.6	0.017	-9.3
C2-28	86	1.2	0.020	-11.7
C2-29	90	3.7	0.025	-11.7
C2-30	95	2.4	0.031	-9.9
C2-31	100	1.3	0.062	-15.6
C2-32	105	0.8	0.075	-15.6
C2-33	115	0.7	0.038	-16.4
C2-34	125	0.2	0.020	-17.0
C2-35	145	0.1	0.039	-18.4
<i>Laboratory Replicates</i>				
C2-3R	-	1.9	-	-9.5
C2-17R	-	2.1	-	-11.5
C2-34R	-	0.2	-	-17.1

Appendix C.3 Total nitrogen and organic carbon data for microbial mat and sediments (Core 3)

Sample ID	Sample Depth mm	Sample Type	Measured Wet Weight (g)	Estimated Dry Weight (g)	Organic Carbon (wt %)
C3-1	1	MM	1.234	0.568	5.3
C3-2	3	MM	2.540	1.168	4.5
C3-3	4	MM	1.155	0.531	3.8
C3-4	5	MM	0.907	0.417	2.8
C3-5	6	MM	0.761	0.350	3.8
C3-6	7	MM	0.823	0.379	4.0
C3-7	9	MM	1.075	0.495	4.3
C3-8	11	MM	1.492	0.686	5.4
C3-9	13	MM	1.369	0.630	5.8
C3-10	14	MM	1.797	0.827	5.1
C3-11	15	MM	1.288	0.592	4.3
C3-12	16	MM	0.924	0.425	2.3
C3-13	17	MM	1.410	0.649	3.0
C3-14	19	MM	1.998	0.919	2.5
C3-15	21	MM	1.541	0.709	3.3
C3-16	23	MM	2.828	1.301	2.1
C3-17	25	MM	2.360	1.086	1.6
C3-18	28	MM	3.064	1.409	1.5
C3-19	29	MM	1.072	0.493	1.0
C3-20	30	MM	1.986	0.913	0.9
C3-21	31	MM	0.845	0.389	0.9
C3-22	32	MM	1.983	0.912	1.0
C3-23	33	MM	1.521	0.700	0.9
C3-24	34	MM	1.242	0.571	0.7
C3-25	35	MM	1.042	0.479	0.9
C3-26	38	MM	3.048	1.402	1.0
C3-27	39	MM	2.520	1.159	1.1
C3-28	40	MM	1.869	0.860	1.5
C3-29	41	MM	1.400	0.644	1.9
C3-30	42	MM	1.549	0.712	2.4
C3-31	43	MM	1.191	0.548	3.0
C3-32	44	MM	1.320	0.607	0.8
C3-33	45	MM	1.181	0.543	2.2
C3-34	46	MM	1.745	0.803	2.3
C3-35	47	MM	1.369	0.630	1.7
C3-36	48	MM	1.330	0.612	1.5
C3-37	49	MM	2.467	1.135	1.7
C3-38	50	MM	1.750	0.805	1.5
C3-39	51	MM	1.491	0.686	1.7

Appendix C.3 Total nitrogen and organic carbon data for microbial mat and sediments (Core 3)

Sample ID	Sample Depth mm	$\delta^{13}\text{C}$ VPBD (‰)	Calculated Organic Carbon Mass (g)	Total Nitrogen (wt %)	$\delta^{15}\text{N}$ AIR (‰)
C3-1	1	-9.2	0.030	0.7	28.76
C3-2	3	ND	0.053	ND	ND
C3-3	4	-8.6	0.020	0.48	27.7
C3-4	5	-10.9	0.012	0.36	27.44
C3-5	6	-10.6	0.013	0.39	26.66
C3-6	7	-9.6	0.015	0.42	27.22
C3-7	9	-8.9	0.021	0.48	28.1
C3-8	11	-9.0	0.037	0.71	28.08
C3-9	13	-8.7	0.037	0.67	25.61
C3-10	14	ND	0.042	ND	ND
C3-11	15	-8.7	0.025	0.52	24.37
C3-12	16	-8.2	0.010	0.41	20.58
C3-13	17	-8.3	0.020	0.43	23.81
C3-14	19	-9.7	0.023	0.28	23.85
C3-15	21	-10.0	0.024	0.44	23.08
C3-16	23	-8.5	0.028	0.34	23.07
C3-17	25	-9.0	0.017	0.16	21.51
C3-18	28	-8.5	0.021	0.13	19.49
C3-19	29	-9.9	0.005	0.28	12.98
C3-20	30	ND	0.009	ND	ND
C3-21	31	-9.6	0.003	0.12	17.91
C3-22	32	-11.1	0.009	0.13	18.26
C3-23	33	-9.9	0.006	0.12	17.04
C3-24	34	-9.7	0.004	0.1	18.35
C3-25	35	-11.3	0.004	0.12	16.72
C3-26	38	-11.1	0.014	0.12	17.82
C3-27	39	-8.4	0.013	0.1	16.95
C3-28	40	-9.3	0.013	0.16	14.29
C3-29	41	-8.6	0.012	0.18	12.03
C3-30	42	ND	0.017	ND	ND
C3-31	43	-6.9	0.016	0.17	15.8
C3-32	44	-9.5	0.005	0.1	18.54
C3-33	45	-8.3	0.012	0.13	17
C3-34	46	-8.0	0.019	0.15	16.4
C3-35	47	-9.7	0.011	0.14	17.19
C3-36	48	-10.4	0.009	0.15	17.43
C3-37	49	-10.7	0.020	0.16	16.68
C3-38	50	-12.6	0.012	0.14	16.75
C3-39	51	-12.0	0.011	0.16	16.48

Appendix C.3 Total nitrogen and organic carbon data for microbial mat and sediments (Core 3)

Sample ID	Sample Depth mm	Sample Type	Measured Wet Weight (g)	Estimated Dry Weight (g)	Organic Carbon (wt %)
C3-40	53	MM	2.628	1.209	1.8
C3-41	54	MM	2.545	1.170	1.8
C3-42	56	MM	2.937	1.351	1.4
C3-43	59	MM	2.839	1.306	1.2
C3-44	60	MM	3.738	1.719	1.1
C3-45	61	Sediment	5.4628	5.193	0.9
C3-46	66	Sediment	5.2742	5.004	1.0
C3-47	71	Sediment	5.5306	5.261	0.9
C3-48	76	Sediment	6.3347	6.065	0.8
C3-49	81	Sediment	9.4003	9.130	0.6
C3-50	86	Sediment	7.2707	7.001	0.3
C3-51	118	Sediment	42.2493	41.979	0.2
C3-52	143	Sediment	17.4539	17.184	0.0
<i>Laboratory Replicates</i>					
C3-3R	-	-	-	-	3.27
C3-4R	-	-	-	-	-
C3-16R	-	-	-	-	2.12
C3-17R	-	-	-	-	-
C3-26R	-	-	-	-	0.98
C3-27R	-	-	-	-	-
C3-37R	-	-	-	-	1.40
C3-38R	-	-	-	-	-
C3-48R	-	-	-	-	-
C3-50R	-	-	-	-	0.33

Samples collected from a split core

Dry weight estimated from wet weigh, assuming average water content from the other two cores (C1, C2): 54% for laminae samples, 27% for sediments

Grey cells are averages of the bounding samples. Select samples were used for alternate analyses and were not measured for org-C abundance

ND = not measured, no data

MM = Microbial Mat

Appendix C.3 Total nitrogen and organic carbon data for microbial mat and sediments (Core 3)

Sample ID	Sample Depth mm	$\delta^{13}\text{C}$ VPBD (‰)	Calculated Organic Carbon Mass (g)	Total Nitrogen (wt %)	$\delta^{15}\text{N}$ AIR (‰)
C3-40	53	ND	0.021	ND	ND
C3-41	54	-12.6	0.022	0.14	17.18
C3-42	56	-11.6	0.019	0.13	17.53
C3-43	59	-11.9	0.016	0.11	17.56
C3-44	60	-13.6	0.019	0.13	17.08
C3-45	61	-14.5	0.046	0.11	18.86
C3-46	66	-14.6	0.048	0.11	17.07
C3-47	71	-14.5	0.050	0.12	16.54
C3-48	76	-14.8	0.051	0.11	16.67
C3-49	81	ND	0.053	ND	ND
C3-50	86	-17.2	0.022	0.07	18.06
C3-51	118	-17.8	0.064	0.05	16.71
C3-52	143	-18.0	0.001	0.05	11.39
<i>Laboratory Replicates</i>					
C3-3R	-	-	-	0.5	28.0
C3-4R	-	-10.0	-	-	-
C3-16R	-	-	-	0.31	23.31
C3-17R	-	-8.7	-	-	-
C3-26R	-	-	-	0.1	17.8
C3-27R	-	-8.3	-	-	-
C3-37R	-	-	-	0.15	16.63
C3-38R	-	-12.7	-	-	-
C3-48R	-	-14.6	-	-	-
C3-50R	-	-	-	0.1	18.6

Appendix C.4 Radiocarbon analysis of organic carbon component of microbial mats and sediments

Sample ID	Depth (mm)	Sample Material	¹⁴ C yr BP	± 2σ	F ¹⁴ C	± 2σ
Core 2						
C2-1	1	Microbial Mats	10052	56	0.2861	0.002
C2-5	9	Microbial Mats	10882	70	0.258	0.0022
C2-8	14	Microbial Mats	9510	64	0.3061	0.0024
C2-9	16	Microbial Mats	11268	104	0.2459	0.0032
C2-12	22	Microbial Mats	11113	58	0.2507	0.0018
C2-19	37	Microbial Mats	11481	60	0.2395	0.0018
C2-29	66	Microbial Mats	13040	76	0.1973	0.0018
C2-30	70	Microbial Mats	12031	68	0.2237	0.0018
Core 3						
C3-1	1	Microbial Mats	9524	48	0.3055	0.0018
C3-2	3	Microbial Mats	10945	82	0.256	0.0026
C3-8	11	Microbial Mats	9791	58	0.2293	0.0016
C3-10	14	Microbial Mats	9419	76	0.3096	0.003
C3-13	17	Microbial Mats	11832	58	0.2293	0.0016
C3-20	30	Microbial Mats	11285	80	0.2454	0.0024
C3-30	42	Microbial Mats	12917	78	0.2003	0.002
C3-40	53	Microbial Mats	13049	90	0.197	0.0022
C3-49	81	Sediments	19370	156	0.0009	0.0018

Radiocarbon analysis of organic carbon fraction

F¹⁴C = fraction modern carbon

¹⁴C yr BP = radiocarbon age, years before 1950

Measurements on organic carbon fraction

Appendix D: Geochemical Modelling (PHREEQC) Output

Input file:
 C:\Users\nicol\Documents\!Antarctica\PHREEQC_Untersee\weathering_forappendice
 s2.pqi
 Output file:
 C:\Users\nicol\Documents\!Antarctica\PHREEQC_Untersee\weathering_forappendice
 s2.pqi
 Database file: C:\Program Files (x86)\USGS\Phreeqc Interactive 3.4.0-
 12927\database\wateq4f.dat

 Reading data base.

SOLUTION_MASTER_SPECIES
 SOLUTION_SPECIES
 PHASES
 EXCHANGE_MASTER_SPECIES
 EXCHANGE_SPECIES
 SURFACE_MASTER_SPECIES
 SURFACE_SPECIES
 RATES
 END

 Reading input data for simulation 1.

DATABASE C:\Program Files (x86)\USGS\Phreeqc Interactive 3.4.0-
 12927\database\wateq4f.dat

SOLUTION 1 Glacial Meltwater (Closed-System Weathering)

temp 0.1
 pH 5.6
 pe 4
 redox pe
 units ppb
 density 1
 C 0.0014 mMol/kgs
 Ca 12
 N(5) 26
 Na 70
 S(6) 137
 water 1 # kg

EQUILIBRIUM_PHASES 1

Albite 0 10
 Anorthite 0 10
 Kaolinite 0 10

SELECTED_OUTPUT 1

file selected_output_weathering1.sel
 totals Na Mg K Ca S(6) C
 molalities Ca+2 Na+ S6-2 K+

```

                                Mg+2  CO2  CO3-2  HCO3-
equilibrium_phases  Albite  Anorthite  Kaolinite
end
-----
Beginning of initial solution calculations.
-----

Initial solution 1.      Glacial Meltwater (Closed-System Weathering)
-----Solution composition-----
--

Elements                Molality                Moles
C                        1.400e-06              1.400e-06
Ca                       2.994e-07              2.994e-07
N(5)                     1.856e-06              1.856e-06
Na                       3.045e-06              3.045e-06
S(6)                     1.426e-06              1.426e-06
-----Description of solution-----
--

                                pH = 5.600
                                pe = 4.000
                                Activity of water = 1.000
                                Ionic strength (mol/kgw) = 7.228e-06
                                Mass of water (kg) = 1.000e+00
                                Total alkalinity (eq/kg) = -2.385e-06
                                Total CO2 (mol/kg) = 1.400e-06
                                Temperature (°C) = 0.10
                                Electrical balance (eq) = 1.320e-06
Percent error, 100*(Cat-|An|)/(Cat+|An|) = 12.00
                                Iterations = 5
                                Total H = 1.110124e+02
                                Total O = 5.550623e+01
-----Distribution of species-----
--

mole V
Species                Molality                Activity                Log                Log                Log
cm³/mol
H+                     2.519e-06              2.512e-06              -5.599              -5.600              -0.001
0.00
OH-                     4.608e-10              4.594e-10              -9.336              -9.338              -0.001
(0)
H2O                    5.551e+01              1.000e+00              1.744              -0.000              0.000
18.02
C(-4)                  0.000e+00
CH4                    0.000e+00              0.000e+00              -54.754              -54.754              0.000
(0)
C(4)                   1.400e-06
CO2                    1.266e-06              1.266e-06              -5.898              -5.898              0.000
(0)

```

HCO3-	1.338e-07	1.334e-07	-6.873	-6.875	-0.001
(0)					
CO3-2	1.269e-12	1.254e-12	-11.896	-11.902	-0.005
(0)					
CaHCO3+	2.625e-13	2.617e-13	-12.581	-12.582	-0.001
(0)					
NaHCO3	2.278e-13	2.278e-13	-12.642	-12.642	0.000
(0)					
CaCO3	5.049e-16	5.049e-16	-15.297	-15.297	0.000
(0)					
NaCO3-	1.806e-17	1.800e-17	-16.743	-16.745	-0.001
(0)					
Ca	2.994e-07				
Ca+2	2.993e-07	2.957e-07	-6.524	-6.529	-0.005
(0)					
CaSO4	6.449e-11	6.449e-11	-10.190	-10.190	0.000
(0)					
CaHCO3+	2.625e-13	2.617e-13	-12.581	-12.582	-0.001
(0)					
CaOH+	1.960e-14	1.954e-14	-13.708	-13.709	-0.001
(0)					
CaHSO4+	7.583e-16	7.560e-16	-15.120	-15.121	-0.001
(0)					
CaCO3	5.049e-16	5.049e-16	-15.297	-15.297	0.000
(0)					
H(0)	1.171e-22				
H2	5.854e-23	5.854e-23	-22.233	-22.233	0.000
(0)					
N(5)	1.856e-06				
NO3-	1.856e-06	1.851e-06	-5.731	-5.733	-0.001
(0)					
Na	3.045e-06				
Na+	3.045e-06	3.036e-06	-5.516	-5.518	-0.001
(0)					
NaSO4-	1.810e-11	1.804e-11	-10.742	-10.744	-0.001
(0)					
NaHCO3	2.278e-13	2.278e-13	-12.642	-12.642	0.000
(0)					
NaCO3-	1.806e-17	1.800e-17	-16.743	-16.745	-0.001
(0)					
O(0)	0.000e+00				
O2	0.000e+00	0.000e+00	-56.683	-56.683	0.000
(0)					
S(6)	1.426e-06				
SO4-2	1.426e-06	1.409e-06	-5.846	-5.851	-0.005
(0)					
HSO4-	2.133e-10	2.126e-10	-9.671	-9.672	-0.001
(0)					
CaSO4	6.449e-11	6.449e-11	-10.190	-10.190	0.000
(0)					
NaSO4-	1.810e-11	1.804e-11	-10.742	-10.744	-0.001
(0)					
CaHSO4+	7.583e-16	7.560e-16	-15.120	-15.121	-0.001
(0)					

-----Saturation indices-----
 --

Phase	SI**	log IAP	log K(273 K,	1 atm)	
Anhydrite	-8.01	-12.38	-4.37		CaSO4
Aragonite	-10.21	-18.43	-8.22		CaCO3
Calcite	-10.05	-18.43	-8.38		CaCO3
CH4(g)	-52.12	-54.75	-2.63		CH4
CO2(g)	-4.79	-5.90	-1.11		CO2
Gypsum	-7.76	-12.38	-4.62		CaSO4:2H2O
H2(g)	-19.20	-22.23	-3.03		H2
H2O(g)	-2.21	-0.00	2.21		H2O
Mirabilite	-14.50	-16.89	-2.38		Na2SO4:10H2O
Nahcolite	-11.60	-12.39	-0.80		NaHCO3
Natron	-20.57	-22.94	-2.36		Na2CO3:10H2O
O2(g)	-54.02	-56.68	-2.66		O2
Portlandite	-20.20	4.67	24.87		Ca(OH)2
Thenardite	-16.75	-16.89	-0.14		Na2SO4
Thermonatrite	-23.25	-22.94	0.31		Na2CO3:H2O
Trona	-35.74	-35.33	0.41		NaHCO3:Na2CO3:2H2O

**For a gas, SI = log10(fugacity). Fugacity = pressure * phi / 1 atm.
For ideal gases, phi = 1.

Beginning of batch-reaction calculations.

Reaction step 1.

Using solution 1. Glacial Meltwater (Closed-System Weathering)
Using pure phase assemblage 1.

-----Phase assemblage-----
--

Phase	SI	log IAP	log K(T, P)	Moles in assemblage		
				Initial	Final	Delta
Albite	0.00	-19.73	-19.73	1.000e+01	9.998e+00	-1.762e-03
Anorthite	0.00	-20.49	-20.49	1.000e+01	9.999e+00	-1.432e-03
Kaolinite	-0.00	9.79	9.79	1.000e+01	1.000e+01	2.300e-03

-----Solution composition-----
--

Elements	Molality	Moles
Al	2.537e-05	2.537e-05
C	1.400e-06	1.400e-06
Ca	1.432e-03	1.432e-03
N	1.857e-06	1.856e-06
Na	1.766e-03	1.765e-03
S	1.426e-06	1.426e-06

Si 3.550e-03 3.550e-03

-----Description of solution-----
 --

equilibrium

	pH =	11.885	Charge balance
	pe =	8.692	Adjusted to redox
	Activity of water =	1.000	
	Ionic strength (mol/kgw) =	5.832e-03	
	Mass of water (kg) =	9.998e-01	
	Total alkalinity (eq/kg) =	4.700e-03	
	Total CO2 (mol/kg) =	1.400e-06	
	Temperature (°C) =	0.10	
	Electrical balance (eq) =	1.320e-06	
	Percent error, 100*(Cat- An)/(Cat+ An) =	0.01	
	Iterations =	25	
	Total H =	1.110032e+02	
	Total O =	5.551108e+01	

-----Distribution of species-----
 --

mole V			Log	Log	Log
Species	Molality	Activity	Molality	Activity	Gamma
cm ³ /mol					
OH-	9.583e-04	8.851e-04	-3.018	-3.053	-0.034
(0)					
H+	1.399e-12	1.304e-12	-11.854	-11.885	-0.031
0.00					
H2O	5.551e+01	9.999e-01	1.744	-0.000	0.000
18.02					
Al	2.537e-05				
Al (OH) 4-	2.537e-05	2.348e-05	-4.596	-4.629	-0.034
(0)					
Al (OH) 3	1.866e-11	1.868e-11	-10.729	-10.729	0.001
(0)					
Al (OH) 2+	1.577e-15	1.462e-15	-14.802	-14.835	-0.033
(0)					
AlOH+2	4.151e-21	3.061e-21	-20.382	-20.514	-0.132
(0)					
Al+3	4.198e-27	2.224e-27	-26.377	-26.653	-0.276
(0)					
AlSO4+	5.030e-30	4.654e-30	-29.298	-29.332	-0.034
(0)					
Al (SO4) 2-	1.319e-34	1.221e-34	-33.880	-33.913	-0.034
(0)					
AlHSO4+2	0.000e+00	0.000e+00	-42.189	-42.325	-0.136
(0)					
C(-4)	0.000e+00				
CH4	0.000e+00	0.000e+00	-149.525	-149.524	0.001
(0)					
C(4)	1.400e-06				
CO3-2	6.962e-07	5.134e-07	-6.157	-6.290	-0.132
(0)					

CaCO3	6.690e-07	6.699e-07	-6.175	-6.174	0.001
(0)					
HCO3-	3.060e-08	2.836e-08	-7.514	-7.547	-0.033
(0)					
NaCO3-	4.282e-09	3.968e-09	-8.368	-8.401	-0.033
(0)					
CaHCO3+	1.943e-10	1.802e-10	-9.712	-9.744	-0.033
(0)					
NaHCO3	2.602e-11	2.605e-11	-10.585	-10.584	0.001
(0)					
CO2	1.395e-13	1.397e-13	-12.856	-12.855	0.001
(0)					
Ca	1.432e-03				
Ca+2	1.300e-03	9.583e-04	-2.886	-3.019	-0.132
(0)					
CaOH+	1.315e-04	1.220e-04	-3.881	-3.914	-0.033
(0)					
CaCO3	6.690e-07	6.699e-07	-6.175	-6.174	0.001
(0)					
CaSO4	1.394e-07	1.396e-07	-6.856	-6.855	0.001
(0)					
CaHCO3+	1.943e-10	1.802e-10	-9.712	-9.744	-0.033
(0)					
CaHSO4+	9.183e-19	8.492e-19	-18.037	-18.071	-0.034
(0)					
H(0)	0.000e+00				
H2	0.000e+00	0.000e+00	-44.186	-44.186	0.001
(0)					
N(-3)	0.000e+00				
NH3	0.000e+00	0.000e+00	-60.773	-60.773	0.000
(0)					
NH4+	0.000e+00	0.000e+00	-62.544	-62.578	-0.034
(0)					
NH4SO4-	0.000e+00	0.000e+00	-67.461	-67.494	-0.033
(0)					
N(0)	1.447e-13				
N2	7.237e-14	7.247e-14	-13.140	-13.140	0.001
(0)					
N(3)	4.050e-16				
NO2-	4.050e-16	3.745e-16	-15.393	-15.427	-0.034
(0)					
N(5)	1.857e-06				
NO3-	1.857e-06	1.713e-06	-5.731	-5.766	-0.035
(0)					
Na	1.766e-03				
Na+	1.765e-03	1.634e-03	-2.753	-2.787	-0.034
(0)					
NaSO4-	6.999e-09	6.486e-09	-8.155	-8.188	-0.033
(0)					
NaCO3-	4.282e-09	3.968e-09	-8.368	-8.401	-0.033
(0)					
NaHCO3	2.602e-11	2.605e-11	-10.585	-10.584	0.001
(0)					
O(0)	3.340e-13				
O2	1.670e-13	1.672e-13	-12.777	-12.777	0.001
(0)					
S(-2)	0.000e+00				

S6-2	0.000e+00	0.000e+00	-142.744	-142.855	-0.111
(0)					
S5-2	0.000e+00	0.000e+00	-143.075	-143.190	-0.116
(0)					
S4-2	0.000e+00	0.000e+00	-143.331	-143.451	-0.120
(0)					
HS-	0.000e+00	0.000e+00	-144.824	-144.859	-0.034
(0)					
S-2	0.000e+00	0.000e+00	-146.567	-146.700	-0.133
(0)					
S3-2	0.000e+00	0.000e+00	-146.826	-146.951	-0.125
(0)					
S2-2	0.000e+00	0.000e+00	-148.134	-148.264	-0.129
(0)					
H2S	0.000e+00	0.000e+00	-149.395	-149.394	0.001
(0)					
S(6)	1.426e-06				
SO4-2	1.280e-06	9.410e-07	-5.893	-6.026	-0.134
(0)					
CaSO4	1.394e-07	1.396e-07	-6.856	-6.855	0.001
(0)					
NaSO4-	6.999e-09	6.486e-09	-8.155	-8.188	-0.033
(0)					
HSO4-	7.966e-17	7.371e-17	-16.099	-16.132	-0.034
(0)					
CaHSO4+	9.183e-19	8.492e-19	-18.037	-18.071	-0.034
(0)					
AlSO4+	5.030e-30	4.654e-30	-29.298	-29.332	-0.034
(0)					
Al(SO4)2-	1.319e-34	1.221e-34	-33.880	-33.913	-0.034
(0)					
AlHSO4+2	0.000e+00	0.000e+00	-42.189	-42.325	-0.136
(0)					
NH4SO4-	0.000e+00	0.000e+00	-67.461	-67.494	-0.033
(0)					
Si	3.550e-03				
H3SiO4-	3.438e-03	3.178e-03	-2.464	-2.498	-0.034
(0)					
H4SiO4	7.836e-05	7.847e-05	-4.106	-4.105	0.001
(0)					
H2SiO4-2	3.418e-05	2.521e-05	-4.466	-4.598	-0.132
(0)					

-----Saturation indices-----
 --

Phase	SI**	log IAP	log K(273 K,	1 atm)
Al(OH)3(a)	-3.57	9.00	12.57	Al(OH)3
Albite	0.00	-19.73	-19.73	NaAlSi3O8
Analcime	-1.71	-15.63	-13.92	NaAlSi2O6:H2O
Anhydrite	-4.68	-9.04	-4.37	CaSO4
Anorthite	0.00	-20.49	-20.49	CaAl2Si2O8
Aragonite	-1.09	-9.31	-8.22	CaCO3
Basaluminite	-16.49	6.21	22.70	Al4(OH)10SO4
Boehmite	-1.46	9.00	10.47	AlOOH
Calcite	-0.93	-9.31	-8.38	CaCO3

CH4 (g)	-146.89	-149.52	-2.63	CH4
Chalcedony	-0.24	-4.11	-3.87	SiO2
CO2 (g)	-11.74	-12.85	-1.11	CO2
Cristobalite	-0.15	-4.11	-3.95	SiO2
Diaspore	0.47	9.00	8.53	AlOOH
Gibbsite	-0.63	9.00	9.63	Al (OH) 3
Gypsum	-4.43	-9.05	-4.62	CaSO4:2H2O
H2 (g)	-41.15	-44.19	-3.03	H2
H2O (g)	-2.21	-0.00	2.21	H2O
H2S (g)	-148.70	-149.39	-0.69	H2S
Halloysite	-5.37	9.79	15.16	Al2Si2O5 (OH) 4
Jurbanite	-17.56	-20.79	-3.23	AlOHSO4
Kaolinite	-0.00	9.79	9.79	Al2Si2O5 (OH) 4
Laumontite	4.91	-28.70	-33.61	CaAl2Si4O12:4H2O
Leonhardite	18.38	-57.40	-75.77	Ca2Al4Si8O24:7H2O
Magadiite	-5.34	-19.64	-14.30	NaSi7O13 (OH) 3:3H2O
Mirabilite	-9.22	-11.60	-2.38	Na2SO4:10H2O
Montmorillonite-Ca	-1.19	-50.12	-48.93	Ca0.165Al2.33Si3.67O10 (OH) 2
N2 (g)	-9.97	-13.14	-3.17	N2
Nahcolite	-9.54	-10.33	-0.80	NaHCO3
Natron	-9.50	-11.86	-2.36	Na2CO3:10H2O
NH3 (g)	-63.09	-60.77	2.32	NH3
O2 (g)	-10.12	-12.78	-2.66	O2
Portlandite	-4.12	20.75	24.87	Ca (OH) 2
Prehnite	8.55	-3.84	-12.39	Ca2Al2Si3O10 (OH) 2
Pyrophyllite	-1.14	-49.45	-48.31	Al2Si4O10 (OH) 2
Quartz	0.28	-4.11	-4.38	SiO2
Silicagel	-0.79	-4.11	-3.31	SiO2
SiO2 (a)	-1.17	-4.11	-2.94	SiO2
Sulfur	-113.76	-129.32	-15.55	S
Thenardite	-11.46	-11.60	-0.14	Na2SO4
Thermonatrite	-12.18	-11.86	0.31	Na2CO3:H2O
Trona	-22.60	-22.20	0.41	NaHCO3:Na2CO3:2H2O
Wairakite	-0.24	-28.70	-28.45	CaAl2Si4O12:2H2O

**For a gas, $SI = \log_{10}(\text{fugacity})$. Fugacity = pressure * phi / 1 atm.
For ideal gases, phi = 1.

End of simulation.

Reading input data for simulation 2.

SOLUTION 2 Glacial Meltwater (Open-System Weathering)

temp 0.1
pH 5.6
pe 4
redox pe
units ppb
density 1
C 0.0014 mMol/kgs
Ca 12
N(5) 26
Na 70

```

S(6)      137
water     1 # kg
EQUILIBRIUM_PHASES 1
Albite    0 10
Anorthite 0 10
Kaolinite 0 10
CO2(g)    -3.43 10
O2(g)     -0.679 10
SELECTED_OUTPUT 2
file      selected_output_weathering2.sel
totals    Na Mg K Ca S(6) C
molalities Ca+2 Na+ S6-2 K+
           Mg+2 CO2 CO3-2 HCO3-
equilibrium_phases Albite Anorthite Kaolinite
end

```

Beginning of initial solution calculations.

Initial solution 2. Glacial Meltwater (Open-System Weathering)

-----Solution composition-----
--

Elements	Molality	Moles
C	1.400e-06	1.400e-06
Ca	2.994e-07	2.994e-07
N(5)	1.856e-06	1.856e-06
Na	3.045e-06	3.045e-06
S(6)	1.426e-06	1.426e-06

-----Description of solution-----
--

```

pH = 5.600
pe = 4.000
Activity of water = 1.000
Ionic strength (mol/kgw) = 7.228e-06
Mass of water (kg) = 1.000e+00
Total alkalinity (eq/kg) = -2.385e-06
Total CO2 (mol/kg) = 1.400e-06
Temperature (°C) = 0.10
Electrical balance (eq) = 1.320e-06
Percent error, 100*(Cat-|An|)/(Cat+|An|) = 12.00
Iterations = 5
Total H = 1.110124e+02
Total O = 5.550623e+01

```

-----Distribution of species-----
--

mole V Species cm ³ /mol	Molality	Activity	Log	Log	Log
			Molality	Activity	Gamma

H+	2.519e-06	2.512e-06	-5.599	-5.600	-0.001
0.00					
OH-	4.608e-10	4.594e-10	-9.336	-9.338	-0.001
(0)					
H2O	5.551e+01	1.000e+00	1.744	-0.000	0.000
18.02					
C(-4)	0.000e+00				
CH4	0.000e+00	0.000e+00	-54.754	-54.754	0.000
(0)					
C(4)	1.400e-06				
CO2	1.266e-06	1.266e-06	-5.898	-5.898	0.000
(0)					
HCO3-	1.338e-07	1.334e-07	-6.873	-6.875	-0.001
(0)					
CO3-2	1.269e-12	1.254e-12	-11.896	-11.902	-0.005
(0)					
CaHCO3+	2.625e-13	2.617e-13	-12.581	-12.582	-0.001
(0)					
NaHCO3	2.278e-13	2.278e-13	-12.642	-12.642	0.000
(0)					
CaCO3	5.049e-16	5.049e-16	-15.297	-15.297	0.000
(0)					
NaCO3-	1.806e-17	1.800e-17	-16.743	-16.745	-0.001
(0)					
Ca	2.994e-07				
Ca+2	2.993e-07	2.957e-07	-6.524	-6.529	-0.005
(0)					
CaSO4	6.449e-11	6.449e-11	-10.190	-10.190	0.000
(0)					
CaHCO3+	2.625e-13	2.617e-13	-12.581	-12.582	-0.001
(0)					
CaOH+	1.960e-14	1.954e-14	-13.708	-13.709	-0.001
(0)					
CaHSO4+	7.583e-16	7.560e-16	-15.120	-15.121	-0.001
(0)					
CaCO3	5.049e-16	5.049e-16	-15.297	-15.297	0.000
(0)					
H(0)	1.171e-22				
H2	5.854e-23	5.854e-23	-22.233	-22.233	0.000
(0)					
N(5)	1.856e-06				
NO3-	1.856e-06	1.851e-06	-5.731	-5.733	-0.001
(0)					
Na	3.045e-06				
Na+	3.045e-06	3.036e-06	-5.516	-5.518	-0.001
(0)					
NaSO4-	1.810e-11	1.804e-11	-10.742	-10.744	-0.001
(0)					
NaHCO3	2.278e-13	2.278e-13	-12.642	-12.642	0.000
(0)					
NaCO3-	1.806e-17	1.800e-17	-16.743	-16.745	-0.001
(0)					
O(0)	0.000e+00				
O2	0.000e+00	0.000e+00	-56.683	-56.683	0.000
(0)					
S(6)	1.426e-06				

SO4-2	1.426e-06	1.409e-06	-5.846	-5.851	-0.005
(0)					
HSO4-	2.133e-10	2.126e-10	-9.671	-9.672	-0.001
(0)					
CaSO4	6.449e-11	6.449e-11	-10.190	-10.190	0.000
(0)					
NaSO4-	1.810e-11	1.804e-11	-10.742	-10.744	-0.001
(0)					
CaHSO4+	7.583e-16	7.560e-16	-15.120	-15.121	-0.001
(0)					

-----Saturation indices-----
--

Phase	SI**	log IAP	log K(273 K,	1 atm)	
Anhydrite	-8.01	-12.38	-4.37	CaSO4	
Aragonite	-10.21	-18.43	-8.22	CaCO3	
Calcite	-10.05	-18.43	-8.38	CaCO3	
CH4 (g)	-52.12	-54.75	-2.63	CH4	
CO2 (g)	-4.79	-5.90	-1.11	CO2	
Gypsum	-7.76	-12.38	-4.62	CaSO4:2H2O	
H2 (g)	-19.20	-22.23	-3.03	H2	
H2O (g)	-2.21	-0.00	2.21	H2O	
Mirabilite	-14.50	-16.89	-2.38	Na2SO4:10H2O	
Nahcolite	-11.60	-12.39	-0.80	NaHCO3	
Natron	-20.57	-22.94	-2.36	Na2CO3:10H2O	
O2 (g)	-54.02	-56.68	-2.66	O2	
Portlandite	-20.20	4.67	24.87	Ca (OH) 2	
Thenardite	-16.75	-16.89	-0.14	Na2SO4	
Thermonatrite	-23.25	-22.94	0.31	Na2CO3:H2O	
Trona	-35.74	-35.33	0.41	NaHCO3:Na2CO3:2H2O	

**For a gas, SI = log10(fugacity). Fugacity = pressure * phi / 1 atm.
For ideal gases, phi = 1.

Beginning of batch-reaction calculations.

Reaction step 1.

Using solution 2. Glacial Meltwater (Open-System Weathering)
Using pure phase assemblage 1.

-----Phase assemblage-----
--

Phase	SI	log IAP	log K(T, P)	Moles in assemblage		Delta
				Initial	Final	
Albite	0.00	-19.73	-19.73	1.000e+01	1.000e+01	-4.853e-04
Anorthite	0.00	-20.49	-20.49	1.000e+01	1.074e-01	-9.893e+00

CO2 (g)	-3.87	-4.98	-1.11	1.000e+01	0	-
1.000e+01						
Kaolinite	-0.00	9.79	9.79	1.000e+01	1.989e+01	
9.893e+00						
O2 (g)	-0.68	-3.34	-2.66	1.000e+01	1.000e+01	-1.618e-04

-----Solution composition-----
--

Elements	Molality	Moles
Al	1.843e-07	1.182e-07
C	1.559e+01	1.000e+01
Ca	1.542e+01	9.893e+00
N	2.893e-06	1.856e-06
Na	7.612e-04	4.884e-04
S	2.223e-06	1.426e-06
Si	1.513e-03	9.707e-04

-----Description of solution-----
--

equilibrium

pH	=	10.643	Charge balance
pe	=	12.363	Adjusted to redox
Activity of water	=	0.725	
Ionic strength (mol/kgw)	=	2.595e+00	
Mass of water (kg)	=	6.416e-01	
Total alkalinity (eq/kg)	=	3.084e+01	
Total CO2 (mol/kg)	=	1.559e+01	
Temperature (°C)	=	0.10	
Electrical balance (eq)	=	1.320e-06	
Percent error, 100*(Cat- An)/(Cat+ An)	=	0.00	
Iterations	=	18	
Total H	=	7.144101e+01	
Total O	=	6.561564e+01	

-----Distribution of species-----
--

mole V Species cm ³ /mol	Molality	Activity	Log		Log Gamma
			Molality	Activity	
OH-	6.990e-05	3.674e-05	-4.156	-4.435	-0.279
(0)					
H+	3.133e-11	2.277e-11	-10.504	-10.643	-0.139
0.00					
H2O	5.551e+01	7.249e-01	1.744	-0.140	0.000
18.02					
Al	1.843e-07				
Al (OH) 4-	1.843e-07	1.071e-07	-6.734	-6.970	-0.236
(0)					
Al (OH) 3	1.130e-12	2.053e-12	-11.947	-11.688	0.259
(0)					

Al(OH) ₂ ⁺	6.231e-15	3.870e-15	-14.205	-14.412	-0.207
(0)					
AlOH ₂ ⁺	1.312e-18	1.953e-19	-17.882	-18.709	-0.827
(0)					
Al ³⁺	6.041e-23	3.419e-24	-22.219	-23.466	-1.247
(0)					
AlSO ₄ ⁺	1.055e-27	6.128e-28	-26.977	-27.213	-0.236
(0)					
Al(SO ₄) ₂ ⁻	2.370e-33	1.377e-33	-32.625	-32.861	-0.236
(0)					
AlHSO ₄ ⁺	5.242e-40	1.088e-39	-39.281	-38.964	0.317
(0)					
C(-4)	0.000e+00				
CH ₄	0.000e+00	0.000e+00	-161.061	-160.801	0.259
(0)					
C(4)	1.559e+01				
CaCO ₃	1.463e+01	2.659e+01	1.165	1.425	0.259
(0)					
CO ₃ ²⁻	6.189e-01	9.214e-02	-0.208	-1.036	-0.827
(0)					
CaHCO ₃ ⁺	1.941e-01	1.250e-01	-0.712	-0.903	-0.191
(0)					
HCO ₃ ⁻	1.431e-01	8.889e-02	-0.844	-1.051	-0.207
(0)					
NaCO ₃ ⁻	2.840e-04	1.764e-04	-3.547	-3.753	-0.207
(0)					
NaHCO ₃	1.113e-05	2.023e-05	-4.953	-4.694	0.259
(0)					
CO ₂	5.804e-06	1.055e-05	-5.236	-4.977	0.259
(0)					
Ca	1.542e+01				
CaCO ₃	1.463e+01	2.659e+01	1.165	1.425	0.259
(0)					
Ca ²⁺	5.932e-01	2.120e-01	-0.227	-0.674	-0.447
(0)					
CaHCO ₃ ⁺	1.941e-01	1.250e-01	-0.712	-0.903	-0.191
(0)					
CaOH ⁺	1.739e-03	1.120e-03	-2.760	-2.951	-0.191
(0)					
CaSO ₄	1.455e-06	2.645e-06	-5.837	-5.578	0.259
(0)					
CaHSO ₄ ⁺	2.342e-16	2.810e-16	-15.630	-15.551	0.079
(0)					
H(0)	0.000e+00				
H ₂	0.000e+00	0.000e+00	-49.304	-49.044	0.259
(0)					
N(-3)	0.000e+00				
NH ₃	0.000e+00	0.000e+00	-78.627	-78.627	0.000
(0)					
NH ₄ ⁺	0.000e+00	0.000e+00	-79.268	-79.189	0.079
(0)					
NH ₄ SO ₄ ⁻	0.000e+00	0.000e+00	-84.954	-85.173	-0.219
(0)					
N(0)	5.896e-35				
N ₂	2.948e-35	5.358e-35	-34.531	-34.271	0.259
(0)					
N(3)	4.955e-21				

NO2-	4.955e-21	5.947e-21	-20.305	-20.226	0.079
(0)					
N(5)	2.893e-06				
NO3-	2.893e-06	1.424e-06	-5.539	-5.846	-0.308
(0)					
Na	7.612e-04				
Na+	4.660e-04	4.048e-04	-3.332	-3.393	-0.061
(0)					
NaCO3-	2.840e-04	1.764e-04	-3.547	-3.753	-0.207
(0)					
NaHCO3	1.113e-05	2.023e-05	-4.953	-4.694	0.259
(0)					
NaSO4-	2.216e-10	1.376e-10	-9.654	-9.861	-0.207
(0)					
O(0)	5.045e-04				
O2	2.522e-04	4.584e-04	-3.598	-3.339	0.259
(0)					
S(-2)	0.000e+00				
S6-2	0.000e+00	0.000e+00	-162.418	-162.798	-0.380
(0)					
S5-2	0.000e+00	0.000e+00	-162.699	-163.133	-0.435
(0)					
S4-2	0.000e+00	0.000e+00	-162.886	-163.394	-0.508
(0)					
HS-	0.000e+00	0.000e+00	-163.280	-163.560	-0.279
(0)					
S-2	0.000e+00	0.000e+00	-165.768	-166.643	-0.875
(0)					
S3-2	0.000e+00	0.000e+00	-166.284	-166.894	-0.610
(0)					
H2S	0.000e+00	0.000e+00	-167.112	-166.853	0.259
(0)					
S2-2	0.000e+00	0.000e+00	-167.488	-168.207	-0.719
(0)					
S(6)	2.223e-06				
CaSO4	1.455e-06	2.645e-06	-5.837	-5.578	0.259
(0)					
SO4-2	7.676e-07	8.060e-08	-6.115	-7.094	-0.979
(0)					
NaSO4-	2.216e-10	1.376e-10	-9.654	-9.861	-0.207
(0)					
CaHSO4+	2.342e-16	2.810e-16	-15.630	-15.551	0.079
(0)					
HSO4-	1.898e-16	1.103e-16	-15.722	-15.957	-0.236
(0)					
AlSO4+	1.055e-27	6.128e-28	-26.977	-27.213	-0.236
(0)					
Al(SO4)2-	2.370e-33	1.377e-33	-32.625	-32.861	-0.236
(0)					
AlHSO4+2	5.242e-40	1.088e-39	-39.281	-38.964	0.317
(0)					
NH4SO4-	0.000e+00	0.000e+00	-84.954	-85.173	-0.219
(0)					
Si	1.513e-03				
H3SiO4-	1.335e-03	7.408e-04	-2.875	-3.130	-0.256
(0)					

H4SiO4	1.758e-04	3.195e-04	-3.755	-3.496	0.259
(0)					
H2SiO4-2	2.260e-06	3.364e-07	-5.646	-6.473	-0.827
(0)					

-----Saturation indices-----
--

Phase	SI**	log IAP	log K(273 K,	1 atm)	
Al (OH) 3 (a)	-4.53	8.04	12.57		Al (OH) 3
Albite	0.00	-19.73	-19.73		NaAlSi3O8
Analcime	-2.74	-16.66	-13.92		NaAlSi2O6:H2O
Anhydrite	-3.40	-7.77	-4.37		CaSO4
Anorthite	0.00	-20.49	-20.49		CaAl2Si2O8
Aragonite	6.51	-1.71	-8.22		CaCO3
Basaluminite	-18.63	4.07	22.70		Al4 (OH) 10SO4
Boehmite	-2.28	8.18	10.47		AlOOH
Calcite	6.67	-1.71	-8.38		CaCO3
CH4 (g)	-158.17	-160.80	-2.63		CH4
Chalcedony	0.65	-3.22	-3.87		SiO2
CO2 (g)	-3.87	-4.98	-1.11		CO2
Cristobalite	0.74	-3.22	-3.95		SiO2
Diaspore	-0.35	8.18	8.53		AlOOH
Gibbsite	-1.59	8.04	9.63		Al (OH) 3
Gypsum	-3.43	-8.05	-4.62		CaSO4:2H2O
H2 (g)	-46.01	-49.04	-3.03		H2
H2O (g)	-2.35	-0.14	2.21		H2O
H2S (g)	-166.16	-166.85	-0.69		H2S
Halloysite	-5.37	9.79	15.16		Al2Si2O5 (OH) 4
Jurbanite	-16.83	-20.06	-3.23		AlOHSO4
Kaolinite	-0.00	9.79	9.79		Al2Si2O5 (OH) 4
Laumontite	6.13	-27.48	-33.61		CaAl2Si4O12:4H2O
Leonhardite	20.95	-54.82	-75.77		Ca2Al4Si8O24:7H2O
Magadiite	-1.66	-15.96	-14.30		NaSi7O13 (OH) 3:3H2O
Mirabilite	-12.89	-15.28	-2.38		Na2SO4:10H2O
Montmorillonite-Ca	0.14	-48.79	-48.93		Ca0.165Al2.33Si3.67O10 (OH) 2
N2 (g)	-31.10	-34.27	-3.17		N2
Nahcolite	-3.65	-4.44	-0.80		NaHCO3
Natron	-6.86	-9.22	-2.36		Na2CO3:10H2O
NH3 (g)	-80.94	-78.63	2.32		NH3
O2 (g)	-0.68	-3.34	-2.66		O2
Portlandite	-4.54	20.33	24.87		Ca (OH) 2
Prehnite	9.02	-3.37	-12.39		Ca2Al2Si3O10 (OH) 2
Pyrophyllite	0.78	-47.53	-48.31		Al2Si4O10 (OH) 2
Quartz	1.16	-3.22	-4.38		SiO2
Silicagel	0.10	-3.22	-3.31		SiO2
SiO2 (a)	-0.28	-3.22	-2.94		SiO2
Sulfur	-126.36	-141.92	-15.55		S
Thenardite	-13.74	-13.88	-0.14		Na2SO4
Thermonatrite	-8.27	-7.96	0.31		Na2CO3:H2O
Trona	-12.95	-12.54	0.41		NaHCO3:Na2CO3:2H2O
Wairakite	1.25	-27.20	-28.45		CaAl2Si4O12:2H2O

**For a gas, SI = log10(fugacity). Fugacity = pressure * phi / 1 atm.
For ideal gases, phi = 1.

End of simulation.

Reading input data for simulation 3.

SOLUTION 3 North Basin (Closed-System)

```
temp      1
pH        10.6
pe        3
units     ppm
density   1
Al        0.0787
Br        0.035
C         0.3
Ca        46
Cl        38.6
F         0.15
K         3.5
Mg        0.15
N(3)     0.19
N(5)     0.5
Na        62
O(0)     20.5
S(6)     166
Si        2.25
Sr        0.0181
Ba        0.001
water     1 # kg
EQUILIBRIUM_PHASES 1
Albite    0 10
Anorthite 0 10
Kaolinite 0 10
SELECTED_OUTPUT 3
file      selected_output_weathering3.sel
totals    Na Mg K Ca S(6) C
molalities Ca+2 Na+ S6-2 K+
           Mg+2 CO2 CO3-2 HCO3-
equilibrium_phases Albite Anorthite Kaolinite
end
```

Beginning of initial solution calculations.

Initial solution 3. North Basin (Closed-System)

-----Solution composition-----

--

Elements	Molality	Moles
Al	2.918e-06	2.918e-06
Ba	7.284e-09	7.284e-09
Br	4.382e-07	4.382e-07
C	4.918e-06	4.918e-06

Ca	1.148e-03	1.148e-03
Cl	1.089e-03	1.089e-03
F	7.898e-06	7.898e-06
K	8.954e-05	8.954e-05
Mg	6.172e-06	6.172e-06
N(3)	1.357e-05	1.357e-05
N(5)	3.571e-05	3.571e-05
Na	2.698e-03	2.698e-03
O(0)	1.282e-03	1.282e-03
S(6)	1.729e-03	1.729e-03
Si	3.746e-05	3.746e-05
Sr	2.066e-07	2.066e-07

-----Description of solution-----

--

pH = 10.600
pe = 3.000
Activity of water = 1.000
Ionic strength (mol/kgw) = 7.229e-03
Mass of water (kg) = 1.000e+00
Total alkalinity (eq/kg) = 1.065e-04
Total CO2 (mol/kg) = 4.918e-06
Temperature (°C) = 1.00
Electrical balance (eq) = 3.945e-04
Percent error, 100*(Cat-|An|)/(Cat+|An|) = 4.27
Iterations = 6
Total H = 1.110126e+02
Total O = 5.551478e+01

-----Redox couples-----

--

Redox couple	pe	Eh (volts)
N(3)/N(5)	5.2986	0.2882
O(-2)/O(0)	12.2842	0.6682

-----Distribution of species-----

--

mole V Species cm ³ /mol	Molality	Activity	Log		Log Gamma
			Molality	Activity	
OH-	5.481e-05	5.021e-05	-4.261	-4.299	-0.038
(0)					
H+	2.713e-11	2.512e-11	-10.567	-10.600	-0.033
0.00					
H2O	5.551e+01	9.999e-01	1.744	-0.000	0.000
18.02					
Al	2.918e-06				
Al(OH)4-	2.918e-06	2.678e-06	-5.535	-5.572	-0.037
(0)					
Al(OH)3	4.112e-11	4.119e-11	-10.386	-10.385	0.001
(0)					

Al (OH) 2+	6.156e-14	5.662e-14	-13.211	-13.247	-0.036
(0)					
AlOH+2	2.874e-18	2.056e-18	-17.541	-17.687	-0.145
(0)					
AlF2+	5.686e-21	5.229e-21	-20.245	-20.282	-0.036
(0)					
AlF+2	2.321e-21	1.660e-21	-20.634	-20.780	-0.145
(0)					
AlF3	4.608e-22	4.615e-22	-21.337	-21.336	0.001
(0)					
AlSO4+	7.490e-23	6.876e-23	-22.126	-22.163	-0.037
(0)					
Al+3	5.397e-23	2.697e-23	-22.268	-22.569	-0.301
(0)					
Al (SO4) 2-	2.373e-24	2.178e-24	-23.625	-23.662	-0.037
(0)					
AlF4-	1.433e-24	1.315e-24	-23.844	-23.881	-0.037
(0)					
AlHSO4+2	1.903e-34	1.348e-34	-33.721	-33.870	-0.150
(0)					
Ba	7.284e-09				
Ba+2	5.185e-09	3.697e-09	-8.285	-8.432	-0.147
(0)					
BaSO4	2.092e-09	2.095e-09	-8.679	-8.679	0.001
(0)					
BaOH+	5.427e-12	4.987e-12	-11.265	-11.302	-0.037
(0)					
BaCO3	1.645e-12	1.647e-12	-11.784	-11.783	0.001
(0)					
BaHCO3+	2.613e-14	2.397e-14	-13.583	-13.620	-0.037
(0)					
Br	4.382e-07				
Br-	4.382e-07	4.020e-07	-6.358	-6.396	-0.037
(0)					
C (-4)	0.000e+00				
CH4	0.000e+00	0.000e+00	-90.868	-90.867	0.001
(0)					
C (4)	4.918e-06				
CO3-2	1.952e-06	1.397e-06	-5.709	-5.855	-0.145
(0)					
HCO3-	1.565e-06	1.439e-06	-5.805	-5.842	-0.036
(0)					
CaCO3	1.368e-06	1.371e-06	-5.864	-5.863	0.001
(0)					
NaCO3-	1.869e-08	1.719e-08	-7.728	-7.765	-0.036
(0)					
CaHCO3+	7.789e-09	7.172e-09	-8.108	-8.144	-0.036
(0)					
MgCO3	3.681e-09	3.687e-09	-8.434	-8.433	0.001
(0)					
NaHCO3	1.992e-09	1.995e-09	-8.701	-8.700	0.001
(0)					
CO2	1.327e-10	1.329e-10	-9.877	-9.876	0.001
(0)					
MgHCO3+	7.055e-11	6.469e-11	-10.152	-10.189	-0.038
(0)					

SrCO3	5.809e-11	5.809e-11	-10.236	-10.236	0.000
(0)					
BaCO3	1.645e-12	1.647e-12	-11.784	-11.783	0.001
(0)					
SrHCO3+	1.394e-12	1.282e-12	-11.856	-11.892	-0.036
(0)					
BaHCO3+	2.613e-14	2.397e-14	-13.583	-13.620	-0.037
(0)					
Ca	1.148e-03				
Ca+2	1.014e-03	7.247e-04	-2.994	-3.140	-0.146
(0)					
CaSO4	1.279e-04	1.281e-04	-3.893	-3.892	0.001
(0)					
CaOH+	5.200e-06	4.788e-06	-5.284	-5.320	-0.036
(0)					
CaCO3	1.368e-06	1.371e-06	-5.864	-5.863	0.001
(0)					
CaF+	2.688e-08	2.472e-08	-7.571	-7.607	-0.036
(0)					
CaHCO3+	7.789e-09	7.172e-09	-8.108	-8.144	-0.036
(0)					
CaHSO4+	1.645e-14	1.510e-14	-13.784	-13.821	-0.037
(0)					
Cl	1.089e-03				
Cl-	1.089e-03	9.979e-04	-2.963	-3.001	-0.038
(0)					
F	7.898e-06				
F-	7.860e-06	7.199e-06	-5.105	-5.143	-0.038
(0)					
CaF+	2.688e-08	2.472e-08	-7.571	-7.607	-0.036
(0)					
NaF	1.020e-08	1.021e-08	-7.992	-7.991	0.001
(0)					
MgF+	1.292e-09	1.186e-09	-8.889	-8.926	-0.037
(0)					
HF	1.799e-13	1.802e-13	-12.745	-12.744	0.001
(0)					
HF2-	4.176e-18	3.825e-18	-17.379	-17.417	-0.038
(0)					
AlF2+	5.686e-21	5.229e-21	-20.245	-20.282	-0.036
(0)					
AlF+2	2.321e-21	1.660e-21	-20.634	-20.780	-0.145
(0)					
AlF3	4.608e-22	4.615e-22	-21.337	-21.336	0.001
(0)					
AlF4-	1.433e-24	1.315e-24	-23.844	-23.881	-0.037
(0)					
H2F2	1.914e-25	1.917e-25	-24.718	-24.717	0.001
(0)					
SiF6-2	0.000e+00	0.000e+00	-46.843	-46.990	-0.147
(0)					
H(0)	1.157e-30				
H2	5.783e-31	5.793e-31	-30.238	-30.237	0.001
(0)					
K	8.954e-05				
K+	8.909e-05	8.163e-05	-4.050	-4.088	-0.038
(0)					

KSO4-	4.472e-07	4.113e-07	-6.349	-6.386	-0.036
(0)					
Mg	6.172e-06				
Mg+2	5.567e-06	3.999e-06	-5.254	-5.398	-0.144
(0)					
MgSO4	5.403e-07	5.412e-07	-6.267	-6.267	0.001
(0)					
MgOH+	5.939e-08	5.474e-08	-7.226	-7.262	-0.035
(0)					
MgCO3	3.681e-09	3.687e-09	-8.434	-8.433	0.001
(0)					
MgF+	1.292e-09	1.186e-09	-8.889	-8.926	-0.037
(0)					
MgHCO3+	7.055e-11	6.469e-11	-10.152	-10.189	-0.038
(0)					
N (3)	1.357e-05				
NO2-	1.357e-05	1.245e-05	-4.867	-4.905	-0.037
(0)					
N (5)	3.571e-05				
NO3-	3.571e-05	3.267e-05	-4.447	-4.486	-0.039
(0)					
Na	2.698e-03				
Na+	2.685e-03	2.465e-03	-2.571	-2.608	-0.037
(0)					
NaSO4-	1.287e-05	1.184e-05	-4.890	-4.927	-0.036
(0)					
NaCO3-	1.869e-08	1.719e-08	-7.728	-7.765	-0.036
(0)					
NaF	1.020e-08	1.021e-08	-7.992	-7.991	0.001
(0)					
NaHCO3	1.992e-09	1.995e-09	-8.701	-8.700	0.001
(0)					
O (0)	1.282e-03				
O2	6.408e-04	6.419e-04	-3.193	-3.193	0.001
(0)					
S (6)	1.729e-03				
SO4-2	1.587e-03	1.131e-03	-2.799	-2.947	-0.147
(0)					
CaSO4	1.279e-04	1.281e-04	-3.893	-3.892	0.001
(0)					
NaSO4-	1.287e-05	1.184e-05	-4.890	-4.927	-0.036
(0)					
MgSO4	5.403e-07	5.412e-07	-6.267	-6.267	0.001
(0)					
KSO4-	4.472e-07	4.113e-07	-6.349	-6.386	-0.036
(0)					
SrSO4	2.143e-08	2.146e-08	-7.669	-7.668	0.001
(0)					
BaSO4	2.092e-09	2.095e-09	-8.679	-8.679	0.001
(0)					
HSO4-	1.887e-12	1.732e-12	-11.724	-11.761	-0.037
(0)					
CaHSO4+	1.645e-14	1.510e-14	-13.784	-13.821	-0.037
(0)					
AlSO4+	7.490e-23	6.876e-23	-22.126	-22.163	-0.037
(0)					

Al (SO4)2-	2.373e-24	2.178e-24	-23.625	-23.662	-0.037
(0)					
AlHSO4+2	1.903e-34	1.348e-34	-33.721	-33.870	-0.150
(0)					
Si	3.746e-05				
H3SiO4-	2.643e-05	2.423e-05	-4.578	-4.616	-0.038
(0)					
H4SiO4	1.102e-05	1.104e-05	-4.958	-4.957	0.001
(0)					
H2SiO4-2	1.508e-08	1.079e-08	-7.822	-7.967	-0.145
(0)					
SiF6-2	0.000e+00	0.000e+00	-46.843	-46.990	-0.147
(0)					
Sr	2.066e-07				
Sr+2	1.849e-07	1.324e-07	-6.733	-6.878	-0.145
(0)					
SrSO4	2.143e-08	2.146e-08	-7.669	-7.668	0.001
(0)					
SrOH+	2.941e-10	2.702e-10	-9.532	-9.568	-0.037
(0)					
SrCO3	5.809e-11	5.809e-11	-10.236	-10.236	0.000
(0)					
SrHCO3+	1.394e-12	1.282e-12	-11.856	-11.892	-0.036
(0)					

-----Saturation indices-----
--

Phase	SI**	log IAP	log K(274 K, 1 atm)	
Adularia	-1.98	-24.53	-22.55	KAlSi3O8
Al (OH)3 (a)	-3.27	9.23	12.50	Al (OH)3
Albite	-3.39	-23.05	-19.66	NaAlSi3O8
AlumK	-26.92	-32.55	-5.63	KAl (SO4)2:12H2O
Alunite	-15.91	-14.09	1.82	KAl3 (SO4)2 (OH)6
Analcime	-4.23	-18.09	-13.87	NaAlSi2O6:H2O
Anhydrite	-1.73	-6.09	-4.36	CaSO4
Anorthite	-3.74	-24.20	-20.46	CaAl2Si2O8
Aragonite	-0.77	-8.99	-8.22	CaCO3
Artinite	-6.90	4.55	11.44	MgCO3:Mg (OH)2:3H2O
BaF2	-12.89	-18.72	-5.82	BaF2
Barite	-0.92	-11.38	-10.45	BaSO4
Basaluminite	-9.92	12.78	22.70	Al4 (OH)10SO4
Beidellite	-4.26	-53.41	-49.14	
(NaKMg0.5)0.11Al2.33Si3.67O10 (OH)2				
Boehmite	-1.16	9.23	10.39	AlOOH
Brucite	-2.78	15.80	18.58	Mg (OH)2
Calcite	-0.61	-8.99	-8.38	CaCO3
Celestite	-3.13	-9.82	-6.69	SrSO4
CH4 (g)	-88.22	-90.87	-2.64	CH4
Chalcedony	-1.10	-4.96	-3.85	SiO2
Chlorite14A	4.50	82.60	78.10	Mg5Al2Si3O10 (OH)8
Chlorite7A	0.89	82.60	81.71	Mg5Al2Si3O10 (OH)8
Chrysotile	2.06	37.49	35.43	Mg3Si2O5 (OH)4
Clinoenstatite	-1.78	10.84	12.63	MgSiO3
CO2 (g)	-8.75	-9.88	-1.13	CO2
Cristobalite	-1.02	-4.96	-3.94	SiO2

Diaspore	0.77	9.23	8.46	AlOOH
Diopside	1.98	23.95	21.97	CaMgSi2O6
Dolomite	-3.76	-20.25	-16.48	CaMg (CO3) 2
Dolomite (d)	-4.42	-20.25	-15.83	CaMg (CO3) 2
Epsomite	-6.02	-8.35	-2.32	MgSO4:7H2O
Fluorite	-2.48	-13.43	-10.94	CaF2
Forsterite	-4.78	26.65	31.42	Mg2SiO4
Gibbsite	-0.34	9.23	9.57	Al (OH) 3
Gypsum	-1.47	-6.09	-4.61	CaSO4:2H2O
H2 (g)	-27.20	-30.24	-3.04	H2
H2O (g)	-2.19	-0.00	2.19	H2O
Halite	-7.13	-5.61	1.52	NaCl
Halloysite	-6.51	8.55	15.06	Al2Si2O5 (OH) 4
Huntite	-14.44	-42.75	-28.32	CaMg3 (CO3) 4
Hydromagnesite	-23.80	-29.21	-5.41	Mg5 (CO3) 4 (OH) 2:4H2O
Illite	-2.91	-46.69	-43.78	K0.6Mg0.25Al2.3Si3.5O10 (OH) 2
Jurbanite	-11.69	-14.92	-3.23	AlOHSO4
Kaolinite	-1.15	8.55	9.70	Al2Si2O5 (OH) 4
Kmica	2.82	19.33	16.51	KAl3Si3O10 (OH) 2
Laumontite	-0.61	-34.11	-33.50	CaAl2Si4O12:4H2O
Leonhardite	7.31	-68.22	-75.54	Ca2Al4Si8O24:7H2O
Magadiite	-12.41	-26.71	-14.30	NaSi7O13 (OH) 3:3H2O
Magnesite	-3.62	-11.25	-7.63	MgCO3
Mirabilite	-5.83	-8.16	-2.33	Na2SO4:10H2O
Montmorillonite-Ca	-4.12	-52.89	-48.77	Ca0.165Al2.33Si3.67O10 (OH) 2
Nahcolite	-7.66	-8.45	-0.79	NaHCO3
Natron	-8.75	-11.07	-2.32	Na2CO3:10H2O
Nesquehonite	-6.00	-11.25	-5.25	MgCO3:3H2O
O2 (g)	-0.52	-3.19	-2.67	O2
Phillipsite	-3.92	-23.79	-19.87	Na0.5K0.5AlSi3O8:H2O
Phlogopite	2.26	48.28	46.01	KMg3AlSi3O10 (OH) 2
Portlandite	-6.73	18.06	24.79	Ca (OH) 2
Prehnite	1.27	-11.09	-12.36	Ca2Al2Si3O10 (OH) 2
Pyrophyllite	-3.86	-52.17	-48.31	Al2Si4O10 (OH) 2
Quartz	-0.59	-4.96	-4.36	SiO2
Sepiolite	0.29	16.73	16.45	Mg2Si3O7.5OH:3H2O
Sepiolite (d)	-1.93	16.73	18.66	Mg2Si3O7.5OH:3H2O
Silicagel	-1.65	-4.96	-3.30	SiO2
SiO2 (a)	-2.03	-4.96	-2.93	SiO2
SrF2	-8.54	-17.16	-8.62	SrF2
Strontianite	-3.40	-12.73	-9.33	SrCO3
Talc	3.20	27.58	24.37	Mg3Si4O10 (OH) 2
Thenardite	-8.02	-8.16	-0.14	Na2SO4
Thermonatrite	-11.38	-11.07	0.30	Na2CO3:H2O
Tremolite	12.68	75.47	62.79	Ca2Mg5Si8O22 (OH) 2
Trona	-19.88	-19.52	0.36	NaHCO3:Na2CO3:2H2O
Wairakite	-5.73	-34.11	-28.39	CaAl2Si4O12:2H2O
Witherite	-5.56	-14.29	-8.72	BaCO3

**For a gas, SI = log10(fugacity). Fugacity = pressure * phi / 1 atm.
For ideal gases, phi = 1.

Beginning of batch-reaction calculations.

Reaction step 1.

Using solution 3. North Basin (Closed-System)
 Using pure phase assemblage 1.

-----Phase assemblage-----
 --

Phase	SI	log IAP	log K(T, P)	Moles in assemblage		
				Initial	Final	
Delta						
Albite	-0.00	-19.66	-19.66	1.000e+01	9.999e+00	-1.131e-03
Anorthite	-0.00	-20.46	-20.46	1.000e+01	9.999e+00	-1.037e-03
Kaolinite	-0.00	9.70	9.70	1.000e+01	1.000e+01	1.589e-03

-----Solution composition-----
 --

Elements	Molality	Moles
Al	3.032e-05	3.032e-05
Ba	7.285e-09	7.284e-09
Br	4.382e-07	4.382e-07
C	4.919e-06	4.918e-06
Ca	2.185e-03	2.185e-03
Cl	1.089e-03	1.089e-03
F	7.899e-06	7.898e-06
K	8.955e-05	8.954e-05
Mg	6.173e-06	6.172e-06
N	4.929e-05	4.928e-05
Na	3.829e-03	3.829e-03
S	1.729e-03	1.729e-03
Si	2.327e-03	2.327e-03
Sr	2.067e-07	2.066e-07

-----Description of solution-----
 --

equilibrium

	pH =	11.777	Charge balance
	pe =	11.106	Adjusted to redox
	Activity of water =	1.000	
	Ionic strength (mol/kgw) =	1.095e-02	
	Mass of water (kg) =	9.999e-01	
	Total alkalinity (eq/kg) =	3.394e-03	
	Total CO2 (mol/kg) =	4.919e-06	
	Temperature (°C) =	1.00	
	Electrical balance (eq) =	3.945e-04	
	Percent error, 100*(Cat- An)/(Cat+ An) =	2.61	
	Iterations =	20	
	Total H =	1.110063e+02	
	Total O =	5.551783e+01	

-----Distribution of species-----

--

mole V Species cm ³ /mol	Molality	Activity	Log		Log Gamma
			Molality	Activity	
OH-	8.397e-04	7.554e-04	-3.076	-3.122	-0.046
(0)					
H+	1.828e-12	1.669e-12	-11.738	-11.777	-0.039
0.00					
H2O	5.551e+01	9.998e-01	1.744	-0.000	0.000
18.02					
Al	3.032e-05				
Al (OH) 4-	3.032e-05	2.736e-05	-4.518	-4.563	-0.045
(0)					
Al (OH) 3	2.790e-11	2.797e-11	-10.554	-10.553	0.001
(0)					
Al (OH) 2+	2.824e-15	2.555e-15	-14.549	-14.593	-0.043
(0)					
AlOH+2	9.205e-21	6.168e-21	-20.036	-20.210	-0.174
(0)					
AlF2+	1.105e-24	1.000e-24	-23.956	-24.000	-0.043
(0)					
AlF+2	4.838e-25	3.242e-25	-24.315	-24.489	-0.174
(0)					
AlF3	8.624e-26	8.645e-26	-25.064	-25.063	0.001
(0)					
AlSO4+	1.358e-26	1.225e-26	-25.867	-25.912	-0.045
(0)					
Al+3	1.216e-26	5.378e-27	-25.915	-26.269	-0.354
(0)					
Al (SO4) 2-	3.843e-28	3.468e-28	-27.415	-27.460	-0.045
(0)					
AlF4-	2.674e-28	2.413e-28	-27.573	-27.618	-0.045
(0)					
AlHSO4+2	2.414e-39	1.596e-39	-38.617	-38.797	-0.180
(0)					
Ba	7.285e-09				
Ba+2	5.387e-09	3.593e-09	-8.269	-8.444	-0.176
(0)					
BaSO4	1.815e-09	1.820e-09	-8.741	-8.740	0.001
(0)					
BaOH+	8.069e-11	7.292e-11	-10.093	-10.137	-0.044
(0)					
BaCO3	1.723e-12	1.727e-12	-11.764	-11.763	0.001
(0)					
BaHCO3+	1.852e-15	1.670e-15	-14.732	-14.777	-0.045
(0)					
Br	4.382e-07				
Br-	4.382e-07	3.951e-07	-6.358	-6.403	-0.045
(0)					
C(-4)	0.000e+00				
CH4	0.000e+00	0.000e+00	-167.455	-167.454	0.001
(0)					
C(4)	4.919e-06				

CaCO3	2.524e-06	2.530e-06	-5.598	-5.597	0.001
(0)					
CO3-2	2.248e-06	1.507e-06	-5.648	-5.822	-0.174
(0)					
HCO3-	1.141e-07	1.032e-07	-6.943	-6.986	-0.043
(0)					
NaCO3-	2.861e-08	2.589e-08	-7.543	-7.587	-0.043
(0)					
MgCO3	3.342e-09	3.351e-09	-8.476	-8.475	0.001
(0)					
CaHCO3+	9.708e-10	8.798e-10	-9.013	-9.056	-0.043
(0)					
NaHCO3	1.992e-10	1.997e-10	-9.701	-9.700	0.001
(0)					
SrCO3	5.862e-11	5.862e-11	-10.232	-10.232	0.000
(0)					
MgHCO3+	4.337e-12	3.908e-12	-11.363	-11.408	-0.045
(0)					
BaCO3	1.723e-12	1.727e-12	-11.764	-11.763	0.001
(0)					
CO2	6.317e-13	6.333e-13	-12.199	-12.198	0.001
(0)					
SrHCO3+	9.500e-14	8.595e-14	-13.022	-13.066	-0.043
(0)					
BaHCO3+	1.852e-15	1.670e-15	-14.732	-14.777	-0.045
(0)					
Ca	2.185e-03				
Ca+2	1.851e-03	1.240e-03	-2.733	-2.907	-0.174
(0)					
CaSO4	1.954e-04	1.959e-04	-3.709	-3.708	0.001
(0)					
CaOH+	1.360e-04	1.233e-04	-3.866	-3.909	-0.043
(0)					
CaCO3	2.524e-06	2.530e-06	-5.598	-5.597	0.001
(0)					
CaF+	4.578e-08	4.143e-08	-7.339	-7.383	-0.043
(0)					
CaHCO3+	9.708e-10	8.798e-10	-9.013	-9.056	-0.043
(0)					
CaHSO4+	1.701e-15	1.534e-15	-14.769	-14.814	-0.045
(0)					
Cl	1.089e-03				
Cl-	1.089e-03	9.803e-04	-2.963	-3.009	-0.046
(0)					
F	7.899e-06				
F-	7.838e-06	7.051e-06	-5.106	-5.152	-0.046
(0)					
CaF+	4.578e-08	4.143e-08	-7.339	-7.383	-0.043
(0)					
NaF	1.393e-08	1.397e-08	-7.856	-7.855	0.001
(0)					
MgF+	1.084e-09	9.784e-10	-8.965	-9.009	-0.045
(0)					
HF	1.170e-14	1.173e-14	-13.932	-13.931	0.001
(0)					
HF2-	2.711e-19	2.438e-19	-18.567	-18.613	-0.046
(0)					

AlF2+	1.105e-24	1.000e-24	-23.956	-24.000	-0.043
(0)					
AlF+2	4.838e-25	3.242e-25	-24.315	-24.489	-0.174
(0)					
AlF3	8.624e-26	8.645e-26	-25.064	-25.063	0.001
(0)					
H2F2	8.101e-28	8.122e-28	-27.091	-27.090	0.001
(0)					
AlF4-	2.674e-28	2.413e-28	-27.573	-27.618	-0.045
(0)					
SiF6-2	0.000e+00	0.000e+00	-50.833	-51.009	-0.176
(0)					
H(0)	0.000e+00				
H2	0.000e+00	0.000e+00	-48.805	-48.803	0.001
(0)					
K	8.955e-05				
K+	8.915e-05	8.023e-05	-4.050	-4.096	-0.046
(0)					
KSO4-	3.992e-07	3.612e-07	-6.399	-6.442	-0.043
(0)					
Mg	6.173e-06				
Mg+2	4.997e-06	3.370e-06	-5.301	-5.472	-0.171
(0)					
MgOH+	7.646e-07	6.939e-07	-6.117	-6.159	-0.042
(0)					
MgSO4	4.065e-07	4.075e-07	-6.391	-6.390	0.001
(0)					
MgCO3	3.342e-09	3.351e-09	-8.476	-8.475	0.001
(0)					
MgF+	1.084e-09	9.784e-10	-8.965	-9.009	-0.045
(0)					
MgHCO3+	4.337e-12	3.908e-12	-11.363	-11.408	-0.045
(0)					
N(-3)	0.000e+00				
NH3	0.000e+00	0.000e+00	-78.164	-78.164	0.000
(0)					
NH4+	0.000e+00	0.000e+00	-79.849	-79.894	-0.045
(0)					
NH4SO4-	0.000e+00	0.000e+00	-81.735	-81.779	-0.044
(0)					
N(0)	2.064e-34				
N2	1.032e-34	1.035e-34	-33.986	-33.985	0.001
(0)					
N(3)	2.008e-19				
NO2-	2.008e-19	1.810e-19	-18.697	-18.742	-0.045
(0)					
N(5)	4.929e-05				
NO3-	4.929e-05	4.426e-05	-4.307	-4.354	-0.047
(0)					
Na	3.829e-03				
Na+	3.813e-03	3.442e-03	-2.419	-2.463	-0.044
(0)					
NaSO4-	1.633e-05	1.477e-05	-4.787	-4.831	-0.043
(0)					
NaCO3-	2.861e-08	2.589e-08	-7.543	-7.587	-0.043
(0)					

NaF	1.393e-08	1.397e-08	-7.856	-7.855	0.001
(0)					
NaHCO3	1.992e-10	1.997e-10	-9.701	-9.700	0.001
(0)					
O(0)	1.268e-03				
O2	6.341e-04	6.357e-04	-3.198	-3.197	0.001
(0)					
S(-2)	0.000e+00				
S6-2	0.000e+00	0.000e+00	-158.291	-158.430	-0.139
(0)					
S5-2	0.000e+00	0.000e+00	-158.595	-158.741	-0.146
(0)					
S4-2	0.000e+00	0.000e+00	-158.847	-159.001	-0.154
(0)					
HS-	0.000e+00	0.000e+00	-160.281	-160.327	-0.046
(0)					
S-2	0.000e+00	0.000e+00	-162.068	-162.244	-0.176
(0)					
S3-2	0.000e+00	0.000e+00	-162.337	-162.498	-0.162
(0)					
S2-2	0.000e+00	0.000e+00	-163.640	-163.809	-0.169
(0)					
H2S	0.000e+00	0.000e+00	-164.773	-164.772	0.001
(0)					
S(6)	1.729e-03				
SO4-2	1.516e-03	1.010e-03	-2.819	-2.995	-0.176
(0)					
CaSO4	1.954e-04	1.959e-04	-3.709	-3.708	0.001
(0)					
NaSO4-	1.633e-05	1.477e-05	-4.787	-4.831	-0.043
(0)					
MgSO4	4.065e-07	4.075e-07	-6.391	-6.390	0.001
(0)					
KSO4-	3.992e-07	3.612e-07	-6.399	-6.442	-0.043
(0)					
SrSO4	1.790e-08	1.794e-08	-7.747	-7.746	0.001
(0)					
BaSO4	1.815e-09	1.820e-09	-8.741	-8.740	0.001
(0)					
HSO4-	1.140e-13	1.029e-13	-12.943	-12.988	-0.045
(0)					
CaHSO4+	1.701e-15	1.534e-15	-14.769	-14.814	-0.045
(0)					
AlSO4+	1.358e-26	1.225e-26	-25.867	-25.912	-0.045
(0)					
Al(SO4)2-	3.843e-28	3.468e-28	-27.415	-27.460	-0.045
(0)					
AlHSO4+2	2.414e-39	1.596e-39	-38.617	-38.797	-0.180
(0)					
NH4SO4-	0.000e+00	0.000e+00	-81.735	-81.779	-0.044
(0)					
Si	2.327e-03				
H3SiO4-	2.246e-03	2.024e-03	-2.649	-2.694	-0.045
(0)					
H4SiO4	6.111e-05	6.126e-05	-4.214	-4.213	0.001
(0)					

(0)	H2SiO4-2	2.022e-05	1.355e-05	-4.694	-4.868	-0.174
(0)	SiF6-2	0.000e+00	0.000e+00	-50.833	-51.009	-0.176
Sr		2.067e-07				
(0)	Sr+2	1.845e-07	1.238e-07	-6.734	-6.907	-0.173
(0)	SrSO4	1.790e-08	1.794e-08	-7.747	-7.746	0.001
(0)	SrOH+	4.208e-09	3.803e-09	-8.376	-8.420	-0.044
(0)	SrCO3	5.862e-11	5.862e-11	-10.232	-10.232	0.000
(0)	SrHCO3+	9.500e-14	8.595e-14	-13.022	-13.066	-0.043

-----Saturation indices-----
--

Phase	SI**	log IAP	log K(274 K, 1 atm)	
Adularia	1.25	-21.30	-22.55	KAlSi3O8
Al(OH)3(a)	-3.44	9.06	12.50	Al(OH)3
Albite	-0.00	-19.66	-19.66	NaAlSi3O8
AlumK	-30.72	-36.36	-5.63	KAl(SO4)2·12H2O
Alunite	-20.06	-18.23	1.82	KAl3(SO4)2(OH)6
Analcime	-1.58	-15.45	-13.87	NaAlSi2O6·H2O
Anhydrite	-1.54	-5.90	-4.36	CaSO4
Anorthite	-0.00	-20.46	-20.46	CaAl2Si2O8
Aragonite	-0.51	-8.73	-8.22	CaCO3
Artinite	-4.66	6.79	11.44	MgCO3:Mg(OH)2:3H2O
BaF2	-12.92	-18.75	-5.82	BaF2
Barite	-0.99	-11.44	-10.45	BaSO4
Basaluminite	-13.00	9.70	22.70	Al4(OH)10SO4
Beidellite	-1.52	-50.67	-49.14	
(NaKMg0.5)0.11Al2.33Si3.67O10(OH)2				
Boehmite	-1.33	9.06	10.39	AlOOH
Brucite	-0.50	18.08	18.58	Mg(OH)2
Calcite	-0.34	-8.73	-8.38	CaCO3
Celestite	-3.21	-9.90	-6.69	SrSO4
CH4(g)	-164.81	-167.45	-2.64	CH4
Chalcedony	-0.36	-4.21	-3.85	SiO2
Chlorite14A	17.80	95.90	78.10	Mg5Al2Si3O10(OH)8
Chlorite7A	14.18	95.90	81.71	Mg5Al2Si3O10(OH)8
Chrysotile	10.40	45.82	35.43	Mg3Si2O5(OH)4
Clinoenstatite	1.24	13.87	12.63	MgSiO3
CO2(g)	-11.07	-12.20	-1.13	CO2
Cristobalite	-0.27	-4.21	-3.94	SiO2
Diaspore	0.60	9.06	8.46	AlOOH
Diopside	8.34	30.31	21.97	CaMgSi2O6
Dolomite	-3.54	-20.02	-16.48	CaMg(CO3)2
Dolomite(d)	-4.19	-20.02	-15.83	CaMg(CO3)2
Epsomite	-6.15	-8.47	-2.32	MgSO4·7H2O
Fluorite	-2.27	-13.21	-10.94	CaF2
Forsterite	0.53	31.95	31.42	Mg2SiO4
Gibbsite	-0.51	9.06	9.57	Al(OH)3
Gypsum	-1.29	-5.90	-4.61	CaSO4·2H2O

H2 (g)	-45.77	-48.80	-3.04	H2
H2O (g)	-2.19	-0.00	2.19	H2O
H2S (g)	-164.07	-164.77	-0.70	H2S
Halite	-6.99	-5.47	1.52	NaCl
Halloysite	-5.36	9.70	15.06	Al2Si2O5 (OH) 4
Huntite	-14.30	-42.61	-28.32	CaMg3 (CO3) 4
Hydromagnesite	-21.69	-27.10	-5.41	Mg5 (CO3) 4 (OH) 2:4H2O
Illite	0.58	-43.20	-43.78	K0.6Mg0.25Al2.3Si3.5O10 (OH) 2
Jurbanite	-14.26	-17.49	-3.23	AlOHSO4
Kaolinite	-0.00	9.70	9.70	Al2Si2O5 (OH) 4
Kmica	5.72	22.23	16.51	KAl3Si3O10 (OH) 2
Laumontite	4.62	-28.88	-33.50	CaAl2Si4O12:4H2O
Leonhardite	17.77	-57.77	-75.54	Ca2Al4Si8O24:7H2O
Magadiite	-5.87	-20.17	-14.30	NaSi7O13 (OH) 3:3H2O
Magnesite	-3.66	-11.29	-7.63	MgCO3
Mirabilite	-5.59	-7.92	-2.33	Na2SO4:10H2O
Montmorillonite-Ca	-1.35	-50.13	-48.77	Ca0.165Al2.33Si3.67O10 (OH) 2
N2 (g)	-30.81	-33.99	-3.17	N2
Nahcolite	-8.66	-9.45	-0.79	NaHCO3
Natron	-8.43	-10.75	-2.32	Na2CO3:10H2O
Nesquehonite	-6.05	-11.29	-5.25	MgCO3:3H2O
NH3 (g)	-80.46	-78.16	2.29	NH3
O2 (g)	-0.53	-3.20	-2.67	O2
Phillipsite	-0.61	-20.48	-19.87	Na0.5K0.5AlSi3O8:H2O
Phlogopite	12.34	58.35	46.01	KMg3AlSi3O10 (OH) 2
Portlandite	-4.14	20.65	24.79	Ca (OH) 2
Prehnite	8.34	-4.02	-12.36	Ca2Al2Si3O10 (OH) 2
Pyrophyllite	-1.22	-49.53	-48.31	Al2Si4O10 (OH) 2
Quartz	0.15	-4.21	-4.36	SiO2
Sepiolite	7.08	23.53	16.45	Mg2Si3O7.5OH:3H2O
Sepiolite (d)	4.87	23.53	18.66	Mg2Si3O7.5OH:3H2O
Silicagel	-0.91	-4.21	-3.30	SiO2
SiO2 (a)	-1.29	-4.21	-2.93	SiO2
SrF2	-8.59	-17.21	-8.62	SrF2
Strontianite	-3.40	-12.73	-9.33	SrCO3
Sulfur	-124.50	-140.03	-15.53	S
Talc	13.02	37.40	24.37	Mg3Si4O10 (OH) 2
Thenardite	-7.78	-7.92	-0.14	Na2SO4
Thermonatrite	-11.05	-10.75	0.30	Na2CO3:H2O
Tremolite	35.22	98.01	62.79	Ca2Mg5Si8O22 (OH) 2
Trona	-20.56	-20.20	0.36	NaHCO3:Na2CO3:2H2O
Wairakite	-0.50	-28.88	-28.39	CaAl2Si4O12:2H2O
Witherite	-5.54	-14.27	-8.72	BaCO3

**For a gas, SI = log10(fugacity). Fugacity = pressure * phi / 1 atm.
For ideal gases, phi = 1.

End of simulation.

Reading input data for simulation 4.

SOLUTION 4 North Basin (Open-System)
temp 1

```

pH          10.6
pe          3
units       ppm
density     1
Al          0.0787
Br          0.035
C           0.3
Ca          46
Cl          38.6
F           0.15
K           3.5
Mg          0.15
N(3)       0.19
N(5)       0.5
Na          62
O(0)       20.5
S(6)       166
Si          2.25
Sr          0.0181
Ba          0.001
water      1 # kg
EQUILIBRIUM_PHASES 4
  Albite    0 10
  Anorthite 0 10
  CO2(g)    -3.43 10
  Kaolinite 0 10
  O2(g)     -0.679 10
SELECTED_OUTPUT 4
  file              selected_output_weathering4.sel
  totals            Na Mg K Ca S(6) C
  molalities        Ca+2 Na+ S6-2 K+
                    Mg+2 CO2 CO3-2 HCO3-
  equilibrium_phases Albite Anorthite Kaolinite
end

```

Beginning of initial solution calculations.

Initial solution 4. North Basin (Open-System)

-----Solution composition-----

--

Elements	Molality	Moles
Al	2.918e-06	2.918e-06
Ba	7.284e-09	7.284e-09
Br	4.382e-07	4.382e-07
C	4.918e-06	4.918e-06
Ca	1.148e-03	1.148e-03
Cl	1.089e-03	1.089e-03
F	7.898e-06	7.898e-06
K	8.954e-05	8.954e-05
Mg	6.172e-06	6.172e-06
N(3)	1.357e-05	1.357e-05
N(5)	3.571e-05	3.571e-05
Na	2.698e-03	2.698e-03

O(0)	1.282e-03	1.282e-03
S(6)	1.729e-03	1.729e-03
Si	3.746e-05	3.746e-05
Sr	2.066e-07	2.066e-07

-----Description of solution-----
--

pH	=	10.600
pe	=	3.000
Activity of water	=	1.000
Ionic strength (mol/kgw)	=	7.229e-03
Mass of water (kg)	=	1.000e+00
Total alkalinity (eq/kg)	=	1.065e-04
Total CO2 (mol/kg)	=	4.918e-06
Temperature (°C)	=	1.00
Electrical balance (eq)	=	3.945e-04
Percent error, 100*(Cat- An)/(Cat+ An)	=	4.27
Iterations	=	6
Total H	=	1.110126e+02
Total O	=	5.551478e+01

-----Redox couples-----
--

Redox couple	pe	Eh (volts)
N(3)/N(5)	5.2986	0.2882
O(-2)/O(0)	12.2842	0.6682

-----Distribution of species-----
--

mole V Species cm ³ /mol	Molality	Activity	Log	Log	Log
			Molality	Activity	Gamma
OH-	5.481e-05	5.021e-05	-4.261	-4.299	-0.038
(0)					
H+	2.713e-11	2.512e-11	-10.567	-10.600	-0.033
0.00					
H2O	5.551e+01	9.999e-01	1.744	-0.000	0.000
18.02					
Al	2.918e-06				
Al(OH)4-	2.918e-06	2.678e-06	-5.535	-5.572	-0.037
(0)					
Al(OH)3	4.112e-11	4.119e-11	-10.386	-10.385	0.001
(0)					
Al(OH)2+	6.156e-14	5.662e-14	-13.211	-13.247	-0.036
(0)					
AlOH+2	2.874e-18	2.056e-18	-17.541	-17.687	-0.145
(0)					
AlF2+	5.686e-21	5.229e-21	-20.245	-20.282	-0.036
(0)					
AlF+2	2.321e-21	1.660e-21	-20.634	-20.780	-0.145
(0)					

AlF3	4.608e-22	4.615e-22	-21.337	-21.336	0.001
(0)					
AlSO4+	7.490e-23	6.876e-23	-22.126	-22.163	-0.037
(0)					
Al+3	5.397e-23	2.697e-23	-22.268	-22.569	-0.301
(0)					
Al (SO4) 2-	2.373e-24	2.178e-24	-23.625	-23.662	-0.037
(0)					
AlF4-	1.433e-24	1.315e-24	-23.844	-23.881	-0.037
(0)					
AlHSO4+2	1.903e-34	1.348e-34	-33.721	-33.870	-0.150
(0)					
Ba	7.284e-09				
Ba+2	5.185e-09	3.697e-09	-8.285	-8.432	-0.147
(0)					
BaSO4	2.092e-09	2.095e-09	-8.679	-8.679	0.001
(0)					
BaOH+	5.427e-12	4.987e-12	-11.265	-11.302	-0.037
(0)					
BaCO3	1.645e-12	1.647e-12	-11.784	-11.783	0.001
(0)					
BaHCO3+	2.613e-14	2.397e-14	-13.583	-13.620	-0.037
(0)					
Br	4.382e-07				
Br-	4.382e-07	4.020e-07	-6.358	-6.396	-0.037
(0)					
C(-4)	0.000e+00				
CH4	0.000e+00	0.000e+00	-90.868	-90.867	0.001
(0)					
C(4)	4.918e-06				
CO3-2	1.952e-06	1.397e-06	-5.709	-5.855	-0.145
(0)					
HCO3-	1.565e-06	1.439e-06	-5.805	-5.842	-0.036
(0)					
CaCO3	1.368e-06	1.371e-06	-5.864	-5.863	0.001
(0)					
NaCO3-	1.869e-08	1.719e-08	-7.728	-7.765	-0.036
(0)					
CaHCO3+	7.789e-09	7.172e-09	-8.108	-8.144	-0.036
(0)					
MgCO3	3.681e-09	3.687e-09	-8.434	-8.433	0.001
(0)					
NaHCO3	1.992e-09	1.995e-09	-8.701	-8.700	0.001
(0)					
CO2	1.327e-10	1.329e-10	-9.877	-9.876	0.001
(0)					
MgHCO3+	7.055e-11	6.469e-11	-10.152	-10.189	-0.038
(0)					
SrCO3	5.809e-11	5.809e-11	-10.236	-10.236	0.000
(0)					
BaCO3	1.645e-12	1.647e-12	-11.784	-11.783	0.001
(0)					
SrHCO3+	1.394e-12	1.282e-12	-11.856	-11.892	-0.036
(0)					
BaHCO3+	2.613e-14	2.397e-14	-13.583	-13.620	-0.037
(0)					
Ca	1.148e-03				

Ca+2	1.014e-03	7.247e-04	-2.994	-3.140	-0.146
(0)					
CaSO4	1.279e-04	1.281e-04	-3.893	-3.892	0.001
(0)					
CaOH+	5.200e-06	4.788e-06	-5.284	-5.320	-0.036
(0)					
CaCO3	1.368e-06	1.371e-06	-5.864	-5.863	0.001
(0)					
CaF+	2.688e-08	2.472e-08	-7.571	-7.607	-0.036
(0)					
CaHCO3+	7.789e-09	7.172e-09	-8.108	-8.144	-0.036
(0)					
CaHSO4+	1.645e-14	1.510e-14	-13.784	-13.821	-0.037
(0)					
Cl	1.089e-03				
Cl-	1.089e-03	9.979e-04	-2.963	-3.001	-0.038
(0)					
F	7.898e-06				
F-	7.860e-06	7.199e-06	-5.105	-5.143	-0.038
(0)					
CaF+	2.688e-08	2.472e-08	-7.571	-7.607	-0.036
(0)					
NaF	1.020e-08	1.021e-08	-7.992	-7.991	0.001
(0)					
MgF+	1.292e-09	1.186e-09	-8.889	-8.926	-0.037
(0)					
HF	1.799e-13	1.802e-13	-12.745	-12.744	0.001
(0)					
HF2-	4.176e-18	3.825e-18	-17.379	-17.417	-0.038
(0)					
AlF2+	5.686e-21	5.229e-21	-20.245	-20.282	-0.036
(0)					
AlF+2	2.321e-21	1.660e-21	-20.634	-20.780	-0.145
(0)					
AlF3	4.608e-22	4.615e-22	-21.337	-21.336	0.001
(0)					
AlF4-	1.433e-24	1.315e-24	-23.844	-23.881	-0.037
(0)					
H2F2	1.914e-25	1.917e-25	-24.718	-24.717	0.001
(0)					
SiF6-2	0.000e+00	0.000e+00	-46.843	-46.990	-0.147
(0)					
H(0)	1.157e-30				
H2	5.783e-31	5.793e-31	-30.238	-30.237	0.001
(0)					
K	8.954e-05				
K+	8.909e-05	8.163e-05	-4.050	-4.088	-0.038
(0)					
KSO4-	4.472e-07	4.113e-07	-6.349	-6.386	-0.036
(0)					
Mg	6.172e-06				
Mg+2	5.567e-06	3.999e-06	-5.254	-5.398	-0.144
(0)					
MgSO4	5.403e-07	5.412e-07	-6.267	-6.267	0.001
(0)					
MgOH+	5.939e-08	5.474e-08	-7.226	-7.262	-0.035
(0)					

MgCO3	3.681e-09	3.687e-09	-8.434	-8.433	0.001
(0)					
MgF+	1.292e-09	1.186e-09	-8.889	-8.926	-0.037
(0)					
MgHCO3+	7.055e-11	6.469e-11	-10.152	-10.189	-0.038
(0)					
N(3)	1.357e-05				
NO2-	1.357e-05	1.245e-05	-4.867	-4.905	-0.037
(0)					
N(5)	3.571e-05				
NO3-	3.571e-05	3.267e-05	-4.447	-4.486	-0.039
(0)					
Na	2.698e-03				
Na+	2.685e-03	2.465e-03	-2.571	-2.608	-0.037
(0)					
NaSO4-	1.287e-05	1.184e-05	-4.890	-4.927	-0.036
(0)					
NaCO3-	1.869e-08	1.719e-08	-7.728	-7.765	-0.036
(0)					
NaF	1.020e-08	1.021e-08	-7.992	-7.991	0.001
(0)					
NaHCO3	1.992e-09	1.995e-09	-8.701	-8.700	0.001
(0)					
O(0)	1.282e-03				
O2	6.408e-04	6.419e-04	-3.193	-3.193	0.001
(0)					
S(6)	1.729e-03				
SO4-2	1.587e-03	1.131e-03	-2.799	-2.947	-0.147
(0)					
CaSO4	1.279e-04	1.281e-04	-3.893	-3.892	0.001
(0)					
NaSO4-	1.287e-05	1.184e-05	-4.890	-4.927	-0.036
(0)					
MgSO4	5.403e-07	5.412e-07	-6.267	-6.267	0.001
(0)					
KSO4-	4.472e-07	4.113e-07	-6.349	-6.386	-0.036
(0)					
SrSO4	2.143e-08	2.146e-08	-7.669	-7.668	0.001
(0)					
BaSO4	2.092e-09	2.095e-09	-8.679	-8.679	0.001
(0)					
HSO4-	1.887e-12	1.732e-12	-11.724	-11.761	-0.037
(0)					
CaHSO4+	1.645e-14	1.510e-14	-13.784	-13.821	-0.037
(0)					
AlSO4+	7.490e-23	6.876e-23	-22.126	-22.163	-0.037
(0)					
Al(SO4)2-	2.373e-24	2.178e-24	-23.625	-23.662	-0.037
(0)					
AlHSO4+2	1.903e-34	1.348e-34	-33.721	-33.870	-0.150
(0)					
Si	3.746e-05				
H3SiO4-	2.643e-05	2.423e-05	-4.578	-4.616	-0.038
(0)					
H4SiO4	1.102e-05	1.104e-05	-4.958	-4.957	0.001
(0)					

(0)	H2SiO4-2	1.508e-08	1.079e-08	-7.822	-7.967	-0.145
(0)	SiF6-2	0.000e+00	0.000e+00	-46.843	-46.990	-0.147
Sr		2.066e-07				
(0)	Sr+2	1.849e-07	1.324e-07	-6.733	-6.878	-0.145
(0)	SrSO4	2.143e-08	2.146e-08	-7.669	-7.668	0.001
(0)	SrOH+	2.941e-10	2.702e-10	-9.532	-9.568	-0.037
(0)	SrCO3	5.809e-11	5.809e-11	-10.236	-10.236	0.000
(0)	SrHCO3+	1.394e-12	1.282e-12	-11.856	-11.892	-0.036

-----Saturation indices-----
--

Phase	SI**	log IAP	log K(274 K, 1 atm)	
Adularia	-1.98	-24.53	-22.55	KAlSi3O8
Al(OH)3(a)	-3.27	9.23	12.50	Al(OH)3
Albite	-3.39	-23.05	-19.66	NaAlSi3O8
AlumK	-26.92	-32.55	-5.63	KAl(SO4)2·12H2O
Alunite	-15.91	-14.09	1.82	KAl3(SO4)2(OH)6
Analcime	-4.23	-18.09	-13.87	NaAlSi2O6·H2O
Anhydrite	-1.73	-6.09	-4.36	CaSO4
Anorthite	-3.74	-24.20	-20.46	CaAl2Si2O8
Aragonite	-0.77	-8.99	-8.22	CaCO3
Artinite	-6.90	4.55	11.44	MgCO3:Mg(OH)2:3H2O
BaF2	-12.89	-18.72	-5.82	BaF2
Barite	-0.92	-11.38	-10.45	BaSO4
Basaluminite	-9.92	12.78	22.70	Al4(OH)10SO4
Beidellite	-4.26	-53.41	-49.14	
(NaKMg0.5)0.11Al2.33Si3.67O10(OH)2				
Boehmite	-1.16	9.23	10.39	AlOOH
Brucite	-2.78	15.80	18.58	Mg(OH)2
Calcite	-0.61	-8.99	-8.38	CaCO3
Celestite	-3.13	-9.82	-6.69	SrSO4
CH4(g)	-88.22	-90.87	-2.64	CH4
Chalcedony	-1.10	-4.96	-3.85	SiO2
Chlorite14A	4.50	82.60	78.10	Mg5Al2Si3O10(OH)8
Chlorite7A	0.89	82.60	81.71	Mg5Al2Si3O10(OH)8
Chrysotile	2.06	37.49	35.43	Mg3Si2O5(OH)4
Clinoenstatite	-1.78	10.84	12.63	MgSiO3
CO2(g)	-8.75	-9.88	-1.13	CO2
Cristobalite	-1.02	-4.96	-3.94	SiO2
Diaspore	0.77	9.23	8.46	AlOOH
Diopside	1.98	23.95	21.97	CaMgSi2O6
Dolomite	-3.76	-20.25	-16.48	CaMg(CO3)2
Dolomite(d)	-4.42	-20.25	-15.83	CaMg(CO3)2
Epsomite	-6.02	-8.35	-2.32	MgSO4·7H2O
Fluorite	-2.48	-13.43	-10.94	CaF2
Forsterite	-4.78	26.65	31.42	Mg2SiO4
Gibbsite	-0.34	9.23	9.57	Al(OH)3
Gypsum	-1.47	-6.09	-4.61	CaSO4·2H2O

H2 (g)	-27.20	-30.24	-3.04	H2
H2O (g)	-2.19	-0.00	2.19	H2O
Halite	-7.13	-5.61	1.52	NaCl
Halloysite	-6.51	8.55	15.06	Al2Si2O5 (OH) 4
Huntite	-14.44	-42.75	-28.32	CaMg3 (CO3) 4
Hydromagnesite	-23.80	-29.21	-5.41	Mg5 (CO3) 4 (OH) 2:4H2O
Illite	-2.91	-46.69	-43.78	K0.6Mg0.25Al2.3Si3.5O10 (OH) 2
Jurbanite	-11.69	-14.92	-3.23	AlOHSO4
Kaolinite	-1.15	8.55	9.70	Al2Si2O5 (OH) 4
Kmica	2.82	19.33	16.51	KAl3Si3O10 (OH) 2
Laumontite	-0.61	-34.11	-33.50	CaAl2Si4O12:4H2O
Leonhardite	7.31	-68.22	-75.54	Ca2Al4Si8O24:7H2O
Magadiite	-12.41	-26.71	-14.30	NaSi7O13 (OH) 3:3H2O
Magnesite	-3.62	-11.25	-7.63	MgCO3
Mirabilite	-5.83	-8.16	-2.33	Na2SO4:10H2O
Montmorillonite-Ca	-4.12	-52.89	-48.77	Ca0.165Al2.33Si3.67O10 (OH) 2
Nahcolite	-7.66	-8.45	-0.79	NaHCO3
Natron	-8.75	-11.07	-2.32	Na2CO3:10H2O
Nesquehonite	-6.00	-11.25	-5.25	MgCO3:3H2O
O2 (g)	-0.52	-3.19	-2.67	O2
Phillipsite	-3.92	-23.79	-19.87	Na0.5K0.5AlSi3O8:H2O
Phlogopite	2.26	48.28	46.01	KMg3AlSi3O10 (OH) 2
Portlandite	-6.73	18.06	24.79	Ca (OH) 2
Prehnite	1.27	-11.09	-12.36	Ca2Al2Si3O10 (OH) 2
Pyrophyllite	-3.86	-52.17	-48.31	Al2Si4O10 (OH) 2
Quartz	-0.59	-4.96	-4.36	SiO2
Sepiolite	0.29	16.73	16.45	Mg2Si3O7.5OH:3H2O
Sepiolite(d)	-1.93	16.73	18.66	Mg2Si3O7.5OH:3H2O
Silicagel	-1.65	-4.96	-3.30	SiO2
SiO2 (a)	-2.03	-4.96	-2.93	SiO2
SrF2	-8.54	-17.16	-8.62	SrF2
Strontianite	-3.40	-12.73	-9.33	SrCO3
Talc	3.20	27.58	24.37	Mg3Si4O10 (OH) 2
Thenardite	-8.02	-8.16	-0.14	Na2SO4
Thermonatrite	-11.38	-11.07	0.30	Na2CO3:H2O
Tremolite	12.68	75.47	62.79	Ca2Mg5Si8O22 (OH) 2
Trona	-19.88	-19.52	0.36	NaHCO3:Na2CO3:2H2O
Wairakite	-5.73	-34.11	-28.39	CaAl2Si4O12:2H2O
Witherite	-5.56	-14.29	-8.72	BaCO3

**For a gas, SI = log10(fugacity). Fugacity = pressure * phi / 1 atm.
For ideal gases, phi = 1.

Beginning of batch-reaction calculations.

Reaction step 1.

Using solution 4. North Basin (Open-System)
Using pure phase assemblage 4.

-----Phase assemblage-----
--

Moles in assemblage

Phase	SI	log IAP	log K(T, P)	Initial	Final	
Delta						
Albite	0.00	-19.66	-19.66	1.000e+01	1.000e+01	-1.835e-
04						
Anorthite	0.00	-20.46	-20.46	1.000e+01	1.213e-01	-
9.879e+00						
CO2 (g)	-3.77	-4.90	-1.13	1.000e+01	0	-
1.000e+01						
Kaolinite	0.00	9.70	9.70	1.000e+01	1.988e+01	
9.879e+00						
O2 (g)	-0.68	-3.35	-2.67	1.000e+01	1.000e+01	4.773e-
04						

-----Solution composition-----
--

Elements	Molality	Moles
Al	4.302e-07	2.761e-07
Ba	1.135e-08	7.284e-09
Br	6.827e-07	4.382e-07
C	1.558e+01	1.000e+01
Ca	1.539e+01	9.880e+00
Cl	1.697e-03	1.089e-03
F	1.231e-05	7.898e-06
K	1.395e-04	8.954e-05
Mg	9.616e-06	6.172e-06
N	7.678e-05	4.928e-05
Na	4.489e-03	2.881e-03
S	2.693e-03	1.729e-03
Si	6.262e-04	4.019e-04
Sr	3.220e-07	2.066e-07

-----Description of solution-----
--

pH = 10.590 Charge balance
 pe = 12.325 Adjusted to redox
 equilibrium

Activity of water = 0.725
 Ionic strength (mol/kgw) = 2.629e+00
 Mass of water (kg) = 6.418e-01
 Total alkalinity (eq/kg) = 3.078e+01
 Total CO2 (mol/kg) = 1.558e+01
 Temperature (°C) = 1.00
 Electrical balance (eq) = 3.945e-04
 Percent error, 100*(Cat-|An|)/(Cat+|An|) = 0.02
 Iterations = 18
 Total H = 7.149727e+01
 Total O = 6.563571e+01

-----Distribution of species-----
--

mole V Log Log Log

Species cm ³ /mol	Molality	Activity	Molality	Activity	Gamma
OH-	6.780e-05	3.556e-05	-4.169	-4.449	-0.280
(0)					
H+	3.540e-11	2.571e-11	-10.451	-10.590	-0.139
0.00					
H2O	5.551e+01	7.249e-01	1.744	-0.140	0.000
18.02					
Al	4.302e-07				
Al (OH) 4-	4.302e-07	2.496e-07	-6.366	-6.603	-0.236
(0)					
Al (OH) 3	2.958e-12	5.418e-12	-11.529	-11.266	0.263
(0)					
Al (OH) 2+	1.695e-14	1.052e-14	-13.771	-13.978	-0.207
(0)					
AlOH+2	3.641e-18	5.393e-19	-17.439	-18.268	-0.829
(0)					
AlF+2	2.012e-21	2.981e-22	-20.696	-21.526	-0.829
(0)					
AlF2+	7.335e-22	4.550e-22	-21.135	-21.342	-0.207
(0)					
Al+3	1.775e-22	9.989e-24	-21.751	-23.000	-1.250
(0)					
AlF3	1.063e-23	1.947e-23	-22.974	-22.711	0.263
(0)					
AlSO4+	3.757e-24	2.179e-24	-23.425	-23.662	-0.236
(0)					
AlF4-	4.634e-26	2.688e-26	-25.334	-25.570	-0.236
(0)					
Al (SO4) 2-	1.019e-26	5.908e-27	-25.992	-26.229	-0.236
(0)					
AlHSO4+2	2.024e-36	4.373e-36	-35.694	-35.359	0.334
(0)					
Ba	1.135e-08				
BaCO3	7.603e-09	1.393e-08	-8.119	-7.856	0.263
(0)					
Ba+2	3.561e-09	4.723e-10	-8.448	-9.326	-0.877
(0)					
BaHCO3+	1.711e-10	2.074e-10	-9.767	-9.683	0.084
(0)					
BaSO4	1.250e-11	2.290e-11	-10.903	-10.640	0.263
(0)					
BaOH+	7.476e-13	4.511e-13	-12.126	-12.346	-0.219
(0)					
Br	6.827e-07				
Br-	6.827e-07	8.276e-07	-6.166	-6.082	0.084
(0)					
C(-4)	0.000e+00				
CH4	0.000e+00	0.000e+00	-160.389	-160.126	0.263
(0)					
C(4)	1.558e+01				
CaCO3	1.458e+01	2.670e+01	1.164	1.426	0.263
(0)					
CO3-2	6.240e-01	9.243e-02	-0.205	-1.034	-0.829
(0)					

CaHCO3+	2.223e-01	1.430e-01	-0.653	-0.845	-0.192
(0)					
HCO3-	1.572e-01	9.752e-02	-0.804	-1.011	-0.207
(0)					
NaCO3-	1.738e-03	1.078e-03	-2.760	-2.967	-0.207
(0)					
NaHCO3	6.996e-05	1.282e-04	-4.155	-3.892	0.263
(0)					
MgCO3	8.594e-06	1.574e-05	-5.066	-4.803	0.263
(0)					
CO2	6.941e-06	1.271e-05	-5.159	-4.896	0.263
(0)					
MgHCO3+	5.105e-07	2.828e-07	-6.292	-6.549	-0.257
(0)					
SrCO3	2.793e-07	2.793e-07	-6.554	-6.554	0.000
(0)					
SrHCO3+	1.017e-08	6.308e-09	-7.993	-8.200	-0.207
(0)					
BaCO3	7.603e-09	1.393e-08	-8.119	-7.856	0.263
(0)					
BaHCO3+	1.711e-10	2.074e-10	-9.767	-9.683	0.084
(0)					
Ca	1.539e+01				
CaCO3	1.458e+01	2.670e+01	1.164	1.426	0.263
(0)					
Ca+2	5.925e-01	2.133e-01	-0.227	-0.671	-0.444
(0)					
CaHCO3+	2.223e-01	1.430e-01	-0.653	-0.845	-0.192
(0)					
CaSO4	1.762e-03	3.228e-03	-2.754	-2.491	0.263
(0)					
CaOH+	1.551e-03	9.980e-04	-2.809	-3.001	-0.192
(0)					
CaF+	5.649e-06	3.527e-06	-5.248	-5.453	-0.205
(0)					
CaHSO4+	3.211e-13	3.893e-13	-12.493	-12.410	0.084
(0)					
Cl	1.697e-03				
Cl-	1.697e-03	9.745e-04	-2.770	-3.011	-0.241
(0)					
F	1.231e-05				
F-	6.654e-06	3.490e-06	-5.177	-5.457	-0.280
(0)					
CaF+	5.649e-06	3.527e-06	-5.248	-5.453	-0.205
(0)					
NaF	2.562e-09	4.693e-09	-8.591	-8.329	0.263
(0)					
MgF+	6.392e-11	3.708e-11	-10.194	-10.431	-0.236
(0)					
HF	4.882e-14	8.942e-14	-13.311	-13.049	0.263
(0)					
HF2-	1.754e-18	9.200e-19	-17.756	-18.036	-0.280
(0)					
AlF+2	2.012e-21	2.981e-22	-20.696	-21.526	-0.829
(0)					
AlF2+	7.335e-22	4.550e-22	-21.135	-21.342	-0.207
(0)					

AlF3	1.063e-23	1.947e-23	-22.974	-22.711	0.263
(0)					
AlF4-	4.634e-26	2.688e-26	-25.334	-25.570	-0.236
(0)					
H2F2	2.576e-26	4.720e-26	-25.589	-25.326	0.263
(0)					
SiF6-2	0.000e+00	0.000e+00	-46.292	-47.169	-0.877
(0)					
H(0)	0.000e+00				
H2	0.000e+00	0.000e+00	-49.130	-48.867	0.263
(0)					
K	1.395e-04				
K+	1.395e-04	8.009e-05	-3.856	-4.096	-0.241
(0)					
KSO4-	5.567e-08	3.453e-08	-7.254	-7.462	-0.207
(0)					
Mg	9.616e-06				
MgCO3	8.594e-06	1.574e-05	-5.066	-4.803	0.263
(0)					
MgHCO3+	5.105e-07	2.828e-07	-6.292	-6.549	-0.257
(0)					
Mg+2	5.059e-07	2.580e-07	-6.296	-6.588	-0.292
(0)					
MgOH+	3.788e-09	2.501e-09	-8.422	-8.602	-0.180
(0)					
MgSO4	1.632e-09	2.989e-09	-8.787	-8.525	0.263
(0)					
MgF+	6.392e-11	3.708e-11	-10.194	-10.431	-0.236
(0)					
N(-3)	0.000e+00				
NH3	0.000e+00	0.000e+00	-76.881	-76.881	0.000
(0)					
NH4+	0.000e+00	0.000e+00	-77.507	-77.423	0.084
(0)					
NH4SO4-	0.000e+00	0.000e+00	-80.108	-80.327	-0.219
(0)					
N(0)	6.451e-32				
N2	3.225e-32	5.908e-32	-31.491	-31.229	0.263
(0)					
N(3)	1.516e-19				
NO2-	1.516e-19	1.838e-19	-18.819	-18.736	0.084
(0)					
N(5)	7.678e-05				
NO3-	7.678e-05	3.770e-05	-4.115	-4.424	-0.309
(0)					
Na	4.489e-03				
Na+	2.680e-03	2.337e-03	-2.572	-2.631	-0.059
(0)					
NaCO3-	1.738e-03	1.078e-03	-2.760	-2.967	-0.207
(0)					
NaHCO3	6.996e-05	1.282e-04	-4.155	-3.892	0.263
(0)					
NaSO4-	1.548e-06	9.606e-07	-5.810	-6.017	-0.207
(0)					
NaF	2.562e-09	4.693e-09	-8.591	-8.329	0.263
(0)					
O(0)	4.886e-04				

O2	2.443e-04	4.475e-04	-3.612	-3.349	0.263
(0)					
S(-2)	0.000e+00				
S6-2	0.000e+00	0.000e+00	-158.763	-159.144	-0.381
(0)					
S5-2	0.000e+00	0.000e+00	-159.019	-159.455	-0.436
(0)					
S4-2	0.000e+00	0.000e+00	-159.206	-159.714	-0.509
(0)					
HS-	0.000e+00	0.000e+00	-159.572	-159.853	-0.280
(0)					
S-2	0.000e+00	0.000e+00	-162.080	-162.957	-0.877
(0)					
S3-2	0.000e+00	0.000e+00	-162.601	-163.212	-0.612
(0)					
H2S	0.000e+00	0.000e+00	-163.374	-163.111	0.263
(0)					
S2-2	0.000e+00	0.000e+00	-163.802	-164.522	-0.721
(0)					
S(6)	2.693e-03				
CaSO4	1.762e-03	3.228e-03	-2.754	-2.491	0.263
(0)					
SO4-2	9.297e-04	9.677e-05	-3.032	-4.014	-0.983
(0)					
NaSO4-	1.548e-06	9.606e-07	-5.810	-6.017	-0.207
(0)					
KSO4-	5.567e-08	3.453e-08	-7.254	-7.462	-0.207
(0)					
MgSO4	1.632e-09	2.989e-09	-8.787	-8.525	0.263
(0)					
SrSO4	7.285e-11	1.334e-10	-10.138	-9.875	0.263
(0)					
BaSO4	1.250e-11	2.290e-11	-10.903	-10.640	0.263
(0)					
CaHSO4+	3.211e-13	3.893e-13	-12.493	-12.410	0.084
(0)					
HSO4-	2.616e-13	1.518e-13	-12.582	-12.819	-0.236
(0)					
AlSO4+	3.757e-24	2.179e-24	-23.425	-23.662	-0.236
(0)					
Al(SO4)2-	1.019e-26	5.908e-27	-25.992	-26.229	-0.236
(0)					
AlHSO4+2	2.024e-36	4.373e-36	-35.694	-35.359	0.334
(0)					
NH4SO4-	0.000e+00	0.000e+00	-80.108	-80.327	-0.219
(0)					
Si	6.262e-04				
H3SiO4-	5.480e-04	3.036e-04	-3.261	-3.518	-0.257
(0)					
H4SiO4	7.727e-05	1.415e-04	-4.112	-3.849	0.263
(0)					
H2SiO4-2	8.910e-07	1.320e-07	-6.050	-6.879	-0.829
(0)					
SiF6-2	0.000e+00	0.000e+00	-46.292	-47.169	-0.877
(0)					
Sr	3.220e-07				

SrCO3	2.793e-07	2.793e-07	-6.554	-6.554	0.000
(0)					
Sr+2	3.240e-08	9.616e-09	-7.490	-8.017	-0.527
(0)					
SrHCO3+	1.017e-08	6.308e-09	-7.993	-8.200	-0.207
(0)					
SrSO4	7.285e-11	1.334e-10	-10.138	-9.875	0.263
(0)					
SrOH+	2.304e-11	1.390e-11	-10.638	-10.857	-0.219
(0)					

-----Saturation indices-----
--

Phase	SI**	log IAP	log K(274 K,	1 atm)	
Adularia	1.42	-21.13	-22.55	KAlSi3O8	
Al(OH)3(a)	-4.15	8.35	12.50	Al(OH)3	
Albite	0.00	-19.66	-19.66	NaAlSi3O8	
AlumK	-31.17	-36.80	-5.63	KAl(SO4)2:12H2O	
Alunite	-20.25	-18.43	1.82	KAl3(SO4)2(OH)6	
Analcime	-2.36	-16.23	-13.87	NaAlSi2O6:H2O	
Anhydrite	-0.32	-4.69	-4.36	CaSO4	
Anorthite	0.00	-20.46	-20.46	CaAl2Si2O8	
Aragonite	6.52	-1.71	-8.22	CaCO3	
Artinite	-5.17	6.27	11.44	MgCO3:Mg(OH)2:3H2O	
BaF2	-14.42	-20.24	-5.82	BaF2	
Barite	-2.89	-13.34	-10.45	BaSO4	
Basaluminite	-14.22	8.48	22.70	Al4(OH)10SO4	
Beidellite	-0.97	-50.12	-49.14		
(NaKMg0.5)0.11Al2.33Si3.67O10(OH)2					
Boehmite	-1.90	8.49	10.39	AlOOH	
Brucite	-4.27	14.31	18.58	Mg(OH)2	
Calcite	6.68	-1.71	-8.38	CaCO3	
Celestite	-5.34	-12.03	-6.69	SrSO4	
CH4(g)	-157.48	-160.13	-2.64	CH4	
Chalcedony	0.28	-3.57	-3.85	SiO2	
Chloritel4A	0.01	78.11	78.10	Mg5Al2Si3O10(OH)8	
Chlorite7A	-3.61	78.11	81.71	Mg5Al2Si3O10(OH)8	
Chrysotile	0.51	35.94	35.43	Mg3Si2O5(OH)4	
Clinoenstatite	-1.75	10.88	12.63	MgSiO3	
CO2(g)	-3.77	-4.90	-1.13	CO2	
Cristobalite	0.37	-3.57	-3.94	SiO2	
Diaspore	0.03	8.49	8.46	AlOOH	
Diopside	5.71	27.68	21.97	CaMgSi2O6	
Dolomite	7.16	-9.33	-16.48	CaMg(CO3)2	
Dolomite(d)	6.50	-9.33	-15.83	CaMg(CO3)2	
Epsomite	-9.26	-11.58	-2.32	MgSO4:7H2O	
Fluorite	-0.64	-11.59	-10.94	CaF2	
Forsterite	-6.09	25.33	31.42	Mg2SiO4	
Gibbsite	-1.22	8.35	9.57	Al(OH)3	
Gypsum	-0.35	-4.96	-4.61	CaSO4:2H2O	
H2(g)	-45.83	-48.87	-3.04	H2	
H2O(g)	-2.32	-0.14	2.19	H2O	
H2S(g)	-162.41	-163.11	-0.70	H2S	
Halite	-7.17	-5.64	1.52	NaCl	
Halloysite	-5.36	9.70	15.06	Al2Si2O5(OH)4	

Huntite	3.74	-24.57	-28.32	CaMg3 (CO3) 4
Hydromagnesite	-11.33	-16.74	-5.41	Mg5 (CO3) 4 (OH) 2:4H2O
Illite	-0.13	-43.91	-43.78	K0.6Mg0.25Al2.3Si3.5O10 (OH) 2
Jurbanite	-13.33	-16.56	-3.23	AlOHSO4
Kaolinite	0.00	9.70	9.70	Al2Si2O5 (OH) 4
Kmica	4.74	21.25	16.51	KAl3Si3O10 (OH) 2
Laumontite	5.35	-28.16	-33.50	CaAl2Si4O12:4H2O
Leonhardite	19.36	-56.17	-75.54	Ca2Al4Si8O24:7H2O
Magadiite	-3.43	-17.73	-14.30	NaSi7O13 (OH) 3:3H2O
Magnesite	0.01	-7.62	-7.63	MgCO3
Mirabilite	-8.34	-10.67	-2.33	Na2SO4:10H2O
Montmorillonite-Ca	-0.35	-49.12	-48.77	Ca0.165Al2.33Si3.67O10 (OH) 2
N2 (g)	-28.06	-31.23	-3.17	N2
Nahcolite	-2.86	-3.64	-0.79	NaHCO3
Natron	-5.37	-7.69	-2.32	Na2CO3:10H2O
Nesquehonite	-2.79	-8.04	-5.25	MgCO3:3H2O
NH3 (g)	-79.18	-76.88	2.29	NH3
O2 (g)	-0.68	-3.35	-2.67	O2
Phillipsite	-0.66	-20.54	-19.87	Na0.5K0.5AlSi3O8:H2O
Phlogopite	1.47	47.49	46.01	KMg3AlSi3O10 (OH) 2
Portlandite	-4.56	20.23	24.79	Ca (OH) 2
Prehnite	8.56	-3.80	-12.36	Ca2Al2Si3O10 (OH) 2
Pyrophyllite	0.21	-48.11	-48.31	Al2Si4O10 (OH) 2
Quartz	0.80	-3.57	-4.36	SiO2
Sepiolite	1.26	17.71	16.45	Mg2Si3O7.5OH:3H2O
Sepiolite (d)	-0.95	17.71	18.66	Mg2Si3O7.5OH:3H2O
Silicagel	-0.27	-3.57	-3.30	SiO2
SiO2 (a)	-0.64	-3.57	-2.93	SiO2
SrF2	-10.31	-18.93	-8.62	SrF2
Strontianite	0.28	-9.05	-9.33	SrCO3
Sulfur	-122.77	-138.31	-15.53	S
Talc	4.56	28.94	24.37	Mg3Si4O10 (OH) 2
Thenardite	-9.13	-9.28	-0.14	Na2SO4
Thermonatrite	-6.74	-6.44	0.30	Na2CO3:H2O
Tremolite	21.51	84.30	62.79	Ca2Mg5Si8O22 (OH) 2
Trona	-10.58	-10.22	0.36	NaHCO3:Na2CO3:2H2O
Wairakite	0.51	-27.88	-28.39	CaAl2Si4O12:2H2O
Witherite	-1.64	-10.36	-8.72	BaCO3

**For a gas, SI = log10(fugacity). Fugacity = pressure * phi / 1 atm.
For ideal gases, phi = 1.

End of simulation.

Reading input data for simulation 5.

SOLUTION 5 North Basin (Open-System, no weathering)
temp 1
pH 10.6
pe 3
units ppm
density 1
Al 0.0787

```

Br          0.035
C           0.3
Ca          46
Cl          38.6
F           0.15
K           3.5
Mg          0.15
N(3)       0.19
N(5)       0.5
Na          62
O(0)       20.5
S(6)       166
Si          2.25
Sr          0.0181
Ba          0.001
water      1 # kg
EQUILIBRIUM_PHASES 5
CO2(g)     -3.43 10
O2(g)      -0.679 10
SELECTED_OUTPUT 5
file                selected_output_weathering5.sel
totals              Na Mg K Ca S(6) C
molalities          Ca+2 Na+ S6-2 K+
                    Mg+2 CO2 CO3-2 HCO3-
equilibrium_phases Albite Anorthite Kaolinite
end

```

Beginning of initial solution calculations.

Initial solution 5. North Basin (Open-System, no weathering)

-----Solution composition-----

--

Elements	Molality	Moles
Al	2.918e-06	2.918e-06
Ba	7.284e-09	7.284e-09
Br	4.382e-07	4.382e-07
C	4.918e-06	4.918e-06
Ca	1.148e-03	1.148e-03
Cl	1.089e-03	1.089e-03
F	7.898e-06	7.898e-06
K	8.954e-05	8.954e-05
Mg	6.172e-06	6.172e-06
N(3)	1.357e-05	1.357e-05
N(5)	3.571e-05	3.571e-05
Na	2.698e-03	2.698e-03
O(0)	1.282e-03	1.282e-03
S(6)	1.729e-03	1.729e-03
Si	3.746e-05	3.746e-05
Sr	2.066e-07	2.066e-07

-----Description of solution-----

--

```

pH = 10.600
pe = 3.000
Activity of water = 1.000
Ionic strength (mol/kgw) = 7.229e-03
Mass of water (kg) = 1.000e+00
Total alkalinity (eq/kg) = 1.065e-04
Total CO2 (mol/kg) = 4.918e-06
Temperature (°C) = 1.00
Electrical balance (eq) = 3.945e-04
Percent error, 100*(Cat-|An|)/(Cat+|An|) = 4.27
Iterations = 6
Total H = 1.110126e+02
Total O = 5.551478e+01

```

-----Redox couples-----
--

Redox couple	pe	Eh (volts)
N(3)/N(5)	5.2986	0.2882
O(-2)/O(0)	12.2842	0.6682

-----Distribution of species-----
--

mole V Species cm ³ /mol	Molality	Activity	Log		Log Gamma
			Molality	Activity	
OH-	5.481e-05	5.021e-05	-4.261	-4.299	-0.038
(0)					
H+	2.713e-11	2.512e-11	-10.567	-10.600	-0.033
0.00					
H2O	5.551e+01	9.999e-01	1.744	-0.000	0.000
18.02					
Al	2.918e-06				
Al(OH)4-	2.918e-06	2.678e-06	-5.535	-5.572	-0.037
(0)					
Al(OH)3	4.112e-11	4.119e-11	-10.386	-10.385	0.001
(0)					
Al(OH)2+	6.156e-14	5.662e-14	-13.211	-13.247	-0.036
(0)					
AlOH+2	2.874e-18	2.056e-18	-17.541	-17.687	-0.145
(0)					
AlF2+	5.686e-21	5.229e-21	-20.245	-20.282	-0.036
(0)					
AlF+2	2.321e-21	1.660e-21	-20.634	-20.780	-0.145
(0)					
AlF3	4.608e-22	4.615e-22	-21.337	-21.336	0.001
(0)					
AlSO4+	7.490e-23	6.876e-23	-22.126	-22.163	-0.037
(0)					
Al+3	5.397e-23	2.697e-23	-22.268	-22.569	-0.301
(0)					
Al(SO4)2-	2.373e-24	2.178e-24	-23.625	-23.662	-0.037
(0)					

AlF4-	1.433e-24	1.315e-24	-23.844	-23.881	-0.037
(0)					
AlHSO4+2	1.903e-34	1.348e-34	-33.721	-33.870	-0.150
(0)					
Ba	7.284e-09				
Ba+2	5.185e-09	3.697e-09	-8.285	-8.432	-0.147
(0)					
BaSO4	2.092e-09	2.095e-09	-8.679	-8.679	0.001
(0)					
BaOH+	5.427e-12	4.987e-12	-11.265	-11.302	-0.037
(0)					
BaCO3	1.645e-12	1.647e-12	-11.784	-11.783	0.001
(0)					
BaHCO3+	2.613e-14	2.397e-14	-13.583	-13.620	-0.037
(0)					
Br	4.382e-07				
Br-	4.382e-07	4.020e-07	-6.358	-6.396	-0.037
(0)					
C(-4)	0.000e+00				
CH4	0.000e+00	0.000e+00	-90.868	-90.867	0.001
(0)					
C(4)	4.918e-06				
CO3-2	1.952e-06	1.397e-06	-5.709	-5.855	-0.145
(0)					
HCO3-	1.565e-06	1.439e-06	-5.805	-5.842	-0.036
(0)					
CaCO3	1.368e-06	1.371e-06	-5.864	-5.863	0.001
(0)					
NaCO3-	1.869e-08	1.719e-08	-7.728	-7.765	-0.036
(0)					
CaHCO3+	7.789e-09	7.172e-09	-8.108	-8.144	-0.036
(0)					
MgCO3	3.681e-09	3.687e-09	-8.434	-8.433	0.001
(0)					
NaHCO3	1.992e-09	1.995e-09	-8.701	-8.700	0.001
(0)					
CO2	1.327e-10	1.329e-10	-9.877	-9.876	0.001
(0)					
MgHCO3+	7.055e-11	6.469e-11	-10.152	-10.189	-0.038
(0)					
SrCO3	5.809e-11	5.809e-11	-10.236	-10.236	0.000
(0)					
BaCO3	1.645e-12	1.647e-12	-11.784	-11.783	0.001
(0)					
SrHCO3+	1.394e-12	1.282e-12	-11.856	-11.892	-0.036
(0)					
BaHCO3+	2.613e-14	2.397e-14	-13.583	-13.620	-0.037
(0)					
Ca	1.148e-03				
Ca+2	1.014e-03	7.247e-04	-2.994	-3.140	-0.146
(0)					
CaSO4	1.279e-04	1.281e-04	-3.893	-3.892	0.001
(0)					
CaOH+	5.200e-06	4.788e-06	-5.284	-5.320	-0.036
(0)					
CaCO3	1.368e-06	1.371e-06	-5.864	-5.863	0.001
(0)					

CaF+	2.688e-08	2.472e-08	-7.571	-7.607	-0.036
(0)					
CaHCO3+	7.789e-09	7.172e-09	-8.108	-8.144	-0.036
(0)					
CaHSO4+	1.645e-14	1.510e-14	-13.784	-13.821	-0.037
(0)					
Cl	1.089e-03				
Cl-	1.089e-03	9.979e-04	-2.963	-3.001	-0.038
(0)					
F	7.898e-06				
F-	7.860e-06	7.199e-06	-5.105	-5.143	-0.038
(0)					
CaF+	2.688e-08	2.472e-08	-7.571	-7.607	-0.036
(0)					
NaF	1.020e-08	1.021e-08	-7.992	-7.991	0.001
(0)					
MgF+	1.292e-09	1.186e-09	-8.889	-8.926	-0.037
(0)					
HF	1.799e-13	1.802e-13	-12.745	-12.744	0.001
(0)					
HF2-	4.176e-18	3.825e-18	-17.379	-17.417	-0.038
(0)					
AlF2+	5.686e-21	5.229e-21	-20.245	-20.282	-0.036
(0)					
AlF+2	2.321e-21	1.660e-21	-20.634	-20.780	-0.145
(0)					
AlF3	4.608e-22	4.615e-22	-21.337	-21.336	0.001
(0)					
AlF4-	1.433e-24	1.315e-24	-23.844	-23.881	-0.037
(0)					
H2F2	1.914e-25	1.917e-25	-24.718	-24.717	0.001
(0)					
SiF6-2	0.000e+00	0.000e+00	-46.843	-46.990	-0.147
(0)					
H(0)	1.157e-30				
H2	5.783e-31	5.793e-31	-30.238	-30.237	0.001
(0)					
K	8.954e-05				
K+	8.909e-05	8.163e-05	-4.050	-4.088	-0.038
(0)					
KSO4-	4.472e-07	4.113e-07	-6.349	-6.386	-0.036
(0)					
Mg	6.172e-06				
Mg+2	5.567e-06	3.999e-06	-5.254	-5.398	-0.144
(0)					
MgSO4	5.403e-07	5.412e-07	-6.267	-6.267	0.001
(0)					
MgOH+	5.939e-08	5.474e-08	-7.226	-7.262	-0.035
(0)					
MgCO3	3.681e-09	3.687e-09	-8.434	-8.433	0.001
(0)					
MgF+	1.292e-09	1.186e-09	-8.889	-8.926	-0.037
(0)					
MgHCO3+	7.055e-11	6.469e-11	-10.152	-10.189	-0.038
(0)					
N(3)	1.357e-05				

NO2-	1.357e-05	1.245e-05	-4.867	-4.905	-0.037
(0)					
N(5)	3.571e-05				
NO3-	3.571e-05	3.267e-05	-4.447	-4.486	-0.039
(0)					
Na	2.698e-03				
Na+	2.685e-03	2.465e-03	-2.571	-2.608	-0.037
(0)					
NaSO4-	1.287e-05	1.184e-05	-4.890	-4.927	-0.036
(0)					
NaCO3-	1.869e-08	1.719e-08	-7.728	-7.765	-0.036
(0)					
NaF	1.020e-08	1.021e-08	-7.992	-7.991	0.001
(0)					
NaHCO3	1.992e-09	1.995e-09	-8.701	-8.700	0.001
(0)					
O(0)	1.282e-03				
O2	6.408e-04	6.419e-04	-3.193	-3.193	0.001
(0)					
S(6)	1.729e-03				
SO4-2	1.587e-03	1.131e-03	-2.799	-2.947	-0.147
(0)					
CaSO4	1.279e-04	1.281e-04	-3.893	-3.892	0.001
(0)					
NaSO4-	1.287e-05	1.184e-05	-4.890	-4.927	-0.036
(0)					
MgSO4	5.403e-07	5.412e-07	-6.267	-6.267	0.001
(0)					
KSO4-	4.472e-07	4.113e-07	-6.349	-6.386	-0.036
(0)					
SrSO4	2.143e-08	2.146e-08	-7.669	-7.668	0.001
(0)					
BaSO4	2.092e-09	2.095e-09	-8.679	-8.679	0.001
(0)					
HSO4-	1.887e-12	1.732e-12	-11.724	-11.761	-0.037
(0)					
CaHSO4+	1.645e-14	1.510e-14	-13.784	-13.821	-0.037
(0)					
AlSO4+	7.490e-23	6.876e-23	-22.126	-22.163	-0.037
(0)					
Al(SO4)2-	2.373e-24	2.178e-24	-23.625	-23.662	-0.037
(0)					
AlHSO4+2	1.903e-34	1.348e-34	-33.721	-33.870	-0.150
(0)					
Si	3.746e-05				
H3SiO4-	2.643e-05	2.423e-05	-4.578	-4.616	-0.038
(0)					
H4SiO4	1.102e-05	1.104e-05	-4.958	-4.957	0.001
(0)					
H2SiO4-2	1.508e-08	1.079e-08	-7.822	-7.967	-0.145
(0)					
SiF6-2	0.000e+00	0.000e+00	-46.843	-46.990	-0.147
(0)					
Sr	2.066e-07				
Sr+2	1.849e-07	1.324e-07	-6.733	-6.878	-0.145
(0)					

SrSO4	2.143e-08	2.146e-08	-7.669	-7.668	0.001
(0)					
SrOH+	2.941e-10	2.702e-10	-9.532	-9.568	-0.037
(0)					
SrCO3	5.809e-11	5.809e-11	-10.236	-10.236	0.000
(0)					
SrHCO3+	1.394e-12	1.282e-12	-11.856	-11.892	-0.036
(0)					

-----Saturation indices-----
--

Phase	SI**	log IAP	log K(274 K,	1 atm)	
Adularia	-1.98	-24.53	-22.55	KAlSi3O8	
Al(OH)3(a)	-3.27	9.23	12.50	Al(OH)3	
Albite	-3.39	-23.05	-19.66	NaAlSi3O8	
AlumK	-26.92	-32.55	-5.63	KAl(SO4)2:12H2O	
Alunite	-15.91	-14.09	1.82	KAl3(SO4)2(OH)6	
Analcime	-4.23	-18.09	-13.87	NaAlSi2O6:H2O	
Anhydrite	-1.73	-6.09	-4.36	CaSO4	
Anorthite	-3.74	-24.20	-20.46	CaAl2Si2O8	
Aragonite	-0.77	-8.99	-8.22	CaCO3	
Artinite	-6.90	4.55	11.44	MgCO3:Mg(OH)2:3H2O	
BaF2	-12.89	-18.72	-5.82	BaF2	
Barite	-0.92	-11.38	-10.45	BaSO4	
Basaluminite	-9.92	12.78	22.70	Al4(OH)10SO4	
Beidellite	-4.26	-53.41	-49.14		
(NaKMg0.5)0.11Al2.33Si3.67O10(OH)2					
Boehmite	-1.16	9.23	10.39	AlOOH	
Brucite	-2.78	15.80	18.58	Mg(OH)2	
Calcite	-0.61	-8.99	-8.38	CaCO3	
Celestite	-3.13	-9.82	-6.69	SrSO4	
CH4(g)	-88.22	-90.87	-2.64	CH4	
Chalcedony	-1.10	-4.96	-3.85	SiO2	
Chlorite14A	4.50	82.60	78.10	Mg5Al2Si3O10(OH)8	
Chlorite7A	0.89	82.60	81.71	Mg5Al2Si3O10(OH)8	
Chrysotile	2.06	37.49	35.43	Mg3Si2O5(OH)4	
Clinoenstatite	-1.78	10.84	12.63	MgSiO3	
CO2(g)	-8.75	-9.88	-1.13	CO2	
Cristobalite	-1.02	-4.96	-3.94	SiO2	
Diaspore	0.77	9.23	8.46	AlOOH	
Diopside	1.98	23.95	21.97	CaMgSi2O6	
Dolomite	-3.76	-20.25	-16.48	CaMg(CO3)2	
Dolomite(d)	-4.42	-20.25	-15.83	CaMg(CO3)2	
Epsomite	-6.02	-8.35	-2.32	MgSO4:7H2O	
Fluorite	-2.48	-13.43	-10.94	CaF2	
Forsterite	-4.78	26.65	31.42	Mg2SiO4	
Gibbsite	-0.34	9.23	9.57	Al(OH)3	
Gypsum	-1.47	-6.09	-4.61	CaSO4:2H2O	
H2(g)	-27.20	-30.24	-3.04	H2	
H2O(g)	-2.19	-0.00	2.19	H2O	
Halite	-7.13	-5.61	1.52	NaCl	
Halloysite	-6.51	8.55	15.06	Al2Si2O5(OH)4	
Huntite	-14.44	-42.75	-28.32	CaMg3(CO3)4	
Hydromagnesite	-23.80	-29.21	-5.41	Mg5(CO3)4(OH)2:4H2O	
Illite	-2.91	-46.69	-43.78	K0.6Mg0.25Al2.3Si3.5O10(OH)2	

Jurbanite	-11.69	-14.92	-3.23	AlOHSO4
Kaolinite	-1.15	8.55	9.70	Al2Si2O5(OH)4
Kmica	2.82	19.33	16.51	KAl3Si3O10(OH)2
Laumontite	-0.61	-34.11	-33.50	CaAl2Si4O12:4H2O
Leonhardite	7.31	-68.22	-75.54	Ca2Al4Si8O24:7H2O
Magadiite	-12.41	-26.71	-14.30	NaSi7O13(OH)3:3H2O
Magnesite	-3.62	-11.25	-7.63	MgCO3
Mirabilite	-5.83	-8.16	-2.33	Na2SO4:10H2O
Montmorillonite-Ca	-4.12	-52.89	-48.77	Ca0.165Al2.33Si3.67O10(OH)2
Nahcolite	-7.66	-8.45	-0.79	NaHCO3
Natron	-8.75	-11.07	-2.32	Na2CO3:10H2O
Nesquehonite	-6.00	-11.25	-5.25	MgCO3:3H2O
O2(g)	-0.52	-3.19	-2.67	O2
Phillipsite	-3.92	-23.79	-19.87	Na0.5K0.5AlSi3O8:H2O
Phlogopite	2.26	48.28	46.01	KMg3AlSi3O10(OH)2
Portlandite	-6.73	18.06	24.79	Ca(OH)2
Prehnite	1.27	-11.09	-12.36	Ca2Al2Si3O10(OH)2
Pyrophyllite	-3.86	-52.17	-48.31	Al2Si4O10(OH)2
Quartz	-0.59	-4.96	-4.36	SiO2
Sepiolite	0.29	16.73	16.45	Mg2Si3O7.5OH:3H2O
Sepiolite(d)	-1.93	16.73	18.66	Mg2Si3O7.5OH:3H2O
Silicagel	-1.65	-4.96	-3.30	SiO2
SiO2(a)	-2.03	-4.96	-2.93	SiO2
SrF2	-8.54	-17.16	-8.62	SrF2
Strontianite	-3.40	-12.73	-9.33	SrCO3
Talc	3.20	27.58	24.37	Mg3Si4O10(OH)2
Thenardite	-8.02	-8.16	-0.14	Na2SO4
Thermonatrite	-11.38	-11.07	0.30	Na2CO3:H2O
Tremolite	12.68	75.47	62.79	Ca2Mg5Si8O22(OH)2
Trona	-19.88	-19.52	0.36	NaHCO3:Na2CO3:2H2O
Wairakite	-5.73	-34.11	-28.39	CaAl2Si4O12:2H2O
Witherite	-5.56	-14.29	-8.72	BaCO3

**For a gas, SI = log10(fugacity). Fugacity = pressure * phi / 1 atm.
For ideal gases, phi = 1.

Beginning of batch-reaction calculations.

Reaction step 1.

Using solution 5. North Basin (Open-System, no weathering)
Using pure phase assemblage 5.

-----Phase assemblage-----
--

Phase	SI	log IAP	log K(T, P)	Moles in assemblage		
				Initial	Final	Delta
CO2(g)	-3.43	-4.56	-1.13	1.000e+01	1.000e+01	-1.210e-04
O2(g)	-0.68	-3.35	-2.67	1.000e+01	1.000e+01	1.873e-04

-----Solution composition-----

--

Elements	Molality	Moles
Al	2.918e-06	2.918e-06
Ba	7.284e-09	7.284e-09
Br	4.382e-07	4.382e-07
C	1.259e-04	1.259e-04
Ca	1.148e-03	1.148e-03
Cl	1.089e-03	1.089e-03
F	7.898e-06	7.898e-06
K	8.954e-05	8.954e-05
Mg	6.172e-06	6.172e-06
N	4.928e-05	4.928e-05
Na	2.698e-03	2.698e-03
S	1.729e-03	1.729e-03
Si	3.746e-05	3.746e-05
Sr	2.066e-07	2.066e-07

-----Description of solution-----

--

	pH =	7.073	Charge balance
	pe =	15.772	Adjusted to redox
equilibrium	Activity of water =	1.000	
	Ionic strength (mol/kgw) =	7.240e-03	
	Mass of water (kg) =	1.000e+00	
	Total alkalinity (eq/kg) =	1.065e-04	
	Total CO2 (mol/kg) =	1.259e-04	
	Temperature (°C) =	1.00	
	Electrical balance (eq) =	3.945e-04	
	Percent error, 100*(Cat- An)/(Cat+ An) =	4.26	
	Iterations =	17	
	Total H =	1.110126e+02	
	Total O =	5.551465e+01	

-----Distribution of species-----

--

mole V Species cm ³ /mol	Molality	Activity	Log		Log Gamma
			Molality	Activity	
H+	9.124e-08	8.447e-08	-7.040	-7.073	-0.033
0.00 OH-	1.630e-08	1.493e-08	-7.788	-7.826	-0.038
(0) H2O	5.551e+01	9.999e-01	1.744	-0.000	0.000
18.02 Al	2.918e-06				
Al (OH) 4-	1.794e-06	1.647e-06	-5.746	-5.783	-0.037
(0) Al (OH) 2+	4.280e-07	3.936e-07	-6.369	-6.405	-0.036
(0)					

AlF ₂ ⁺	3.477e-07	3.198e-07	-6.459	-6.495	-0.036
(0)					
AlF ₂	1.609e-07	1.151e-07	-6.793	-6.939	-0.146
(0)					
Al(OH) ₃	8.500e-08	8.514e-08	-7.071	-7.070	0.001
(0)					
AlOH ₂ ⁺	6.721e-08	4.807e-08	-7.173	-7.318	-0.146
(0)					
AlF ₃	2.485e-08	2.489e-08	-7.605	-7.604	0.001
(0)					
AlSO ₄ ⁺	5.885e-09	5.402e-09	-8.230	-8.267	-0.037
(0)					
Al ³⁺	4.244e-09	2.120e-09	-8.372	-8.674	-0.301
(0)					
Al(SO ₄) ₂ ⁻	1.863e-10	1.710e-10	-9.730	-9.767	-0.037
(0)					
AlF ₄ ⁻	6.814e-11	6.255e-11	-10.167	-10.204	-0.037
(0)					
AlHSO ₄ ²⁺	5.028e-17	3.560e-17	-16.299	-16.448	-0.150
(0)					
Ba	7.284e-09				
Ba ²⁺	5.190e-09	3.700e-09	-8.285	-8.432	-0.147
(0)					
BaSO ₄	2.092e-09	2.096e-09	-8.679	-8.679	0.001
(0)					
BaHCO ₃ ⁺	1.627e-12	1.493e-12	-11.789	-11.826	-0.037
(0)					
BaCO ₃	3.046e-14	3.052e-14	-13.516	-13.515	0.001
(0)					
BaOH ⁺	1.615e-15	1.484e-15	-14.792	-14.829	-0.037
(0)					
Br	4.382e-07				
Br ⁻	4.382e-07	4.020e-07	-6.358	-6.396	-0.037
(0)					
C(-4)	0.000e+00				
CH ₄	0.000e+00	0.000e+00	-159.507	-159.506	0.001
(0)					
C(4)	1.259e-04				
HCO ₃ ⁻	9.742e-05	8.959e-05	-4.011	-4.048	-0.036
(0)					
CO ₂	2.777e-05	2.782e-05	-4.556	-4.556	0.001
(0)					
CaHCO ₃ ⁺	4.874e-07	4.487e-07	-6.312	-6.348	-0.036
(0)					
NaHCO ₃	1.240e-07	1.242e-07	-6.907	-6.906	0.001
(0)					
CO ₃ ²⁻	3.614e-08	2.585e-08	-7.442	-7.588	-0.146
(0)					
CaCO ₃	2.546e-08	2.550e-08	-7.594	-7.593	0.001
(0)					
MgHCO ₃ ⁺	4.433e-09	4.065e-09	-8.353	-8.391	-0.038
(0)					
NaCO ₃ ⁻	3.459e-10	3.181e-10	-9.461	-9.497	-0.036
(0)					
SrHCO ₃ ⁺	8.684e-11	7.986e-11	-10.061	-10.098	-0.036
(0)					

MgCO3	6.877e-11	6.888e-11	-10.163	-10.162	0.001
(0)					
BaHCO3+	1.627e-12	1.493e-12	-11.789	-11.826	-0.037
(0)					
SrCO3	1.076e-12	1.076e-12	-11.968	-11.968	0.000
(0)					
BaCO3	3.046e-14	3.052e-14	-13.516	-13.515	0.001
(0)					
Ca	1.148e-03				
Ca+2	1.019e-03	7.285e-04	-2.992	-3.138	-0.146
(0)					
CaSO4	1.285e-04	1.287e-04	-3.891	-3.890	0.001
(0)					
CaHCO3+	4.874e-07	4.487e-07	-6.312	-6.348	-0.036
(0)					
CaCO3	2.546e-08	2.550e-08	-7.594	-7.593	0.001
(0)					
CaF+	2.383e-08	2.192e-08	-7.623	-7.659	-0.036
(0)					
CaOH+	1.554e-09	1.431e-09	-8.808	-8.844	-0.036
(0)					
CaHSO4+	5.559e-11	5.100e-11	-10.255	-10.292	-0.037
(0)					
Cl	1.089e-03				
Cl-	1.089e-03	9.978e-04	-2.963	-3.001	-0.038
(0)					
F	7.898e-06				
F-	6.932e-06	6.350e-06	-5.159	-5.197	-0.038
(0)					
AlF2+	3.477e-07	3.198e-07	-6.459	-6.495	-0.036
(0)					
AlF+2	1.609e-07	1.151e-07	-6.793	-6.939	-0.146
(0)					
AlF3	2.485e-08	2.489e-08	-7.605	-7.604	0.001
(0)					
CaF+	2.383e-08	2.192e-08	-7.623	-7.659	-0.036
(0)					
NaF	8.991e-09	9.006e-09	-8.046	-8.045	0.001
(0)					
MgF+	1.150e-09	1.056e-09	-8.939	-8.977	-0.037
(0)					
HF	5.336e-10	5.345e-10	-9.273	-9.272	0.001
(0)					
AlF4-	6.814e-11	6.255e-11	-10.167	-10.204	-0.037
(0)					
HF2-	1.092e-14	1.001e-14	-13.962	-14.000	-0.038
(0)					
H2F2	1.683e-18	1.686e-18	-17.774	-17.773	0.001
(0)					
SiF6-2	2.937e-33	2.094e-33	-32.532	-32.679	-0.147
(0)					
H(0)	0.000e+00				
H2	0.000e+00	0.000e+00	-48.728	-48.727	0.001
(0)					
K	8.954e-05				
K+	8.909e-05	8.162e-05	-4.050	-4.088	-0.038
(0)					

KSO4-	4.470e-07	4.110e-07	-6.350	-6.386	-0.036
(0)					
Mg	6.172e-06				
Mg+2	5.621e-06	4.037e-06	-5.250	-5.394	-0.144
(0)					
MgSO4	5.451e-07	5.460e-07	-6.264	-6.263	0.001
(0)					
MgHCO3+	4.433e-09	4.065e-09	-8.353	-8.391	-0.038
(0)					
MgF+	1.150e-09	1.056e-09	-8.939	-8.977	-0.037
(0)					
MgCO3	6.877e-11	6.888e-11	-10.163	-10.162	0.001
(0)					
MgOH+	1.783e-11	1.643e-11	-10.749	-10.784	-0.035
(0)					
N(-3)	0.000e+00				
NH4+	0.000e+00	0.000e+00	-70.135	-70.173	-0.037
(0)					
NH4SO4-	0.000e+00	0.000e+00	-71.973	-72.010	-0.037
(0)					
NH3	0.000e+00	0.000e+00	-73.147	-73.147	0.000
(0)					
N(0)	1.320e-24				
N2	6.600e-25	6.611e-25	-24.180	-24.180	0.001
(0)					
N(3)	2.396e-19				
NO2-	2.396e-19	2.198e-19	-18.620	-18.658	-0.037
(0)					
N(5)	4.928e-05				
NO3-	4.928e-05	4.509e-05	-4.307	-4.346	-0.039
(0)					
Na	2.698e-03				
Na+	2.685e-03	2.465e-03	-2.571	-2.608	-0.037
(0)					
NaSO4-	1.287e-05	1.183e-05	-4.891	-4.927	-0.036
(0)					
NaHCO3	1.240e-07	1.242e-07	-6.907	-6.906	0.001
(0)					
NaF	8.991e-09	9.006e-09	-8.046	-8.045	0.001
(0)					
NaCO3-	3.459e-10	3.181e-10	-9.461	-9.497	-0.036
(0)					
O(0)	8.935e-04				
O2	4.468e-04	4.475e-04	-3.350	-3.349	0.001
(0)					
S(-2)	0.000e+00				
H2S	0.000e+00	0.000e+00	-155.011	-155.010	0.001
(0)					
HS-	0.000e+00	0.000e+00	-155.231	-155.269	-0.038
(0)					
S6-2	0.000e+00	0.000e+00	-157.956	-158.077	-0.121
(0)					
S5-2	0.000e+00	0.000e+00	-158.262	-158.387	-0.126
(0)					
S4-2	0.000e+00	0.000e+00	-158.516	-158.647	-0.131
(0)					

S-2	0.000e+00	0.000e+00	-161.743	-161.890	-0.147
(0)					
S3-2	0.000e+00	0.000e+00	-162.008	-162.145	-0.137
(0)					
S2-2	0.000e+00	0.000e+00	-163.313	-163.455	-0.142
(0)					
S(6)	1.729e-03				
SO4-2	1.586e-03	1.130e-03	-2.800	-2.947	-0.147
(0)					
CaSO4	1.285e-04	1.287e-04	-3.891	-3.890	0.001
(0)					
NaSO4-	1.287e-05	1.183e-05	-4.891	-4.927	-0.036
(0)					
MgSO4	5.451e-07	5.460e-07	-6.264	-6.263	0.001
(0)					
KSO4-	4.470e-07	4.110e-07	-6.350	-6.386	-0.036
(0)					
SrSO4	2.144e-08	2.147e-08	-7.669	-7.668	0.001
(0)					
HSO4-	6.343e-09	5.823e-09	-8.198	-8.235	-0.037
(0)					
AlSO4+	5.885e-09	5.402e-09	-8.230	-8.267	-0.037
(0)					
BaSO4	2.092e-09	2.096e-09	-8.679	-8.679	0.001
(0)					
Al(SO4)2-	1.863e-10	1.710e-10	-9.730	-9.767	-0.037
(0)					
CaHSO4+	5.559e-11	5.100e-11	-10.255	-10.292	-0.037
(0)					
AlHSO4+2	5.028e-17	3.560e-17	-16.299	-16.448	-0.150
(0)					
NH4SO4-	0.000e+00	0.000e+00	-71.973	-72.010	-0.037
(0)					
Si	3.746e-05				
H4SiO4	3.743e-05	3.750e-05	-4.427	-4.426	0.001
(0)					
H3SiO4-	2.670e-08	2.448e-08	-7.574	-7.611	-0.038
(0)					
H2SiO4-2	4.530e-15	3.240e-15	-14.344	-14.489	-0.146
(0)					
SiF6-2	2.937e-33	2.094e-33	-32.532	-32.679	-0.147
(0)					
Sr	2.066e-07				
Sr+2	1.851e-07	1.325e-07	-6.733	-6.878	-0.145
(0)					
SrSO4	2.144e-08	2.147e-08	-7.669	-7.668	0.001
(0)					
SrHCO3+	8.684e-11	7.986e-11	-10.061	-10.098	-0.036
(0)					
SrCO3	1.076e-12	1.076e-12	-11.968	-11.968	0.000
(0)					
SrOH+	8.755e-14	8.045e-14	-13.058	-13.094	-0.037
(0)					

-----Saturation indices-----
 --

Phase	SI**	log IAP	log K(274 K, 1 atm)	
Adularia	-0.60	-23.15	-22.55	KAlSi3O8
Al(OH)3(a)	0.05	12.55	12.50	Al(OH)3
Albite	-2.01	-21.67	-19.66	NaAlSi3O8
AlumK	-13.02	-18.66	-5.63	KAl(SO4)2·12H2O
Alunite	4.61	6.44	1.82	KAl3(SO4)2(OH)6
Analcime	-3.37	-17.24	-13.87	NaAlSi2O6·H2O
Anhydrite	-1.72	-6.08	-4.36	CaSO4
Anorthite	-3.10	-23.56	-20.46	CaAl2Si2O8
Aragonite	-2.50	-10.73	-8.22	CaCO3
Artinite	-15.67	-4.23	11.44	MgCO3:Mg(OH)2·3H2O
BaF2	-13.00	-18.83	-5.82	BaF2
Barite	-0.92	-11.38	-10.45	BaSO4
Basaluminite	10.39	33.09	22.70	Al4(OH)10SO4
Beidellite	4.25	-44.90	-49.14	
(NaK _{0.5} Al _{2.33} Si _{3.67} O ₁₀ (OH) ₂				
Boehmite	2.15	12.55	10.39	AlOOH
Brucite	-9.83	8.75	18.58	Mg(OH)2
Calcite	-2.34	-10.73	-8.38	CaCO3
Celestite	-3.13	-9.82	-6.69	SrSO4
CH4(g)	-156.86	-159.51	-2.64	CH4
Chalcedony	-0.57	-4.43	-3.85	SiO2
Chlorite14A	-22.52	55.58	78.10	Mg5Al2Si3O10(OH)8
Chlorite7A	-26.14	55.58	81.71	Mg5Al2Si3O10(OH)8
Chrysotile	-18.02	17.41	35.43	Mg3Si2O5(OH)4
Clinoenstatite	-8.30	4.33	12.63	MgSiO3
CO2(g)	-3.43	-4.56	-1.13	CO2
Cristobalite	-0.49	-4.43	-3.94	SiO2
Diaspore	4.08	12.55	8.46	AlOOH
Diopside	-11.06	10.91	21.97	CaMgSi2O6
Dolomite	-7.22	-23.71	-16.48	CaMg(CO3)2
Dolomite(d)	-7.88	-23.71	-15.83	CaMg(CO3)2
Epsomite	-6.02	-8.34	-2.32	MgSO4·7H2O
Fluorite	-2.59	-13.53	-10.94	CaF2
Forsterite	-18.34	13.08	31.42	Mg2SiO4
Gibbsite	2.97	12.55	9.57	Al(OH)3
Gypsum	-1.47	-6.08	-4.61	CaSO4·2H2O
H2(g)	-45.69	-48.73	-3.04	H2
H2O(g)	-2.19	-0.00	2.19	H2O
H2S(g)	-154.31	-155.01	-0.70	H2S
Halite	-7.13	-5.61	1.52	NaCl
Halloysite	1.18	16.24	15.06	Al2Si2O5(OH)4
Huntite	-21.35	-49.67	-28.32	CaMg3(CO3)4
Hydromagnesite	-37.76	-43.17	-5.41	Mg5(CO3)4(OH)2·4H2O
Illite	2.69	-41.08	-43.78	K0.6Mg0.25Al2.3Si3.5O10(OH)2
Jurbanite	-1.32	-4.55	-3.23	AlOHSO4
Kaolinite	6.54	16.24	9.70	Al2Si2O5(OH)4
Kmica	10.83	27.35	16.51	KAl3Si3O10(OH)2
Laumontite	1.09	-32.41	-33.50	CaAl2Si4O12·4H2O
Leonhardite	10.72	-64.82	-75.54	Ca2Al4Si8O24·7H2O
Magadiite	-12.22	-26.52	-14.30	NaSi7O13(OH)3·3H2O
Magnesite	-5.35	-12.98	-7.63	MgCO3
Mirabilite	-5.83	-8.16	-2.33	Na2SO4·10H2O
Montmorillonite-Ca	4.39	-44.38	-48.77	Ca0.165Al2.33Si3.67O10(OH)2
N2(g)	-21.01	-24.18	-3.17	N2
Nahcolite	-5.87	-6.66	-0.79	NaHCO3

Natron	-10.48	-12.80	-2.32	Na2CO3:10H2O
Nesquehonite	-7.73	-12.98	-5.25	MgCO3:3H2O
NH3 (g)	-75.44	-73.15	2.29	NH3
O2 (g)	-0.68	-3.35	-2.67	O2
Phillipsite	-2.54	-22.41	-19.87	Na0.5K0.5AlSi3O8:H2O
Phlogopite	-17.50	28.51	46.01	KMg3AlSi3O10 (OH) 2
Portlandite	-13.78	11.01	24.79	Ca (OH) 2
Prehnite	-4.61	-16.97	-12.36	Ca2Al2Si3O10 (OH) 2
Pyrophyllite	4.90	-43.42	-48.31	Al2Si4O10 (OH) 2
Quartz	-0.06	-4.43	-4.36	SiO2
Sepiolite	-12.22	4.23	16.45	Mg2Si3O7.5OH:3H2O
Sepiolite(d)	-14.43	4.23	18.66	Mg2Si3O7.5OH:3H2O
Silicagel	-1.12	-4.43	-3.30	SiO2
SiO2 (a)	-1.50	-4.43	-2.93	SiO2
SrF2	-8.65	-17.27	-8.62	SrF2
Strontianite	-5.13	-14.47	-9.33	SrCO3
Sulfur	-114.81	-130.35	-15.53	S
Talc	-15.82	8.55	24.37	Mg3Si4O10 (OH) 2
Thenardite	-8.02	-8.16	-0.14	Na2SO4
Thermonatrite	-13.11	-12.80	0.30	Na2CO3:H2O
Tremolite	-32.42	30.37	62.79	Ca2Mg5Si8O22 (OH) 2
Trona	-19.82	-19.46	0.36	NaHCO3:Na2CO3:2H2O
Wairakite	-4.02	-32.41	-28.39	CaAl2Si4O12:2H2O
Witherite	-7.30	-16.02	-8.72	BaCO3

**For a gas, SI = log10(fugacity). Fugacity = pressure * phi / 1 atm.
For ideal gases, phi = 1.

End of simulation.

Reading input data for simulation 6.

End of Run after 0.3 Seconds.
